CLIMATE HAZARD MAPS – A TOOL TO SUPPORT COMMUNICATION WITH STAKEHOLDERS.
A SHOWCASE OF BAIA MARE DEPRESSION, ROMANIA

INES GRIGORESCU[*], MIHAELA SIMA[*], CARMEN-SOFIA DRAGOTĂ[*],
CRISTINA DUMITRICĂ[*]

Key words: extreme weather events, multi-hazard map, stakeholder communication, Baia Mare Depression.

Abstract. Baia Mare Depression is an inter-hilly depression located in the north-western part of Romania bounded by mountain and hilly areas. Its position has granted it with specific environmental features which had exposed it to several climatic hazards while the historical industrial profile of the area (non-ferrous mining and metallurgical industry) and the related emissions (CO_2, SO_X, particulate matters and Pb) might still pose threats to the environment and human health. The article proposes a methodology for producing multi-hazard climate information (layers) and designing communication products (hazard maps) on extreme weather phenomena, to be used by relevant stakeholders at local level. The scientific method relies on the occurrence, frequency, and amplitude of the foremost extreme weather phenomena (snow cover, glazed frost, fog, heavy rainfall, strong winds) based on monthly and daily extreme climatic values from several weather stations. The stakeholder's interaction through focus groups meetings and cross analysis validated the resulted maps. The main findings of the current study are the assessment, and spatial (visual) representation of the climate hazards the study area is exposed to as key step in supporting adaptation strategies and increasing resilience at regional and local levels.

1. INTRODUCTION

Development will continue to occur in hazard-prone areas which is enhancing the potential for climate change induced damages (Balogun *et al*., 2020). Over the last few decades, climate- and water-related hazards have increased in occurrence (IPCC, 2014) and served as trigger for more than 75% of the disasters globally, hence being tightly connected with issues such as food security, migration, and even national security (Mcbean and Rodgers, 2010). The impacts on local economies and communities are massive, and the recovery usually involves significant financial resources and takes a very long time (Newman *et al*., 2017). That being so, between 1970 and 2019, over 11,000 disasters were attributed to climate and water-related hazards which accounted for over 2 million deaths and US$ 3.64 trillion in losses and they will continue to adversely affect human health, economic and social development in the future (WMO, 2021). Europe has faced several changes in its physical, technological and human/social systems. On that account, climate change impacts and responses are observed in the physical and ecological systems (Adger *et al*., 2005; Kreibich *et al*., 2014), this leading to an increasing effect of disasters caused by natural hazards and technological accidents (EEA, 2010). Evidence shows that Europe will likely face a progressive increase in overall climate hazards affecting highly populated areas, multiple sectors and causing systemic failures (IPCC, 2014); floods and windstorms, in particular, have become critical in combination with other climate hazards (Forzieri *et al*., 2016). Accordingly, a continuous population growth will bring about an increased exposure of communities; hence a changing climate will lead to more people at risk (Mcbean and Rodgers, 2010). To better handle this unprecedented situation, there is need to build

[*] Senior Researcher, Institute of Geography, Romanian Academy, 12 Dimitrie Racoviţă Street, 023993, Bucharest, Romania, inesgrigorescu@yahoo.com; simamik@yahoo.com; dragotacarmensofia@gmail.com; geocrisro@yahoo.com.

scientific capacity in disaster risk reduction through data collection and analysis infrastructure to maintain the complexity of the social and environmental interlinkages (Chen *et al*., 2021).

Europe suffered some of the world's damaging disasters: *e.g.*, storms (western, central, and parts of Eastern Europe), floods (central parts of the continent and the United Kingdom), forest fires (Greece), drought (Iberian Peninsula), several countries being more affected, *i.e.*, Turkey, Romania and France (EEA, 2010, 2017). Within the EEA-32 member countries, between 1980 and 2019, weather- and climate-related extremes accounted for around 81% of total economic losses driven by natural hazards which caused economic losses totalling nearly EUR 446 billion, of which 12,118 million euros in Romania (EEA, 2020). The growing interlinkage between our societies and countries have determined some of these impacts to cascade up from local to national and even international levels (WMO, 2021). As shown, climate change is likely to enhance the risk posed by extreme weather events considering the reported losses which are reaching historical high levels (Forzieri *et al*., 2016), cities being more affected in this respect by concentrating the largest population and buildings (OECD, 2014), thus increasing urban resilience to climate change being a major concern worldwide (World Bank, 2010). Because of the widespread negative impacts of climate change across different economic sectors (*e.g.*, aviation, farming, tourism), the demand for tailored weather information is constantly growing (Mills *et al*., 2016). To avoid such undesirable consequences in the future, the European Commission adopted its new EU Strategy on Adaptation to Climate Change to support climate change adaptation, particularly in key vulnerable sectors[1]. In addition, the Climate-ADAPT platform (developed by the European Commission and the EEA) was created to support climate action and governmental policy by sharing knowledge on climate change and its impacts, adaptation strategies and plans, and case studies[2]. The EU also supports the UN Sendai Framework for Disaster Risk Reduction 2015–2030 (Sendai Framework) in the evaluation of disaster-related losses and economic impacts, as well as in reducing such losses by 2030[3].

It has been estimated that environmental and social threats will be more pronounced in areas prone to multiple climate hazards. In this context, a multi-hazard assessment accounting for possible regional variations in intensity and frequency of climate extremes is essential to identify areas potentially more exposed to climate change (Forzieri *et al*., 2016). However, making scientific information on key environmental concerns available and easy to be used by different stakeholders is an issue researchers are dealing with even more in the recent years. In view of that, climate change "hotspots" mapping has become an important visual tool used by researchers to communicate issues in a manner that may be easier to interpret than text (De Sherbinin, 2014; De Sherbinin *et al*., 2019) and to be understood by different stakeholders and decision makers. Thus, a system mapping framework will turn into a helpful analytical and visual support tool able to enhance stakeholders' knowledge, experience and perception (Nikas *et al*., 2017). More recently, participatory mapping was widely used as effective techniques aimed at engaging local communities in developing decision support tools towards climate change adaptation (Nkoana *et al*., 2018; Yen *et al*., 2019; Mabon, 2020). As a result, an important step for carrying out impact and risk analysis consists in identifying areas where climate phenomena manifest on at larger scales and their intensities (Turco *et al*., 2015). On the long run, through climate mapping, identifying areas considered particularly vulnerable to different climate impacts might also have political, economic, and social consequences to spot regions at climate security risk (Gemenne *et al*., 2014).

The current paper aims to propose a methodology for the elaboration of GIS climate hazards maps at small spatial scale, *i.e.*, Baia Mare Depression, an area with particular local conditions in terms of the natural settings (*e.g.*, climate, relief, hydrology) and human-related impacts (exploitation

---

[1] https://ec.europa.eu/clima/eu-action/adaptation-climate-change/eu-adaptation-strategy_en
[2] https://climate-adapt.eea.europa.eu/
[3] https://ec.europa.eu/echo/sites/default/files/sendai_leaflet_draft_v6.pdf

and processing of mineral ore deposits, road traffic). As a first step, single hazards maps have been elaborated and, using standard indicators, a complex map resulted, which indicates areas considered as potential climate-related "hotspots". The maps can be used as a support during the interaction with local stakeholders to increase their awareness and interest in climate change issues. Hence, this type of approach can be considered a climate service by way of the scientific information it provides to stakeholders. The study is part of a larger survey undertaken in the Baia Mare Municipality, where an intense interaction with stakeholders in terms of providing climate-tailored data and information has been undertaken, the results being reported in a previous paper (Sima *et al*., 2016).

2. STUDY AREA

The study area, Baia Mare Depression, located in the north-western part of Romania, is bordered by the Igniş Massive and by the Gutâi Mountains raised to over 1200 m altitude in the North and North-East, and by the Codrului and Chioarului Hills at 650–800 m in the West and South, framing into the Crişana Hills (Posea and Badea 1984; Badea *et al*. 2008). The area is drained by the Someş River and its tributaries Lăpus, Bârsău etc. (Fig. 1) According to the climatic regionalization, the area under analysis is part of the *low hills and tablelands climatic region*, since it benefits from a shelter topoclimate specific to depressionary areas imposed by its relief particular features (Bălteanu, 2016). The *western and northern climatic influences* complete the moderate temperate-continental climate of the Baia Mare Depression. These major climatic traits are completed by the variety of factors imposed by the local geographical environment (*e.g.*, orographic barrier of the mountains situated in the north and north-east and hills in the west and south, exposure, fragmentation, vegetation, soil and water bodies as well as the man-made changes) determining a wide range of local climatic features and exposing the area to several extreme weather phenomena.

The effects of observed and future climate change are differentiated both spatially and socially (Adger, 2010). That being so, the natural conditions of the study area (inter-hilly depression) have a particular influence on the distribution, dynamics and intensity of the extreme weather phenomena and the related impacts on the ecological and social systems. Thus, the intensity of weather phenomena can be smoothened (summer heat waves) or enhanced to the extreme (fog and acid depositions) by its sheltered position provided by the inner hilly area (Sima *et al*., 2012). In the previous years, the pollutant emissions (CO_2, SO_X, particulate matters and Pb) in relation to the industrial profile of Baia Mare, Baia Sprie or Cavnic cities (non-ferrous mining and metallurgical industry) posed significant threat to environment and human health by increasing in concentration in the presence of some weather phenomena (*e.g.*, fog, snow cover, wind, temperature inversions) (Dragotă *et al*., 2013).

During winter the depressionary relief favours the persistence of low temperatures driven by temperature inversions under the atmospheric calm. At inferior levels, where the entire human activity unfolds, this phenomenon is amplified and upheld. Under specific genetic (advective-radiating and orographic processes) and local (*e.g.*, the presence of the solid snow layer, the existence of closed depressions) conditions, the combination of some extreme weather events becomes significantly dangerous. In these conditions, the gravitational leakage of the cold air on the surrounding slopes generates temperature inversions of orographic nature which contribute to the intensification of the cooling process and to the increase in thickness of the inversion stratum. The more closed the depression, the more shielded is the horizon by the bordering mountain slopes which leads to the reduction of the insolation time, and implicitly to the increase in duration and intensity of the thermal inversions that, on a daily regime occurs in the early evening and persists longer in the mornings. That being so, the narrow opening of the depression to the north-west gives a slight smoothening of the

extreme weather events in the centre and north-western parts, while the narrowing of the depression in the southern and south-eastern parts under the form of tapered valleys surrounded by mountains, the effects of the extreme weather phenomena are amplified.
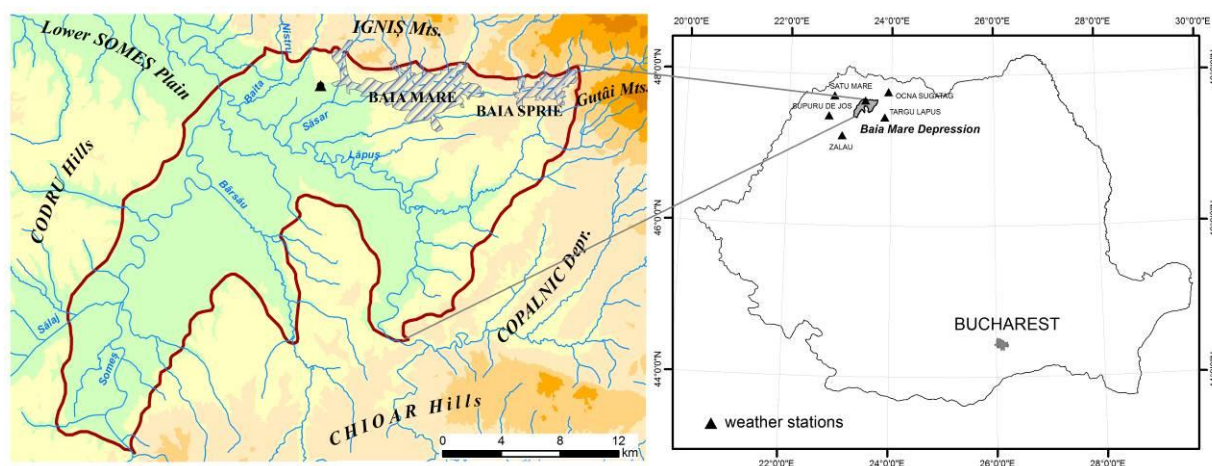

Fig. 1 – The physical-geographical location of the Baia Mare Depression.

Nevertheless, the general climatic feature of the Baia Mare Depression is characterized by a spatial uniformity of thermal parameters imprinting the type of climate known as moderate temperate continental with hot summers and gentle winters, early springs, and late autumns. The most important climate hazards the study area is exposed to, are generated by the main climatic factors: the general atmospheric circulation, solar radiation, and the active surface.

3. METHODOLOGY

A large body of literature on climate change-related events and impacts has been mainly dedicated to issues that involve vulnerability assessment of different weather events, mostly drought or heavy rainfall and vulnerable communities (Wilhite, 2000; Brooks *et al*., 2005; Füssel and Klein, 2006; Iglesias *et al*., 2009; Yusuf and Francisco, 2009; Preston *et al*., 2011), impacts on vulnerable sectors such as agriculture (Van der Velde *et al*., 2012; Sima *et al*., 2015; Lesk *et al*., 2016), urban areas and human health (Stone *et al*., 2010; Bambic *et al*., 2011; Schmeltz and Marcotullio, 2019) etc. More recently, climate change "hotspots" mapping has become of growing concern in the scientific community (De Sherbinin, 2014; Turco *et al*., 2015; De Sherbinin *et al*., 2019) because of the extended range of practical applications the resulted maps provide. Above all, the development of adaptation and mitigation measures and strategies (Wilhite *et al*., 2007; Füssel, 2009; Reckien *et al*., 2014; Felton *et al*., 2016) with implications across various regions or fields is another research direction largely addressed in relation to climate change-related maps. In addition, several theoretical (Peduzzi *et al*. 2005; Gwilliam *et al*. 2006; Helmer and Hilhorst, 2006; De Sherbinin *et al*. 2007; IPCC 2007; IPCC 2014; Cueva-Luna *et al*. 2008) and applied (Yusuf and Francisco, 2009; Amarnath *et al*., 2017; Leis and Kienberger, 2020; Sutanto *et al*., 2020) studies have been elaborated on the impact extreme events have on the environment (climate-related, in particular). Most of them used the overlaying climate hazard sensitivity, and adaptive capacity maps following the vulnerability assessment framework of the United Nations' Inter-Governmental Panel on Climate Change (IPCC) to

identify regions most vulnerable to climate change. However, spatial assessments of the extreme weather events which included mapping, spatial analysis and regionalisation have been little addressed in the scientific literature. At larger scales (European level), several impact studies have often relied on a single decisive factor, *i.e.*, climate hazard or extreme weather event, such as heat waves (Fischer and Schär, 2010; Russo *et al*., 2015; Papathoma-Köhle *et al*., 2016; Savić *et al*., 2018), heat stress (Vitolo *et al*., 2019), droughts (Lehner *et al*., 2006; Kim *et al*., 2014) or windstorms (Outten and Esau 2013). These studies described a limited set of climate hazards which limits the delineation of areas potentially affected by climate change-related events. This is also the case of a risk assessment and mapping methodology developed within the European project SEERISK and adapted for a number of climate change-related hazards individually (floods, heat waves, wildfires, and storms) which was applied to some areas of central and south-eastern Europe (Papathoma-Köhle *et al*., 2016; Savić *et al*., 2018). Hence, considering multiple, compound, or cascading hazards for future approaches becomes critical to identifying areas potentially more exposed to the complex effects of climate change (Forzieri *et al*., 2016) and understanding the transformations in the ecological and social systems, given that the impacts of one hazardous event are often exacerbated by interaction with another (Marzocchi *et al*. 2009), causing more severe impacts than a single hazard event alone (Sutanto *et al*., 2020). As a result, Sutanto *et al*. (2020) developed a novel methodology for the identification of hotspots and patterns of compound and cascading dry hazards (heatwaves, droughts, and fire) at pan-European scale.

In Romania, some studies have attempted to develop a methodology to map and regionalise climate hazards (Dragotă *et al*., 2013; Dragotă *et al*., 2016; Dumitraşcu *et al*., 2016). These studies have used the classification of hazardous meteorological phenomena carried out for the Romanian territory by Croitoru and Moldovan (2005) derived from the complex classification of Bryant (1991). Based on these classifications, and yet adapted to the particularities (*e.g.*, climate, relief, industrial profile, associated economic effects) and the scale of the study area, the authors have selected the foremost climatic hazards with impact on both ecological and social systems: snow cover, glazed frost, fog, heavy rainfall, strong wind (Fig. 2).

Forzieri *et al*. (2016) pinpointed as major challenges in addressing multiple hazards the lack of compatibility in relation to the different metrics used to measure the processes and their interaction triggering cascade effects and coupled dynamics. Hence, standardization approaches are required (Kappes *et al*, 2012; Lung *et al*., 2013). That being so, the authors have chosen to use a standard indicator for the statistical reckoning of each extreme climate phenomena selected, *i.e.*, the *maximum absolute frequency* (Fq) which plays a key role in the hazard assessment (Dragotă *et al*., 2009b; Dragotă *et al*., 2013; Grigorescu *et al*., 2013). The maximum absolute frequency was calculated using the real data (1896–2010 period) from the Baia Mare weather station, considered as a reference station for the study area. In addition, due to the lack of additional backing weather stations, the database of Satu Mare, Târgu Lăpuş, Ocna Şugatag, Supuru de Jos and Zalău adjacent weather stations was also used in order to obtain a good GIS interpolation. Furthermore, based on the selected class values, three hazard classes have been set up: high, medium and low (Fig. 2).

Each climate hazard was spatially represented in GIS as a single-hazard layer and, based on its significance for the study area, was not considered as equally contributing to the overall equation, being evaluated on a 1 to 3 scale and assigned with a ***weight (w).*** Having in view its attributed hazard class (3 – high, 2 – medium and 1 – low), a ***rank (r)*** has been also assigned (Tab. 1) (Dragotă *et al*., 2013; Dragotă *et al*., 2016; Dumitraşcu *et al*., 2016).
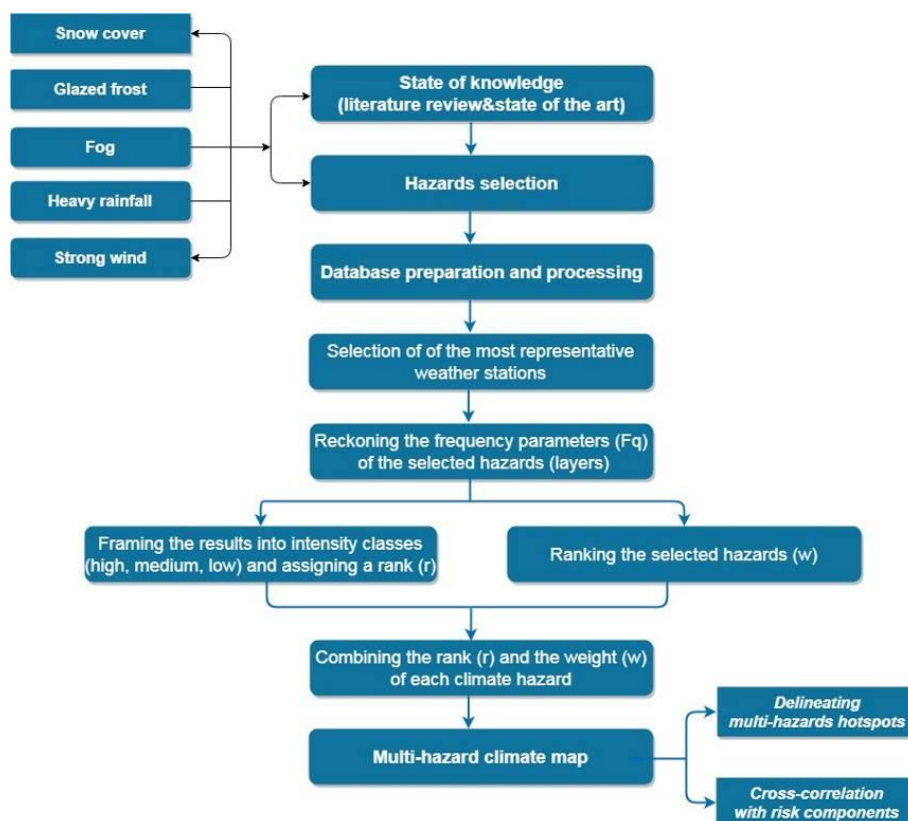
Fig. 2 – Methodological flow of the climate multi-hazard mapping and assessment.

Table 1

The selected climate hazards and the assigned classification (rank)
importance (weight)

Climate hazards		rank	weight
F	*Fog*	3...1	3
Sw	*Strong wind*	2	3
H$_{rf}$	*Heavy rainfall*	3...1	2
Gf	*Glazed frost*	3...1	2
S$_{cov}$	*Snow cover*	3...1	1

Finally, the mathematical formula summing up the layers and the assigned *weight (w)* and *rank (r)* was computed with the aim of completing the complex multi-hazard climate map:

$$\text{Scov}r + 2(\text{Gf}r + \text{Hrf}r) + 3(\text{Sw}r + \text{F}r)$$

Thus, the resulted GIS-based complex multi-hazard climate map is a comprehensive way of representing the spatial susceptibility to a group of severe climatic events at regional scale (Baia Mare Depression). By weighting and ranking the selected extreme weather events, the resulted final map clearly delineates which areas or identifies which communities are more exposed in order to provide effective monitoring and coordination of the mitigation actions. However, it should be noted that the weight might have a significant influence in upgrading or downgrading the hazard classes in the final map. *E.g.*, low fog hazard will be multiplied by 3 or low heavy rainfall hazard will be multiplied by 2, thus increasing the overall hazard class of the area due to a higher rank.

The visual impact and effectiveness of the climate hazard map has been subjected to **stakeholder analysis** using the focus group research method. Two meetings with local stakeholders were organised at Baia Mare City Hall. For each of the two meetings, two focus groups were established: (1) an *institutional focus group* consisting in local authorities and selected institutions (*e.g.*, Regional Meteorological Centre North Transylvania, Counties Inspectorates for Emergency Situations – Maramureş, Satu Mare and Zalău, Maramures Public Health Authority) and (2) an *academic focus group* with experts in climate hazards assessment, mapping and communication. These two focus groups provided qualitative information and feedbacks on the easiness of understanding and readability of the data which significantly improved the visual display of the maps. The interaction between the outcomes of the two focus groups allowed the authors to select the best way to transpose the climate information to be better interpreted by the potential users.

4. RESULTS AND DISCUSSIONS

Given the specific environmental features of the Baia Mare Depression, the selected extreme weather events occurring during the cold semester of the year (snow cover, glazed frost, fog) stand out due to their increased hazardous potential as compared to the warm semester (heavy rainfall, strong winds). Generally, they are triggered by the negative thermal deviations from the normal state caused by the positioning of the baric centres in relation to the study area, the frequency and intensity of the cooling processes and the speed of air masses. These genetic conditions are amplified or diminished by the characteristics of the active surface.

The *fog* is basically represented by atmospheric suspensions in the form of microscopic droplets which reduce visibility on a horizontal level to less than 1 km. The presence of the fog, no matter in what form, has a negative impact on the transportation means and on the state of health of the population. The highest monthly value for the fog frequency throughout the year is registered during winter (December–January), and the lowest during the summer months (June–August). Fog becomes significantly dangerous on certain sectors of the European roads where, the low visibility along with the higher speeds and increased traffic can result into severe accidents with casualties and property damages (Dragotă *et al.*, 2016).

Whenever fog is associated with different polluting substances, its effect on the environment increases in direct proportion with the polluting factor's concentration level, and the intensity and duration of the parameters characteristic for this meteorological phenomenon amplify or decrease the content of polluting substances existing in the microclimatic space (Bogdan and Frumuşelu 2002).

In polluted areas, *i.e.*, Baia Mare Depression, 5% of the polluting factors present in the free atmosphere can be engulfed by the precipitations fallen on the earth (*wash-out*). When these precipitations come from a dirty cloud with a high concentration of polluting substances (*rain-out*), these substances reach the soil at the same time the precipitations do, at large distances from the emission source. The Baia Mare Depression was one of the three *hotspots* in the country, alongside Copşa Mică and Zlatna, which has been facing atmospheric pollution for the last decades (Farcaş and Croitoru, 2003; ANPM, 2020). Thus, Baia Mare town was a historical hot spot in terms of atmospheric pollution with sulfuric dioxide, sulfuric trioxide, and sulfuric acid from the non-ferrous metallurgy activity (S.C. ROMPLUMB Company) which thrived during the communist period (before 1990). By its position in the north-eastern part of the Baia Mare Depression (Firiza Valley), and because of the reduced dispersion of polluting agents (low air circulation, atmospheric calm and frequent thermal inversions) high levels of pollution with specific toxic substances (heavy metals such as Cd, As, Pb) were registered (Şerban and Bălteanu, 2005). Recently, reducing its capacity and the implementation of new technologies after 1990, the air pollution level in and around Baia Mare had decreased significantly. However, the main environmental threat comes from the heavy metal dust of the tailing

ponds and waste dumps in relation to the former non-ferrous metallurgy activity (Baia Mare, Baia Sprie areas), as well as from the polluting emissions in the atmosphere from the fuel burnings (*e.g.*, steam power plants) and from the road traffic (Fig. 3). All of these are more likely to expose Baia Mare Depression to acid rains, the surrounding heights in the north being an obstacle against the dispersion of the polluting air (Dragotă *et al*., 2013).
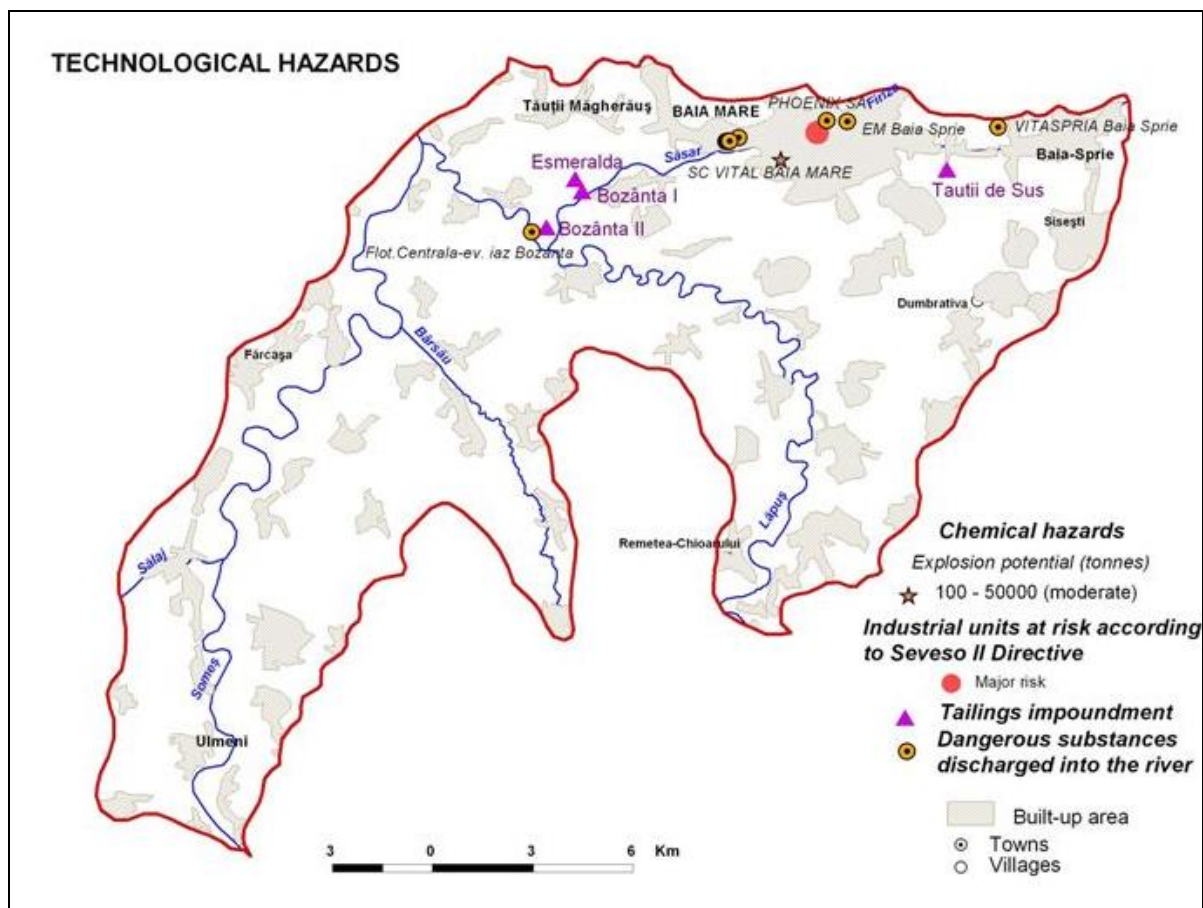

Fig. 3 – Industrial hot-spots in the Baia Mare Depression.

In the absence of rain or other types of precipitation, the atmospheric polluting substances are taken from the atmosphere and deposited on various surfaces (soil, vegetation and buildings). The dry deposition could also contribute to the increasing of the acidity level and together with humid deposition are known as *acid depositions* (Farcaş and Croitoru, 2003). When associated with fog, acid deposition may increase the environmental risk in the topoclimatic conditions of the Baia Mare *heat island*. The increase in road traffic has amplified the contamination sources and in association with the risk meteorological phenomena (*e.g.*, smog, mist, acid depositions) have had a major impact on the environment and on population health.

The areas most exposed to this couple of extreme weather and human-induced phenomena have the largest extent in the northern and north-eastern parts of the study area where the industry (pollution sources) and the foremost settlements are located (Fig. 4), thus posing an increased threat to the natural ecosystems and human health.
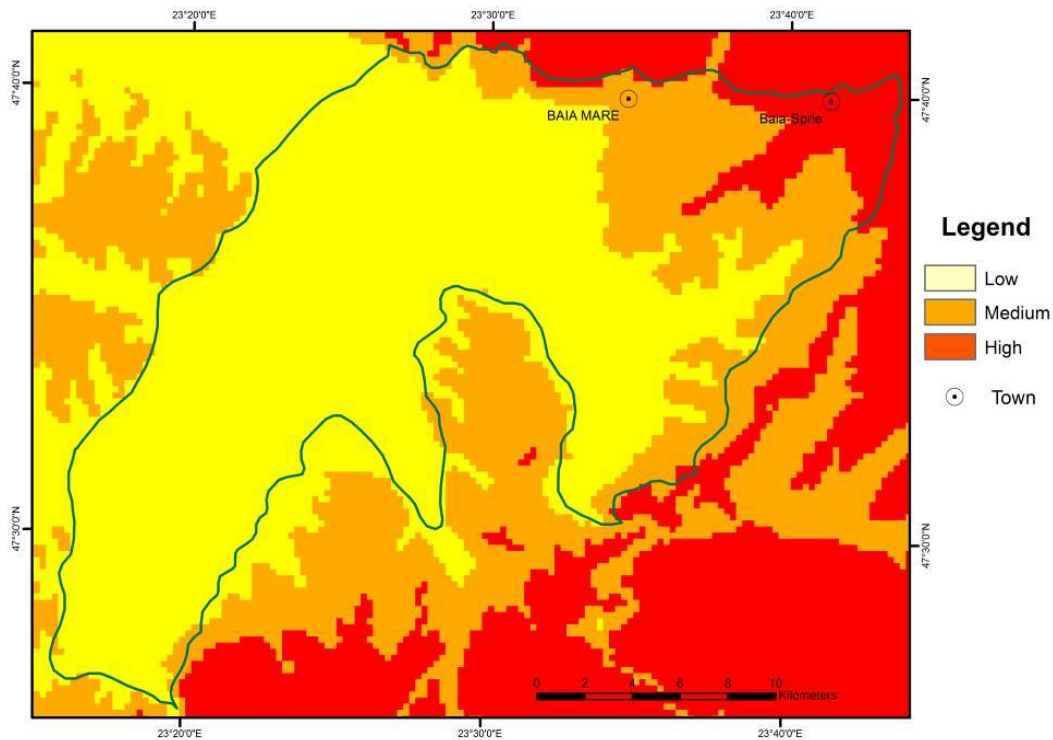
Fig. 4 – The annual frequency of days with fog.

Strong wind is generated by the thermo-baric contrasts between the regions characterized by high-value horizontally gradients and can occur any time of the year. If, during the cold semester of the year, wind is associated with the snow layer and snowfall, during the warm semester of the year it become climate hazard when associated with extreme heat episodes or with heavy rainfall, in particular. Also, it has a key role in changing the dispersion of polluting substances into the atmosphere in relation to the air circulation at the terrestrial surface, which depends on the speed of air masses, as well as on the relief morphology. On the other hand, the atmospheric calm, coupled with the lack of precipitation could lead to the stagnation of polluting substances for long periods of time, usually at low altitudes, in the same regions of their emission. The annual mean value of the wind's dominant frequency is from the western direction (12.5% of cases), followed by the eastern direction (11.9%), and the atmospheric calm is felt in over 50% of cases (51.2%).

The climate hazard aspect induced by the wind is related to its strong intensifications characterized by the sudden shifts in direction and intensities higher than 16 m/s. These can manifest themselves as strong winds and windstorms of a convective origin or associated with the passing of cold air fronts, causing severe damages to buildings, road infrastructure causing restrictions to traffic flow, breaking the aerial cables, toppling the electricity transmission poles, falling over the trees along the transportations means (Dragotă *et al*., 2016) and vegetation, especially in the case of frontal winds (due to their large expansion). At Baia Mare meteorological station, the mean annual number of days with strong winds exceeds 10 days, and the maximum number can exceed, during the warm semester of the year, 40 cases (Sandu *et al*., 2008). The mechanic effect generated by the strong winds is doubled by the amount of polluting substances dispersed into the atmosphere. The obstruction of the depression to the north by the Igniş Massif determines an annual (%) prevalence of air masses coming from western and north-western (19%), as well as eastern and south-eastern (19.8%) directions. This leads to an increased effect of the wind activity in the northern and north-eastern parts of the

depression in relation to potential transportation of pollutant substances, thus enhancing its environmental damaging effects. On the other hand, the specific topography of Baia Mare depression determines a high frequency of the atmospheric calm (51.2%) which enables the stagnation of pollutants in the lower atmosphere. This situation also applies to the most urbanised areas located in the northern and north-eastern parts where the main pollutant sources are located.

The hazardous character of the **heavy rainfall** depends on its specific parameters (intensity, length, quantity), as well as on the particular features of the active surface: lithology, presence/absence of the vegetation cover, declivity, occurrence period (*e.g.* after long periods of drought when the soil is extremely dry and has a low cohesion; after a rainy period; before or after snowmelt when soil is over-moist), and on the role Carpathian Mountains play against the humid air advections. The highly active dynamics of the humid tropical air or of the polar maritime air over the Romanian territory, as well as the unequal heating of the terrestrial surface leads, during summer leads to heavy rainfalls triggering floods. The hilly regions, wherein the study area falls into, the occurrence of floods is conditioned by a certain amount of rainfall water (Milea et. al. 1974): in the case of dry soil, an amount of water of 30 l/m^2 or more is needed within a 24-hour time span; in the case of moist or humid soil, an amount of water between 10 and 20 l/m^2 or more is needed within a 24-hour time span.

In the Baia Mare Depression, the maximum monthly pluviometric value is registered in June when on a multi-annual scale reaches 103.5 mm. The maximum precipitation amounts accumulated in short intervals (24 h, 48 h or 72 h) are mostly owed to the torrential character of the summer rains in terms of high intensities and relatively small durations, having significant effects on the environment by triggering erosional processes on the mountain slopes (*e.g.*, floods, landslides), as well as in riverbeds (lateral erosion). The pluvial intensity reaches values that rank among the highest in Romania: the mean intensity of between 0.03 and 0.04 mm/minute, the maximum mean intensity of 0.20 and 0.30 mm/minute and the average of the highest 5 pluvial intensity ranging between 3 and 4 mm/minute (Dragotă *et al.*, 2013). By way of the floods they cause, exceeding rainfall affects the crops, the economic infrastructure (*e.g.*, roads, bridges, railroads, electric energy transportation networks, sewage system, water pipes, gas pipes), and the houses, having a direct and incidental influence on people's lives. The frequency of days with rain showers pinpoints high and medium hazard in the northern, north-eastern and eastern parts of the analysed territory and low in the central, western and southern parts (Fig. 5). Once more, the areas most exposed to this hazardous phenomenon overlap the areas where human communities are more developed.

The **glazed frost** corresponds to a crystal ice deposit with a very fine structure that generally comes from the freezing of overcooled water drops out of fog or clouds during very cold weather and mild winds. The wind favours the deposition of white frost leading to ice deposits of significant sizes and shapes influenced by its direction. In the study area, the mean annual number of days with glazed frost is up to 4 and a maximum number reaches or exceeds 10 days per year, posing a significant threat to the environment and human health. It has a negative impact on all transport means primarily due to the significant decrease of friction coefficient on ice layer that hinders transportation and increases the risk of accidents. In addition, ice accumulations can cause breaks in the canopy of trees (Dragotă *et al.*, 2016). The areas most affected by glazed frost are located in the central, south-western and western parts of the Baia Mare Depression, generally overlapping the roads that connect the city of Baia Mare with other important cities outside the analysed area: Satu Mare to the north-west, Zalău to the south-west or Cluj-Napoca to the south (Fig. 6).
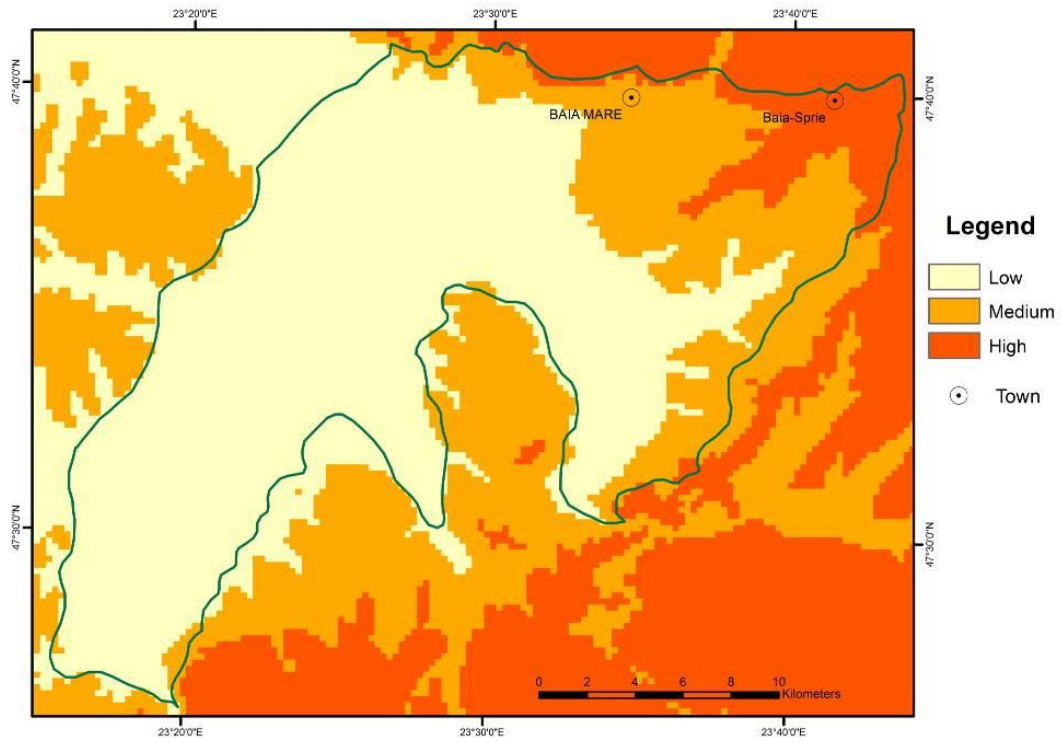
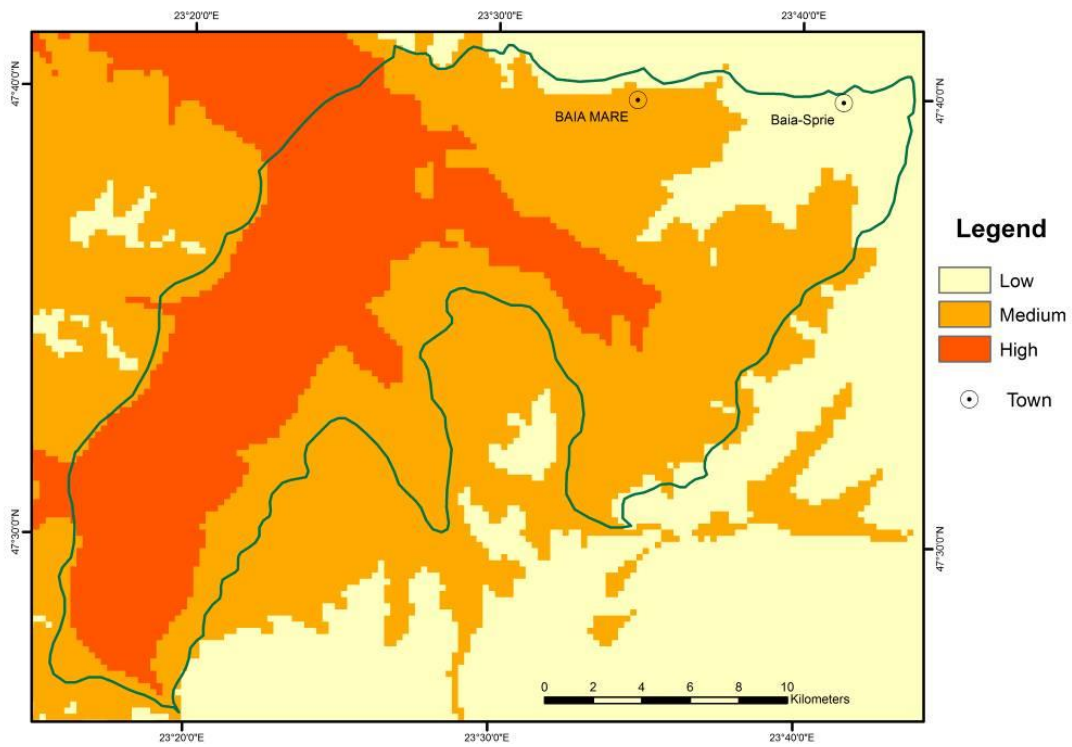Fig. 5 – The annual frequency of days with heavy rainfall.

Fig. 6 – The annual frequency of days with glazed frost.

The ***snow cover*** is considered a dangerous winter phenomenon, and it occurs in Baia Mare Depression almost every year. It is characterized by thickness, uniformity, structure and density. On a multi-annual mean value, the first day with snow layer usually occurs in the second third of November in the eastern and north-eastern sectors, expanding up on the slopes of Igniş and Gutâi Mountains, and in the western sector in the last third of November. The last day with snow cover is usually registered in the second third of March for the western sector, while in the eastern and northern sectors they last longer, until the end of March. Thus, a mean duration of a stable snow layer ranges from 50 to 100 days in the western side of the depression to 150 days in the rest of the area. The maximum thickness of the snow layer has reached 98 cm, and under the action of the wind, the layer is not levelled, and the snow is blasted over distances and piled up in mounds.

Generally, the snow cover becomes climate hazard when its thickness is significantly high and the wind has elevated speeds (Dragotă *et al.*, 2016); mounds of snow are causing damages both related to its presence and its absence. Thus, under the influence of the atmospheric calm or of the wind with speeds lower than 2 m/s, as well as under the influence of the active surface's particularities, significant snow depositions are favoured. On the other hand, in particular synoptic conditions and in association with wind speeds exceeding 15 m/s, the snow cover could enhance its hazardous character turning into blizzard. That being so, blizzards-built snowbanks on all the traffic routes that are perpendicular on the wind direction, especially on the European and national roads that cross Baia Mare Depression. When the blizzards become violent, and the mean snow layer thickness goes over 25 cm, significant damages and environmental unbalances might result (Fig. 7).
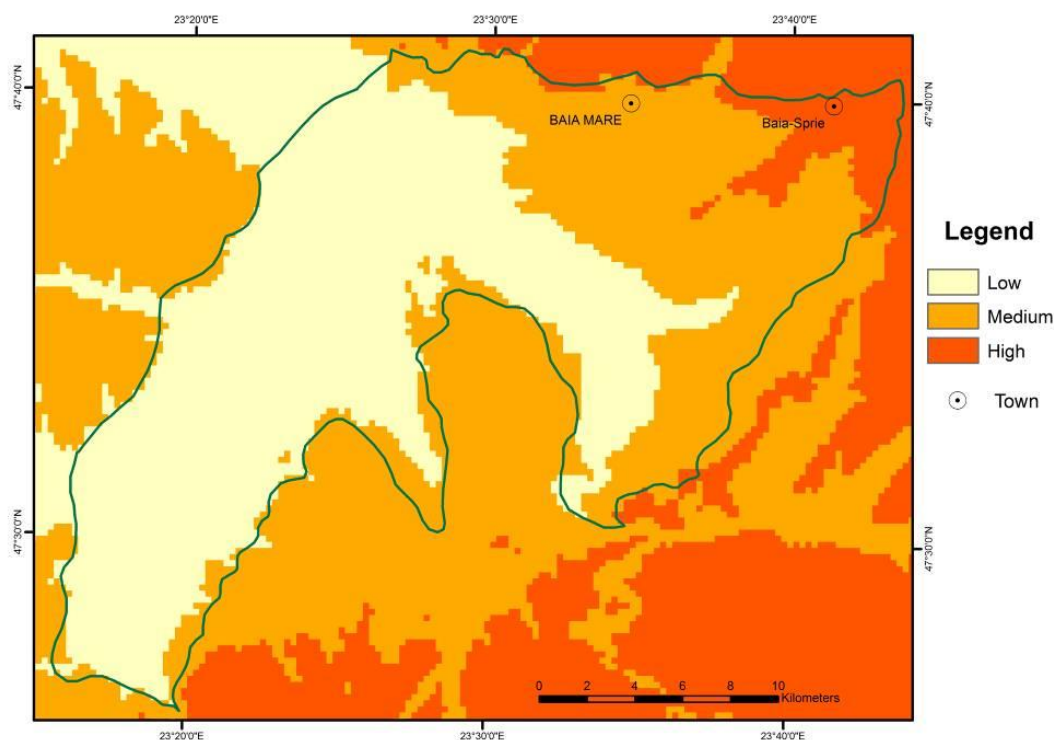

Fig. 7 – The annual frequency of days with snow cover.

During early springs, sudden snow melts can trigger floods, as well as river blocking caused by ice breakup having major impact on river transportation. Under partial or total absence of the snow layer, the frostiness is favoured at the soil level leading to severe damages to vegetation and crops

(especially during fall). The northern, north-eastern and eastern parts of the Baia Mare Depression are highly exposed to this climate hazard putting at risk the main settlements, as well as the roads connecting them.

The final ***multi-hazard climate map*** indicates that 88.8 % of the study area is highly and medium exposed to the selected extreme weather events. Geographically, the exposed territory overlies a large depressionary area which favours the persistence and even intensification of some weather phenomena, *i.e.*, fog, due to the topography and the mixture with different pollutant substances. The lowest exposure (11.2 %) overlaps the north-eastern extremity (Baia Sprie area), where the proximity to the mountain areas provides shelter to the occurrence of most of the extreme phenomena (Fig. 8).

An extension of the current study is a cross-correlation between the multi-hazard climate map and the local conditions to quantify the potential risk which might involve population or infrastructure. At local administrative units' level, the localities with high exposure to the selected extreme weather phenomena (with over 90% of their surface) are Ardusat, Ariniş, Farcaşa, Salsig, Satulung etc. These localities are highly exposed to at least three of the four analysed phenomena (primarily snow cover, glazed frost and heavy rainfall). Medium exposure is depicted by some localities (*e.g.*, Recea, Sisteşti, Salsig, Satulung) with relatively low to moderate exposure to all considered climate hazards.
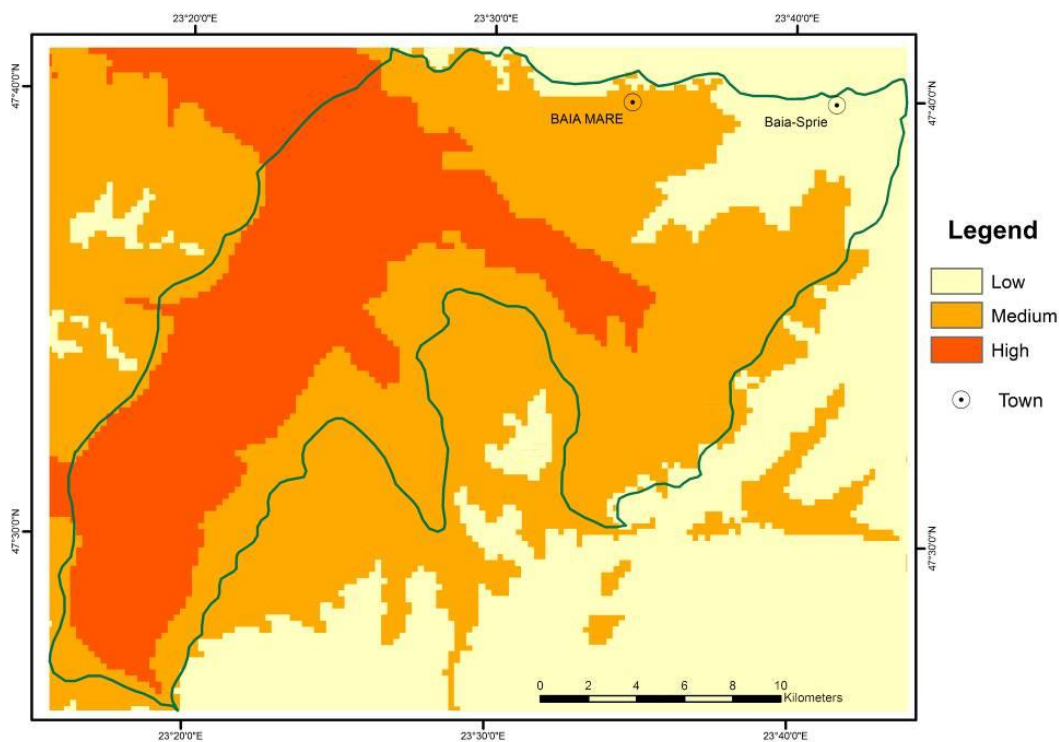

Fig. 8 – Climate hazards in Baia Mare Depression.

A reduced number of localities (*e.g.*, Baia Sprie, Copalnic-Mănăştur, Siseşti) have low exposure to this group of dangerous weather phenomena, generally given by the lowest values recorded to all extreme weather events (Fig. 9).

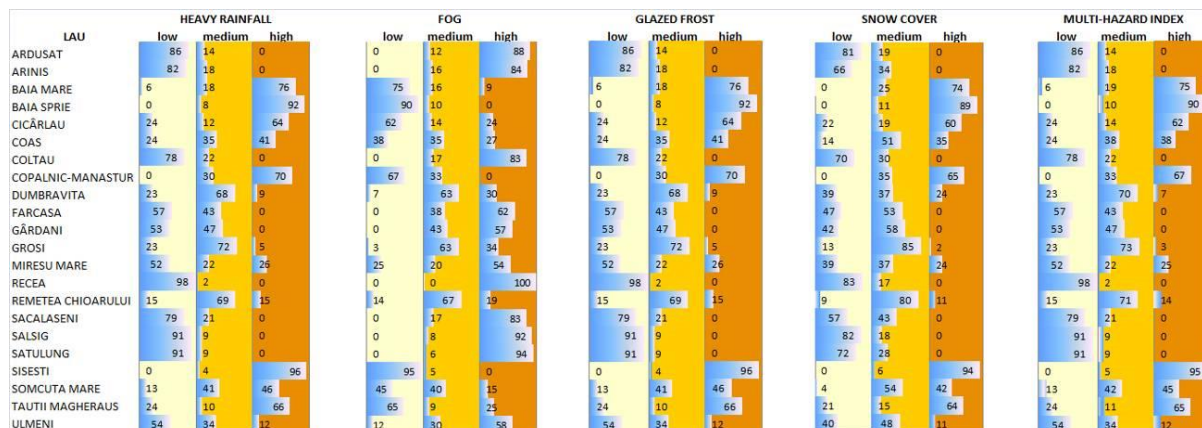| LAU	HEAVY RAINFALL			FOG			GLAZED FROST			SNOW COVER			MULTI-HAZARD INDEX		
	low	medium	high	low	medium	high	low	medium	high	low	medium	high	low	medium	high
ARDUSAT	86	14	0	0	12	88	86	14	0	81	19	0	86	14	0
ARINIS	82	18	0	0	16	84	82	18	0	66	34	0	82	18	0
BAIA MARE	6	18	76	75	16	9	6	18	76	0	25	74	6	19	75
BAIA SPRIE	0	8	92	90	10	0	0	8	92	0	11	89	0	10	90
CICĂRLAU	24	12	64	62	14	24	24	12	64	22	19	60	24	14	62
COAS	24	35	41	38	35	27	24	35	41	14	51	35	24	38	38
COLTAU	78	22	0	0	17	83	78	22	0	70	30	0	78	22	0
COPALNIC-MANASTUR	0	30	70	67	33	0	0	30	70	0	35	65	0	33	67
DUMBRAVITA	23	68	9	7	63	30	23	68	9	39	37	24	23	70	7
FARCASA	57	43	0	0	38	62	57	43	0	47	43	0	57	43	0
GÂRDANI	53	47	0	0	43	57	53	47	0	42	58	0	53	47	0
GROSI	23	72	5	3	63	34	23	72	5	13	85	2	23	73	3
MIRESU MARE	52	22	26	25	20		52	22	26	39	37	24	52	22	25
RECEA	98	2	0	0	0	100	98	2	0	83	17	0	98	2	0
REMETEA CHIOARULUI	15	69	15	14	67	19	15	69	15	9	80	11	15	71	14
SACALASENI	79	21	0	0	17	83	79	21	0	57	43	0	79	21	0
SALSIG	91	9	0	0	8	92	91	9	0	82	18	0	91	9	0
SATULUNG	91	9	0	0	6	94	91	9	0	72	28	0	91	9	0
SISESTI	0	4	96	95	5	0	0	4	96	0	6	94	0	5	95
SOMCUTA MARE	13	41	46	45	40	15	13	41	46	4	54	42	13	42	45
TAUTII MAGHERAUS	24	10	66	65	9	25	24	10	66	21	15	64	24	11	65
ULMENI	54	34	12	12	30	58	54	34	12	40	48	11	54	34	12

Fig. 9 – The share of climate hazards & multi-hazard classes at LAU level in Baia Mare Depression.

Following the focus groups meetings and interactions, the mapping of the selected extreme weather events was constantly improved so as the scientific information to be better visualised and understood by the potential end users. As a result, the main purpose of the climate map is to provide a simple tool to identify and prioritise areas ("hotspots") where extreme weather-related impacts are assumed to be the greatest. The resulted product becomes a valuable climate service to be further used for adaptation interventions by different stakeholders in relation to the specific needs of different sectors of local importance (*e.g.*, tourism, agriculture, transport, health). In the study area, two sectors stand out: transport and health which can be analysed through assessing the interaction between the hazard classes and infrastructure (road, rail) and population (Fig. 10).
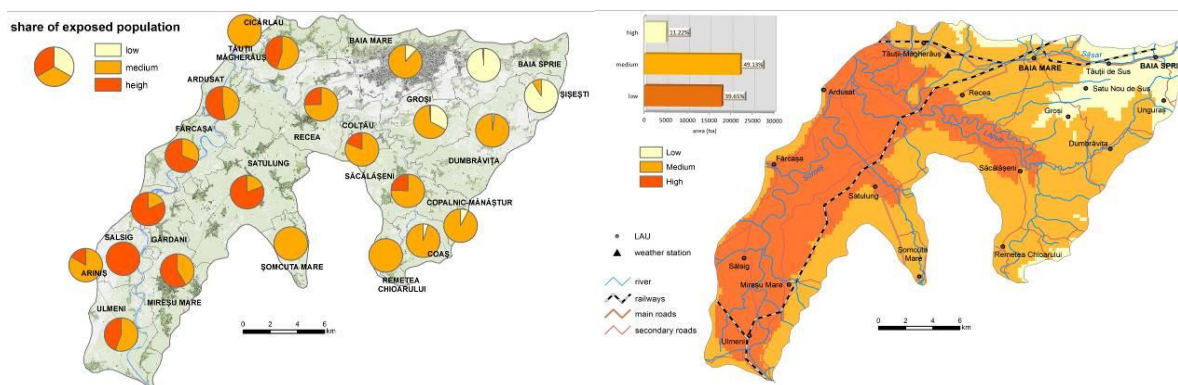

Fig. 10 – Communicating handy climate hazards to stakeholders. Share of exposed population (left) and distribution of exposed transport infrastructure (right)

Depending on the addressed extreme weather events, the climate hazard map turns into a useful tool for different categories of stakeholders and decision-makers: farmers, local/regional authorities, Emergency Inspectorates etc. However, to better communicate the climate information, the interaction with the potential end users (*i.e.*, stakeholders) is crucial since it provides the realistic feedback which allows scholars to design and produce useful final scientific products.

5. CONCLUSIONS

In the Baia Mare Depression out of the assemblage of the hazardous climate phenomena one could identify a distribution of "hotspot" areas according to the distribution of the main genetic factors: the altitude (from the surrounding mountain and hilly slopes), and air circulation (from west to east). In terms of intensity, frequency and duration, the extreme climate phenomena occurred during the cold semester of the year (snow cover, glazed frost) have an increased negative impact upon the environment then the ones unfolding during the warm semester (heavy rainfall) or throughout the year (fog). This is largely due to the general display of the relief, as well as to the dominant air circulation, favouring a sheltered climate for the cold, polar and arctic air advections.

In preparing the tailored scientific (*i.e.*, climate) information, the role of the GIS techniques is particularly important since it enables the creation of an interactive database, easily updatable and accessible to different users involved in disaster mitigation and management, as well as in the elaboration of the sustainable development strategies (Bălteanu and Șerban, 2004). These data can be further transposed into GIS-based climate hazard maps which are visually comprehensive communication tools in representing, at different scales, the spatial vulnerability to a single climatic phenomenon or to an association of other severe climatic events. These maps might also rank the natural hazards in a certain area and monitor the state of the environment to diminish and even avoid the damaging consequences resulting from their occurrence and in further supporting adaptation strategies and increase resilience.

Climate hazards mapping is an important component of the climate change mitigation and adaptation processes in terms of identifying areas prone to different extreme events in order to further design and apply tailored strategies at different spatial scales. Climate hazards maps, as comprehensible visual tools, have become increasingly useful in the communication process between academia and different categories of potential beneficiaries. On that account, they can be use not only to spatially identify areas exposed to different extreme events, but to understand the environmental, social and economic impacts and perform in-depth quantitative investigations on the potentially affected population, goods, assets and ecosystems through vulnerability and risk assessments. They come as an addition to the landslides and floods hazard maps, compulsory by legislation to be adopted by each municipality, offering them a more complex multi-hazard view on the natural dangerous phenomena.

Compared to an extended literature on single risks (Iglesias *et al*., 2009; Yusuf and Francisco 2009; Preston *et al*., 2011), integrating multi-hazards into a complex index (based on classifications and ranking) is a more comprehensive approach since it takes into consideration the possible interactions among them which often exacerbate their effects (Marzocchi *et al*., 2009). The combination of multiple extreme weather phenomena relied on both objective (with the highest impact on the study area) and subjective (expert judgement on ranking or assigning the weight of the selected phenomena) approaches. Thus, spatio-temporal information layers to be tailored in order to identify the concurrence of multiple hazards become necessary, especially in the context of Early Warning Systems (Vitolo *et al*., 2019). In line with the above, the current work proposes a simple methodology to integrate several climate extreme phenomena (layers) with impacts on a broader spectrum of sectors (*e.g.*, agriculture, health, infrastructure) and visually display (map) them in order to delineate areas prone to their effects. In this way, the overall multi-hazard exposure of the study area has been quantified in a more accurate manner, to identify areas that are likely to be most exposed ("hotspots"). The resulted multi-hazard information (layers and final map) could be valuable in disaster risk reduction and emergency response management to develop or to improve (according to the case) evidence-based decision making (Vitolo *et al*., 2019) at different spatial scales. Thus, cross-examining the spatial response of local administrative units, inquiring the share of exposed population or infrastructure were among some of the practical applications proposed by the authors that might be used to prepare handy products (maps, graphs) able to communicate climate hazards to stakeholders. They better illustrate the relationships between the spatial distribution of the multi-hazards and the environmental

components, to be easily understood by the potential end users and to improve the knowledge about and response to change-related impacts.

Uncertainties. Even though it uses real data to integrate the key extreme weather events the area is exposed to, the proposed methodology has, however, several objective and subjective uncertainties. The objective uncertainties refer to the data limitations in terms of spatial and temporal resolution. It applies to the data used for the elaboration of the multi-hazard map (*e.g.*, climate data, Digital Elevation Model) and in the cross-correlation with the risk components (*e.g.*, statistical socio-economic data) to obtain the quantitative evaluation of hazard impacts. On the other hand, the subjective uncertainties reside in the use of expert judgement for the selection of extreme weather events and ranking them according to importance (weight). However, a qualitative approach to hazard, impact, and risk assessment is often preferred due to data limitations (Papathoma-Köhle *et al.*, 2016). The overall uncertainties of the methodology were generally reduced by the stakeholder analysis which provided positive feedback, supported the overall scope of our research, *i.e.*, communicating handy multi-hazards climatic products to end users. Thus, stakeholder involvement throughout the process of building up the multi-hazard assessment and mapping has been recognized to improve the effectiveness of the final products.

Regardless of some data limitations, the output of the current study is expected to be useful to different stakeholders (*e.g.*, policymakers, local authorities, NGOs) and academics in better attracting financial resources towards developing mitigation and adaptation measures. In order to deliver a more complete picture of the potential risks an area is subject to, additional information on exposure and vulnerability would be required to quantify and spatialize the expected response of the risk components (*e.g.*, population, infrastructure). Moreover, visualising scientific data helps improve the access to transparent, updated and easy-to-read scientific information that can be used to improve social and economic progress at regional and local levels. Also, the possibility to regularly updating the resulted climate products would be another plus of the methodology, given the increasing variability of temporal and spatial patterns of extremes, as well as a in the magnitude and frequency of climate hazards (Forzieri *et al.*, 2016). The current study proposes a simple methodology to generate climate hazard maps based on integrating multi-hazards information layers that can be easily replicated to different regions and adapted to local scale assessments. Such approach would contribute to one of UN Sendai Framework for Disaster Risk Reduction 2015–2030 (Sendai Framework) key targets, *i.e.*, increasing the availability and access to multi-hazard early warning systems and disaster risk information and assessments to people by 2030[4].

REFERENCES

Adger, W. N. (2010), *Social capital, collective action, and adaptation to climate change*. In Der klimawandel. VS Verlag für Sozialwissenschaften, pp. 327–345.

Adger, W. N., Arnell, N. W., Tompkins, E. L. (2005), *Successful adaptation to climate change across scales*. Global environmental change, **15**, *2*, pp. 77–86.

Amarnath, G., Alahacoon, N., Smakhtin, V., Aggarwal, P. (2017), *Mapping multiple climate-related hazards in South Asia,* International Water Management Institute (IWMI), Research Report 170, 41 p. doi: 10.5337/2017.207.

ANPM (2020), *Raport privind starea mediului în România, anul 2019*, Agenția Națională pentru Protecția Mediului, Ministerul Mediului, București.

Badea L., Niculescu, Gh., Sandu, M., Roată, S., Micu, M., Sima, M., Jurchescu, M. (2008), *Unitățile de relief ale României III. Dealurile pericarpatice. Dealurile Crișanei și Banatului. Subcarpații*. Editura Academiei Române, București. 143 p.

---

[4] https://sustainabledevelopment.un.org/frameworks/sendaiframework

Balogun, A. L., Marks, D., Sharma, R., Shekhar, H., Balmes, C., Maheng, D., Adnan A., Salehi, P. (2020), *Assessing the potentials of digitalization as a tool for climate change adaptation and sustainable development in urban centres,* Sustainable Cities and Society, **53**, 101888.

Bălteanu D. (2016), *The Relief. Pericarpahian Regions in Romania*, in vol. Romania. Spaţiu şi Societate (Bălteanu D., Dumitraşcu M., Geacu S., Mitrică B., Sima M. Ed..), Publishing House of the Romanian Academy, pp. 82–101.

Bălteanu, D., Badea, L., Buza, M., Niculescu, Gh., Popescu, C., Dumitraşcu, M., (Eds.), (2006), *Romania. Space, Society, Environment*. The Publishing House of the Romanian Academy, Bucharest. 384 p.

Bălteanu, D., Şerban, M. (2004), *Natural and technological hazards in Romania*. In: Environmental Change and Sustainable Development, Proceedings of the second Romanian – Turkish Workshop of Geography, Bucharest, Romania/June 15–22, 2003, Editura Universitară, Bucharest, pp. 155–164.

Bambrick, H. J., Capon, A. G., Barnett, G. B., Beaty, R. M., Burton, A. J. (2011), *Climate change and health in the urban environment: adaptation opportunities in Australian cities,* Asia Pacific Journal of Public Health, **23**(2_suppl), pp. 67S–79S.

Bogdan, O. Niculescu, E. (1999), *Riscurile climatice din România*. Institutul de Geografie, Bucureşti. 279 p.

Bogdan, O., Frumuşelu, D. (Eds.) (2002), *Romania. The Environment and the Electric Transportation Network. Geographical Atlas*. The Publishing House of the Romanian Academy, Bucharest, 52 p.

Bogdan, O., Marinică, I. (2007), *Hazarde meteo-climatice din zona temperată. Factori genetici şi vulnerabilitate cu aplicaţii la România*. Editura Lucian Blaga, Sibiu. 422 p.

Brooks N, Neil Adger W, Mick Kelly P (2005), *The determinants of vulnerability and adaptive capacity at the national level and the implications for adaptation*. Global Environmental Change Part A, **15**, 2, pp. 151–163.

Bryant E. A. (1991), *Natural Hazards*. Cambridge University Press. 294 p.

Chen, F., Shirazi, Z., Wang, L. (2021), *Building scientific capacity in disaster risk reduction for sustainable development*, Cultures of Science, pp. 1–15.

Croitoru A., Moldovan F., (2005), *Vulnerability of Romanian territory to climatic hazards,* Analele Universităţii de Vest din Timişoara, Seria Geografie, **XV**, pp. 55–64.

Cueva-Luna, T. E., Few, R., Mercado, A., Graizbord, B. (2008), *Climatic hazards, health risk and response. Case study 3: Chihuahua, Mexico*. Research report, University of East Anglia, Norwich, UK, 59 p.

De Sherbinin, A. (2014), *Climate change hotspots mapping: what have we learned?*. Climatic Change, **123**, *1*, pp. 23–37.

De Sherbinin, A., Bukvic, A., Rohat, G., Gall, M., McCusker, B., Preston, B., Apotsos A., Zhang, S. (2019), *Climate vulnerability mapping: A systematic review and future prospects,* Wiley Interdisciplinary Reviews: Climate Change, **10**, *5*, e600.

De Sherbinin, A., Schiller, A., Pulsipher, A. (2007), *The vulnerability of global cities to climate hazards*. Environment and Urbanization, **19**, pp. 39–64.

Dragotă Carmen, Grigorescu Ines, Mihaela Sima, Kucsicsa Gh., Mihalache S. (2013), *The vulnerability of the Baia Mare Urban System (Romania) to extreme climate phenomena during the warm semester of the year*, Simpozionul "Air and Water Components of the Environment", Air and Water Components of the Environment, Presa Universitară Clujeană, Cluj-Napoca, pp. 71–78.

Dragotă Carmen-Sofia, Grigorescu Ines, Kucsicsa Gheorghe, Dumitraşcu Monica (2016), *Multiple climate hazards with impact on transport systems in Dolj Country, Romania*, Air and Water Components of the Environment, Universitară Clujeană, Cluj-Napoca, pp. 28–33.

Dragotă Carmen-Sofia, Grigorescu Ines, Nikolova Maryiana, Kucsicsa Gheorghe (2013), *Climatic hazards, in Hazard assessment and mitigation in the Danube Floodplain (Calafat-Vidin – Turnu Măgurele-Nikopol sector)*, Technical Guide, Edit. Universitaria, Craiova, pp. 127–134.

Dragotă, C. (2006), *Precipitaţiile excedentare din România*. Editura Academiei Române, Bucureşti. 174 p.

Dragotă, C., Grigorescu, I., Dumitraşcu, M., Dumitraşcu C., (2009a), *Regionalization of the main climatic hazard phenomena in the South-West Development Region*. Romania. In: Proceedings of the 11th International Conference on Environmental Science and Technology, 3–5 September 2009, Chania, Crete, pp. 206–213.

Dragotă, C., Grigorescu, I., Sima, M. (2009b), *The main climatic hazard phenomena and their environmental impact in the Râmnicu Vâlcea – Ocnele Mari Depression*. Environment & Progress, **13**, pp. 131–140.

Dumitraşcu Monica, Carmen Dragotă, Grigorescu Ines, Kuscicsa Gheorghe, Dumitrică Cristina (2016), *Extreme weather phenomena with impact on agriculture in Dolj Country, Romania*, Proceedings of the 16th International Multidisciplinary Scientific GeoConference SGEM, Air Pollution and Climate Change, Albena, Bulgaria, **II**, pp. 381–388.

EEA – European Environment Agency (2010), Mapping the impacts of natural hazards and technological accidents in Europe: An overview of the last decade. Report Number 13/2010.

EEA – European Environment Agency (2017), *Climate change adaptation and disaster risk reduction in Europe. Enhancing coherence of the knowledge base, policies and practices*, Report number 15, European Environment Agency.

EEA – European Environment Agency (2021), *Economic losses from climate-related extremes in Europe*, https://www.eea.europa.eu/data-and-maps/indicators/direct-losses-from-weather-disasters-4/assessment.

Fărcaş I., Croitoru Adina-Eliza (2003): Poluarea atmosferei şi schimbările climatice, cauze, efecte, măsuri de protecţie. Editura Casa Cărţii de Ştiinţă, Cluj Napoca. 110 p.

Felton, A., Gustafsson, L., Roberge, J. M., Ranius, T., Hjältén, J., Rudolphic, J., Lindbladh M., Weslien J., Rist L., Brunet J., Felton, A. M. (2016): How climate change adaptation and mitigation strategies can threaten or enhance the biodiversity of production forests: Insights from Sweden. Biological Conservation, 194, 11–20.

Fischer Em, Schär C (2010): Consistent geographical patterns of changes in high-impact European heatwaves. Nat Geosci 3:398–403. doi: 10.1038/ngeo866.

Forzieri, G., Feyen, L., Russo, S., Vousdoukas, M., Alfieri, L., Outten, S., Migliavacca M., Bianchi A., Rojas R., Cid, A. (2016), *Multi-hazard assessment in Europe under climate change*. Climatic Change, **137**, *1–2*, pp. 105–119.

Füssel H-M, Klein R (2006), *Climate Change Vulnerability Assessments: An Evolution of Conceptual Thinking*. Climatic Change, **75**, *3*, pp. 301–329.

Füssel, H. (2009), *Review and quantitative analysis of indices of climate change exposure, adaptive capacity, sensitivity, and impacts,* Background note to the world development report 2010 on development and climate change, Washington, DC: World Bank.

Gemenne, F., Barnett, J., Adger, W.N., Dabelko, G.D. (2014), *Climate and security: Evidence, emerging risks, and a new agenda*. Climatic Change, **123**, *1*, pp. 1–9.

Grigorescu Ines, Dragotă Carmen, Kucsicsa Gheorghe, Nikolova Mariyana (2013), *Joint assessment of climate hazards in the Danube Floodplain: the Calafat-Vidin – Turnu Măgurele-Nikopole Sector. A preliminary approach*, The 13th International Multidisciplinary Scientific GeoConference SGEM, 16–22 iunie, 2013, Albena, Bulgaria, Energy and Clean Technologies Conference Proceedings, Section Air Pollution and Climate Change, pp. 689–695.

Gwilliam, J., Fedeski, M., Lindley, S., Theuray, N., Handley, J. (2006), *Methods for assessing risk from climate hazards in urban areas*. In: Proceedings of the Institution of Civil Engineers, Municipal Engineer 159, Issue ME4: 245–255.

Helmer, M., Hilhorst, D. (2006), *Natural Disasters and Climate Change*. Disasters, **30**, *1*, pp. 1–4.

Iglesias, A., Moneo, M., Quiroga, S. (2009), *Methods for evaluating social vulnerability to drought*. In Coping with Drought Risk in Agriculture and Water Supply Systems. Springer Netherlands pp. 153–159.

IPCC (2007), *Climate change 2007: The physical science basis contribution of working group to the 4th assessment report of the Intergovernmental Panel on Climate Change*. Cambridge University Press, Cambridge, UK and NY. 996 p.

IPCC (2014), *Climate Change 2014 – Impacts, Adaptation and Vulnerability: Regional Aspects*. Cambridge University Press.

Kappes Ms, Keiler M, Von Elverfeldt K, Glade T. (2012), *Challenges of analyzing multi-hazard risk: a review*. Nat Hazards, **64**, pp. 1925–1958. doi: 10.1007/s11069-012-0294-2.

Kim, C. J., Park, M. J., Lee, J. H. (2014), *Analysis of climate change impacts on the spatial and frequency patterns of drought using a potential drought hazard mapping approach*. International Journal of Climatology, **34,** *1*, pp. 61–80.

Kreibich H, Van Den Bergh Jcjm, Bouwer Lm (2014), *Costing natural hazards*. Nat. Clim. Chang **4**, pp. 303–306. doi: 10.1038/nclimate2182.

Lehner B., Döll P, Alcamo J. (2006), *Estimating the impact of Global change on flood and drought risks in Europe: A Continental, Integrated analysis*. Clim Chang **75**, pp. 273–299. doi: 10.1007/s10584-006-6338-4.

Leis, J. L., Kienberger, S. (2020), *Climate Risk and Vulnerability Assessment of Floods in Austria: Mapping Homogenous Regions, Hotspots and Typologies*. Sustainability, **12**, *16*, 6458.

Lesk, C., Rowhani, P., Ramankutty, N. (2016). *Influence of extreme weather disasters on global crop production*. Nature, **529**, pp. 84–87.

Lung T., Lavalle C., Hiederer R. (2013), *A multi-hazard regional level impact assessment for Europe combining indicators of climatic and non-climatic change*. Glob Environ Change 23:522–536. doi: 10.1016/j.gloenvcha.2012.11.009.

Mabon, L. (2020), *Making climate information services accessible to communities: What can we learn from environmental risk communication research?*. Urban climate, **31**, 100537.

Marinică, I. (2006), *Fenomene climatice de risc în Oltenia*. Editura Autograf MJM, Craiova. 385 p.

Marzocchi, W., Mastellone, M., Di Ruocco, A., Novelli, P., Romeo, E., Gasparini, P. (2009), *Principles of multi-risk assessment: interactions amongst natural and man-induced risks*. Directorate-General for Research, Environment Directorate, European Commission http://publications.europa.eu/resource/cellar/22eb788f-5d0a-496a-92d4-4759b0b57fde.0001.03/DOC_2.

Mcbean Gordon, Rodgers Caroline (2010), *Climate hazards and disasters: the need for capacity building*, Wiley Interdisciplinary Reviews: Climate Change, **1**, *6*, pp. 871–884, DOI: 10.1002/wcc.77.

Milea Elena, Bacinski D, Doneau A. (1974), *Studiu meteorologic al apelor mari din 4–12 octombrie 1972 în sudul ţării*. Meteorology and Hidrology, **1**, pp. 41–55.

Mills A., Huyser O., Van den Pol O., Zoeller K., Snyman D., Tye N., Mcclure A. (2016), *Revenue-generating opportunities through tailored weather information products*, UNDP Market Assessment, 151 p. https://www.adaptation-undp.org/sites/default/files/resources/revenue-generating-opportunities-for-tailored-weather-information-productions-undp-june-2-2016_0.pdf.

Newman, J. P., Maier, H. R., Riddell, G. A., Zecchin, A. C., Daniell, J. E., Schaefer, A. M., ... & Newland, C. P. (2017). *Review of literature on decision support systems for natural hazard risk reduction: Current status and future research directions*. Environmental Modelling & Software, **96**, pp. 378–409.

Nikas, A., Doukas, H., Lieu, J., Tinoco, R. A., Charisopoulos, V., van der Gaast, W. (2017), *Managing stakeholder knowledge for the evaluation of innovation systems in the face of climate change*, Journal of Knowledge Management, **21**, *5*, pp. 1013–1034.

Nkoana, E. M., Verbruggen, A., Hugé, J. (2018), *Climate change adaptation tools at the community level: An integrated literature review*, Sustainability, **10**, *3*, 796.

OECD (2014), *Cities and Climate Change. Policy perspectives*, OECD Publishing, Paris, https://www.oecd.org/env/cc/Cities-and-climate-change-2014-Policy-Perspectives-Final-web.pdf

Outten SD, Esau I (2013), *Extreme winds over Europe in the ENSEMBLES regional climate models*. Atmos Chem Phys, **13**, pp. 5163–5172. doi: 10.5194/acp-13-5163-2013.

Papathoma-Köhle, M., Promper, C., Glade, T. (2016), *A common methodology for risk assessment and mapping of climate change related hazards – implications for climate change adaptation policies*. Climate, **4(1)**, *8*, pp. 1–23.

Peduzzi, P., H. Dao, Herold, C. (2005), *Mapping Disastrous Natural Hazards Using Global Datasets*. Natural Hazards, **35**, *2*, pp. 265–289.

Posea Gr., Badea L. (1984), *România – unitățile de relief, hartă, scara 1:750000*. Editura Ştiinţifică şi Enciclopedică, Bucureşti.

Preston, B. L., Yuen, E. J., Westaway, R. M. (2011), *Putting vulnerability to climate change on the map: a review of approaches, benefits, and risks*. Sustainability Science, **6**, *2*, pp. 177–202.

Reckien, D., Flacke, J., Dawson, R. J., Heidrich, O., Olazabal, M., Foley, A., Hamann J. J.-P. Orru H., Salvia M., De Gregorio Hurtado S., Geneletti, D. Pietrapertosa F. (2014), *Climate change response in Europe: what's the reality? Analysis of adaptation and mitigation plans from 200 urban areas in 11 countries*. Climatic change, **122**, *1–2*, pp. 331–340.

Russo S., Sillmann J., Fischer Em. (2015), *Top ten European heatwaves since 1950 and their occurrence in the coming decades*. Environ Res Lett, **10**, 124003. doi: 10.1088/1748-9326/10/12/124003.

Sandu, I., Pescaru, V., I., Poiană, I., Geicu, A., Cândea, I., Ţâştea, D., (Eds.) (2008), *Clima României*. Editura Academiei Române, Bucureşti. 365 p.

Savić, S., Marković, V., Šećerov, I., Pavić, D., Arsenović, D., Milošević, D., Dolinaj D., Nagy I, Pantelić, M. (2018), *Heat wave risk assessment and mapping in urban areas: case study for a midsized Central European city, Novi Sad (Serbia)*. Natural hazards, **91**, *3*, pp. 891–911.

Schmeltz, M. T., Marcotullio, P. J. (2019), *Examination of human health impacts due to adverse climate events through the use of vulnerability mapping: A scoping review*, International Journal of Environmental Research and Public Health, **16**, *17*, 3091.

Şerban, Mihaela, Bălteanu, D. (2005), *Hazardele tehnologice induse de hazardele naturale în contextul modificărilor globale ale mediului*, Environment & Progress, **4**, pp. 591–595.

Sima Mihaela, Bălteanu D., Grigorescu Ines (2012), *Connecting universities and stakeholders through integrated climate services at local and regional level*. The EU-FP7 ECLISE project experience, In "Sustainable Development at Universities. New Horizons", Peter Lang Scientific Publishers, pp. 691–696.

Sima, M., Popovici, E. A., Bălteanu, D., Micu, D. M., Kucsicsa, G., Dragotă, C., Grigorescu, I. (2015), *A farmer-based analysis of climate change adaptation options of agriculture in the Bărăgan Plain*, Romania. Earth Perspectives, **2**, *1*, 5.

Stone, B., Hess, J. J., Frumkin, H. (2010). Urban form and extreme heat events: are sprawling cities more vulnerable to climate change than compact cities?. Environmental health perspectives, **118**, *10*, 1425.

Sutanto, S. J., Vitolo, C., Di Napoli, C., D'Andrea, M., Van Lanen, H. A. (2020), *Heatwaves, droughts, and fires: Exploring compound and cascading dry hazards at the pan-European scale,* Environment international, **134**, 105276.

Turco, M., Palazzi, E., Hardenberg, J., Provenzale, A. (2015), *Observed climate change hotspots.* Geophysical Research Letters, **42**, *9*, pp. 3521–3528.

Van der Velde, M., Tubiello, F. N., Vrieling, A., Bouraoui, F. (2012), *Impacts of extreme weather on wheat and maize in France: evaluating regional crop simulations against observed data*. Climatic Change, **113**, *3–4*, pp. 751–765.

Vitolo, C., Di Napoli, C., Di Giuseppe, F., Cloke, H. L., Pappenberger, F. (2019), *Mapping combined wildfire and heat stress hazards to improve evidence-based decision making*. Environment International, **127**, pp. 21–34.

Wilhite, D. A., Svoboda, M. D., Hayes, M. J. (2007), Understanding the complex impacts of drought: a key to enhancing drought mitigation and preparedness. Water resources management, **21**, *5*, pp. 763–774.

Wilhite, D.A. (2000), *Drought as a Natural Hazard: Concepts and Definitions*. In D.A. Wilhite (ed.), Drought: A Global Assessment. Hazards and Disasters: A Series of Definitive Major Works, Routledge, London, pp 1–21.

WMO (2021), *Atlas of Mortality and Economic Losses from Weather, Climate and Water Extremes (1970–2019),* World Meteorological Organization (WMO), no. 1267.

World Bank (2010), *Cities and climate change: An urgent Agenda*, December 2010, **10**, The International Bank for Reconstruction and Development, Washington.

Yen, B. T., Son, N. H., Amjath-Babu, T. S., Sebastian, L. (2019), *Development of a participatory approach for mapping climate risks and adaptive interventions (CS-MAP) in Vietnam's Mekong River Delta,* Climate Risk Management, **24**, pp. 59–70.

Yusuf, A., A., Francisco, Herminia (2009), *Climate Change Vulnerability Mapping for Southeast Asia*. Economy and Environment Program for Southeast Asia (EEPSEA) Report, 26 p.

IDENTIFYING POTENTIAL LANDSLIDE AREAS
BY EMPLOYING THE EROSION RELIEF INDEX AND METEOROLOGICAL
CRITERIA IN UKRAINE

ALEXANDR APOSTOLOV[*], LESIA YELISTRATOVA[**],
INNA ROMANCIUC[***], IULIIA ZAKHARCHUK[****]

Abstract. A method for determining landslide-prone areas based on remote sensing data and meteorological data is proposed for the Ukrainian territory. It was tested within different landscape sites of the country: the Ukrainian Carpathians, the Dniester river valley, the right-bank of Dnieper river within Kyiv and Kaniv, right side of the Dnieper-Donets Rift within Kharkiv, and the Black Sea Lowland within the Odessa city. The digital elevation model (DEM) data based on the topographic survey by Shuttle Radar Topography Mission (SRTM) as well as data from meteorological stations were used. The Erosion Relief Index (ER) method was obtained based on terrain morphology as reflected by the DEM. The index considers vertical and horizontal terrain dissection. The potential areas prone to erosion and landslide risks were identified by the ER index values. On the background of the Köppen climatic classification, the potential of rainfall events to cause the activation and intensification of landslides was analyzed by adopting threshold curves of meteorological criteria. The study argues that the use of the ER index in conjunction with meteorological data is an effective method to identify potential areas with erosion and landslide risks.

1. INTRODUCTION

Modern conditions are characterized by intensive engineering and economic land development. The global technogenic and natural processes lead to the activation of negative factors. These natural and anthropogenic factors intensify social and economic problems. Prevention is possible by rational use of natural resources and the introduction of measures. It will be possible to prevent occurrence of the new areas of natural disasters: mudflows, landslides *et al*. The main causes of such disasters are factors of hydrogeology and geomorphology.

Human safety, well-being and health depend on climate conditions. Climate determines complex of the weather and natural state. The modern climate situation leads to considerable environmental changes. The last decades showed the increase of catastrophic natural disasters worldwide. The most of the catastrophic natural disasters are related with hazardous exogenous variables: landslides, mudflows *et al*. The activities of exogenous variables are changed to more susceptible to the weather conditions.

---

[*] Researcher Officer, State Institution "Scientific Centre for Aerospace Research of the Earth of the Institute of Geological Sciences of the National Academy of Sciences of Ukraine", O. Gonchar str., 55-b, 01054, Kyiv, Ukraine, alex@casre.kiev.ua.

[**] PhD, Senior Researcher, State Institution "Scientific Centre for Aerospace Research of the Earth of the Institute of Geological Sciences of the National Academy of Sciences of Ukraine", O. Gonchar str., 55-b, 01054, Kyiv, Ukraine, tkach_lesya@ukr.net.

[***] PhD, Lead Engineer, State Institution "Scientific Centre for Aerospace Research of the Earth of the Institute of Geological Sciences of the National Academy of Sciences of Ukraine", O. Gonchar str., 55-b, 01054, Kyiv, Ukraine, romanciuc@nas.gov.ua, i.romanciuc@gmail.com.

[****] Lead Engineer, State Institution "Scientific Centre for Aerospace Research of the Earth of the Institute of Geological Sciences of the National Academy of Sciences of Ukraine", O. Gonchar str., 55-b, 01054, Kyiv, Ukraine, yulia.zakharchuk@gmail.com.

Climate change and global warming assign to safety of ecological environment. The global warming has expressed in physical characteristics of the atmosphere and lithosphere during the last ears of XXth century and within XXIth century. Increases of global average temperature of 1,4–5,8°C till the end of current century are projected (Suruchi *et al.*, 2021). The high temperatures destruct soil layers. During intensive sunshine, the soil drains, and become a dry crust. The drops of heavy rain are more heavily and stronger. Heavy rains destroy soils. In such cases, rains do not saturate soils with necessary water. The soil layer erodes and forms gullies. Gullies with time become deepen and induce strengthening erosion and destruction. So, considerable land areas become decommission. Such land areas are unusable in agronomy and construction (Belayneh *et al.*, 2020; Bastola *et al.*, 2018).

It is expected further increase of the water vapor, evaporation and precipitation size on the global level. On the regional level, increases and decreases of precipitation within different areas are predicted. The changes in dynamic intensity, frequency and variability of heavy, catastrophic rains are observed (Hosseinzadehtalaei *et al.*, 2020; Li *et al.*, 2019; Wasko and Sharma, 2017; Kundzewicz *et al.*, 2014). The increase of significant ecosystems dislocations in consequence of drought and freshet is expected. Heavy rainfalls will lead to freshets, floods, mudflows. The reduction of frosty days and cols waves is possible. In conditions of air temperature increasing, it will facilitate decline freezing of the soil in winter. It is observing acceleration in water infiltration of soils and increasing groundwater level. Floods and landslides will intensify and activate (Gariano and Guzzetti, 2016; Panek, 2019).

Attention must be paid to operational developments for detecting potential hazard areas especially areas with landslide activity. It is optional and effective to involve the remote sensing data. Such methods can detect areas with potential environmental problems. Based on remote sensing data is possible development prevention and operational observing of landslides.

Landslide hazard is a negative factor of ecological and technogenic safety of terrain on the regional and local level. Landslides lead to huge losses in nature, agriculture, economics and humans' life. The evolution of landslide is caused by many factors. The most significant factor is action of hydrometeorological processes during anthropogenic disorders of vegetation cover, surface and underground runoff. During the spring melting snow process and summer heavy rains the maximum of landslide activity is observed. The landslide studies must include characteristics of liquid and solid precipitation on the soil substance.

The landslides are a dangerous hazard. During landslide activity the huge soil masses can be displaced. The movements may cause damages to buildings, communications, and threaten human lives.

The natural origin of landslides is localized mainly within ravine-beam lands, river valley slopes, along the coasts, in the mountains, on the watersheds.

The aim of this study is to identify the potential areas with erosion and landslide risks within Ukraine as well as landslide intensification and triggering thresholds of unexpected climatological indicators, by employing data derived from remote sensing and meteorological stations.

This study is concentrated on addressing some unresolved tasks, such as: (a) generalized characterization of the impact of climatological indicators on landslides; (b) the identification of threshold values of unexpected meteorological factors, which determine the activation of landslide processes in Ukraine.

2. BACKGROUND

The erosion and landslides are widely distributed all around the world, with numerous cases reported especially in USA (Smith and Wegmann, 2018), China (Tang *et al.*, 2020; Zhang *et al.*, 2020), Indonesia (Nugraha *et al.*, 2015), Italia (Cencetti *et al.*, 2020), Pakistan (Khan *et al.*, 2019), Brazil (Mendonca and Silva, 2020) etc.

To study the natural and anthropogenic landslides by remote sensing data many sensor systems were developed: radiolocation, active and passive systems, radiometers, scatterometers (Zhao and Lu, 2018; Casagli *et al.*, 2016).

Synthetic-aperture radar (SAR) has wide coverage and high spatial resolution. The significant advantage is its independence of weather conditions and capability of day and night imaging. For landslide detection and exploration widely used are: European Remote Sensing Satellites (ERS-1, ERS-2) (Refice *et al.*, 2019; Hayati *et al.*, 2020), Envisat ASAR (Frangioni *et al.*, 2013), COSMO, SkyMED (Soldato *et al.*, 2019; Konishi and Suga, 2018), Terra SAR-X (Liu *et al.*, 2020; Zhao *et al.*, 2018), Sentinal-1 (Solari *et al.*, 2019; Mondini *et al.*, 2019). The main radiolocation sensing direction is measuring earth and water surface. Based on this data, digital elevation models are derived.

The optical remote sensing data are in use also for landslide research and monitoring. Optical methods are used for landslide inventory and mapping (Kyriou and Nikolakopoulos, 2020; Fang, 2020; Ramos-Bernal, 2018). The most useful optical systems for this purpose are considered Landsat (Hashim *et al.*, 2018; Cahalane *et al.*, 2019), SPOT (Khan *et al.*, 2019), ASTER (Ramos-Bernal *et al.*, 2018; Chang *et al.*, 2019), RapidEye (Kim and Kim, 2018; Cahalane *et al.*, 2019).

One of the most popular and useful method of erosion observing is digital elevation model (DEM). It identifies terrain changes. The LiDAR systems obtain long-term imaging. It is effective for quantitative assessment of landscape changes within large areas. The Terrestrial Laser Scanning (TLS) obtains three-dimensional relief changes with the high level of detail, that is effective for landslide researches (Li and Tomas, 2017; Pradhan, 2017). The digital elevation model from the Indian satellite IRS obtains stereophotogrammetric images. Such images are better to use for mapping and quantitative assessment of landscape erosion and landslide processes (Chen *et al.*, 2020; Chang *et al.*, 2019).

The textural features analysis method is used for landslide detection. It is based on difference in textures and features of objects on the satellite images. The method is used as additional and subsidiary in complex with other methods (Knevels *et al.*, 2019; Timchenko *et al.*, 2016). The method is used to detect the difference between the roughness and smooth of the surface. It is possible to determine the landslide bounds, stability and instability zones, zones with active and passive phases. Detecting the erosion with high-spectral and temporal remote sensing frequently based on the qualitative colored background method. Different color corrections, color combinations, color compositions, merging images are also effective to erosion signification (Fauzi *et al.*, 2015; Fernandez *et al.*, 2008). In this case the vegetation cover is good separated, forming the high contrast in vegetation and non-vegetation zones. The near infrared (NIR) band is widely used for vegetation separation. As the control data points are usually used the Normalized Difference Vegetation Index (NDVI) which is calculated based on remote sensing data (Lin *et al.*, 2005). Interpretation of space images include filtrating of polyline features, slope gradients, different object classification methodic.

Spectroscopic and 3D effect analyses permit to identify landslides by morphological features, such as borders, earthfall and accumulation zones, elevations. Complex long-term monitoring observations and momentary images enables to assess activity of landslides, displayed by pixel movement and changes. The pixel changes in subsequence satellite images shows the intensity, dynamics and trends of the process.

Since the erosion is worldwide spread, many scientists develop monitoring and research methods. One of the methods is the detection of the dynamics of landslides (Gatter *et al.*, 2018), observing the impacts of landslide on the social-economic systems (Perera, 2018), ecosystems and environment (Nicolic, 2014). Quantitative evaluation of landslide susceptibility using multiple regression methods and principal component analysis is used for landslides estimation. Physically-based modelling illustrates the physical processes of landslide formation and rainfall impacts. The combination of field surveys and remote sensing techniques is widely applied due to multifactorial consideration of landslide processing. The modelling methods are effective, because they are based on quantitative and different features consideration: slope angle, curvature of the slopes, soil features,

precipitation conditions etc. The landslide monitoring must be improved for later prevention of negative societal consequences. The detection of erosion processes and of their impact on the environment allow to proceed with modeling of vulnerability risks on natural disasters and hydrogeological risks (Kostyuchenko, 2015; Kostyuchenko *et al.*, 2016).

The observation and study of denudation processes is a significant task in Ukraine as well. Based on Landsat 5/TM remote data a modeling of the land degradation risk assessment was performed within the Oleshky Sand dunes during two periods: 1983–1991 and 1991–2010, while considering vegetation cover changes and soil erosion dynamics (Popov *et al.*, 2012). It was ground different aspects of remote sensing data application as a component of landscape monitoring conditions using geoinformation systems (GIS) (Lai and Tsai, 2019; Mersha and Meten, 2018). Besides it was considered the main approaches of assessment erosion within wide areas based on remote sensing data, determined dangerous of erosion process manifestation using GIS, based on spatial geoinformation erosion modeling of soil losses, develop approaches for water soil erosion modeling, identified measures, diagnostic parameters, quantitative and qualitative assessment of soil degradation, using integral assessment of relief identified erosion risks (Svetlitchnyi, 2009; Svetlitchnyi, 2018).

The tendency of ecological hazard increasing with intensity of precipitation (heavy rains) was estimated by Ukrainian and world scientists (Lyalko *et al.*, 2018; Dourte *et al.*, 2015).

3. CHARACTERISTICS OF THE STUDY AREA

The Ukraine is situated on the southwest part of East European Plain. Ukrainian Carpathians are located in the western part and the Crimean Mountains in the southern part of Ukraine. Within the Ukraine there are mountains, uplands and lowlands, plains. Such physiographic conditions vary due to climate changing from perhumid on the west part to arid on the south of the country. The climate is favorable for human life and activity. However, location features, evolution of atmospheric processes establish conditions for adverse meteorological phenomena formation, which increase during XXI century.

Therefore, the Ukraine is characterized by wide diversity of natural, climatic and geological conditions. It determines formation of different exogenous geomorphological processes. Some of them have a negative influence on the human lives and activities. This category includes erosion, landslides, anthropogenic and other processes. Beside natural exogenous processes defined anthropogenic processes that are widespread on the east of the Ukraine. It's spreading caused by development of mineral deposits.

Combined manifestation of different exogenous processes leads to increase of unusable land areas. The intensification of exogenous processes including landslides as a result of global and regional warming is observed. A comprehensive study of these both problems and their interdependence is an interesting aspect.

4. DATA AND METHODOLOGY

This study is based on the complexion of methods, include the national and world experience. The methodological workflow is reflected in the Figure 1. The statistical data of the ground meteorological stations within Ukraine were used. For geological observations the cartographic data were applied. The remote sensing data, such as digital elevation model (DEM) with 30m resolution form the Shuttle (SRTM) were used for landslide assessment. The field measurements include the data from 60 ground-based meteorological instrumental stations, verified by Central Geophysical Observatory of Ukraine named after Boris Sreznevsky. Field meteorological surveys include quantity of monthly precipitations from 1900 to 2018: rainfall events (30 mm precipitation in 12 hours); heavy rainfall events (precipitation 50 mm and more in 12 hours); long-term rainfall events (precipitation 100 mm and more).
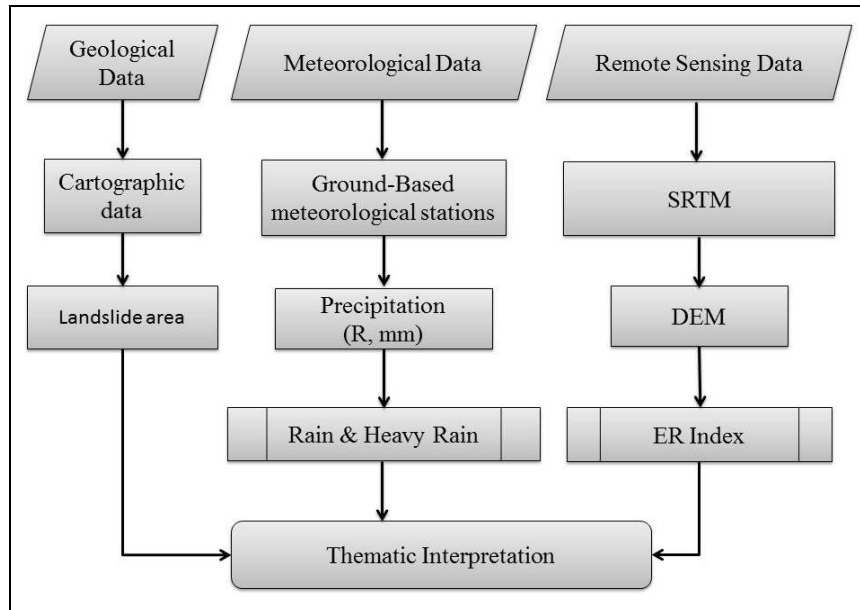
Fig. 1 – The scheme for the assessmant of landslide-prone areas in Ukraine.

For determining threshold values of climatological factors the next algorithm was put in practice: 1) the analysis of a multiannual precipitation data carried out for diagnostic estimation of the precipitation distribution changing in Ukraine; 2) the compilation of the structured dataset on precipitation which can lead to the landslides intensification. The intensity of each heavy rainfall event was estimated; 3) the threshold values were obtained in accordance to the Guzzetti approach (Guzzetti *et al.*, 2007) which describe the landslides activation in Ukraine; 4) rainfall events which can provoke the landslides were determined by exceeding the actual rainfall average intensity over the threshold proposed by Guzzetti *et al.*, 2007.

The intensity of relief dissection was derived through the Erosion Relief Index (ER) used as a methodological tool to assess potential landslide areas. ER Index were developed and tested in Ukrainian Carpatians (Lyalko *et al.*, 2018) and Dnieper River Vally withib Kyiv region (Lyalko *et al.*, 2017). The intensity of erosion dissection (Q) is estimated by equation 1:

$$Q = \frac{\Delta H * L}{P^2} \tag{1}$$

where, $\Delta H / P$ is the vertical amplitude (vertical dissection) of relief, ΔH is the difference between the highest and lowest points in a particular area within moving window (relative relief), P is the area of moving window, L / P is the interfluvial amplitude (horizontal dissection), L is the total length of river in the moving window.

In this study, it has been suggested to use the length of contour lines in the moving window instead of total length of the river. In this way, the equation for intensity of erosion dissection of the area (Erosion Relief Index) takes the following form:

$$ER = \frac{\Delta H * (N * l)}{P^2} \tag{2}$$

where, $(N * l) / P$ is the interfluvial amplitude (horizontal dissection), N is the number of contour line pixels in the moving window, l – length of the pixel.

Based on the digital elevation model from the reusable spacecraft Shuttle was obtained for Ukraine. The spatial resolution of 30 m was too low for this purpose. Therefore, the ERDAS Imagine software product was used for processing digital elevation model data with the *Bilinear Interpolation* procedure. According to this procedure, the changing in the heights between nearest pixels was assumed as linear with 30 m change degree.

To estimate the vertical dissection of the relief the *Spatial Modeler* module within ERDAS Imagine was used to implement the following equation:

$$\frac{\Delta H}{P} = (H_{max} - H_{min})/P \tag{3}$$

where, H_{min} and H_{max} are the minimum and maximum elevation values in the moving window.

Using the *Interpreter* module from ERDAS Imagine, the contour lines for all Ukraine territory were obtained with 5m horizontal interval for estimation of the relief dissection.

The next step was focused on estimating the horizontal dissection of relief within the moving window according to the equation:

$$(N*l)/P \tag{4}$$

Thus, using the ERDAS Imagine software the intensity of erosion dissection (ER) was estimated with equation 2.

The erosion relief index (ER) was estimated from the DEM. The values of ER index depend on the latitudes. To compare different areas, the values of ER were scaled according to the following equation:

$$ER_{new} = 100*(\frac{ER - ER_{min}}{ER_{max} - ER_{min}}) \tag{5}$$

where, *ER* is the current value, ER_{min} and ER_{max} are the minimal and maximal value of ER index within the study area.

This allows comparing areas in different physiographic regions. Without scale normalization by equation 5, it is hard to observe the local erosion features of different areas, including plains (Lyalko *et al.*, 2017; Lyalko *et al.*, 2018).

5. RESULTS AND DISCUSSIONS

Monitoring and modeling studies shown the significant impact of climate change on stability of natural and engineering slopes of activating landslides. The mechanisms and intensity of such processes in space and time, as well as the frequency of landslides during climate changing are unclear (Kovrov *et al.*, 2018).

Multiannual values of weather define the concept of climate as a characteristic of natural conditions of an area. Due to the general circulation of atmosphere, the climatic fluctuations spread through the planet. The physical aspects of global climate changes have been studied for a long time. Currently, the greenhouse effect, created by greenhouse gases is considered as main impact on climate (Hertzberg *et al.*, 2017).

The unstable climatic conditions are manifested in Ukraine. In order to complete analysis of the modern exogenous processes, in particular landslides, the diagnostic assessment of the modern climate of Ukraine were done in this study. The warming, which has no analogues in duration and intensity began from 1989 in Ukraine (Elistratova and Apostolov, 2018; Lyalko, 2015).

Deviation of air temperature (ΔT, °C) from the climatic norm of 1981–2010 in Ukraine from 2001 to 2017

Years	Months												Average
	I	II	III	IV	V	VI	VII	VIII	IX	X	XI	XII	(ΔT, °C)
2001–2017	0,1	0,3	1,2	1,0	0,7	0,9	1,5	1,2	1,0	0,1	1,5	0,5	0,8

Table 1 shows the deviation of air temperature from the climatic norm within 1981–2010 in Ukraine. The total air temperature deviation for 17 years in the XXI century is 0.8. Annual observations demonstrated that the average of annual temperature is increasing (Lyalko *et al.*, 2020).

Particularities of climate in Ukraine depend on the global climate system, as well as from the general circulation processes which take place in the European area. Ambiguous causes of climate change in Ukraine are characterized by precipitation distribution. The formation and fall of precipitation in Ukraine is a consequence of macrocirculary processes that determine heat and moisture changes in the atmosphere. The essence of these processes consists in transferring heat and moisture over a considerable distance from the Atlantic Ocean and the Mediterranean Sea. Under the influence of cyclones, the large-scale vertical air movements develop that lead to the precipitation (Martazinova, 2019). The average amount of annual precipitation in Ukraine has not changed significantly, but it was observed its distribution by months. Precipitation fluctuations relative to the norm persist, although there is a tendency to precipitations decreasing. During the decades 1981–1990, 1991–2000, 2001–2010, 2011–2020 the decrease in precipitation fluctuations is observed, which indicates a slight weakening of precipitation processes. Despite this, the humidification becomes more stable (Lyalko *et al.*, 2015).

The map of average annual of precipitation (R) in Ukraine for the period 1900–2018 is created on the bases of meteorological data from the Central Geophysical Observatory of Ukraine named after Boris Sreznevsky and presented in Fig. 2. The largest values of average annual precipitation occur in the northern, western and northwestern parts of the territory.

The main feature in the precipitation characteristic is the increase expectations of heavy rainfalls. Due to both the global and regional (Ukraine) warming, the frequency and intensity of heavy rainfalls are increasing. It is the main cause of the rapid landslide processes. The natural phenomena, including precipitation, snowmelt, temperature changes as well as anthropogenic activity are the dominant factors for slope instability. In the long run, the climate changes will affect the slopes stability at different temporal and spatial scales. Therefore, it is expedient to study the influence of meteorological factors (especially heavy rains) on landslide occurence in Ukraine.

Exogenous processes develop the modern relief of Ukraine and depend on neotectonic vertical movements. Ukraine territory is affected by neotectonic uplifts for a long time. Neotectonic structures of Ukraine represent a system of closely related elements of the relief in the modern deposits. Neotectonic vertical movements imprinted the elevations of relief, slopes, form of slopes where the exogenous processes take place.

Thus, the diversity of natural, climatic, geological and geomorphological conditions in Ukraine contributes to the formation and development of different exogenous processes. In particular, erosion in Ukraine has a high dynamic and destructive ability.

Analysis of long-term monitoring of exogenous processes (EGP) in Ukraine shows the fundamental changes of slopes during technological development. It is manifested in the disbalance of the upper zone of geological environment by unfavorable constructions. Industrial-urban agglomerations, degradation and soil subsidence processes are constantly increasing. The soil weakening increases the tendency of landslides intensifies. The number and frequency of its activation over time are increasing (Kovrov *et al.*, 2018; Kovrov *et al.*, 2020).
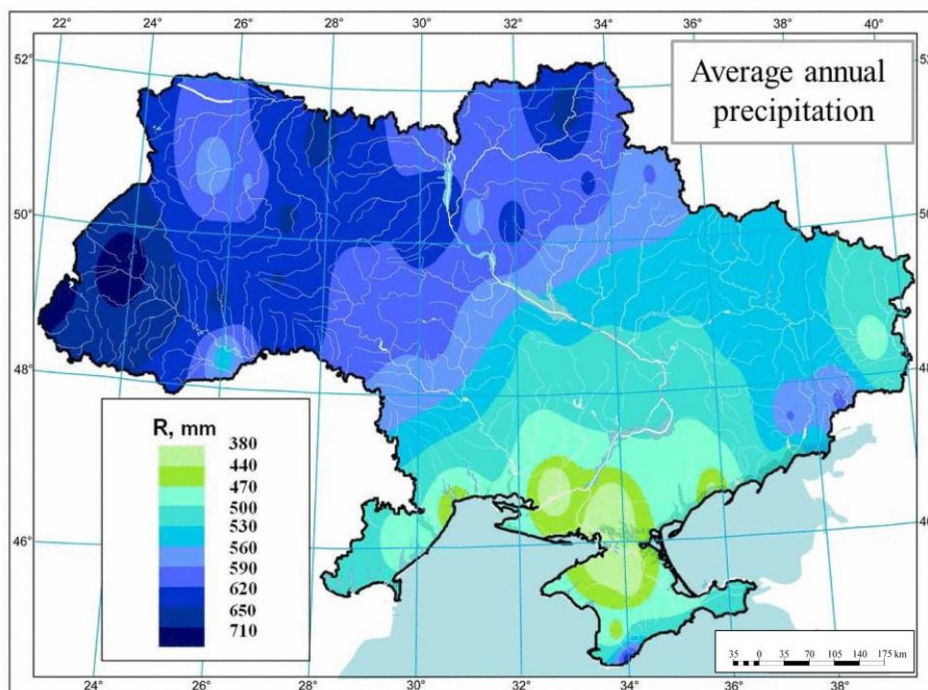
Fig. 2 – Map of the disturbtion of average annual precipitation (R)
in Ukraine for the 1900–2018 period.

The majority of landslide processes appear on the slopes and in the coastal areas, which are composed of unstable rocks subject to deformation. On the river valley slopes these processes develop with the deepening of valleys during tectonic uplift movements. When the potential energy of relief increases the unilateral displacement of watercourses takes place imprinting an asymmetry to river valleys. The landslide development in mountain areas occurs due to the significant elevation and steepness of the slopes, when the thick layer of weathered rocks and intensive dissection of the terrain take place.

The largest areas of landslides in Ukraine are observed on the Black and Azov Sea coasts, within the basin the Seversky Donets River (Donetsk region), the right bank of the Dnieper River and its right part tributaries. For the climatic and geographical conditions of Ukraine, the intensification of landslides will remain at a high level due to the growth of anthropogenic impacts on the environment and global climate change (Kovrov *et al.*, 2018). The precipitations can act as a trigger factor in this case.

According to the State Geology Department data (Information yearbook, 2017), the map of landslide distribution in Ukraine was compiled for the year 2016 (Fig. 3).

Figure 3 illustrates the landslide distribution within the Ukraine in 2016. The background color shows the area of landslides in sq. km and the areas with active landslides. The columns of different colors and sizes show the number of slides for each administrative region (oblast in Ukrainian). The most developed landslide areas are in the mountain regions – the Crimean Mountains and the Carpathians. Also, active landslide areas are along the banks of the Dnieper and the Dniester rivers, and in the eastern part of territory due to anthropogenic pressure.

To study the connection between precipitation and exogenous processes (landslides, debris flows, gullies), areas located in different climatic conditions of Ukraine were selected (Fig. 4).
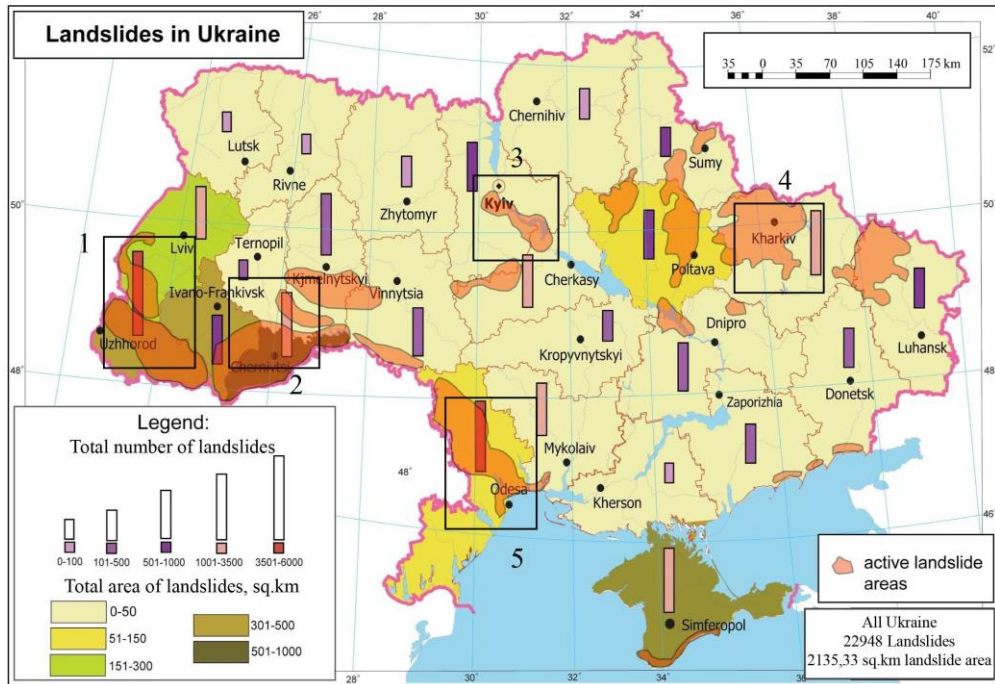
Fig. 3 – The map of landslides within the Ukraine for the year 2016.
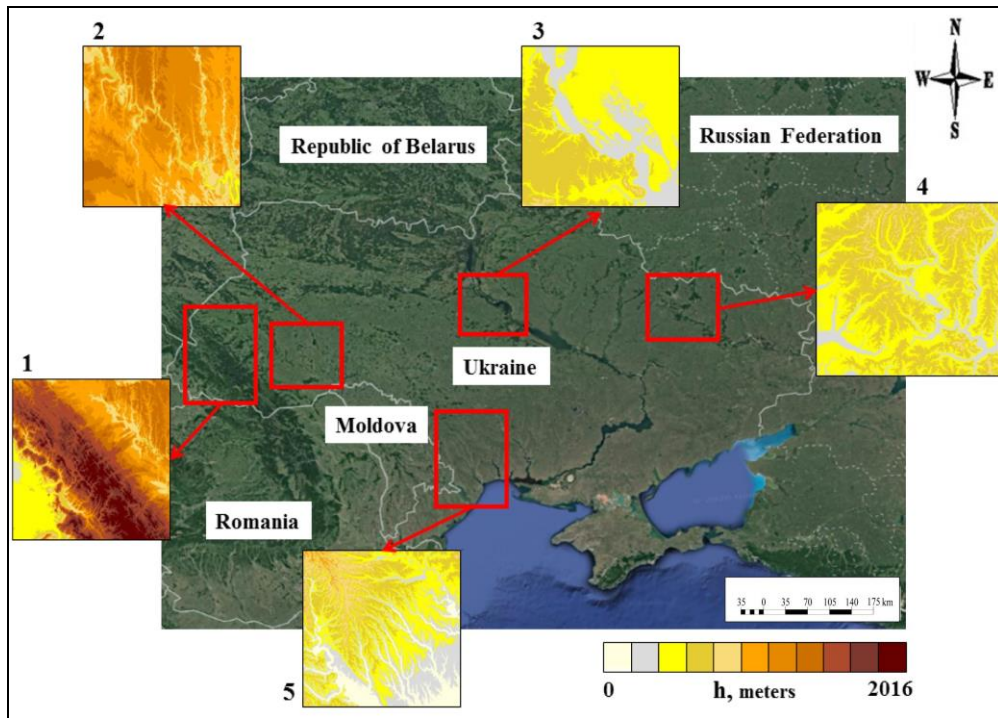

Fig. 4 – Location of the test sites with elevation imaging: 1) Ukrainian Carpathians; 2) Dniester River Valley; 3) the right bank of Dnieper River near Kyiv and Kaniv; 4) the right side of the Dnieper-Donetsk Depression near Kharkiv; 5) Black Sea Lowland near Odessa.

To assess the caabilities of the proposed method, the observations were done within several regions of Ukraine, which are in terms neotectonic activity and the level of terrain dissection. The Ukrainian Carpathians were selected as high elevation area. The territory between the Dniester River Valley and the right bank of Dnieper River between Kyiv and Kaniv was studied as a plain area. These two areas are located in the zone of active vertical neotectonic uplifts with a significant amplitude. A territory with weak neotectonic movements and weak erosion dissection is located around the Kharkiv city within the right bank of Dnieper-Donetsk Depression. The area of Black Sea Lowland near Odessa city is characterized ny neotectonic subsidence with intense erosion.

According to the proposed method, the disturibution of the intensity of Erosion Relief Index values for the right bank of the Dnieper River between Kiev and Kaniv is presented in Figure 5a. The color gradation from red to light green demonstrates the level of erosion dissection in the area according to the ER index shown in Table 2. Detailed gradation of of ER Index is eluminated in previous studies (Lyalko *et al.*, 2017; Lyalko *et al.*, 2018). To identified by ER index landslide area confirmation the fragment of the landslide distribution map according to the data from State Geological Department is presented in the Figure 5b (Information yearbook, 2017).
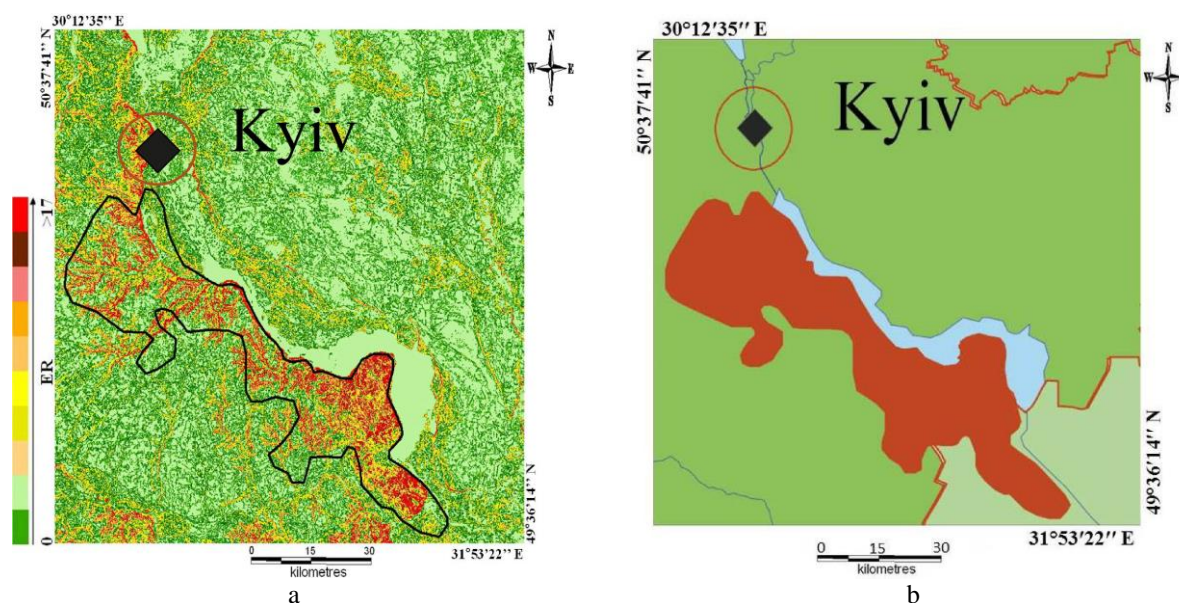

Fig. 5 – a) The relief dissection by Erosion Relief Index for the right bank of the Dnieper River between Kyiv and Kaniv area, according to processed DEM data; b) the fragment of landslide disribution map based on the data from information yearbook of dangerous exogenous geological processes activation in Ukraine according to EGP monitoring (Information yearbook, 2017).

Table 2

The values of ER index

Index values	Color gradation	Danger level
<2	Light to dark green	No danger
2–7	Mustard and yellow	Light
7–10	Light orange	Significant
10–13	Dark orange	Strong
13–17	Dark pink	Very strong
>17	Dark brown and red	Catastrophic

The results analysis showed that maximum values of the ER index are confined to the sloping surfaces. These relief elements are naturally affected by erosion. They are complicated by ravines and gullies of different ages and origins and require special erosion safety actions. There is a clear relationship between the vertical dissection and density of the ravines. This reflects the specificity of the area affected by linear water erosion. Besides, the morphometric parameters are of significant importance – *e.g.* slope angle, slope shape, slope length etc. By using the ER index it is possible to identify potentially threatened erosion areas. The index values obtained in this study can be used for other areas where the digital elevation model is obtained. According to the ER index, areas with very high potential of landslide activity are observed for the right bank of the Dnieper River between Kyiv and Kaniv. These areas will very likely respond to extreme meteorological values.

The total number of landslides in Ukraine does not change, but the number of active landslides depends on the precipitation. The threshold values of climatological indicators, more precisely of precipitations (R), were estimated in order to distinguish areas with high moisture and potential landslide hazard. The landslide activation depends on the amount of precipitation, its seasonal distribution, precipitation regime, temperature changes in annual and multiannual terms.

To determine potential landslide hazard areas, the quantity of precipitation changes for the 1976–2018 period were estimated, based on data from the meteorological stations located on the right bank of the Dnieper River between Kyiv and Kaniv. Changes in the amount of precipitation by seasons for the period 1976–2018, corresponding to the right bank of the Dnieper River between Kyiv and Kaniv are illustrated in Figure 6.
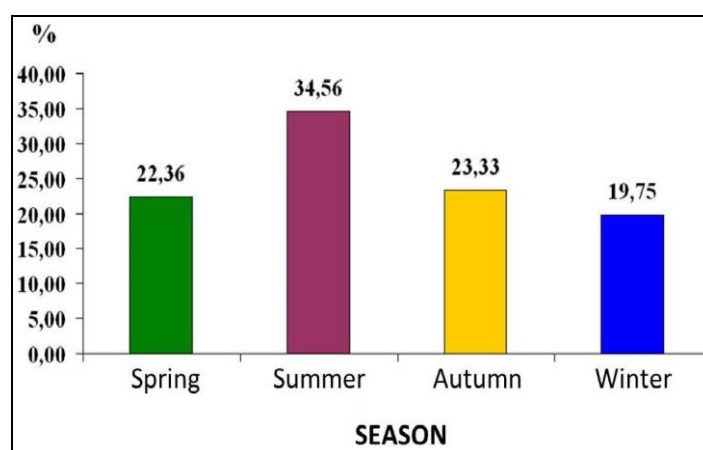

Fig. 6 – The precipitation quantity changes by seasons on the right bank of Dnieper River between Kyiv and Kaniv for the 1976–2018 period.

The average monthly precipitation for the 1976–2018 period was analyzed. For the period studied the excess of precipitations (wet years) was registered in 20 years.

In Table 3, the percentage of monthly precipitation average in comparison to the norm (1981–2010) for the 2001–2015 period was obtained for the right bank of the Dnieper River between Kyiv and Kaniv. According to Table 3, the average percentage of precipitation excess relative to the norm is 2.155 %.

Exceeding the norm 1,5–2 times provides oversaturation of soil with moisture and leads to the intensification of landslides (Matsuyama *et al.*, 2021; Brocca *et al.*, 2012). To identify the threshold values of meteorological factors, a structured dataset of precipitation (heavy rainfall events – HRE and rainfall events RE) was compiled for all tested sites. The dataset includes information about the station names, time and date, duration and intensity of atmospheric phenomena. As an example, the part of

the constructed database is shown in Table 4. The database includes 113 rainfall events that triggered the intensification of landslides in the studied area.

Table 3

Percentage of monthly precipitation average from norm (1981–2010) during the 2001–2015 period
for the right bank of the Dnieper River between Kyiv and Kaniv

Months / Years	I	II	III	IV	V	VI	VII	VIII	IX	X	XI	XII
2001	**118**	**114**	**239**	**120**	93	**197**	79	44	**107**	51	**146**	69
2002	56	92	52	75	**182**	**139**	63	**142**	**190**	**170**	92	27
2003	**137**	50	79	67	51	35	88	**120**	74	**300**	58	80
2004	**182**	**148**	72	54	**108**	27	**160**	**203**	117	68	**114**	50
2005	**132**	**163**	94	**129**	91	**123**	48	**172**	19	**149**	89	**182**
2006	43	**101**	**189**	89	**170**	**145**	67	**118**	115	103	58	26
2007	**137**	**137**	53	27	88	75	**103**	**124**	68	50	**164**	65
2008	89	37	**105**	**181**	79	52	**110**	48	**221**	36	90	**157**
2009	93	**156**	**138**	4	70	67	98	25	31	**129**	64	**195**
2010	**154**	**195**	65	60	**109**	50	**112**	42	82	78	**138**	**153**
2011	78	72	23	48	65	**162**	**189**	101	29	**153**	8	95
2012	**156**	89	89	**154**	55	85	74	**175**	69	**137**	80	**246**
2013	**176**	**168**	**278**	71	**112**	90	41	96	**264**	29	96	38
2014	**101**	28	52	96	**276**	76	96	76	57	55	32	75
2015	**134**	78	**176**	50	**135**	81	57	11	68	66	**127**	61

Table 4

Example of the structure of the constructed precipitation database, corresponding to the right bank
of the Dnieper River between Kyiv and Kaniv

№	Station	Year	Precipitations	Date	Duration (time)	Intensity (mm/hour)
1	Teteriv	1998	HRE	17–17.07	1:00:00	30,00
2	Teteriv	1999	HRE	20–20.06	1:00:00	35,00
3	Teteriv	2001	HRE	04–04.07	1:00:00	41,00
4	Teteriv	2010	HRE	06–06.07	0:45:00	41,33
5	Teteriv	2013	HRE	28–28.06	0:57:00	31,58
6	Baryshivka	1977	HRE	10–10.07	1:00:00	34,00
7	Baryshivka	1988	HRE	25–25.06	1:04:00	45,94
8	Baryshivka	2011	HRE	16–16.08	0:44:00	45,00
9	Kyiv	1983	HRE	02–03.05	2:24:00	37,92
10	Boryspil	1977	HRE	28–28.06	0:48:00	38,75
…	…	…	…	…	…	…

The next step was dedicated to the detection of threshold values of meteorological factors that are causing landslide activation within the studied climatic zone. To select threshold values, a number of publications describing areas with the similar climatic conditions (Guzetti *et al.*, 2007). Determination of precipitation thresholds that can lead to the landslide activation processes at the selected test sites (Fig. 4) was carried out in accordance to the threshold formula (Guzetti *et al.*, 2007), which includes the Ukraine territory:

$$I_{\Pi}=30,53D^{-0,57} \tag{6}$$

where, D is the rainfall duration, in hours; I_{Π} is the average rainfall intensity, mm/h.

The threshold equation (6) was used for climatic class D according to the W. Köppen classification. This classification shows the diagnostic assessment of the climate type and is based on

the temperature and precipitation characteristics. According to this classification, Ukraine makes part of the Dfb zone – temperate-continental climate, which is characterized by equable humidity, with pronounced seasonal differentiations (Beck *et al.*, 2018; Britannica, 2021).

In Figure 7, the map of ER index and threshold rainfall diagrams for the studied test sites within Ukraine are presented. The diagrams in Figure 7 demonstrate the location points (rainfall events) 1) for the Ukrainian Carpathians, where 718 rainfall events at 10 weather stations were observed; 2) for the Dniester River Valley – 372 rainfall events at 13 stations; 3) for the right bank of the Dnieper River between Kyiv and Kaniv – 113 rainfall events at 13 stations; 4) for the right side of the Dnieper-Donetsk Depression near Kharkiv – 59 events at 10 stations; 5) for Black Sea Lowland near Odessa – 97 rainfall events at 10 stations. In the diagrams (Fig. 7), the threshold curves estimated by equation (6) are illustrated for each tested site. The rainfall events points located near and above the threshold curves are expected to cause landslide intensification. They vary by intensity within the different areas of Ukraine. Their variation is a function of the neotectonic movements, the landscape and climatic conditions, anthropogenic impacts, and climate change.

6. FUTURE RESEARCH DIRECTIONS

Future research and monitoring envisage the use of the Sentinel-1 remote sensing data available for free. Considering that landslide processes lead to changes of the terrain surface, the interferometry method permits to assess the landscape changes and landslides detection.

Taking into consideration that global climate change is a long-term process, further monitoring and analysis of exogenous processes (changes is temperature, wind and water regime) will be necessary in the future.
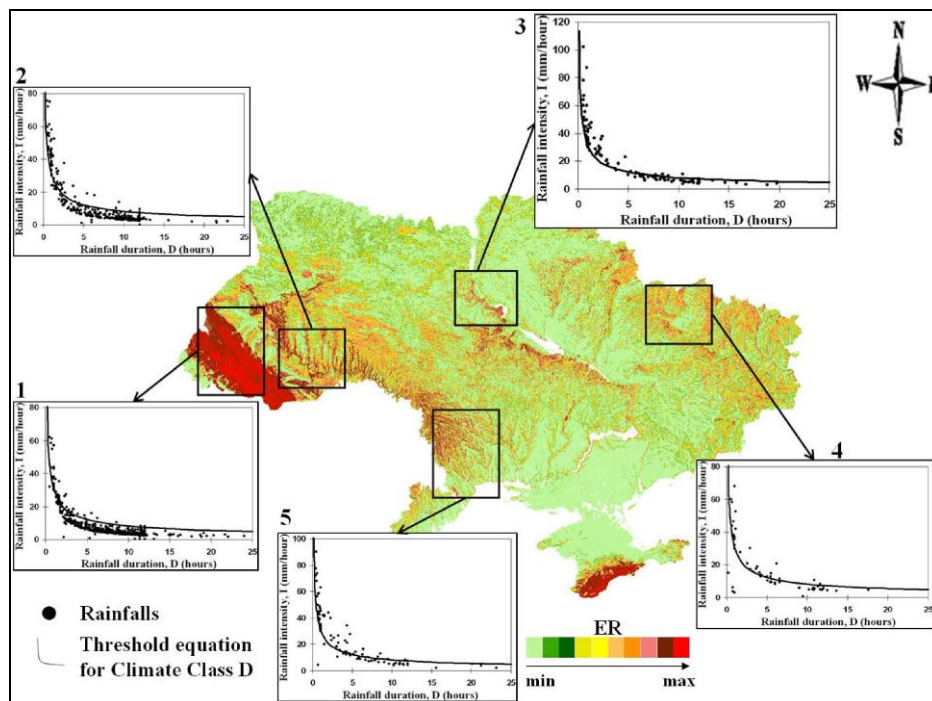

Fig. 7. – The ER index map of the Ukrainian territory and rainfall thresholds for the causing landslide intensification in:
1) the Ukrainian Carpathians; 2) the Dniester River Valley; 3) the right bank of Dnieper River near Kyiv and Kaniv;
4) the right side of the Dnieper-Donetsk Depression near Kharkiv; 5) Black Sea Lowland near Odessa.

7. CONCLUSIONS

The proposed method, based on combination of erosion relief index (ER) and threshold values of meteorological data (heavy rainfall events) allows for the identification of territories with potential erosion processes (landslides, gullies etc.).

In Ukraine, terrains with potential for the occurrence of erosion-type processes can quickly become as active erosion zones. The speed of activation depends on natural loading in conditions when the monthly precipitation average exceed the monthly norm in 1.5–2 times. The intensity of erosion increases with quick water accumulation, increasing of groundwater level. Saturation and waterlogging of soils occurs during rainfalls of high intensity within the long time period. To reduce the negative factors is necessary to implement large-scale geological surveys. It would be a good base for development of effective economic measures which can minimize the geoecological risks. The study performed shows an effective involvement of remote sensing data for prediction of erosion risks within the entire territory of the country. It could serve as a base for operative administrative solutions for relevant government services and governing specialization authorities.

REFERENCES

Bastola, S., Dialynas, Y. G., Bras, R. L., Noto, L. V., Istanbulluoglu, E. (2018), *The role of vegetation on gully erosion stabilization at a severely degraded landscape: a case study from Calhoun Experimental Critical Zone Observatory*, Geomorphology, **308**, pp. 25–39. DOI: 10.1016/j.geomorph.2017.12.032.

Beck, H. B., Zimmermann, N. E., McVicar, T. R., Vergopolan, N., Berg, A., Wood, E. F. (2018), *Present and future Koppen-Geiger climate classification maps at 1-km resolution*, Scientific Data, **5**, 180214. DOI:10.1038/sdata.2018.214.

Belayneh, M., Yirgu, T., Tsegaye, D. (2020), *Current extent, temporal trends, and rates of gully erosion in the Gumara watershed, Northwestern Ethiopia*, Global Ecology and Conservation, **24**, E01255. DOI: 10.1016/j.gecco.2020.e01255.

Brocca, L., Ponziani, F., Moramarco, T., Melone, F., Berni, N. & Wagner, W. (2012), *Improving Landslide Forecasting Using ASCAT-Derived Soil Moisture Data: A Case Study of the Torgivannetto Landslide in Central Italy*, Remote Sensing, **4**, 1232–1244. DOI:10.3390/rs4051232.

Britannica, T., *Editors of Encyclopaedia 2009: Continentality. Encyclopedia Britannica*, https://www.britannica.com/science/continentality (24. 05. 2021).

Cahalane, C., Magee, A., Monteys, X., Casal, G., Hanafin, J., Harris, P. (2019), *A comparison of Landsat 8, RapidEye and Pleiades products for improving empirical predictions of satellite-derived bathymetry,* Remote Sensing of Environment, **233**, 111414. DOI: 10.1016/j.rse.2019.111414.

Casahli, N., Cigna, F., Bianchini, S., Holbling, D., Fureder, P., Righini, G., Conte, S. D., Friedl, B., Schneiderbauer, S., Iasio, C., Vlcko, J., Greif, V., Proske, H., Granica, K., Falco, S., Lozzi, S., Mora, O., Armaud, A., Bianchi, M. (2016), *Landslide mapping and monitoring by using radar and optical remote sensing: Examples from the EC-FP7 project SAFER*, Remote Sensing Applications: Society and Environmental **4**, pp. 92–108. DOI: 10.1016/j.rsase.2016.07.001.

Cencetti, C., Rosa, P. D., Fredduzzi, A. (2020), *Characterization of landslide dams in a sector of the central-northern Apennines (Central Italy),* Heliyon, **6**, 6, e03799. DOI: 10.1016/j.heliyon.2020.e03799.

Chang, K-T., Merghadi, A., Yunus, A. P., Pham, B. T., Dou, J. (2019), *Evaluation scale effects of ropographic variables in landslide susceptibility models using GIS-based machine learning techniques,* Scientific Reports, **9**, 1229. DOI: 10.1038/s41598-019-48773-2.

Chen, Z., Ye, F., Fu, W., Ke, Y., Hong, H. (2020), *The influence of DEM spatial resolution on landslide susceptibility mapping in the Baxie River basin, NW China*, Natural Hazards, **101**, pp. 853–0877. DOI: 10.1007/s11069-020-03899-9.

Dourte, D. R., Fraisse, C. W., Bartels, W. L. (2015), *Exploring changes in rainfall intensity and seasonal variability in the Southeastern U.S.: Stakeholder engagement, observations, and adaptation*, Climate Risk Management, **7**, pp. 11–19. DOI: 10.1016/j.crm.2015.02.001.

Elistratova, L. O., Apostolov, A. A. (2018), *The Climate Changes in Ukraine During Global Warming,* Scientific Notes of Vinnytsa State Pedagogical University Named After Michailo Kotzubynsky. Series: Geography, **30**, pp. 25–34.

Fang, B., Chen, G., Pan, L., Kou, R., Wang, L. (2021), *GAN-Based Siamese Framework for Landslide Inventory Mapping Using Bi-Temporal Optical Remote Sensing Images,* IEEE Geoscience and Remote Sensing Letters, **18**, 3, pp. 391–395. DOI: 10.1109/LGRS.2020.2979693.

Fauzi, M. F. A., Wibowo, A. D. A., Lim, S. L., Tan, W.-N. (2015), *Detection of possible landslides in post-event satellite images using color and texture*, IEEE Region 10 Humanitarian Technology Conference (R10-HTC), Philippines, Cebu. DOI: 10.1109/R10-HTC.2015.7391862.

Fernandez, T., Jimenez, J., Fernandez, P., Hamdouni, R. El., Cardenal, F. J., Delgado, J., Irigaray, C., Chacon, J. (2008), *Automatic Detection of Landslide Features with Remote Sensing Techniques in the Betic Cordilleras (Granada, Southern Spain).* The International Archives of the Photogrammetry. Remote Sensing and Spatial Information Sciences. Vol **XXXVII**. Part B8, Beijing, pp. 351–356.

Frangioni, S., Bianchini, S., Moretti, S. (2015), *Landslide inventory updating by means of Persistent Scatterer Interferometry (PSI): The Setta basin (Italy) case study*, Geomatics, Natural Hazards and Risk, **6**, 5–7, pp. 419–438. DOI: 10.1080/19475705.2013.866985.

Gariano, S. L., Guzzetti, F. (2016), *Landslides in changing climate*, Earth-Science Reviews, **162**, pp. 227–252. DOI: 10.1016/j.earscirev.2016.08.011.

Gatter, R., Cavalli, M., Crema, S., Bossi, G. (2018), *Modelling the dynamics of a large rock landslide in the Dolomites (eastern Italian Alps) using multi-temporal DEMs*, PeerJ, **6**, e5903. DOI: 10.7717/peerj.5903.

Guzetti, F., Peruccacci, S., Rossi, M., Stark, C. P. (2007), *Rainfall thresholds from the initiation of landslides in central and southern Europe*, Meteorology and Atmospheric Physics, **98**, pp. 239–267. DOI: 10.1007/s00703-007-0262-7.

Hayati, N., Niemeier, W., Sadarviana, V. (2020), *Ground Deformation in The Ciloto Landslides Area Revealed by Multi-Temporal InSAR*, Geosciences, **10**, 5, pp. 156–172. DOI: 10.3390/geosciences10050156.

Hashim, M., Misbari, S., Pour, A. B. (2018), *Landslide Mapping and Assessment by Integrating Landsat-8, PALSAR-2 and GIS Techniques: A Case Study from Kelantan State, Peninsular Malaysia*, Journal of the Indian Society of Remote Sensing, **46**, pp. 233–248. DOI: 10.1007/s12524-017-0675-9.

Hertzberg, M., Siddons, A., Schreuder, H. (2017), *Role of greenhouse gases in climate change*. Energy & Environment, **28**, 4, pp. 530–539. DOI: 10.1177/0958305X17706177.

Hosseinzadehtalaei, P., Tabari, Y., Willems, P. (2020), *Climate change impact on short-duration extreme precipitation and intensity-duration-frequency curves over Europe*, Journal of Hydrology, **590**, 125249. DOI: 10.1016/j.jhydrol.2020.125249.

Information yearbook of dangerous exogenous geological processes activation in Ukraine according to EGP monitoring (2017), Ministry of Environmental Protection of Ukraine. Sate. Geol. Service. State Inform. Geol. fund of Ukraine. Kyiv, 100 P. https://geoinf.kiev.ua/publikatsiyi/shchorichnyky/shchorichnyk-egp/.

Khan, H., Shafique, M., Khan, M. A., Bacha, M. A., Shah, S. U., Calligaris, C. (2019), *Landslide susceptibility assessment using Frequency Ratio, a case study of northern Pakistan*, The Egyptian Journal of Remote Sensing and Space Science, **22**, 1, pp. 11–24. DOI: 10.1016/j.ejrs.2018.03.004.

Kim, J. S., Kim, K. H. (2016), *Analysis of 2016 Minamiaso landslides using remote sensing and geographic information system*, J. of Applied Remote Sensing, **12**, 3, 036001. DOI: 10.1117/1.JRS.12.036001.

Knevels, R., Petschko, H., Leopold, P., Brenning, A. (2019), *Geographic Object-Based Image Analysis for Automated Landslide Detection Using Open Source GIS Software*, ISPRS Int. J. Geo-inf, **8**, 12, pp. 551–572. DOI: 10.3390/ijgi8120551.

Konishi, T., Suga, Y. (2018), *Landslide Detection using COSMO-SkyMed images: a case study of a landslide event on Kii Peninsula, Japan*, European Journal of Remote Sensing, **51**, 1, pp. 205–221. DOI: 10.1080/22797254.2017.1418185.

Kostyuchenko, Y. V. (2015), *Geostatistics and remote sensing for extremes forecasting and disaster risk multiscale analysis*, in: Seifedine Kadry, Abdelkhalak El Hami, (eds.): Numerical Methods for Reliability and Safety Assessment, Springer International Publishing, Cham, pp. 439–458. DOI 10.1007/978-3-319-07167-1_16.

Kostyuchenko, Y. V., Movchan, D., Kopachevsky, I., Yuschenko, M. (2016), *Approach to multi-disaster vulnerability analysis based on risk perception model. Prace i Studia Geograficzne*, Prace i Studia Geograficzne, **61**, 4, pp. 63–84.

Kovrov, O. S., Kolesnik, V. Ye., Buchavyi, Yu. V. (2018), *Evaluation of the influence of climatic and geomorphological factors on landslides development*, Environmental Safety and Natural Resources, **25**, 1, pp. 52–63, DOI: 10.32347/2411-4049.2018.1.52-63.

Kovrov, O., Kolesnyk, V., Buchavyi, Y. (2020), *Development of the landslide risk classification for natural and man-made slopes based on soil watering and deformation extent,* Min. miner. depos., **14**, 4, pp. 105–112. DOI: 10.33271/mining14.04.105.

Kundzewicz, Z. W., Kanae, S., Seneviratne, S. I., Handmer, J., Nicholls, N., Peduzzi, P., Mechler, R., Bouwer, L. M., Arnell, N., Mach, K., Muir-Wood, R., Brakenridge, G. R., Kron, W., Benito, G., Honda, T., Takahashi, K., Sherstyukov, B. (2014), *Flood risk and climate change: global and regional perspectives*, Hydrological Sciences Journal, **59**, 1, pp. 1–28. DOI: 10.1080/02626667.2013.857411.

Kyriou, A., Nikolakopoulos, K. (2020), *Landslide mapping using optical and radar data: a case study from Aminteo, Western Macedonia Greece*, European Journal of Remote Sensing, **53**, 2, pp. 17–27. DOI: 10.1080/22797254.2019.1681905.

Lai, J.-S., Tsai, F. (2019), *Improving GIS-Based Landslide Susceptibility Assessments with Multi-Temporal Remote Sensing and Machine Learning*, Sensors, **19**, *17*, 3717. DOI: 10.3390/s19173717.

Li, Z., Li, X., Wang, Y., Quiring, S. M. (2019), *Impact of climate change on precipitation patterns in Huston, Texas, USA*, Anthropocene, **25**, 100193. DOI: 10.1016/j.ancene.2019.100193.

Li, Z., Tomas, R. (2017), *Earth Observation for Geohazards*, Remote Sensing, **386**. DOI: 10.3390/books978-3-03842-399-7.

Lin, W. T., Chou, W. C., Lin, C. Y., Huang, P. H., Tsai, J. S. (2005), *Vegetation recovery monitoring and assessment at landslides caused by earthquake in Central Taiwan*, Forest ecology and Management, **210**, pp. 55–66. DOI:10.1016/j.foreco.2005.02.026.

Liu, Z., Zhao, C., Zhang, Q., Yang, C., Zhu, W. (2020), *Heifangtai Loess landslide type and failure mode analysis with ascending and descending Spot-mode Terra SAR-X dates*, Landslides, **17**, pp. 205–215. DOI: 10.1007/s10346-019-01265-w.

Lyalko, V. I., Romanciuc, I. F., Yelistratova, L. A., Apostolov, A. A., Chekhniy, V. M. (2020), *Detection of Changes in Terrestrial Ecosystems of Ukraine Using Remote Sensing Data*, Journal of Geology, Geography and Geoecology, **29**, *1*, pp. 201–110. DOI: 10.15421/112010.

Lyalko, V. I., Elistratova, L. O., Apostolov, A. A., Khodorovsky, A. Ya., Czechniy, V. M. (2018), *Express-evaluation of potentially erosive soils on the territory of Ukraine, by using the remote sensing data with consideration of climatic factors and vegetation*, Reports of the NAS of Ukraine, **3**, pp. 87–94. DOI: 10.15407/dopovidi2018.03.087.

Lyalko, V. I., Elistratova, L. A., Apostolov, A. A., Chekhniy, V. M. (2017), *Analysis of soil erosion processes in Ukraine on the basis of remote sensing of the Earth*, Visn. Nac. Acad. Nauk Ukr, **10**, pp. 34–41. DOI: 10.15407/visn2017.10.034.

Lyalko, V. I., Elistratova, L. A., Kul'bida, M. I., Apostolov, A. A., Barabash, M. B. (2015), *Climate changes in Ukraine at the end of XX – beginning of XXI century according to ground and remote sensing data*, Ukrainian Journal of Remote Sensing of the Earth, **6**, pp. 33–63.

Lyalko Vadym Ivanovych (Eds.) (2015), *Greenhouse Effect and Climate Change in Ukraine: Assessments and Consequences*, Edit. Scientific Thought Publishing House of the NAS of Ukraine, Kyiv, 283 p.

Mandonca, M. B., Silva, D. R. (2020), *Integration of census data based vulnerability in landslide risk mapping – The case of Angra dos Reis, Rio de Janeiro, Brazil*, International Journal of Disaster Risk Reduction, **50**, 101884. DOI: 10.1016/j.ijdrr.2020.101884.

Martazinova, V. F. (2019), *Instability of daily summer air temperature from the beginning of the XXI century at Kyiv weather station*, Ukrainian Geographical Journal, **3**, pp. 15–21. DOI: 10.15407/ugz2019.03.015.

Matsuyama, H., Saito, H. & Zemtsov, V. (2021), *Application of Soil Water Index to landslide prediction in snowy regions: sensitivity analysis in Japan and preliminary results from Tomsk, Russia.* Prog. Earth Planet Sci. **8**, *17*. https://doi.org/10.1186/s40645-021-00408-9.

Mersha, T., Meten, M. (2020), *GIS-based landslide susceptibility mapping and assessment using bivariate statistical methods in Simada area, northwestern Ethiopia*, Geoenvironmntal Disaster, **7**, *20*. DOI: 10.1186/s40677-020-00155-x.

Mondini, A. C., Santangelo, M., Rocchetti, M., Rossetto, E., Mancioni, A., Monserrat, O. (2019), *Sentinel-1 SAR Amplitude Imagery for Rapid Landslide Detection. Remote Sensing*, Special Issue Landslide Hazard and Risk Assessment, **11**, *7*, 760. DOI: 10.3390/rs11070760.

Nikolic, T. (2014), *Direct and Indirect Impact of Landslide on Environment*, Engineering Geology for Society and Territory, **5**, pp. 1237–1241. DOI: 10.1007/978-3-319-09048-1_236.

Nugraha, H., Wacano, D., Dipayana, G. A., Cahyada, A., Mutaqin, B. W., Larasati, A. (2015), *Geomorphometric Characteristics of the Tinalah, Watershed, Menoreh Mountains*, *Yogyakarta, Indonesia.* Procedia Environmental Sciences, **28**, pp. 578–586. DOI: 10.1016/j.proenv.2015.07.068.

Panek, T. (2019), *Landslides and Quaternary climate changes – The state of the art*, Earth-Science Review, **196**, 102871. DOI: 10.1016/j.earscirev.2019.05.015.

Perera, E. N. C., Jayawardana, D. T., Jayasinghe, P., Bansara, R. M. S., Alahakoon, N. (2018), *Direct impacts of landslides on socio-economic systems: a case of study from Aranayake, Sri Lanka*, Geoenvironmental Disasters, **5**, *11*. DOI: 10.1186/s40677-018-0104-6.

Popov, M. A., Stankievich, S. A., Kozlova, A. A. (2012), *Remote risk assessment of land degradation using satellite images and geospatial modelling*, Reports of the NAS of Ukraine, **6**, pp. 100–104.

Pradhan, B. (2017), Laser Scanning Applications in Landslide Assessment, *Springer International Publishing*, **360**. DOI: 10.1007/978-3-319-55342-9.

Ramos-Bernal, R. N., Jimenez, R. V., Calcerrada, R. R., Funes, P. A., Novillo, C. J. (2018), *Evaluation of Unsuprvisec Change Detection Methods Applied to Landslide Inventory Mapping Using STER Imagery*, Remote Sensing. Special Issue Landslide Hazard and Risk Assessment, **10**, *12*, 1987. DOI: 10.3390/rs10121987.

Refice, A., Spalluto, L., Bovenga, F., Fiore, A., Miccoli, M. N., Muzzicato, P., Nitti, D. O., Nutricato, R., Pasquariello, G. (2019), *Integration of persistent scatterer interferometry and ground data for landslide monitoring: the Pianello landslide (Bovino, Southern Italy)*, Landslides, **16**, pp. 447–468. DOI: 10.1007/s10346-018-01124-0.

Smith, S. G., Wegmann, K. W. (2018), *Precipitation, landsliding, and erosion across the Olympic Mountains, Washington State, USA*, Geomorphology, **300**, pp. 141–150. DOI: 10.1016/j.geomorph.2017.10.008.

Solari, L., Soldato, M. D., Montalti, R., Bianchini, S., Raspini, F., Thuegaz, P., Bertolo, D., Tofani, V., Casagli, N. (2019), *A Sentinel-1 based hot-spot analysis: landslide mapping in north-western Italy,* International Journal of Remote Sensing, **40**, *20*, pp. 7898–7921. DOI: 10.1080/01431161.2019.1607612.

Soldato, M. D., Solari, L., Poggi, F., Raspini, F., Tomas, R., Fanti, R., Casagli, N. (2019), *Landslide-induced Damage Probability Estimation Coupling InSAR and Field Survey Data by Fragility Curves*, Remote Sensing of Landslides II, **11**, *2*, 1486. DOI: 10.3390/rs11121486.

Svetlitchnyi, A. A. (2009), *Soil Erosion Induced Degradation of Agrolandscapes in Ukraine: Modeling, Computation and Prediction in Conditions of the Climate Changes*, in: Groisman, P.Y., Ivanov, S.V. (eds): Regional Aspects of Climate-Terrestrial-Hydrologic Interactions in Non-boreal Eastern Europe. NATO Science for Peace and Security Series C: Environmental Security, Springer, Dordrecht, pp. 191–199. DOI: 10.1007/978-90-481-2283-7_21.

Svetlitchnyi, A. A. (2018), *Evaluation of changes in hydrameteorological conditions of rain storm soil erosion in steppe and forest-steppe zones of Ukraine in connection with climate change,* Visn. Odes. Nat. univ., Geogr. Geol. Sciences, **23**, 1–32, pp. 53-71. DOI: 10.18524/2303-9914.2018.1(32).141951.

Tang, Y., Feng, F., Guo, Z., Feng, W., Li, Z., Wang, J., Sun, Q., Ma, H., Li, T. (2020), *Integrating principal component analysis of casual factors and landslide susceptibility mapping: A comparative study from the leoss plateau area un Shanxi (China),* Journal of Cleaner Production, **277**, 124159. DOI: 10.1016/j.jclepro.2020.124159.

Timchenko, O., Ugnenko, E., Makovyey, R. (2016), *Analysis of Methods of Landslide Processess Forecasting on Highways*, Procedia Engineering, **134**, pp. 146–152. DOI: 10.1016/j.proeng.2016.01.051.

Wasko, C., Sharma, A. (2017), *Global assessment of flood and storm extremes with increased temperatures*, Scientific Reports, **7**, 7945. DOI: 10.1038/s41598-017-08481-1.

Zhang, S., Yin, Y., Hu, X., Wang, W., Zhang, N., Zhu, S., Wang, L. (2020), *Dynamics and emplacement mechanisms of the successive Baige Landslides on the Upper Reaches of the Jinsha River, China,* Engineering geology, **278**, 105819. DOI: 10.1016/j.enggeo.2020.105819.

Zhao, C., Lu, Z. (2018), *Remote Sensing of Landslides-A Review,* Remote Sensing. Remote Sensing of Landslides Special Issue, **10**, *2*, 279. DOI: 10.3390/rs10020279.

Zhao, F., Mallorqui, J. J., Iglesias, R., Gili, J. A., Corominas, J. (2018), *Landslide Monitoring Using Multi-Temporal SAR Interferometry with Advanced Persistent Scatterers Identification Methods and Super High-Spatial Resolution TerraSAR-X Images*, Remote Sensing. Ten Years of Terra SAR-X-Scientific Results, **10**, *6*, 921. DOI: 10.3390/rs10060921.

RECENT DYNAMICS OF THE SECONDARY SECTOR IN ROMANIA. REGIONAL DISPARITIES

BIANCA MITRICĂ[*], RADU SĂGEATĂ[*], IRENA MOCANU[*],
NICOLETA DAMIAN[*], ADRIANA NEAGOE[**]

Abstract. The secondary sector of the Romanian economy has in time suffered several modifications, the most important ones being linked to the political and legislative systems. The present paper, which analyses the secondary sector in the Romanian economy, relies on the following variables: the turnover, the employed population, net investments, as well as various indicators that illustrate the enterprises' demographic picture. This paper is a spatial/geographical approach of the secondary sector in the national economy context; its sub-branches, processes, social and economic actions, which influence its evolution in space, are entirely different. The space dimension of the variables analysed herein emphasizes the structural-quantitative changes which have occurred during the past few decades in the whole secondary sector and in each of the eight development regions. This approach proved useful in completing the more general economic analysis. The time-interval this analysis refers to is not the same for all the indicators chosen. However, the last two decades are fully covered by all the four variables taken into consideration.

1. INTRODUCTION

Once in power, the Romanian communist system focused on industrialization as a way of economic development. The major goal of the then state policy was to achieve a balanced development of the country's territory. Central-based planning, investments in different economic sectors, mostly in the secondary one, were made in all of the country's regions, irrespective of whether they were economically justified, or not. Concentrating industrial investments, especially in towns, made many villagers choose the town area, hence a higher rate of urbanzation. Redistributing the population had a negative effect on the rural environment, reducing its demographic vitality, and thus declining economically. The towns themselves were negatively affected (through swift urbanization), having to cope with demographic and social pressures too high for the available housing stock, as well as for their technical and social infrastructure (Popescu *et al.*, 2016).

After 1990, industry turned from a main way to progress into a main cause of economic decline. That year represents a major breach in the evolution of Romania's industry, and the traits of the secondary sector, characteristic of that moment, are quite relevant for understanding the deeply-rooted structural changes recorded over the last few decades, *i.e.* a gigantic industry (numerous big enterprises) exclusively state property, dominantly heavy industry (metallurgy and machine-building) units, the industry-governed functional specialization of large cities, and the presence of factory-towns (small urban centres under 20,000 inhabitants – whose economy was dependent on one big industrial plant alone); the rural sector featured industrial diffusion, with only a few minor concentrations here and there (Popescu, 2016). After 1990, restructuring was characteristic of the Romanian industrial sector: in-depth changes in the type of property, mode of production, forms of organization, development policies, relationships between activities in the secondary sector and the environmental components.

---

[*] Senior Researcher, Institute of Geography, Romanian Academy, 12 Dimitrie Racoviţă Street, 023993, Bucharest, Romania, biancadumitrescu78@yahoo.com; rsageata@gmail.com; mocanitai@yahoo.com; nicoleta_damian2002@yahoo.com.
[**] PhD student, Aerospace Service, 44/A Ficusului Blvd., Bucharest, Romania, adriana.mateescu93@gmail.com.

A decisive element for industrial evolution after 1990 was the legal framework. Although the mining industry was considered to be a strategic industry, the post-1990 restructuring processes did not spare this sector either, conferring it an unwanted specificity, namely the degradation of the economic structures in mining areas, destroying the miners' social identity and creating severe social imbalances. Based primarily on an economic reason, as well as on environmental protection, restructuring the mining industry showed major temporal discontinuities, among which collective layoffs, reorganization of the extractive activity and the legislative framework regarding the action of restructuring the mining areas. In 1997, the wave of restructuring, began with collective layoffs, which affected the over 200,000 people engaged in mining, adding up to the several hundreds of thousands directly, or indirectly, dependent on that industry. This action did not rely on any single normative act to stipulate the stages, actions, and concrete measures of the restructuring process. The Law of the Mines, passed in March 1998 – *Law No. 61/1998* (Parlamentul României, 1998), although restructuring the mining industry, had begun with massive layoffs in August–September 1997 (Mocanu, 2008). *Law No. 15/1991* (Parlamentul României, 1991)*,* which stipulated that industrial enterprises be turned into commercial societies, was the moment when the processing industry started on a downward trend (Popescu, 2016). Industrial processing branches had to adjust to the new conditions and put up with new challenges. Some of them would choose decentralising in order to fit into the smaller economy of lower-size companies, and develop more flexible collaboration relations. On the other hand, industrial units would merge in order to better cope with competition and, thus, trusts and holdings emerged.

A spatial approach to the secondary sector implies analysing the differences between one type of space and the other (*e.g.* urban versus rural areas, development counties and regions, or historical regions, between various categories of towns etc.). An area's dynamics is generated by the multitude of economic, social, cultural etc. changes. In the post-communist period, modifications, transformations and restructuring were omnipresent in spatial evolution, and when territorial actors – as a major component of territorial development – started to also diversify and multiply, the premises were laid for a very complex process of changing the geographical space. The space-based approach to the industrial sector is beneficial for the economic sciences. Quite often, the macro-space analysis hides and distorts secondary sector dynamics (and not only of this sector) at lower territorial levels, therefore, the all-country level study offers a far too superficial generalization of regional and local trends, which have a greater impact (in terms of economic activities) on the economic communities and economic actors.

Consequently, this paper is aimed at studying the secondary sector in terms of aspects revealed by its relation with space (*i.e.* the level of the 8 Development Regions), but also with homogeneous groups of "economic entities" (*i.e.* through the analyses the secondary sector in terms of the Classification of Activities in the National Economy (CAEN Rev 1, 2) which offer distinct picture of categories of factories or enterprises). Thus, this paper approached the structural-quantitative changes which have occurred during the past few decades in the whole secondary sector, through the following variables: the turnover, the employed population, net investments, as well as various indicators that illustrate the enterprises' demographic context. The economic activities the secondary sector is subdivided into (according to CANE Rev 1 and 2) are: extractive industry; processing industry; construction; electrical and thermal energy, gas and water; gas, hot water and air conditioning; water distribution, scavenging, management of wastes, decontamination activities. The enterprises' demographic component is illustrated by analysing secondary sector units at national level, as well as the economic activities included in this sector.

2. STUDY-AREA

The Romania's administrative-territorial structure has the following levels: NUTS2 (8 development regions without administrative and legal person status, an average population number/region of 2.8 million inhabitants); NUTS3 (41 counties and Bucharest Municipality) and NUTS5/LAU (319 towns, and 2,862 communes). The regional development policy in Romania has been closely correlated with the use of pre-accession instruments offered by the European Union to restart the

national economy after the severe deindustrialization and excessive fragmentation of agriculture, processes with a strong social impetus that marked the 1990s (Mitrică *et al.*, 2020).

The starting point for the delimitation of Romania's Development Regions was the elaboration of a study on regional disparities, on the basis of the socio-economic evolution taking place in the 1990–1994 period. The development-gap analysis took account of indicators grouped into five categories: the economy, infrastructure, household resources, socio-demography and urbanisation. (Hansen, *et al.*, 1996).

The study is focusing on the Development Regions of Romania – the NUTS 2 level (Fig. 1). Designed as regional spaces with specific development problems, the Development Regions were delineated as functional spaces of comparable size composed of units with different levels of economic and social development. In terms of area and demographic size, with the exception of the Bucharest–Ilfov Region, the regions are slightly different, corresponding to NUTS 2 of the EU Territorial Units Nomenclature (Table 1) (Popescu and Săgeată, 2016).

Fig. 1. The Development Regions of Romania.

Table 1

Main characteristics of the Development Regions, 2018

Development region – NUTS2	Counties/NUTS3	Region centre	Population	Area	Share of employees in secondary sector
North-West	Bihor, Cluj, Bistriţa-Năsăud, Maramureş, Satu Mare, Sălaj	Cluj-Napoca	2,836,219	3,416,046	39.4
Centre	Alba, Braşov, Covasna, Harghita, Mureş, Sibiu	Alba-Iulia	2,634,748	3,409,972	42.6
North-East	Bacău, Botoşani, Iaşi, Neamţ, Suceava, Vaslui	Piatra-Neamţ	3,939,938	3,684,983	32.4
South-East	Brăila, Buzău, Constanţa, Galaţi, Tulcea, Vrancea	Brăila	2,859,897	3,576,170	34.2
South-Muntenia	Argeş, Călăraşi, Dâmboviţa, Giurgiu, Ialomiţa, Prahova, Telorman	Călăraşi	3,242,876	3,445,299	40.0
Bucharest–Ilfov	Ilfov, Bucharest Municipality	Bucharest	2,510,877	182,115	21.4
South-West Oltenia	Dolj, Gorj, Olt, Mehedinţi, Vâlcea	Craiova	2,194,235	2,921,169	37.7
West	Arad, Caraş-Severin, Hunedoara, Timiş	Timişoara	2,012,053	3,203,317	42.5

Source: data processed from http://statistici.insse.ro/shop/?lang=ro

In socio-economic terms, differentiations between development regions are moderate, with the exception of the North-East Development Region which has lower performances (Guvernul României, Comisia Europeană, 1997, Popescu, Săgeată, 2016, Mitrică *et al*, 2019).

3. DATA AND METHODOLOGICAL ASPECTS

The methodological approach involves several steps, such as: (1) selecting the statistical indicators, (2) building the database and (3) processing the data into graphics and maps.

(1) ***The selection*** of statistical indicators was generated by the availability of statistical variables contained in the main official source of data, namely the National Institute of Statistics, TEMPO-Online Time Series (National Institute of Statistics, 1992, 2002, 2011, 2015).

(2) These data were organized in a ***database***, structured by variables and indicators (2.1.), by Classification of Activities in the National Economy (CAEN Rev 1, 2) (2.2) and by years (2.3.). (*2.1.*) Analysing the economic sector was based on the following variables and indicators: the turnover, the employed population, and net investments in the whole secondary sector (over two intervals: 2003–2008 and 2008–2015). (*2.2.*) A longer time-interval (1992–2016) is devoted to looking at the employed population, having in view that the demographic component of a territorial system has greater inertia, the current situation of this component is the result/effect of the socio-demographic and economic evolutions developed decades back, while the trends are expected to be seen in coming decades. (*2.3.*) The present study analyses the secondary sector in terms of the Classification of Activities in the National Economy (CAEN Rev 1, 2), so that the observations made and conclusions reached in this paper are distinguished not only in relation to space (at the level of the Eight Development Regions), but also of homogeneous groups of 'statistical units' (*i.e.* a factory, or a group of factories which form an economic entity – an enterprise). The economic activities the secondary sector is subdivided into (according to CANE Rev 1 and 2) are: extractive industry; processing industry; construction; electrical and thermal energy, gas and water; gas, hot water and air conditioning; water distribution, scavenging, management of wastes, decontamination activities. The enterprises' demographic component is illustrated by analysing secondary sector units at national level, as well as the economic activities included in this sector.

(3) An important step of the methodological approach consists in ***processing the data into graphics and maps*** that show the trends and dynamic differences of the secondary sector both, in time and space.

4. RESULTS

4.1. The turnover dynamics

The 1998–2008 turnover is progressively growing throughout the secondary sector, from 255,083 mil. Lei in 1998 to 1,793,653 mil. Lei in 2004, 1,946,530 mil. Lei (*i.e.* 194,653 RON) in 2005 and 316,132 RON (3,161,320 mil. Lei old currency) in 2008.

The highest turnover at sub-sectorial level was registered by the processing industry, followed by the construction, electrical and thermal energy, gas and water industries. At the same time, the extractive industry proved to be less investment-attractive, with the lowest turnover score (Fig. 1).

At regional level, the highest turnover value was registered by the Bucharest–Ilfov and South-Muntenia Regions, the lowest values going to the West, North-East and South-East Regions (the poorest regions, investment-unattractive, having an economy largely based on agriculture and the extractive industry) (Fig. 2).
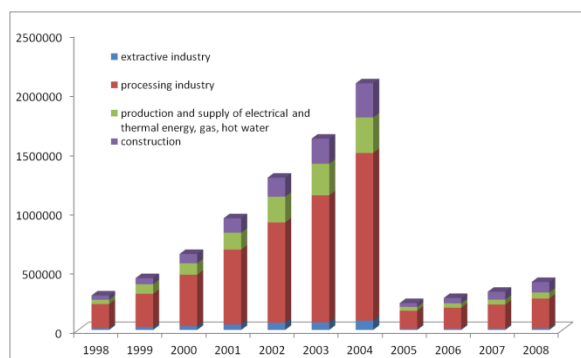
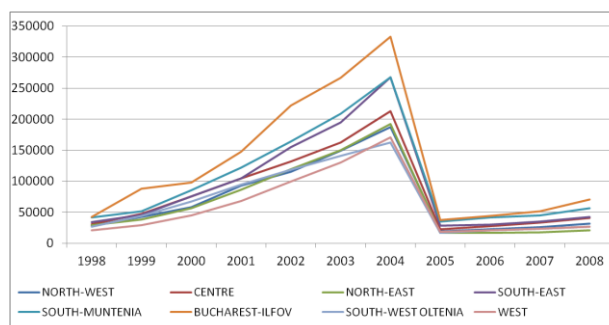Fig.1 – Secondary sector turnover dynamics at national level, 1998–2008 (mil. Lei).

Fig. 2 – Secondary sector turnover dynamics at regional level, 1998–2008 (mil. Lei).

In the first part of 2008–2018, as a result of the economic-financial crisis, the turnover was negative, followed by an increase until 2011 (when it registered higher values than at the beginning of that period), its evolution fluctuating until 2015, when the secondary sector turnover exceeded 450,000 mil. Lei (Fig. 3). Looking at the national activities in this sector, one finds investment to prevail in the processing industry, in construction, energy and the thermal industry, hot water and air conditioning. At the other end of the spectrum lie investments in the extractive industry and in the commercial management sector.
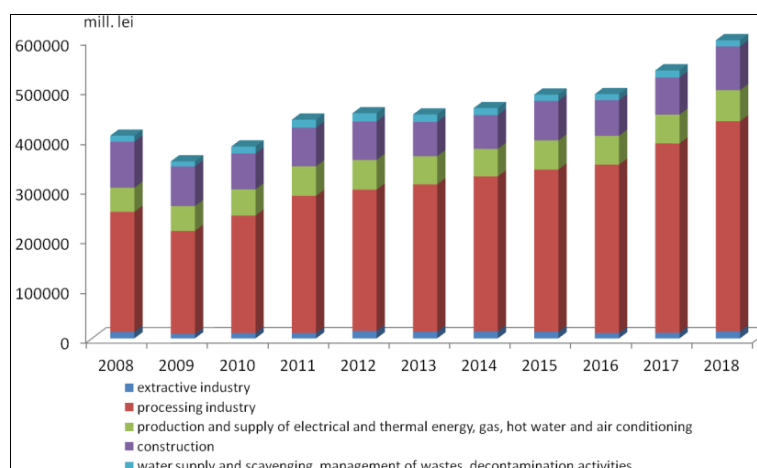
Fig. 3 – Secondary sector turnover dynamics at national level, 2008–2015.

Distinguishing the secondary sector by activities in the national economy shows the following industries having benefitted from major investments: the processing industry, construction, the energy and thermal industry, gas, hot water and air conditioning. At the other end of the spectrum we have investments in the extractive industry; the communal management sector (distribution of water, scavenging, management of waste and decontamination), which proved little investment-attractive.

The fluctuating evolution of the 1998–2008 turnover in the *extractive industry* is the result of legislative inconsistency and of attempts, largely unsuccessful, to restructure and make this industry more efficient. Thus, in 1998, 2000, 2001, 2002 and 2003 the highest turnover values in this industry were registered by the South-West Oltenia Region. At the other end were the South-East and North-East Regions (Fig. 4a). Between 2008–2018, the turnover was constantly positive in the extractive industry due to investments made in the Centre, South-Muntenia, South-East and South-West Regions (Fig. 4b).
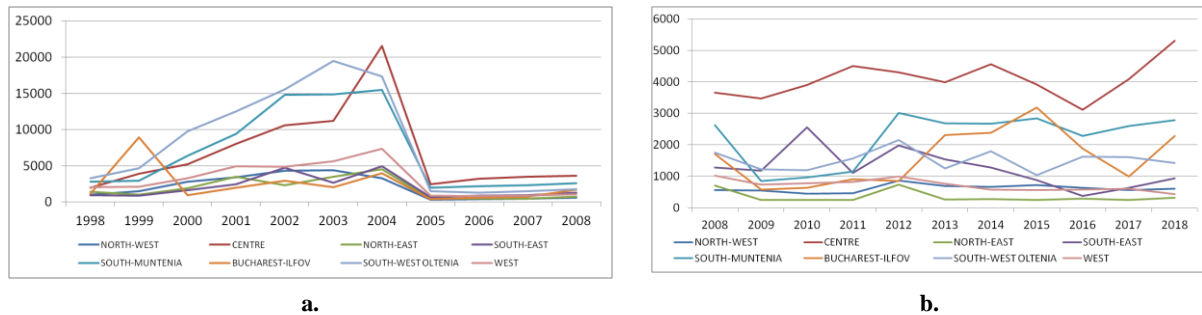
a.   b.

Fig. 4 – Turnover evolution in the extractive industry (mil. Lei): a. 1998–2008; b. 2008–2018.

The processing industry. The turnover registered constant growth, from 203,634 mil. Lei in 1998 to 1,415,109 mil. Lei in 2004, 241,259 mil. Lei in 2008 and 422,916 mil. Lei in 2018. The highest turnover values were registered by Bucharest–Ilfov and South-Muntenia, the lowest ones by the South-West Oltenia, West and North-East Regions (Fig. 5a, b). The capital-city Bucharest and its peripheral zone (Bucharest–Ilfov Region) became increasingly less attractive for investments in the processing industry, successively falling behind South-West Oltenia, Centre, West and even North-East Regions (in 2018) (Fig. 5 b).

a.   b.
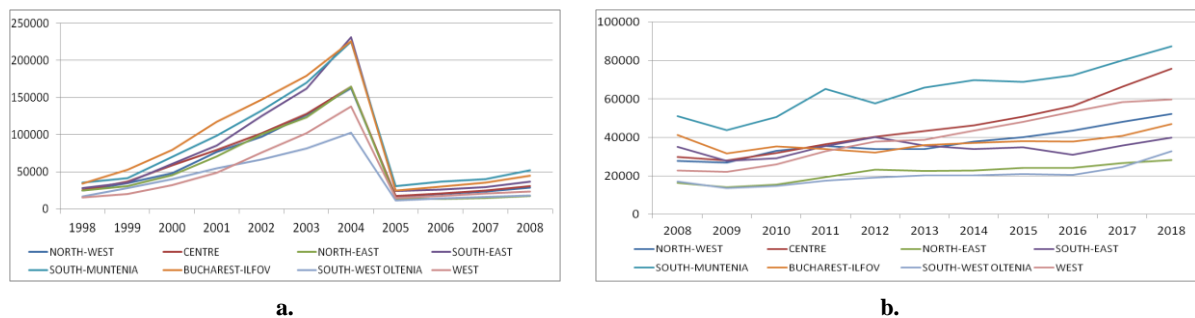
Fig. 5 – Turnover dynamics in the processing industry (mil. Lei): a. 1998–2008; b. 2008–2018.

In the area of production and distribution of electrical and thermal energy, gas, water and scavenging, management of waste and decontamination, a positive turnover evolution was constantly registered, the Bucharest–Ilfov Region being the clear standout.

In the interval between 2008 and 2018, the Bucharest–Ilfov Region headed the charts with a turnover of 2,300,000 and 3,500,000 Lei (top figure in 2011), with the Centre and South-West Oltenia Regions next in line. Regarding water supply, scavenging, management of wastes and decontamination, Bucharest–Ilfov had the lowest turnover score.

For the interval between 1998 and 2008, the turnover in the field of electric power and heating, gas and water the Bucharest–Ilfov region, South-West Oltenia and South-East regions recorded maximum values, while the other development regions registered low values.

For the interval between 2008 and 2018, the situation is quite similar in terms of regional distribution: the Bucharest–Ilfov region recorded a turnover ranging between 2,300,000 and 3,500,000 thousand Lei (with the highest value in 2011), followed by Centre and South-West Oltenia regions with a different dynamic (positive for the first one and negative for the second).

In water distribution, sanitation, waste management and decontamination activities, the highest turnover figures pertained to the Bucharest–Ilfov region, which registered an oscillating dynamic: decreasing between 2008 and 2009, ascending during the interval 2009–2012, followed by a new

downward spiral between 2012 and 2015. This development region was consistently followed by the South-East, South-Muntenia, Centre and West regions, all of them recording oscillating trajectories similar to that of the Bucharest–Ilfov region.

Turnover evolution in *construction* (Fig 6 a, b) was constantly on the increase. However, the economic-financial crisis was being felt in the regression between 2008–2010 and in the oscillating course from 2010 to 2014. Outstanding again was the Bucharest–Ilfov Region in both intervals, followed at a great distance by the North-West Region, with the lowest score in the South-West Oltenia Region.
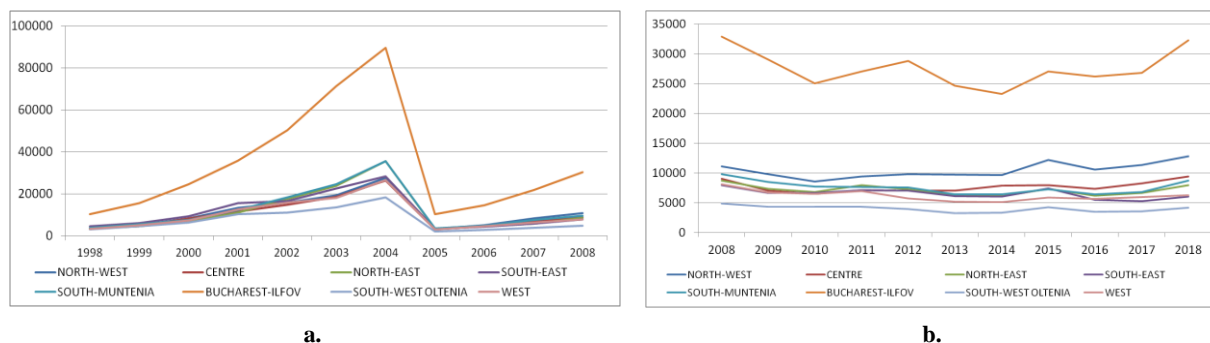
Fig. 6 – Turnover evolution in construction (mil. Lei): a. 1998–2008; b. 2008–2018.

4.2. Employed population dynamics

At national level (1992–2018) the study of the employed population in the secondary sector covered the years 1992–2008 and 2008–2018 (Fig. 7a). Thus, in the first interval, the population employed in this sector was steadily decreasing (from 3,900 to 2,400 people between 1992 and 1999) followed by a period of stagnation at 2,500 employed people. In terms of the types of economic activity in the secondary sector, the majority of the employed population (two–thirds of it worked in the processing industry, then in construction, the extractive industry, electrical and thermal energy, gas and water.
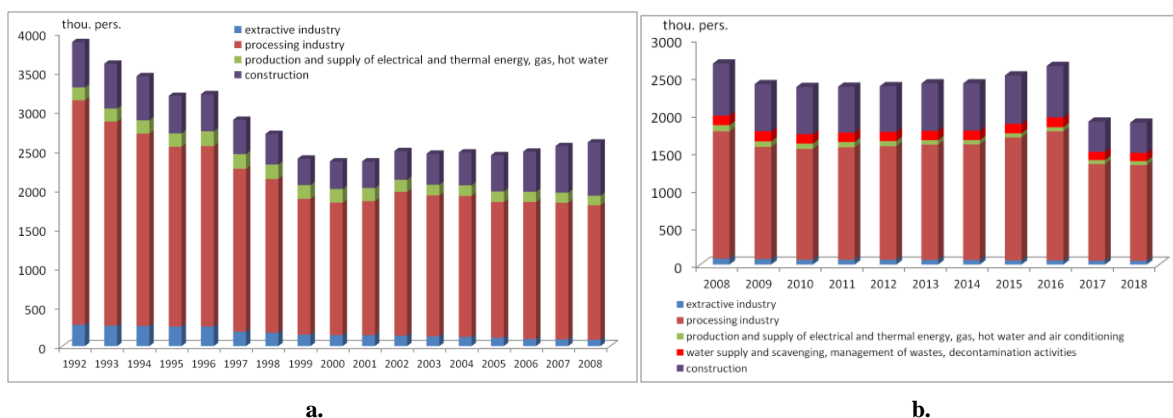

Fig. 7 – Dynamics of the population employed in the secondary sector, a. 1992–2008, b. 2008–2018

The interval between 2008 and 2018 features oscillating evolutions in the secondary sector population (around 2,300–2,600 individuals employed), with the highest values in 2008 before the economic crisis-induced layoffs, and from 2015–2018, when people started being employed given the

post-crisis recovery. Depending on the economic activities discharged in this sector over the same time-interval, most people were employed in the processing industry and in construction (best recovering after the economic-financial crisis). Together, these two types of activity registered over three-fourths of the secondary sector's employed population. At the same time, the population working in the extractive industry, electrical and thermal energy, gas, hot water and air conditioning, water supply, scavenging, management of wastes and decontamination proceeded to personnel cuts (Fig. 7b).

Restructuring the mining sector, which began after 1990, as well as failed privatizations, turned the extractive industry into one of the most vulnerable economic activities, large-scale layoffs join on as numerous production units closed down. Declaring less-favoured mining zones proved an unsuccessful attempt at making up for layoffs by granting investors facilities.

Thus, between 1992 and 2008, *the population employed in the extractive industry* was considerably reduced in all development regions, except for the Bucharest–Ilfov Region where, after 2005, they began employing people in the central administration. Most mining areas experienced steep decreases, especially from 1996 to 1997 (West, South-West Oltenia, North-West, South-Muntenia and North-East Regions), the decline being less obvious in the mining areas of the South-East and Centre Regions because the extractive sector was less developed there. After 2008, differences in the evolution trend became apparent: the regions with a well-developed mining sector (South-West Oltenia, South-Muntenia and the West Regions) continued to lose people employed in extractive activities, while the regions where this industry held a lower share (South-East, Bucharest–Ilfov and North-East) had an oscillating record, employment alternating with layoffs (Figs. 8, 9, 10).
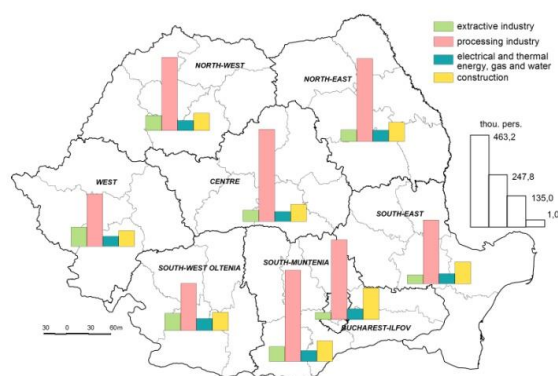

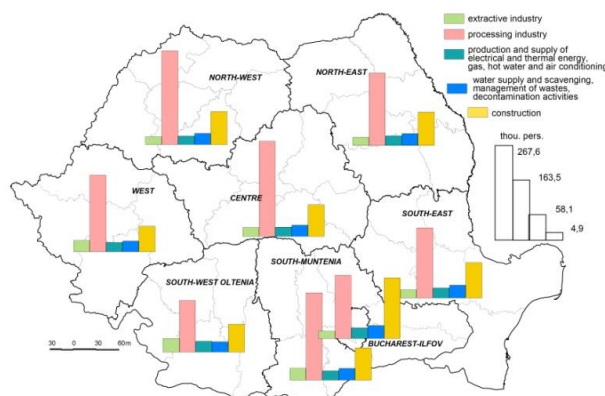Fig. 8 – The structure of the employed population by secondary sector branches, 1992.

Fig. 9 – The structure of the employed population by secondary sector branches, 2008.

Analysing the two reference intervals (1992–2008 and 2008–2018) we found that the evolution trend in the *processing industry workforce* was similar in all the development regions. However, a steeper decline was registered in the first interval in the Centre and South-Muntenia Regions, followed by an oscillating period, mainly of stagnation, and one of increase after 2014. Most people employed in the processing industry were in the Centre and North-West Regions, which had a greater demographic availability and a sustained economic growth (in 2013, the North-West Region was ahead of the Centre Region in regard to the population working in the processing sector), next in line being South-Muntenia and the West Regions (the last one having the most constant growth of population employed in this industry), the North-East, South-East, and Bucharest–Ilfov Regions, with the South-West Oltenia Region coming constantly last (Figs. 8, 9, 10).
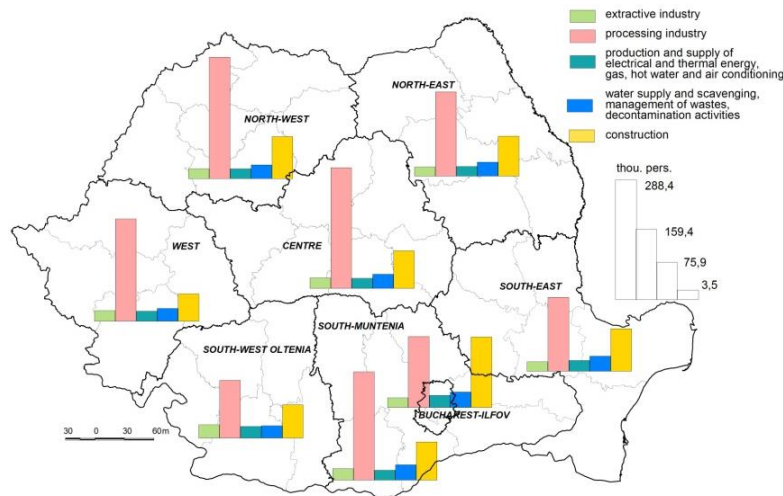
Fig. 10 – The structure of the employed population by secondary sector branches, 2018.

Within the first part of the 1992–2008 interval, the *population employed in the energy and thermal, gas and hot water, and air conditioning industries* experienced an increasing evolution (especially the North-East, South-Muntenia and North-East Regions); however, during 1997–2008 all the eight development regions registered involutions. Thus, in 2008, the hierarchy of development regions had changed, the first positions being occupied by South-Muntenia and South-East Regions followed by Bucharest–Ilfov, North-East, Centre and South-West Oltenia, the last places going to the West and North-West Regions. The evolution of the population employed in the production and supply of electrical and thermal energy, gas, hot water and air conditioning over 2008–2018 indicated a general declining trend, especially in the South-West Oltenia, South-East, South-Muntenia, Centre and North-East Regions (the last one having the worst record) (Figs. 8, 9, 10).

An oscillating evolution between 2008–2018 was recorded by the population working in the water supply, scavenging, management of wastes and decontamination sectors (Fig. 7b), which sharply decreased during certain years in the Bucharest–Ilfov, South-East and Centre Regions, as well as in South-Muntenia. The most important employment of personnel, with positive effects on the evolution of the population working in these fields, took place over various periods of time in Bucharest–Ilfov, South-East, North-East, South-Muntenia, South-West Oltenia and other regions (Figs. 8, 9, 10).

Throughout the 1992–2008 interval, *the population employed in construction* experienced two distinct evolution trends in all the development regions, particularly in 1990. The most obvious evolution record was had by the Bucharest–Ilfov Region, with an explosive growth especially in the City's peri-urban area (from 50,000 pers. to over 160,000 pers.). A stagnation occurred from 2008 to 2018 in the employment of population in this sector, which affected all developed regions, with slight employment decreases from 2009 to 2016 and mild increases over 2015–2016 (Figs. 8, 9, 10).

4.3. Net investments dynamics

Within the 2003–2008 interval (Fig. 11a), net investments in the secondary sector registered consistent growth throughout the country. Most investments were made in the processing industry, which reached impressive growth to the detriment of the extractive industry which was faced with difficulties in being restructured and becoming efficient. After investing in the processing industry, there followed construction, electrical energy, gas and water, and eventually in the extractive industry, which proved to be the least net investment-attractive sector.
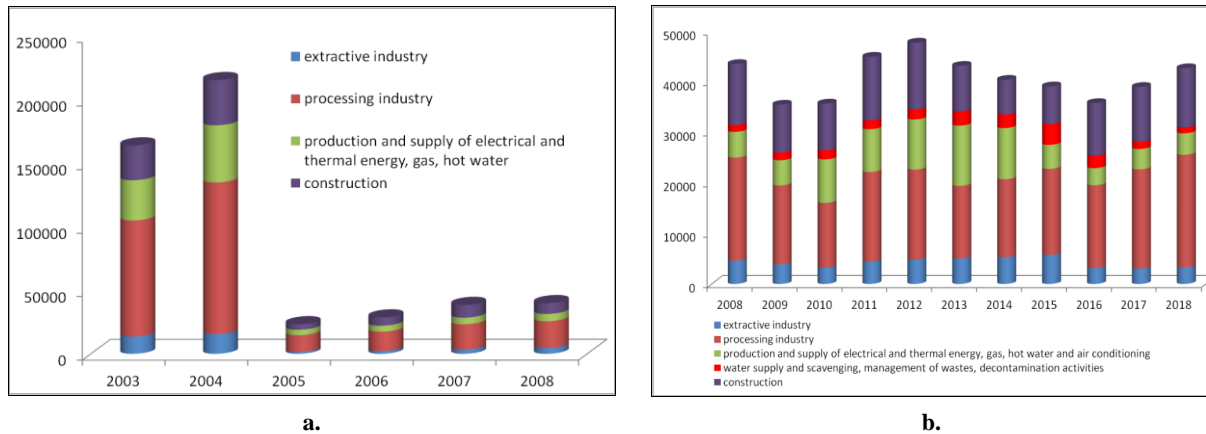
a.   **b.**

Fig. 11 – Net investment evolution in the secondary sector (mil. Lei), a. 2003–2008, b. 2008–2018.

Beginning with 2008, net investments in the secondary sector started oscillating primarily due to the financial crisis-induced decline in 2008–2009, with a second negative trend occurring in 2012–2015 (Fig. 11b).

In the net investment structure, the processing industry held pride of place, next in line standing production and supply of electrical and thermal energy, gas, hot water and air conditioning (a sector that decreased significantly between 2013 and 2015), construction, extractive industry and water supply, scavenging, management of waste and decontamination, the share of the last sector increasing significantly in 2015 versus 2008.

Net investments in the extractive industry at the end of the 1990s suffered sharp cuts in all the development regions because restructuring and effectiveness policies in this economic sector failed. After 2006, it was South-Muntenia Region that headed the list, with the Centre and South-West Oltenia Regions coming next in line (Figs. 12 a, b).
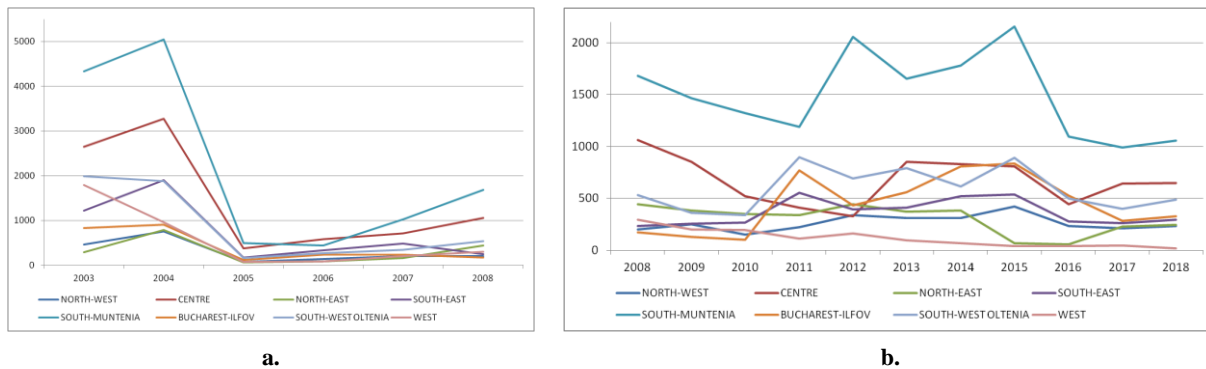

a.   **b.**

Fig. 12 – Net investments in the extractive industry (mil. Lei), a. 2002–2008, b. 2008–2018.

Net investments in the processing industry were concentrated in the South-Muntenia, Bucharest–Ilfov, North-West, Centre and West Regions. Until 2008, all development regions had a pretty similar dynamic in attracting net investments (see the hierarchy in Fig. 13a). However, the economic-financial crisis would disturb the course of capital intake, all development regions having a fluctuating record in this respect (Fig. 13b). At the top of the net investments' hierarchy (basically the net investment value) we may find the South-Muntenia and Centre Regions, with the poorest regions (North-East and South-West Oltenia) falling to the bottom; the Bucharest–Ilfov Region (the last position in 2010–2012) was involved mainly in the third sector.
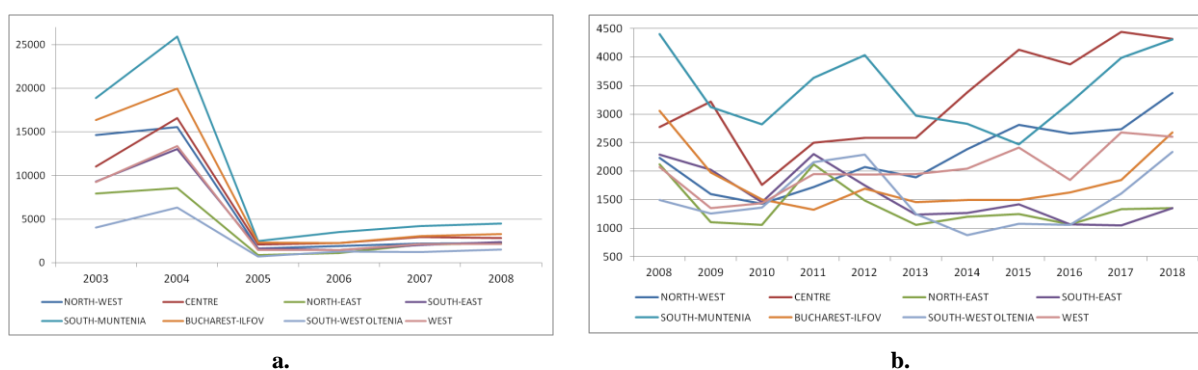
a.

b.

Fig. 13 – Net investments dynamics in the processing industry (mil. Lei), a. 2003–2008, b. 2008–2018.

Net investments in electrical and thermal energy, gas, water, scavenging, air conditioning, management of wastes, and decontamination recorded an evolution relatively similar to that in the processing sector, *i.e.* quite relative from 2003 to 2008, followed by a mild decrease especially in the Bucharest–Ilfov Region during 2007.

After 2008, investments registered great fluctuations. The biggest capital vested in the supply of electrical and thermal energy, gas, hot water and air conditioning went to the South-West Oltenia, South-East and Bucharest–Ilfov Regions. As to net investments in water supply, scavenging, management of waste and decontamination, it was the South-East Region that has stood at the forefront ever since 2010. In 2015, preferential investments were earmarked for the North-West and South-Muntenia Regions.

Net investments in construction were concentrated in the Bucharest–Ilfov Region, being ten times higher than the average value registered by the other regions. During the economic-financial crisis, the land-price increasing fewer net investment went to construction (Fig. 14 a, b).
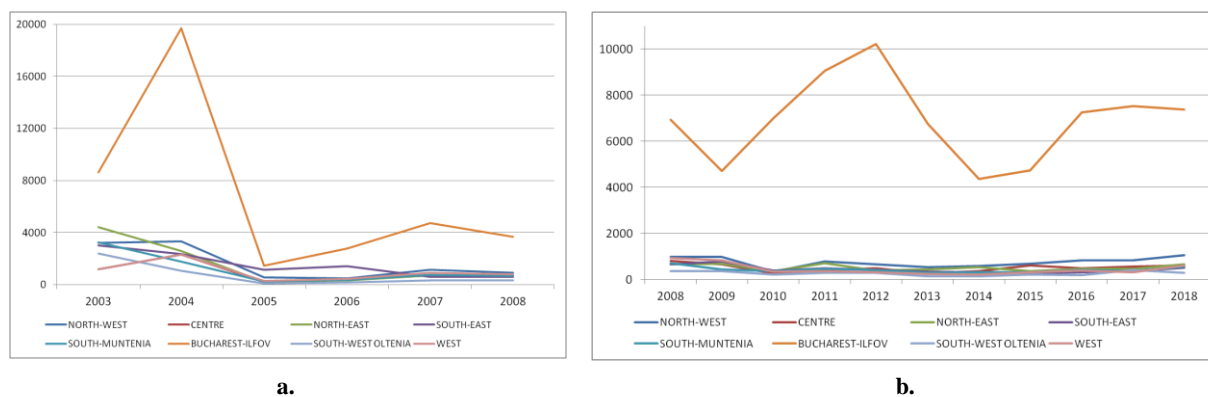

a.

b.

Fig. 14 – Net investment dynamics in construction (mil. Lei), a. 2003–2008, b. 2008–2018.

4.4. Enterprises and their demographic component

Between 2002 and 2008, secondary sector units had been constantly growing all over the country by twice as many units (from 60,000 to 120,000), being set up especially in the processing and construction branches. The share of extractive industry, energy and thermal, gas and water sectors was simply insignificant.

After 2009, the economic-financial crisis marked the evolution of secondary sector units, which decreased from 120,000 to some 90,000 over the 2009–2011 period. What followed was a slow increase and then a stagnation (2014–2015), no more than 100,000 units being left mainly in the processing and construction sectors, themselves numerically reduced in the 2008–2018 interval. An insignificant proportion of units in the extractive industry production and supply of electrical and thermal energy, gas, hot water and air conditioning, water supply, scavenging management in waste and decontamination.

Extractive industry units went on an upward trend but at distinct rates: faster in 2002–2004 and 2006–2008, and slower in 2004–2006. Most extractive industry units were located in the regions North-West, Centre, South-Muntenia, South-West Oltenia and West, with North-East and Bucharest–Ilfov Regions coming next in line, where the latter sector was less represented in the regional economic structure. From 2008 to 2015, the number of extractive industry units would increase beyond the 1,400-threshold fluctuating afterwards around 1,200–1,300 units. Most of them continued to be concentrated in the North-West, Centre, West and South-West Oltenia Regions, their share decreasing in the South-West Oltenia Region because many mining exploitations were being closed (Fig. 15, 16, 17).
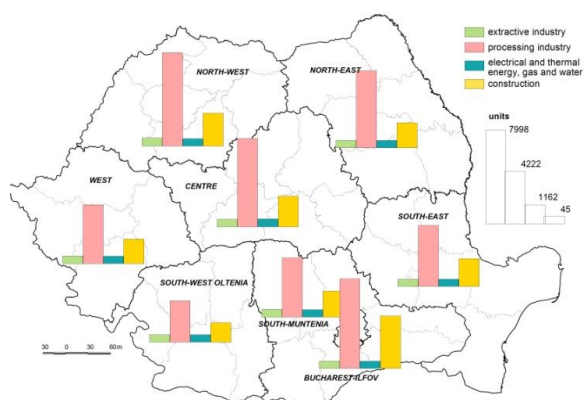

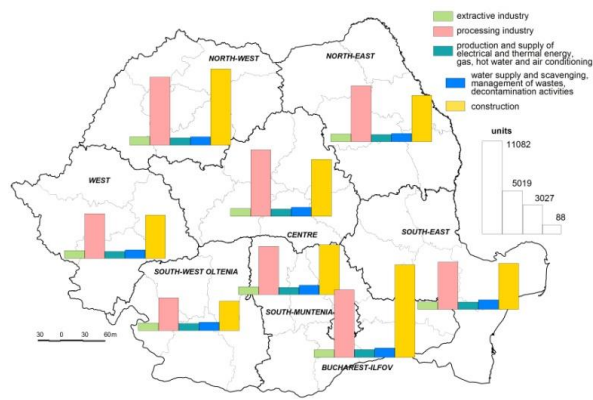Fig. 16 – The structure of secondary sector units, 1992.

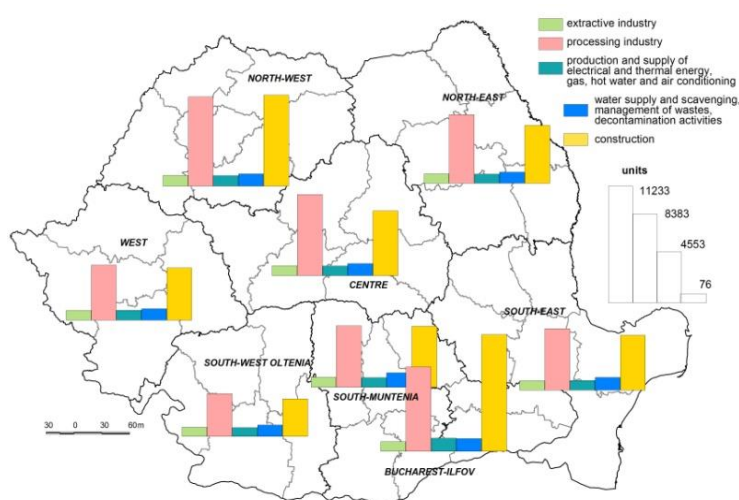Fig. 17 – The structure of secondary sector units, 2008.

Fig. 18 – The structure of secondary sector units, 2018.

Processing industry units registered an upward trend in some 45,000 to over 65,000 units throughout 2003–2008. Outstanding in the territory was the Bucharest–Ilfov Region with more than 10,000 units, followed by the Centre and North-West Regions with above national average evolutions (Figs. 16, 17, 18). After 2008, the economic-financial crisis would be deeply felt, the number of processing industry units dropping from some 58,000 in 2008 to about 45,000 in 2014–2015. As the regional analysis revealed, the Bucharest–Ilfov Region stood at the top of the hierarchy, followed by the Centre and North-West Regions, with the South-West Oltenia, West and South-East Regions standing at the bottom of the table (Figs. 15, 16, 17).

Between 2008 and 2014, the units belonging to the *production and supply of electrical energy, gas, hot water and air conditioning sectors* went on the increase, but at distinct rates and directions of evolutions. The hierarchy was headed by the Bucharest–Ilfov Region with up to one-third of all the units in this field. The South-West Oltenia and North-East Regions fell at the bottom of the list (Figs. 16, 17, 18).

A slow numerical growth between 2008 and 2018 was registered by *the scavenging, management of wastes and decontamination units*, in other years their activity kept stagnating, or decreased. Their distribution at regional level registered a relatively balanced evolution, yet the South-Muntenia Region was slightly ahead of the others (Figs. 15, 16, 17).

From 2002–2018, *the number of construction units* went steadily up between 2003–2008 and at a constant rate until 2007, subsequently declining because of the economic-financial crisis, however, they would slightly recover from 2012 to 2018. In terms of territorial structure, the Bucharest–Ilfov Region stood out with nearly one-third of all construction units, the North-West Region coming second. At the other end of the spectrum there were the South-West Oltenia, the South-East, North-East and West Regions (Figs. 15, 16, 17).

4.5. Secondary sector economic activities and their effects on environment quality

In Romania, the general state of the environment has improved due to the technological progress in some industrial units, as well as because industrial activity was significantly reduced. Air and soil pollution is visible in the areas surrounding pollution sources, *i.e.* industrial mining and oil processing sites, as well as animal breeding zones (Sima, Popovici, 2016). All these secondary sector activities have a significant impact on environmental factors – air, water and soil –, but more especially it is such industries as thermal energy, cement, oil and natural gas, refinery, chemical and petrochemical, as well as metallurgy that may affect these polluting factors. The potential impact is the result of emissions released by the preparation of raw material, the final processing of products, the transport and storage of raw material and auxiliary items (Annual Report on the State of the Environment in Romania 2016–2017).

The quality of air is being changed by atmospheric pollutants up to noxious concentrations produced mostly by burning procedures used in the energy industry. Looking at the evolution and origin of various types of air pollutants, one finds a general tendency towards reducing the mean annual concentrations which, as a rule, fall below limit values. However, it appears that mercury emissions are released during the energy producing process to obtain iron and steel. Also, the highest contributor to the emissions of persistent organic pollutants is just the iron, steel and aluminium manufacturing process; the energy sector does contribute to polluting the air with significant quantities of sulphur dioxide, carbon monoxide, carbon dioxide, nitrogen oxides and powders. Analysing the evolution of the main air-released pollutants one finds a general decreasing trend since big burning installations have been rehabilitated and updated, while sulphur-rich fuels are no longer used. The analyses made by the Ministry of the Environment show that closing down some industrial installations is an important way of reducing air-released pollutants (Annual Report on the State of the Environment in Romania in 2016, 2017). Since the activities of industrial installations can be controlled so that energy consumption-yielded emissions and waste is as decreased as possible, has led to the EU legislation

reform, with the publication in 2010 of *Directive 2010/75/UE on industrial emissions (IED Directive)* included in the national legislation – Law No. 278/2013 on industrial emissions (Parlamentul României, 2013).

The industrial units producing polluting emissions, releasing dangerous substances and used waters put significant pressure on water quality in Romania, water being charged with organic matter, nutrients and dangerous substances. Among secondary sector activities significantly contributing to the degradation of water bodies, we would recall the catchment and processing of water for the population, the production of electrical and thermal energy, as well as the chemical, metallurgical and extractive industries (Guvernul României, Ministerul Mediului, Agenţia Naţională pentru Protecţia Mediului, 2017, Ministerul Economiei, Energiei şi Mediului de Afaceri, 2020). Water management and the monitoring of water body quality in this country are as per the *Water Framework Directive (60/2000/CEE)* aimed primarily at having all water bodies in good condition by acting at drainage basin level (Sima, Popovici, 2016).

The degradation of *soil quality* through various digging works is the severest form of its impairment, a situation occurring especially in the case of open mining. The quality of land affected by this type of pollution is by 1–3 classes lower, some such surfaces having actually become unproductive. Soil degradation is induced by extractive industry works, the presence of waste deposits, mud-setting ponds, dump heaps of debris, wastes produced by the extractive, siderurgical and metallurgical industries, pollutions with various types of chemical components carried by air and water in the proximity of industrial pollution sources, radioactive materials, crude oil, and salt water from oil extraction (Sima, Popovici, 2016, Guvernul României, Ministerul Mediului, Agenţia Naţională pentru Protecţia Mediului, 2017, Ministerul Economiei, Energiei şi Mediului de Afaceri, 2020).

5. CONCLUSIONS

This analysis of the Romanian secondary sector has in view turnover variability, the employed population, net investments and various indicators relevant for the demographic aspects of the enterprises. Thus, some regional profiles may be singled out. Secondary sector territorial characteristics, the specificity of development regions, which is based on in-depth studies of a larger number of variables and statistical indicators (Popescu 2000, Popescu *et al*. 2003, Dumitrescu 2008, Bălteanu *et al*., 2016, Popescu *et al*., 2016) are briefly outlined below:

South-Muntenia Development Region. Secondary sector activities that were restructured and made investment-attractive: oil and natural gas extraction and processing, machine-building, pieces of equipment and means of transport, chemical industry, electrical and household items.

South-East Development Region. The secondary sector featured a steep decline of employed population but also benefitted from natural resources, from the openness to international markets, accessibility to and diversity of a transport infrastructure. The advantages offered by the localisation of secondary sector units and by the Region's industrial specialization proved investment attractive.

North-East Development Region. An underdevelopment secondary sector was among the causes of great poverty here, this Region being one of the poorest in Romania (Mocanu *et al*., 2016), with the least amount of investments in the secondary sector, especially in the processing industry, as opposed to other development regions; a lower turnover than in other regions (again in the processing sector), but a better one in the mining industry.

North-West Development Region. The secondary sector is relatively diversified, tending, however to specialize in machine-building and equipment, furniture, textile and footwear industries. Due to their cross-border co-operation potential and a better development infrastructure than in other regions, important investments could be drawn in.

Centre Development Region. The secondary sector is well represented, especially the energy industry. The Region is specialised in wood processing, food, aeronautics and chemical fertilisers.

West Development Region. Its secondary sector was severely affected by industrial restructuring (of the extractive and metallurgical branches); however, a positive evolution was were recorded in telecommunications, machine-building, chemical and electrochemical industries.

South-West Oltenia Development Region. Failures to privatise some industrial units and dysfunctions in the energy and extractive industry led to it being more poorly developed than other regions.

Bucharest-Ilfov Development Region. The deindustrialization and tertiarization of Bucharest's economy, together with the relocation of some firms in Ilfov County, has forced its secondary sector to heavily restrict its activity. Industrial units are largely connected with the industries working for the urban market; in addition, numerous multinational companies are also involved.

The disparities revealed by this study are consistent with Romania's complex socio-economic discrepancy rooted in the historical background of the country: Romania's economic development follows a West–East direction, thus having a powerful geographical component, the less developed regions being more focused in the Eastern and Southern parts of the country (Ianoş, 1998). Since the early 20th century, Romania has had two space organisation patterns: the Wallachia historical region (corresponding to the South-Muntenia Development Region and parts of the South-East Development Region) follows a North-South development direction with a few scattered nuclei; and Transylvania, Banat and Crişana historical regions (corresponding to the Development Regions located in the Central, Western and North-Western parts of Romania), which have a profile shaped by mining activities and by the main cities encompassing secondary and tertiary sectors). Having been perpetuated over time, these two main opposite space organisation patterns have led to the emergence of regional disparities. However, the South-East–North-West industrial profile has been maintained, leaving discontinuities at the periphery (Popescu 2000; Ministerul Dezvoltării Regionale şi Administraţiei Publice, 2014, Popescu *et al.*, 2016, Mitrică *et al.*, 2017).

REFERENCES

Bălteanu, D., Mitrică, B., Mocanu, I., Sima, M., Popescu, C., (2016). *Caracterizarea geografică a regiunilor de dezvoltare*, in vol. *România. Natură şi societate*, Romanian Academy Publishing House, Bucharest, pp. 621–652.

Dumitrescu, B. (2008), *Oraşele monoindustriale din România între industrializare forţată şi declin economic,* University Publishing House, Bucharest.

European Parliament (2010a), *Directive 2010/75/EU on industrial emissions (integrated pollution prevention and control)*, http://data.europa.eu/eli/dir/2010/75/oj

European Parliament (2010b), *The EU Water Framework Directive – integrated river basin management for Europe*, http://ec.europa.eu

Hansen, T-N., Ianoş, I., Pascariu, G., Platon, V., Sandu, D. (1996). *Regional Disparities in Romania 1990–1994*, Grupul de consultanţă Ramboll, Bucharest.

Ianoş, I. (1998), Restructurarea economică şi fenomenul de migraţie în România. Revista Geografică, V, 8–13.

Ministerul Economiei, Energiei şi Mediului de Afaceri (2020), *Raport de Mediu pentru Strategia Energetică a României 2020–2030, cu perspective anului 2050*, http://www.mmediu.ro/app/webroot/uploads/files/Raport%20de%20 mediu_aug%202020.pdf.

Ministerul Dezvoltării Regionale şi Administraţiei Publice (2014), *Strategia de Dezvoltare Teritorială a României, 2020–2035* (Romania's Territorial Development Strategy, 2020–2035), www.sdtr.ro, Acc. Sept. 18, 2017.

Mitrică, B., Mocanu, I., Dumitraşcu, M. Grigorescu, I. (2017). *Socio-Economic Disparities in the Development of the Romania's Border Areas,* Social Indicators Research, **134**(*3*), pp. 899–916.

Mitrică, B., Damian, N., Mocanu, I., Grigorescu, I. (2019). *Exploring the links between out-migration and social development in Romania. A Development Region-based approach*. Europa XXI(*37*), pp. 53–70. https://doi.org/10.7163/Eu21.2019.37.4

Mitrică, B., Grigorescu, I., Săgeată, R., Mocanu, I., Dumitrașcu, M. (2020). *Territorial Development in Romania: regional disparities*, in vol. *Dilemmas of Regional and Local Development* (ed. J. Banski), Routledge Explorations in Development Studies, Taylor & Francis Group, pp. 206–228.
DOI: 10.4324/9780429433863-13,
https://www.routledge.com/Dilemmas-of-Regional-and-Local-Development/Banski/p/book/9781138359154
Mocanu, I., (2008). *Șomajul din România. Dinamică și diferențieri geografice,* University Publishing House, Bucharest.
Mocanu, I., Guran L., Damian N., Dumitrache, L. (2016). *Elemente de geografie socială*, in vol. *România. Natură și societate*, Romanian Academy Publishing House, Bucharest, pp. 451–480.
National Institute of Statistics (1992), *Recensământul populației și locuințelor din 1992*, Bucharest.
National Institute of Statistics (2002), *Recensământul populației și locuințelor din 2002*, Bucharest.
National Institute of Statistics (2011), *Recensământul populației și locuințelor din 2011*, Bucharest.
National Institute of Statistics (2015), http://statistici.insse.ro/shop/index.jsp?page=tempo2&lang=ro&context=55
Parlamentul României (1991), *Lege pentru soluționarea conflictelor colective de muncă (Legea nr. 15)*, Monitorul Oficial al României, 33, 11 februarie.
Parlamentul României (1998), *Legea minelor (Legea nr. 61)*, Monitorul Oficial al României, 113, 16 martie.
Parlamentul României (2013), *Lege privind emisiile industriale (Legea nr. 278)*, Monitorul Oficial al României, 671, 1 noiembrie.
Popescu, C. (2000), *Industria României în secolul XX. Analiză geografică,* Edit. Oscar Print, Bucharest.
Popescu, C., Săgeată, R., Nancu, D., Mocanu, I., Dumitrescu, B., Simion, G., Damian, N., Borto, G., Guran, L., Persu, M., Dogaru, D. (2003). *Disparități regionale în dezvoltarea economico-socială a României,* Meteor Press Publishing House, Bucharest.
Popescu, C., (2016), *Industria României – de la dezindustrializare la reindustrializare*, in vol. *Natură și societate*, Romanian Academy Publishing House, Bucharest, pp. 375–404.
Popescu, C., Mitrică, B., Mocanu, I., (2016). *Dezvoltarea regională pre- și post-aderare la Uniunea Europeană*, in vol. *România. Natură și societate*, Romanian Academy Publishing House, Bucharest, pp. 613–620.
Popescu, C., Săgeată, R. (2016). *Regiunile de dezvoltare și politica de dezvoltare regională*, in vol. *Romania. Natură și Societate*, Romanian Academy Publishing House, Bucharest, pp. 604–608.
Guvernul României, Comisia Europeană (1997). *Carta Verde. Politica de dezvoltare regională în România*. Bucharest.
Guvernul României, Ministerul Mediului, Agenția Națională pentru Protecția Mediului (2017), *Raport anual privind starea mediului România, în anul 2016* (Annual Report on the State of the Environment in Romania)*,* Bucharest.
Sima, M., Popovici, A-E., (2016), *Calitatea mediului,* in vol. *România. Natură și societate*, in vol. *Romania. Natură și Societate*, Romanian Academy Publishing House, Bucharest, pp. 527–540.

NATURE-BASED TOURISM IN THE KARST GORGES
OF THE SOUTHERN CARPATHIANS

GABRIELA MUNTEANU[1]

Les principales activités de pleine nature pratiquées dans les gorges karstiques des Carpates Méridionales. En ce qui concerne le relief karstique de Roumanie, les Carpates Méridionales ne sont pas un exemple typique, parce qu'elles sont éclipsées par d'autres groupes de montagnes mieux douées de massifs calcaires. Cependant, l'analyse des gorges karstiques de ces montagnes met en évidence un grand nombre de géomorphosites au potentiel attractif important. A partir de ce potentiel touristique, dans cette étude nous décrivons les principales activités de pleine nature pratiquées dans les gorges des Carpates Méridionales: escalade, canyoning, randonnée, VTT (vélo tout terrain), spéléo-tourisme. Nous avons également remarqué les multiples possibilités qu'offrent certaines de ces gorges pour le géotourisme (actuellement sous-développé dans la région étudiée).

1. INTRODUCTION

The touristic role of geomorphosites has been widely covered in the international literature, with several authors approaching the relationship between such landforms and tourism, while other scientists developed specific assessment methods that facilitate comparisons between different sites or ease the identification of most representative resources (Pralong, 2005; Pereira and Pereira, 2009; Reynard *et al.*, 2011; Gordon, 2018 etc.). Many more recent studies have been applied to valleys, gorges and canyons, proving the important touristic role that such sites can have (Božić and Tomić, 2015; Dollma, 2018; Chrobak *et al.*, 2020; Obradović and Stojanović, 2021; Tomic *et al.*, 2021 etc.).

The role that karst gorges play among tourism resources in Romania is undisputed and has been signaled in many general tourism studies (Cocean, 2010; Comănescu *et al.*, 2010; Ielenicz and Comănescu, 2009 etc.) while also analyzed in detail in some other studies (Cocean, 1988; Cocean, 2013; 2014; Cocean and Cocean, 2017). Their importance as a tourism resource is ensured by their specific landscape and intriguing morphologic features that tourists find appealing: the narrow profile, steep slopes, cave entrances, arches, towers and pillars, waterfalls, rapids and plunge pools etc. The number and scale of interesting elements are directly proportional to the potential for tourism development; and so is the length of the engaging sector – not necessarily of the whole gorge sector, when the latter lacks in enticing features (Cocean, 2013).

Gorges offer the ideal setup for practicing various forms of nature-based tourism, from different active outdoor activities practiced by certain categories of tourists, like canyoning, climbing and mountain biking, to hiking over different distances or levels of difficulty. The interesting genesis and evolution of karst gorges have left expressive traces in some cases, especially in the context of the karstic capture scenario, which renders them perfect observation places and didactic destinations, thus important resources for geotourism. The caves and pits found in the slopes of gorges add to their geotouristic value, while also contributing as essential resources for the development of speleotourism. Besides, in many gorges of the region, nature-based tourism intersects and completes other types of tourism, especially cultural and ecumenical tourism, developed due to various well-known monasteries located in the nearby areas.

---

[1] Senior Researcher, Centre for Geographic Research, Cluj-Napoca Branch, Romanian Academy, 42 Treboniu Laurian Street, Cluj-Napoca, Romania, gabriela.munteanu@academia-cj.ro.

The most important tourism resources of the Southern Carpathians are the natural assets: the mountain landscape at high altitudes (the highest in Romania), the suitable conditions for the development of winter sports, well represented in the eastern unit, and the glacial landscape in the higher parts of the mountains. However, our hypothesis is that even if outshined by these other resources, karst gorges still spark relevant tourist flows, thus supporting tourism development in the region.

In theoretical studies, the Southern Carpathians are mostly recognized for their altitude, massiveness and glacial landscape, while the presence of important karst features is still acknowledged (Mihăilescu, 1963; Pop, 2000; Cocean, 2010; Ielenicz and Oprea, 2011; Bălteanu *et al.*, 2012 etc.). While there are numerous studies focusing on the glacial landscape and processes, karst in the Southern Carpathians has not been a frequent subject of research. Even among the valleys of the Southern Carpathians, the transversal valleys (*e.g.*, Olt, Prahova, Jiu) or the Cerna Valley had been more frequently singled out (studies such as those of Orghidan, 1969 or Badea *et al.*, 1981 etc.). Karst gorges did not (and still do not) benefit from the same attention from researchers, although many such sites are mentioned in geomorphologic or geographic studies (Pop, 2000; Posea, 2005; Murătoreanu, 2009; Constantinescu, 2009; Ielenicz and Oprea, 2011 etc.). Some of the karst gorges in the area are however presented in Grigore's study focusing on gorges in Romania (1989), as well as in different studies analyzing geomorphosites in certain parts of the Southern Carpathians (*e.g.*, Albă, 2016) while other gorges appear in various studies due to the caves located in their perimeter, that have long been studied by speleologists and geologists (*e.g.*, Olteţului Gorge or Galbenului Gorge).

Thus, due to the fact that karst gorges are often overlooked or only briefly mentioned in the analyses regarding the tourism potential of the Southern Carpathians, our study has the following main objectives: 1. Create a general image of the potential that karst gorges in the Southern Carpathians have; 2. Present the main types of leisure activities that are already undertaken within the perimeters of such sites.

2. STUDY AREA

The Southern Carpathians (Fig. 1) extend over approximately 14,000 km² (Pop, 2000), between the Timiș–Cerna Corridor in the west and the Prahova Valley – Cerbului Valley – Bârsa Groșetului and Sinca in the east (*Geografia României*, III, 1987). They are east-west oriented, over approximately 250 km, while the north-south distribution varies, stretching as far as 70 km in length (Geografia României, III, 1987).

Karst landscape is not considered representative for these mountains, and indeed the spatial distribution of limestones is not that impressive in this region. Bleahu *et al.* (1976) note that limestone areas in the Southern Carpathians cover 1,597 km². However, the authors include Banat and Poiana Ruscă mountains in the Southern Carpathians, as they have quite extended limestone areas: Banat Mountains have 807 km² of karst areas (Olaru, 1996), while Poiana Ruscă Mountains have about 113 km² in the eastern part, and around 250 km² in the western part (Bandrabur and Bandrabur, 2010). This means that the Southern Carpathians from between the Prahova Valley and the Timiș–Cerna Corridor would only encompass approximately 427 km² of karst areas.

Crystalline schists are the dominant rocks in the Southern Carpathians, with limestone only occupying just above 3% of the total area (one may remark that Bleahu *et al.*, 1976, indicate a percentage of 5,8%, but one must keep in mind the inclusion of Banat and Poiana Ruscă mountains in that estimation). To be put into perspective, in no way do they stand a comparison with Banat Mountains or Apuseni Mountains, where the percentage is 7,8% (Cocean, 2000). Limestone is mostly present in the western and eastern extremities, but one may also notice that the situation for the different mountain groups is much more nuanced. In Bucegi Mountains, the main karst areas are located in the Ialomiţa Basin, the Piatra Craiului Massif, in the west of Leaota Mountains and the Bran–Rucăr Corridor (Pop, 2000). In Făgăraș Mountains, limestone has less extended areas, while in

the Parâng sector, the most expansive karst areas are located in the south-west of Șureanu Mountains, the south-east of Căpățânii Mountains (with the particular landscape of Vânturarița–Buila), the south of Parâng Mountains and smaller areas of Latoriței Mountains. In Retezat–Godeanu, karst is more widespread, especially in the Cernei Basin, Mehedinți Mountains (a particular example of which being Domogled Ridge) and the south of Vâlcan Mountains.
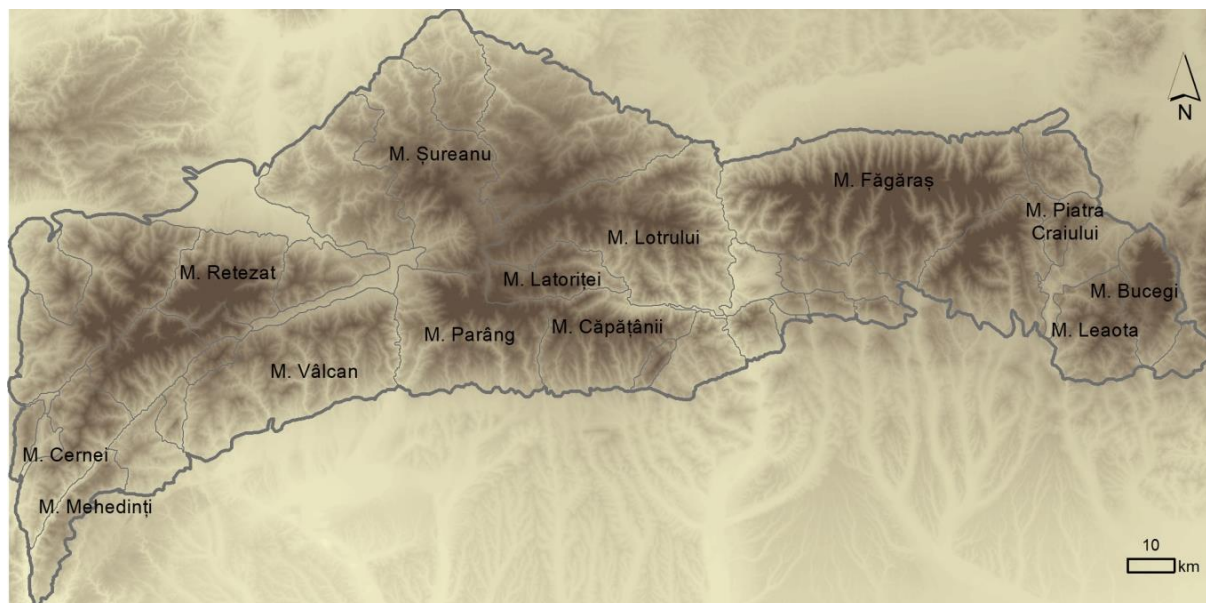

Fig. 1 – The Southern Carpathians. A delimitation of the study area
(Map source: personal production using data from http://geo-spatial.org/vechi/download/romania-seturi-vectoriale,
using the mountain unit limits according to Posea and Badea, 1984).

Naturally, the same differences among the distinct mountain sectors apply to the spatial presence of gorges. Bucegi and Retezat–Godeanu mountains stand out, followed by Parâng Mountains. There are however three main areas where more gorges are clustered: the Dâmbovița Basin (Dâmbovicioarei, Brusturetului, Cheile Mici ale Dâmboviței, Orății, Cheile Mari ale Dâmboviței, Cheița and Ghimbavului gorges), the Ialomița Basin (Urșilor, Peșterii, Horoabei, Coteanu, Tătarului, Zănoaga Mică, Zănoaga, Orzei, Brăteiului and Răteiului gorges) and the Cernei Basin (Corcoaia, Șaua Padinei, Jelărăului, Feregari and Săliștei gorges).

3. MATERIALS AND METHODS

This research is primarily based on a thorough review of scientific content regarding the geomorphology of the Southern Carpathians, karst landscape in Romania and tourism development in the Southern Carpathians. Several official data bases were consulted, such as data from the Ministry of Economy, Entrepreneurship and Tourism or the Ministry of Environment, Water and Forests, management plans for national or natural parks in the area (Piatra Craiului, Domogled – Valea Cernei and Bucegi), as well as other non-formal, online resources for the assessment of climbing sectors and trails, and several webpages of outdoor and speleological associations, and tourism promoters, in order to assess the advertising of gorges in the region in what adventure tourism is concerned. Tourist maps issued by national/natural parks authorities were also consulted, as well as the "Munții noștri" collection of touristic maps.

We have tried to put each analyzed form of nature-based tourism into the context of the whole mountain group in order to understand just how relevant karst gorges actually are to the overall tourist phenomenon in the region.

4. RESULTS AND DISCUSSION

4.1. Main engaging features of karst gorges in the Southern Carpathians

There are over 50 gorges in the Southern Carpathians, many of them having important inviting features. Their lengths are limited by the karst area in which they are located. Hence, we may notice a wide variety of gorges, from the ones stretching over just 100–300 m: Corcoaia, Bănița, Buții, to gorges that span around 1 to 2 km: Brusturetului, Crivadia, Oltețului, Țăsnei, Prisăcinei, Bistriței, Cheița, Cheile Mici ale Dâmboviței etc., gorges that range between 3 and 5 km in length (*e.g.*, Prăpăstiile Zărneștilor or Crovului) or even longer gorges, the longest one being Sohodol Gorge, for which Bleahu *et al.* (1976) indicate a length of 12 km between Luncile Contului and Runcu Village.

All studied gorges have the typical narrow profile, that in some cases can get as narrow as 5 m (the lower part of Oltețului Gorge, Bănița Gorge (Fig. 2A), the median part of Buții Gorge (Fig 2B), Corcoaia Gorge, Râmnuței Canyon, Bobot Canyon etc.). The slopes can even be as close as 1.5 m in Crivadia Gorge (Fig. 2C).

Fig. 2 – Profiles and slopes in the gorges of the Southern Carpathians (A. Bănița Gorge, B. Buții Gorge, C. Crivadia Gorge).

While for most gorges the side slopes are the most impressive due to their relative height, up to 150 m in Buții Gorge, Dâmbovicioarei Gorge, Cheile Mici ale Dâmboviței, Țăsnei Gorge or Taia Gorge, only to name a few, for others, it is their particular shape and overhanging sectors that are most impressive, such as for Bănița Gorge and Corcoaia Gorge. The effect of the general features of these last two gorges created a lot of visibility for the two geomorphosites, rendering them among the most promoted in the region (the easy access definitely helps in making them widely accessible for tourists).

Towers and pillars on the high parts of the slopes add a distinctive note to the landscape of other gorges: Prăpăstiile Zărneștilor, Dâmboviței, Bistriței etc. Cave entrances increase the alluring factor of some gorges (Oltețului, Dâmbovicioarei, Sohodolului, Cheile Mici ale Dâmboviței, Bistriței, Buții,

Scorota etc.), as do the swallets (*e.g.*, swallets form Pecinișcăi or Țăsnei gorges). The small canyons in Cernei Basin, Crivadia Gorge and Valea lui Stan Canyon have eye-catching waterfalls (however, most of the canyons in Cerna Basin can be dry during summertime), while other gorges have polished marmites and pools (Buții, Corcoaiei etc.).

4.2. Main leisure activities performed in the karst gorges of the Southern Carpathians

Due to their particular landscape and tourism potential, gorges are places where fairly active forms of tourism are performed, some characteristic to gorges and canyons alone, and others based on several different tourist resources.

4.2.1. Canyoning can only be practiced along gorges and canyons that have a series of vertical descents, waterfalls, rapids, plunge pools and slides. Thus, it is of no surprise that only few gorges can accommodate this activity in the Southern Carpathians. Țăsnei gorge, Drăstănic, Bobot and Râmnuța canyons in Cerna Basin are the most important ones. These canyons, with some rappelling points reaching 25–30m, are well-known on a national level, also being used as locations for the National Canyoning School, between 2017–2020. They also have the added advantage of being located very close to one another; therefore, tourists have the option of more activities, hence a longer stay in the area. Other canyons worth mentioning are Valea Mării in Retezat Mountains, Jgheabului Canyon in Șureanu Mountains and Orății Canyon in Bucegi Mountains.

Canyoning does not involve great numbers of tourists, as it is practiced by technically trained and experienced mountaineers (or with the assistance of a specialized team). Additionally, there is also a matter of generally good health and fitness level, since most canyons do need a trek uphill to get to the entering point and do not have intermediate exit points, and the entire activity can take up to 8 hours.

Canyoning has its seasonality, especially in what assisted tours offered by private companies are concerned. We have analyzed the offer of seven such companies working in the area and we have found that the canyoning offer refers mainly to the May–October period for dry canyons and to the July–September segment for canyons with a lot of water (such as Valea Mării in Retezat). For individual teams of experienced mountaineers, the season can begin earlier or end later; still, winter and early spring are not suitable time frames for this activity.

4.2.2. Speleotourism. The most important aspect of speleotourism practiced within the perimeter of the gorges of the Southern Carpathians is centered mainly on the five most important show caves in the region: Muierilor Cave (A-class cave, with B sectors, as classified by Order No. 604/2005), Polovragi Cave (B-class cave with A and C sectors – the touristic sector), Ialomiței Cave (B-class cave with a C-class touristic sector), Liliecilor Cave in Bistriței Gorge (B-class) and Dâmbovicioara Cave (C-class cave). Easily accessible by car or, in the case of Ialomiței cave, by the Bușteni–Babele– Peștera cable car as well, and presenting arrangements for easy and safe passage, these caves attract hundreds of thousands of tourists every year.

Polovragi Cave (Fig. 3A,B), in Oltețului Gorge is the longest cave among the four, with 10,793 m long, followed by Muierilor Cave, in Galbenului Gorge, more than 8 km long, Ialomiței Cave 1,130 m long, Dâmbovicioara cave, 555 m long, and Liliecilor cave, 250 m long. However, the sectors that can be visited by the public are much shorter: 800 m in Polovragi Cave, 573 m in Muierilor Cave, 480 m in Ialomiței Cave, and 200 m in Dâmbovicioara Cave. Aside from Dâmbovicioara and Liliecilor caves, which are rather modest in terms of detail morphology, speleothems are present in all of these show caves, although in the case of Ialomița and Polovragi caves, they have been damaged. These caves did not lack in cultural assets either, starting with the little monastery at the entrance of Ialomiței cave and the two chapels built at the entrance of and inside Liliecilor cave, and moving forward with the different artifacts and paleontological assets of Muierilor Cave.

Fig. 3 – Polovragi Cave. Entrance (A) and detail morphology (B).

These caves were among the first in Romania to be included in the tourism phenomenon. For example, Muierilor Cave had its electric network and arrangements set up as early as 1963. However, the need for "a radical redevelopment" has been pointed out by scientists (Constantin *et al.*, 2021) due to the high number of visitors and the vulnerability of this speleosite. The same authors point out the need to open another exit for the tourist flow in Polovragi Cave, in order to achieve a boost in tourist circulation (currently, visitors enter and then exit the cave on the same route). However, such projects of redevelopment are not yet in the cards for most sites. Still, a project targeting the restoration of the touristic path began in 2014 in Ialomiței Cave, with it reopening to the public in July, 2015. Since then, it has had high numbers of visitors; in 2018 there were 87,766 visitors, 125,984 visitors in 2019 and 109,540 visitors in 2020 (data received from the "Curtea Domnească" National Museum Complex in Târgoviște). Muierilor Cave has around 100,000 visitors/year, Polovragi cave around 30,000 visitors/ year (Constantin *et al.*, 2021) and Dâmbovicioara Cave around 20,000 (data retrieved from the Piatra Craiului National Park website).

One may note that all the important show caves in the Southern Carpathians are located within the perimeter of gorges; only Bolii show cave in Sebeș Mountains is not situated on the slopes of a gorge, but in the vicinity of Băniţa Gorge. The cave is 455 m long, has basic arrangements and sometimes holds concerts or other cultural events.

The second aspect of speleotourism practiced in gorges is the exploration of caves that have not been arranged for tourism. This may refer to the small caves near the hiking paths in gorges, most of them of small dimensions, where tourists can briefly observe more of a preview of the endokarst, as well as more secluded caves, with a more difficult access that does require speleological skills.

The Southern Carpathians are home to various caves representative for the Romanian karst, which are included in the A-class, such as Pagodelor, Izverna, Cioclovina, Peștera din Valea Stânii, Bârzoni, Epuran etc., as well as some developed pits, like Avenul de sub Colții Grindului. In the perimeter of the analyzed gorges (alongside the show caves mentioned before) there are a few notable caves in terms of development and complexity, among which: Șura Mare Cave in Sebeș Mountains (A-class cave over 11 km long) and Rătei Cave (B-class cave over 7 km long). The rest of the caves located within the perimeter of karst valleys are mostly more modest speleosites.

There are also some gorges that stand out due to the higher numbers of caves they contain, located in areas where the degree of endokarstic activity had been more intense: Dâmbovicioarei, Cheile Mari ale Dâmboviței, Cheița, Galbenului, Oltețului, Scorotei or Sohodol gorges.

4.2.3. Climbing requires tourists with a certain physical fitness and technical background; it is performed on the steep slopes of mountainous areas, gorges being just one among the favorable locations.

The mountains in the Southern Carpathians with the highest numbers of climbing routes, in general, on limestones and other rocks (schists, granites, gneisses) are: Bucegi (762 routes, among which more than half are clustered in just two climbing areas: Sinaia and Coștila), Piatra Craiului (475), Vâlcan (302), Parâng (193), Căpățânii (168), Făgăraș (125) and Retezat (98), while the other mountains have fewer climbing sectors (all the data regarding the routes were retrieved off of ClimbRomania, a website and data base for active climbers).

Gorges serve as important areas for climbing, with some valleys that gather high numbers of routes standing out, such as Galbenului Gorge, which has 177 routes grouped into 13 sectors. Its most impressive sector is the A Zone – Peretele Peșterii, reaching up to 100 m high and containing 48 routes. Galbenului Gorge is closely followed by Sohodol Gorge, with 153 routes, many of them grouped in the area of the geomorphological feature called "Nările" (direct translation – *The nostrils*). Two other gorges have over 110 routes: Feregari in Cerna Basin and Prăpăstiile Zărneștilor in the Piatra Craiului Massif. Cheii (96 routes), Balomir (72 routes), Folea and Bistriței (57 routes each), Jiu de Vest (49 routes), Crovului (45 routes), Dâmbovicioarei and Brusturetului gorges (with a total of 60 routes) are also worth mentioning.

4.2.4. Hiking. Due to their attractive morphological features, gorges provide both challenging passages and a sense of adventure for tourists, as well as beautiful background scenery for segments of longer distance hikes – many gorges in the area are also entry points of trails leading to the higher parts of the mountains (Scorota Gorge, Buții Gorge, Prăpăstiile Zărneștilor Gorge etc.).

According to data provided by the Ministry of Economy, Entrepreneurship and Tourism, (http://turism.gov.ro/web/autorizare-turism/) there are 306 homologated mountain trails in the Southern Carpathians. The fascination for the high altitudes of these mountains is unmistakable, with most routes heading towards the most important summits of Romania. The highest numbers of hiking routes are cumulated in the following mountains: Făgăraș (68), Bucegi (56), Piatra Craiului (41), Căpățânii and Retezat (30 each), and Mehedinți (23). The other massifs in the analyzed region appear to have a more modest number of such trails.

Among these, less than 50 trails pass through the perimeter of karst gorges, which represents roughly around 16% of the homologated mountain tracks in the area. The highest concentrations of hiking tracks that include the passing by or the stopover at karst gorges are present in the Piatra Craiului Massif (11 trails in the Prăpăstiile Zărneștilor area and Dâmbovița Basin), Mehedinți Mountains (10 trails around Băile Herculane resort, passing through the nearby gorges– Feregari, Jelărău, Pecinișcăi and Șaua Padinei) and Bucegi Mountains (8 trails around Ialomița basin).

Trails have various levels of difficulty, influenced by the particular morphology of each gorge, thus being suitable for different types of tourists. The most accessible trails, for all categories of tourists, pass through gorges with an existing road near the river-bed (Prăpăstiile Zărneștilor – Fig. 4A, Dâmbovicioarei – Fig. 4B, Cheile Mici ale Dâmbovitei, Brusturetului, Tătarului, Taia, Galbenului, Oltețului etc.). However, while the circulation of motor vehicles is not restricted, the downside is that cars, motorcycles, cyclists, pedestrians, all use the same road, which are perhaps narrowed down further by little boutiques placed along the road, all this creating a less than idyllic image of the site (*e.g.*, Dâmbovicioarei Gorge). Another category of accessible gorges are the very short ones, with low-difficulty level trails, like Corcoaia Gorge (Fig. 4C). More demanding trails cross other gorges (Buții, Scorotei, Zănoagei etc.), some of them with higher, significant elevation gains and losses (*e.g.*, Țăsnei –Fig. 4D or Tâmnei).

Only 19 of the 51 analyzed gorges in the Southern Carpathians have homologated hiking trails within their perimeter (some of them having several trails reaching their entrance, different routes in the slopes or along the water); however, of the remaining 32, many are still popular hiking areas. There are many gorges that do have a walking path, and even, in some cases, orientation signs (mostly

placed by locals or different outdoor associations) or basic supporting arrangements (cables, ladders etc.), and which are popular among tourists (Cheile Mari ale Dâmboviței, Ghimbavului, Cheița, Răteiului gorges etc.), while many of them are wilder and require crossing through deeper water that can be up to 1.3 m deep, in Crivadiei Gorge, for example, or even climbing on certain sectors (Orzei or Horoabei gorges). In the absence of marked trails, hiking in such gorges is not recommended for inexperienced tourists; and no hiking route inside gorges is recommended in the absence of basic mountain wear. Finally, there are gorges that do not have homologated mountain trails, but where an access road (more or less modernized) does exist, that can also be used by tourists for a nice walk (Sohodolului, Scocului, Roșiei etc.).
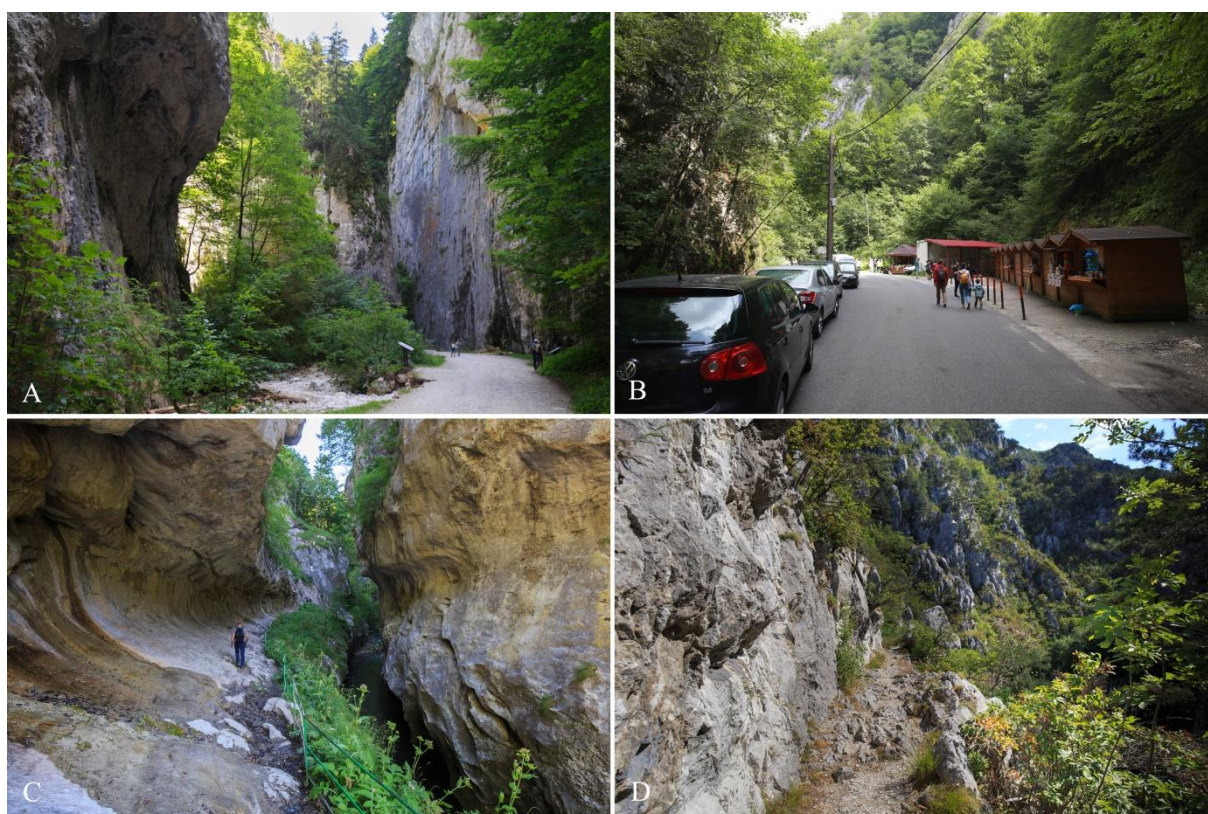

Fig. 4 – Access in gorges: along roads closed for public circulation with motor vehicles (A. Prăpăstiile Zărneștilor Gorge), along roads opened for vehicles (B. Dâmbovicioarei Gorge) and along the slopes (C. Corcoaia Gorge and D. Țăsnei Gorge).

Hiking has its typical seasonality; many trails in the perimeter of gorges are accessible all year round but there are, however, many that are not recommended in winter, especially those that require tourists to pass through water, or climb certain sectors, and especially not for inexperienced tourists. Moreover, in periods of heavy rainfall gorge sectors can be dangerous throughout all seasons, due to the high risk of flash floods (the latest such event taking place in July 2021, when there was serious damage, including to the access road, due to a flashflood in Tătarului and Zănoaga gorges).

Gorges are often visited by travelers involved in other types of tourism. Tourists that visit Polovragi Monastery most often also go for a walk in Oltețului Gorge or visit Polovragi Cave. The same goes for visitors of Bistrița Monastery near Bistrița Gorge and Ialomița Monastery near Peșterii Gorge. For this type of tourists, gorges are merely an additional sight to see; they appreciate an easy access through the gorge, especially since many of them may not even have mountain wear.

4.2.5. Cycling and mountain biking. In many cases, gorges can be a perfect place for mountain biking. We are, of course, referring to those gorges where a road or a dirt road exists, or at least a rather accessible path. Mountain biking usually implies longer distances than hiking, so most gorges constitute merely a stage of the biking track, and not necessarily the destination. For example, passing through Prăpăstiile Zărneștilor, the cycling track continues towards Curmătura Cabin, or through Pisicii Gorge, on Vlădușca Valley, towards Poiana Vlădușca and "La table" area. Here, the track intersects another mountain biking route coming from the Brusturet Gorge, passing by Poiana din Grind (thus, we may note that the segment of the track passing through gorges is rather modest). These are among the clearly signaled and accessible cycling routes in the eastern sector of the mountains. However, for the rest of the units in the Southern Carpathians, information and promotion is scarce and hence, this activity attracts only real connoisseurs, leaving a lot of room for improvement.

4.2.6. Geotourism consists of the observation of geomorphosites, while also having access to information about their geologic and geomorphologic features. Gorges have several assets that are solid bases for the development of geotourism. Firstly, they can provide an understanding to the way water carves its way into limestone (resulting in epigenetic, antecedent, of peripheral subsidence or karstic caption gorges) and the way it models the microforms one can find in the valley (natural bridges, arches, towers, marmites etc.). In the case where a gorge also contains caves, the whole scenario is even more captivating; while visiting Polovragi Cave, tourists should receive information about how the cave was once an underground meander of the Olteț River, and thus get a more detailed picture of the succession and complexity of different evolution phenomena.

The vicinity of Olteț and Galbenului gorges, carved in the same limestone ridge, gives the opportunity of establishing a geotouristic route, which would provide two examples of iconic gorges, in very different evolutionary instances. The landscape is very different among the two, especially when comparing the narrowness of the base sector of Olteț Gorge to the rather wide profile of Galbenului Gorge. The two caves, Muierii and Polovragi, are also good opportunities to provide more understanding of the karst landscape.

Sohodol gorge is another favorable location for the development of geotourism. The complex genesis of this sector, involving both surface evolution and karstic capture has left many clues and traces along the valley. The five swallets, where water continues the underground carving of limestone, together with the many caves (Gârla Vacii, Pârleazului, Izbucului Muschiat, Laptelui etc.) located in the perimeter add to the complexity of the area and subsequently, to the potential for geotourism development. Explanatory panels are now placed near the most important features, like the "Nările" formations, underground meanders of the river, but there is room for improvement in the quality of information and the esthetics of the panels. The presence of an access road, accessible to all types of tourists is an advantage that Sohodol and Olteț gorges have, because one must keep in mind that geotourists are not necessarily looking for a demanding hike during their outing.

There are many other examples of gorges that are valuable geotourism resources, such as Pecinișcăi Gorge, another great didactic site, with a shorter trail leading to the Pecinișcăi swallet after passing through the dry valley downstream, or the Corcoaia Gorge where the erosion levels are displayed in a very illustrative way. All the information regarding these forms and processes ought to be revealed via information panels strategically placed; but until now, we have only observed the presence of satisfactory detailed information panels in Sohodol Gorge and Prăpăstiile Zărneștilor areas. Thus, we may estimate that there is a vast potential for the development of geotourism around these geomorphosites, but that there are only sparse, rudimental arrangements.

5. CONCLUSIONS

The Southern Carpathians have a more solid offer in terms of karst landscape than can be perceived at first glance. There are many types of gorges in terms of morphologic features and enticing offer for different outdoor leisure activities. A wide range of activities and types of tourism is already performed in many of the analyzed gorges but much can still be improved. In the absence of a coherent strategy, these sites of great potential stand only to lose in visibility. The first steps to be taken should fall in the care of researchers, and a detailed inventory and assessment of these valuable geomorphosites should be completed. That data base should be made available to authorities and used in the planning strategies regarding tourism development in the different counties involved, as well as for the whole mountain area, that has much to offer alongside its ski resorts, high altitude trails and picturesque glacial landscape.

REFERENCES

Albă, Claudia Daniela (2016), *Geomorphosites with touristic value in the central – southern part of the Parâng Mountains*, Forum geografic. Studii și cercetări de geografie și protecția mediului, **XV**.*1*, pp. 109–115.

Badea, L. (Eds.) (1981), *Valea Cernei Studiu de geografie*, Edit. Acad. Rep. Socialiste România, București, 149 p.

Bandrabur, G., Bandrabur, Rădița (2010), *Poiana Ruscă Mountains*, in Orășeanu I., Iurkiewicz, A. (Eds.) Karst Hydrogeology of Romania, Belvedere, Oradea, pp. 169–180.

Bălteanu, D., Jurchescu, Marta, Surdeanu, V., Ioniță, I., Goran, C., Urdea P., Rădoane Maria, Rădoane, N., Sima, Mihaela (2012), *Recent Landform Evolution in the Romanian Carpathians and Pericarpathian Regions*, in Lóczy *et al.* (Eds.), Recent Landform Evolution: The Carpatho–Balkan–Dinaric Region, Springer Geography.

Bleahu, M., Decu, V., Negrea S., Plesa, C., Povară, I., Viehmann, I. (1976), *Peșteri din România,* Edit. Științifică și Enciclopedică, București, 415 pp.

Božić, Sanja, Tomić, N. (2015), *Canyons and gorges as potential geotourism destinations in Serbia: comparative analysis from two perspectives – general geotourists' and pure geotourists'*, Open Geosciences 7(*1*):531–546, https://doi.org/ 10.1515/geo-2015-0040.

Chrobak, Anna, Witkowski, K., Szmańda J. (2020), *Assessment of the educational values of geomorphosites based on the expert method, Case Study: the Białkaa Skawa Rivers, The Polish Carpathians*, Quaestiones Geographicae **39**(*1*):45–57, DOI: https://doi.org/10.2478/quageo-2020-0004.

Candrea, B., Candrea, Petronela, Niță, M.D. (2008), *Limite unități relief*: http://geo-spatial.org/vechi/download/romania-seturi-vectoriale.

Cocean, Gabriela (2013), *The current touristic capitalization of the karstic gorges in the Apuseni Mountains*, Geographia Napocensis, **VII**, No *2*, pp. 43–50.

Cocean, Gabriela (2014), *Guidelines for including gorges in the tourist offer of the Apuseni Mountains*, Romanian Review of Regional Studies, **X**, No *2*. pp. 95–102.

Cocean, Gabriela, Cocean, P. (2017), *An assessment of gorges for purposes of identifying geomorphosites of geotourism value in the Apuseni Mountains (Romania)*, Geoheritage, Vol. **9**, Issue *1*, pp 71–81.

Cocean, P. (1988), *Chei și defilee din Munții Apuseni*, Edit. Acad. Rep. Socialiste România, București, 168 p.

Cocean, P. (2000), *Munții Apuseni. Procese și forme carstice*, Edit. Academiei Române, București, 253 p.

Cocean, P. (2010), *Patrimoniul turistic al României*, Edit. Presa Universitară Clujeană, 254 p.

Comănescu, Laura, Ielenicz, M., Nedelea, Al. (2010), *Relieful și valorificarea lui în turism*, Edit. ARS Docendi, Universitatea din București, p. 264.

Constantin, S., Mirea, I.C., Petculescu, A., Arghir, R.A., Mantoiu, D.S., Kenesz, M., Robu, M., Moldovan, Oana Teodora (2021), *Monitoring Human Impact in Show Caves. A Study of Four Romanian Caves*. Sustainability, **13**, 1619.

Constantinescu, T. (2009), *Masivul Piatra Craiului. Studiu geomorfologic*, Edit. Universitară, București, 163 p.

Dollma, Merita (2018), *Canyons of Albania and geotourism development*, Acta Geoturistica, Vol. **9**, No. *2*, pp. 28–34, doi: 10.1515/agta-2018-0008.

Gordon, J.E. (2018), *Geoheritage, Geotourism and the Cultural Landscape: Enhancing the Visitor Experience and Promoting Geoconservation*, Geosciences, **8**, *136*; doi:10.3390/geosciences8040136.

Grigore, M. (1989), *Defileuri, chei și văi de tip canion în România*, Edit. Științifică și Enciclopedică, București, 287 p.

Ielenicz, M., Comănescu, Laura (2009), *România. Potențial turistic*, Edit. Universitară, București, 464 p.

Ielenicz, M., Oprea, R. (2011) *România. Carpații. Caracteristici generale (Partea I),* Edit. Universitară, București, 462 p.

Mihăilescu, V. (1963), *Carpații sud-estici de pe teritoriul R.P. Romîne, Studiu de geografie fizică cu privire specială la relief*, Edit. Științifică, 373 p.

Murătoreanu, G. (2009), *Munții Leaota – studiu de geomorfologie*, Edit. Transversal, 182 p.

Obradović, Sanja, Stojanović, V., (2021), *Measuring residents' attitude toward sustainable tourism development: a case study of the Gradac River gorge, Valjevo (Serbia)*, Tourism Recreation Research, https://doi.org/10.1080/02508281.2020.1870073.

Olaru, M., (1996), *Munții Banatului. Resursele turistice naturale și antropice*, Edit. Hestia, Timișoara, 91 p.

Orghidan, N. (1969), *Văile transversale din România. Studiu geomorphologic*, Edit. Academiei Republicii Socialiste România, București, 188 p.

Pereira, P., Pereira, D. (2009), *The geomorphological heritage approach in protected areas: Geoconservation vs. Geotourism in Portuguese natural parks*, Mem. Descr. Carta Geol. d'It. **LXXXVII**, pp. 135–144.

Pop, G. (2000), *Carpații si Subcarpații României*, Edit. Presa Universitară Clujeană, Cluj-Napoca, 264 p.

Posea G., Badea L. (1984), *România. Unitățile de relief (Regionarea geomorfologică)*, Edit. Științifică și Enciclopedică, București.

Posea, G. (2005) *Geomorfologia României. Relief – Tipuri, geneză, evoluție, regionare*, Edit. Fundației România de Mâine, București, 443 p.

Pralong J.P. (2005), *A method for assessing tourist potential and use of geomorphological sites.* Geomorphologie: relief, processus, environnement, **2005**/*3*, pp. 189–196.

Reynard, E., Coratza, Paola, Giusti, C. (2011), *Geomorphosites and Geotourism*, Geoheritage **3**(*3*):129–130, DOI:10.1007/s12371-011-0041-1.

Tomic, N., Sepehriannasab, B., Markovi´c, S.B., Hao, Q., Lobo, H.A.S. (2021), *Exploring the Preferences of Iranian Geotourists: Case Study of Shadows Canyon and Canyon of Jinns*. Sustainability, **13**, *798*. https://doi.org/10.3390/su13020798.

*** (1987), *Geografia României, vol. III, Carpații Românești și Depresiunea Transilvaniei*, Edit. Academiei Republicii Socialiste România, 655 p.

*** Ministerul Economiei, Antreprenoriatului și Turismului – *Trasee turistice montane omologate* – actualizare 30.07.2021, available at http://turism.gov.ro/web/autorizare-turism/.

*** *Ordinul nr. 604/2005 pentru aprobarea clasificării peșterilor și a sectoarelor de peșteri – arii naturale protejate;* available at http://ananp.gov.ro/wp-content/uploads/O-604-pe-2005.pdf.

*** Plan de management integrat al Parcului Național Domogled – Valea Cernei și al siturilor Natura 2000 ROSCI0069 și ROSPA0035, available at https://domogled.ro/ro/administratia/plan-management/.

*** Plan de management integrat al Parcului Natural Bucegi și al sitului Natura 2000 ROSCI0013, available at http://www.mmediu.ro/app/webroot/uploads/files/2018-03-28_PLAN_MANAGEMENT_FINAL.pdf.

*** Planul de Management al Parcului Național Piatra Craiului, https://www.pcrai.ro/files/pdf/Plan_site.pdf.

*** https://www.climbromania.com/.

COMBINING THE ANALYTIC HIERARCHY PROCESS WITH GIS FOR LANDFILL SITE SELECTION: THE CASE OF THE MUNICIPALITY OF M'SILA, ALGERIA

ALI REDJEM*, AZZEDINE BENYAHIA*, MOSTEFA DOUGHA*, BRAHIM NOUIBAT*, MAHMOUD HASBAIA*, ANDRÉ OZER**

Key-words: Landfill siting**,** Multi-criteria analysis, Analytic Hierarchy Process (AHP), GIS, M'Sila.

Abstract. In Algeria, the most used method for the disposal of municipal solid waste (MSW) is landfills. However, determining the location of landfill sites is a difficult and complex process relying on many criteria, such as technical, environmental and socio-economic parameters. The main objective of this study was to test a methodology, based on a multi-criteria analysis and geographic information systems, aimed at identifying areas potentially suitable for the landfill location of Municipal Solid Waste (MSW) for the municipality of M'sila. To choose the most appropriate landfill site, a geographic information system (GIS) was combined with an analytical hierarchy process (AHP) in order to analyse several criteria, such as land use, slope, distance from residential areas, settlements, surface waters, roads, and sensitive ecosystem areas. The analytical hierarchy process (AHP) was applied to identify the weights on each criterion. To assess the suitability for landfill siting, a simple additive weighting method was used. Each criterion was evaluated with the aid of AHP and mapped by GIS. The resulting land suitability was reported on a scale of 0 to 10, *i.e.*, from least suitable to most suitable sites. As a result, 0.5% of the study area is identified as the most suitable for landfill siting, 4.73% suitable and 7.73% moderately suitable, 14.27% less suitable and 72.93% was seen as being completely unsuitable areas to host sites for MSW landfill.

1. INTRODUCTION

Municipal solid waste (MSW) is generated by households, businesses, institutions and industry. MSW typically contains a wide variety of putrescible (packaging, food waste and paper products) and non-putrescible materials (construction materials). Solid waste has become a global environmental and health issue in today's world both in developing and developed countries (United Nations, 2017).

The increase in the quantity of generated waste arises from the effects of many factors, such as improvements in living standards, rapid population growth, economic growth etc. (Guerrero *et al.*, 2013; Minghua, 2009). For solid waste management, many effective techniques of disposal of municipal solid waste have been used, such as landfills, recycling, thermal treatment and biological treatment (Moeinaddini *et al.*, 2010; Kontos *et al.*, 2003).

---

* Professor, City, Environment, Society and Sustainable Development Laboratory (VESDD), Urban Technology Management Institute, Mohamed Boudiaf University, M'sila, Algeria, ali.redjem@univ-msila.dz.

* Professor, City, Environment, Society and Sustainable Development Laboratory (VESDD), Urban Technology Management Institute, Mohamed Boudiaf University, M'sila, Algeria, azzedine.benyahia@univ-msila.dz.

* Associate Professor, City, Environment, Society and Sustainable Development Laboratory (VESDD), Urban Technology Management Institute, Mohamed Boudiaf University, M'sila, Algeria, mostafa.dougha@univ-msila.dz.

* Professor, City, Environment, Society and Sustainable Development Laboratory (VESDD), Urban Technology Management Institute, Mohamed Boudiaf University, M'sila, Algeria, brahim.nouibat@univ-msila.dz.

* Professor, City, Environment, Society and Sustainable Development Laboratory (VESDD), Urban Technology Management Institute, Mohamed Boudiaf University, M'sila, Algeria, mahmoud.hasbaia@univ-msila.dz.

** Professor, Geomorphology and Remote Sensing Laboratory, Institute of Geography, University of Liège (Ulg), Belgium, a.ozer@ulg.ac.be.

Although waste disposal in most towns and cities, especially those in underdeveloped countries, is done in the simple form of landfill deposition, less attention has been paid to the use of expert and engineering knowledge to find the most optimal waste disposal site in municipal solid waste management (MSWM). One of the most important aspects in well-engineered waste disposal siting is the identification of a long-term optimal waste depot location (Awomeso *et al.*, 2010).

Recently, due to the growing urgency of urban environmental problems, solid waste management in lower income countries has attracted much attention, with actions oriented toward landfills designed to increase environmental protection. Proper waste disposal, without compromising natural reserves and environmental quality, has become an absolute necessity in order to avoid environmental and public health risks (Pires *et al.*, 2011) and is one of the greatest endeavours of our times. Hence, it is necessary to devise suitable waste management and disposal methods (Gizachew *et al.*, 2012; Ebistu and Minale, 2013; Abedi-Varaki and Davtalab, 2016).

Algerian cities are experiencing an accelerated urbanization process (Nemouchi, 2005), high demographic growth and the economic, social and political upheavals have direct effects on the volume of household waste produced every day, which is constantly increasing (Safaa Monqid, 2012). These problems, common for all our cities and characterized by uncontrolled urbanization (Abdelli *et al.*, 2017), weaken the waste management systems in place.

Competent authorities have great difficulty in containing and eliminating them, as evidenced by the spectacle of solid waste indiscriminately discarded around the human environment, which also results in aesthetic problems and a general nuisance (Hafidi, 2015). According to a survey by the services of the Ministry of Land-use Planning and Environment, more than 3000 uncontrolled dumps have been identified. Waste management remains one of the weak links (Bendjoudi *et al.*, 2009) of urban management and urban services in Algeria, prior to the issuing of Law N° 01–19 of December 12, 2001 relating to the management, control and elimination of waste. Most solid waste disposal sites in M'sila were on the borders of urban areas, around water bodies, crop fields, settlements and on road sides (Bendjoudi *et al.*, 2009). Therefore, locating proper sites for dumping solid waste far from environmental resources, residential areas, water bodies, roads, faults and settlements is essential for the proper management of solid waste. (Miezah *et al.*, 2015). Over time, due to accelerated urbanization, many existing disposal sites have been very close to settlements and housing estates (Yousefi *et al.*, 2018). The environmental degradation associated with these dumps is likely to pose several health issues for the population (Nas *et al.*, 2008; Soroudi *et al.*, 2018; Yukalang *et al.*, 2017; Yan *et al.*, 2017), especially in summer, when the temperature is unbearable.

The socio-economic development and urban dynamic that Algeria has been experiencing have led to a series of strategic actions aiming to reform the waste management sector (PROGDEM "National Solid Municipal Waste-Management Programme", PNAGDES "National Special Waste-Management Plan", 2001). The problem of solid waste (about 34 million tons per year in Algeria, including 11 million tonnes of urban solid waste) (Aliouche *et al.*, 2017) arises from its collection, but also from the selection and management of dumps. Recognizing environmental risks related to poor waste management, several Algerian administrative regions envisaged the realization of inter municipal landfills. The information presented in this material forms part of this prospect and tries to suggest favourable sites for installing the controlled landfill in the municipality of M'sila.

Choosing an intelligent and integrated landfill site is considered a complex task for planners and authorities. It is a process that poses many difficulties for them, and which requires the evaluation of many different criteria (Chang *et al.*, 2008) as well as a considerable expertise in various social and environmental fields (Chang *et al.*, 2008; Rahman *et al.*, 2008; Lunkapis, 2010; Nishanth, 2010). Environmental factors are very important because the landfill may affect the biophysical environment and the ecology of the surrounding area (Siddiqui *et al.*, 1996; Kontos *et al.*, 2003; Erkut and Moran 1991). Economic factors must be taken into account in the siting of landfills, including the costs

associated with the acquisition, development, and operation of the site (Delgado *et al.*, 2008; Erkut and Moran, 1991; Kontos *et al.*, 2003).

It is evident that many factors, with spatial dimensions, must be incorporated into landfill siting decisions, and geographic information systems (GIS) are useful for such studies due to their ability to manage (collect, store, manipulate, process and analyse) large volumes of spatial data from a variety of sources (Sener *et al.*, 2006). GIS is a very effective way of managing and integrating the necessary economic, environmental, social, technical, and political constraints.

Many attributes considered in the process of selecting technical landfill sites have a spatial representation, which in recent years has motivated researchers to use geographical approaches that allow for the integration of multiple attributes using geographic information systems (Kontos *et al.*, 2003; Sarptas *et al.*, 2005; Sener *et al.*, 2006; Gomez-Delgado and Tarantola, 2006; Delgado *et al.*, 2008; Chang *et al.*, 2008).

Site selection procedures can benefit from the appropriate use of GIS. A GIS is first and foremost an Information System: an organized set of elements which makes it possible to group, classify, process and disseminate information on any given phenomenon. It is capable of capturing, storing and managing spatially referenced data; provide massive amounts of spatially referenced input data and analyse it; easily perform a sensitivity and optimization analysis; and communicate the results of the model to be able to react quickly after events which have an impact on the territory (Vatalis and Manoliadis, 2002).

The multi-criteria method is used to deal with the problems encountered by decision-makers in the processing of large amounts of complex information. The principle of the method is to divide the decision problems into several smaller understandable parts, analyse each part separately, and then integrate the parts in a logical manner (Malczewski, 1997). To solve the problem of landfills, the integration of the Geographic Information System (GIS) and the Analytic Hierarchy Process (AHP) method were used because GIS provides an efficient manipulation and presentation of spatial data and considers many factors from a variety of sources (Kontos *et al.*, 2003; El Alfy, 2010; Sener *et al.*, 2011), while MCE supplies a consistent ranking of the potential landfill areas based on a variety of criteria (Sener *et al.*, 2006).

Many studies have applied different methods for landfill site selection. Barakat *et al.* (2017) has used GIS-based multi-criteria evaluation techniques for evaluating the suitability for landfill site selection in the common of M'sila, Algeria. Eskandari *et al.* (2016) have used an integrated approach for landfill siting based on conflicting opinions among environmental, economic and social cultural experts. In Alanbari *et al.* (2014), a landfill site selection is performed by using Geographic Information Systems (GIS) and Multi-criteria Decision Analysis (MCDA) in Al-Hashimyah Qadaa. Khan *et al.* (2015) has applied a weighted linear combination (WLC) in GIS using a comparison matrix to aggregate different significant scenarios associated with environmental and economic objectives Dhanbad, India. Uyan (2014), Ramjeawon (2008), Kara (2012), Malczewski (1997), Alavi *et al.*, (2013) and Asif *et al.* (2019) used a combination of AHP, GIS and field analysis in order to find the best solid waste disposal sites.

Therefore, this paper aims to test a methodology based on the application of the Analytic Hierarchy Process (AHP) combined with Geographic Information System (GIS) in order to obtain a map of areas suitable for landfill sites in M'sila, Algeria. This association of MCDA and GIS not only permits us to manage the spatial reference information, but also to apply analysis methods allowing us to have the most pertinent and profitable information at spatial-temporal scales. The use of special tools, such as the GIS software, has enabled us to quickly manage and efficiently process large amounts of input data within a specific geodatabase (geology, geomorphology, hydrology, meteorological and climatic aspects, constraints imposed by regulations and legislation both national and regional, etc. (Mussa *et al.*, 2019).

2. STUDY AREA

The commune of M'sila is located in the plains of Hodna, Algeria. It lies about 35° 42′ 7″ north of the Equator and 4° 32′ 49″ east of the Greenwich Meridian, 250 km southeast of Algiers, the capital city of Algeria. It covers an area of 233.2 km^2, with an average elevation of 471 meters above sea level (Fig. 1). The monthly average temperatures are between -3°C and 40°C, the warmest months are June, July and August, and the coldest months are December, January and February. The main activity in the area is agropastoralism, dependent on low and irregular rainfall under 250 mm per year. The area had a population of 238,689 in 2017, with a density of 925 inhabitants per sqkm (Programming and budget monitoring department "DPAT", 2017).

3. MATERIALS AND METHODS

3.1. Materials

Many available datasets, gathered from different sectors of the country, both digital and hard copies at different scales, were used in this study. The data used was based on its availability and suitability for the purpose of the study.
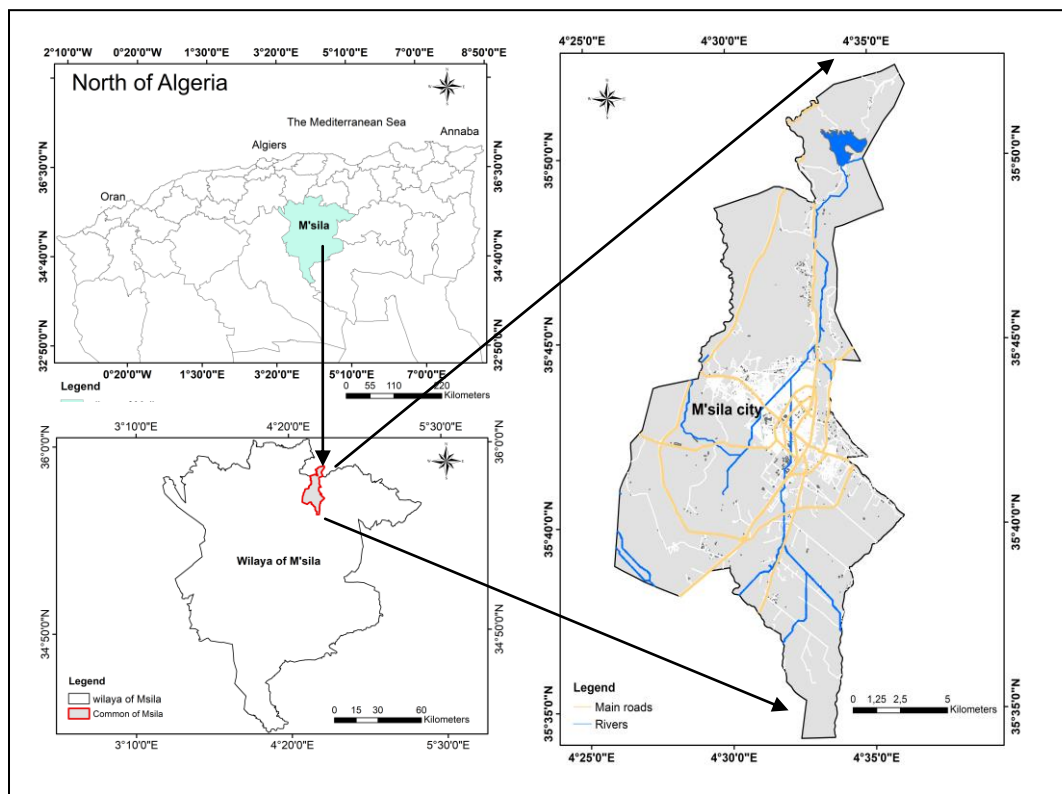

Fig. 1 – Study area – Commune of M'sila.

The Spot 5 imagery that covers M'sila was acquired from the University of Liège (ULg) in Belgium, following a program agreement between the University of M'sila and the University of Liège. The Spot imagery acquisition date was October 26, 2006. This imagery, with a resolution of

10m, was used to prepare primary input thematic maps, such as land-use and hydraulic networks, with the help of field investigations and secondary maps.

The Landsat 8 imagery that covers M'sila (path 195, row 035) was acquired from the United States Geological Survey (USGS) website. The Landsat imagery acquisition date was December 20, 2015. This imagery was used to generate the land use and land slopes.

The aerial photograph, zone F97 (Digital Mapping Camera) that covers M'sila City was acquired from the National Institute of Cartography and Remote Sensing (INCT), Algiers. The Aerial photograph acquisition date was 2011. This aerial photograph with a resolution of GSD-30cm (Ground Sampled Distance) was used to update thematic maps.

In this study, 7 (seven) input map layers, including settlements (urban centres and villages), roads (main roads and village roads), sensitive ecosystems, slope, land use, surface water and residential area were collected and prepared in a GIS environment. All layers were converted to the individual raster maps (Sener *et al.*, 2006; Sener *et al.*, 2011). All input datasets were georeferenced to WGS 1984 UTM Zone 31N coordinate system and reclassified by providing weights, while new maps were generated.

3.2. Methods

3.2.1. The Analytical Hierarchy Process (AHP) method

Currently, the most used methods for the identification of areas potentially suitable for landfills have been generally based on analytical hierarchical approaches (AHP) combined with geographic information systems (GIS), in order to examine various criteria (Kontos *et al.*, 2005; Chang *et al.*, 2008; Sharifi *et al.*, 2009; Carone and Sansò, 2010; Sener *et al.*, 2010; Gbanie *et al.*, 2013). Each criterion is evaluated according to a system based on scores and weights and mapped using GIS techniques. The AHP divides the decision problems into understandable parts; each of these parts is analysed separately and integrated in a logical manner (Demesouka *et al.*, 2013). Therefore, each criterion was allocated a score ranging from 0 to 10, where zero indicates that the area is unsuitable, while 10 describes the best condition.

For this study, we have selected seven criteria for the evaluation of landfill suitability. Establishing the weightings of the sub-criteria is based on the opinion of experts, literature, environmental and scientific requirements and governmental regulations (Table 2), as well as the pre-existing local level factors of M'sila area. The criteria were grouped according to their environmental or socio-economic importance and each criterion was assigned values from three to four classes with scores between 0 and 10.

After defining the importance of each criterion, the next step is to identify the relative importance of the criteria in relation to each other. AHP is one of the most common methods that have been used in recent years. It is a multi-attribute technique that has been integrated into GIS-based land use adequacy procedures.

After defining the importance of each criterion, the next step is to identify the relative importance of criteria to each other. AHP is one of the most common methods that have been used in recent years. It is a multi-attribute technique that has been integrated into GIS-based land use adequacy procedures (Saaty, 1980). It is a reliable decision support method which is widely used to define the relative importance of the different criteria in the landfill site selection (Kontos *et al.*, 2005; Moeinaddini *et al.*, 2010; Sener *et al.*, 2006; 2010; 2011; Sharifi *et al.*, 2009; Yesilnacar and Cetin, 2005). The AHP is based on pairwise comparisons and any criterion or sub-criterion is compared to another criterion at the same time. Decision makers can quantify their opinions about the criteria's magnitude.

The suitability of an area was then assessed by the use of Simple Additive Weighting (SAW) which is one method used to solve the problem of multi-attribute decision making. The basic concept

of the SAW method is to find the sum of the weighted performance rating for each alternative to all attributes. This system is widely used for the calculation of final values in issues using several criteria according to the formula of the following equation (Yoon and Hwang, 1995; Khairul *et al.*, 2016):

$$V_i = \sum_{j=1}^{n} W_j V_{ij} \tag{1}$$

where V_i is the suitability index for the area i, W_j is the relative importance of the weight given to the criterion j, V_{ij} is the priority value of the area *i* with respect to the criterion j, n is the total number of criteria.

The end result of this methodology was the evaluation of the territory on the basis of suitability indices. In this study, the used scale for such indices ranged from 0 (less suitable area) to 10 (most suitable area).

We applied the pair-wise comparison method, which has the added advantages of providing an organized structure for group discussions and helping the decision maker when working with numerous and disputing evaluations, allowing them to obtain an agreement solution when setting criterion weights (Drobne and Lisec, 2009). The pair-wise comparison method in the context of the analytical hierarchy process (AHP) (Saaty, 1980) is now used in various application fields, such as finance, planning, telecommunications and ecology. This method is an effective method for the establishment of relative importance. It uses a ratio matrix to compare one criterion to another (Kontos and Halvadakis, 2002; Kontos *et al.*, 2003; Kontos *et al.*, 2005). Additionally, it uses a numerical scale with values ranging from 1 to 9, as shown in Table 1.

Table 1

The comparison scale in AHP (Saaty 1980)

Value	Intensity of importance
1	Equal importance
3	Moderate importance
5	Strong importance
7	Very strong importance
9	Absolute importance
2, 4, 6, 8	Intermediate values between the two adjacent judgments

The comparison was performed using an integer scale from 1 to 9, with each number having the interpretation shown in Table 1. This pair-wise comparison allowed for an independent evaluation of the contribution of each factor, thereby simplifying the decision-making process.

Table 2

Square matrix of the pair-wise comparisons of various criteria

Criteria	1	2	3	4	5	6	7	Weights	Rank
(1) Distance from water	1.00	5.00	5.00	7.00	1.00	1.00	3.00	0.258	2
(2) Distance from settlement	1/5	1.00	1.00	3.00	1.00	1/3	1/3	0.077	5
(3) Slope	1/5	1.00	1.00	3.00	1/3	1/5	1/3	0.057	6
(4) Distance from roads	1/7	1/3	1/3	1.00	1/7	1/9	1/5	0.026	7
(5) Land use	1.00	1.00	3.00	7.00	1.00	1/3	3.00	0.174	3
(6) Sensitive Ecosystems	1.00	3.00	5.00	9.00	3.00	1.00	3.00	0.288	1
(7) Residential area	1/3	3.00	3.00	5.00	1/3	1/3	1.00	0.120	4
								1.000	
Total	3.88	14.33	18.33	35.00	6.81	3.31	10.87		
	λ max = 7.444			CI= 0.074			C.R = 5,61 %		

Then, the obtained geometric means were normalized and the relative importance weights were extracted. For the decision-making problem mentioned earlier, a structural hierarchy is formed. Where CI is the consistency index, λmax is the largest or principal eigen value of the matrix, and n is

the order of the matrix. This CI can be compared to that of a random matrix, the Random Consistency Index (RI), such that the ratio, CI/RI, is the consistency ratio, CR. As a general rule, for the matrix to be consistent we should have a value of CR $\leq$ 0.1. For this study, (RI = to 1.32) for n = 7 (Table 3), and calculated (λmax = 7.444), producing a value of Consistency Index (CI = 0.074). The consistency ratio CR was 0.0561 < 0.1, thus indicating that a consistent matrix was formed (Alonso and Lamata, 2006).

Table 3

Random inconsistency indices for different values of (n) (Saaty, A980)

N	1	2	3	4	5	6	7	8	9	10	11	12	13	14	15
RI	0	0	0.58	0.90	1.12	1.24	1.32	1.41	1.45	1.49	1.51	1.48	1.56	1.57	1.59

3.2.2. Description of site selection criteria

Generally, selecting a suitable landfill site would minimize the risk to human health as well as decrease the negative effects on the environment. Additionally, it would reduce the costs of waste disposal (Pinar and Akgun, 2014). The selected areas for landfilling should be close to the source of waste and far from protected areas (wildlife refuges, national parks, natural monuments, in addition to protected areas) (Mojtaba, 2019).

The assessment criteria used in this work were divided into two main categories: ecological criteria and socio-economic criteria. We assigned 3 to 4 classes of values to each factor, with a score between 0 and 10 (Table 3). Higher scores are representative of more favourable conditions of the location.

The ecological criteria included the three factors of distance from surface water, distance from residential area and sensitive ecosystems as shown in Table 3.

The socio-economic criteria included factors that affect the construction and the operations management of a landfill. The parameters here considered were land slopes, distance from roads, land use and distance from settlements.

Considering the criteria ascertained through different methods, as shown in Table 1, the information, digital maps, and data related to every criterion were acquired from relevant organizations, including the National Institute of Cartography and Remote Sensing (INCT), the Water Resources Department (DRE), and the Programming and Budget Monitoring Department (Ex DPAT). Since the data used in different organizations and companies are developed and compiled for particular applications, they have different formats and scales, and use different projection systems.

Considering the objective of the current study and the required accuracy, that data was converted into a homogeneous format, scale, and projection system so that all could be used in the defined conceptual model to obtain reliable results.

4. RESULTS AND DISCUSSION

Due to the high rate of population growth in M'sila, as is the case of other Algerian cities, the amount of MSW production is on the rise (Abdelli *et al.*, 2017). One of the major public health problems and environmental pollution factors in this region of Algeria is MSW dumping. MSW dumping in this area has caused environmental and health problems (Pires *et al.*, 2011), such as water and air pollution, disease-causing vectors and odour, especially during summer (Tchobanoglous *et al.*, 1993). Most of these dumps are temporary and are soon to be filled. Hence, it is necessary to look for other suitable sites to dispose of MSW.

GIS data sets of land use, rivers, roads, digital elevation models (DEMs), and slope were collected for this study from: the National Institute of Cartography and Remote Sensing, the Water

Resources Department, and the Programming and Budget Monitoring Department. The criteria for data selection were based on constraints and factors for an ideal landfill siting (Table 4), with terrain parameters, natural resources, and human infrastructure numbering among the broad criteria. The most significant criteria were selected according to landfill site selection regulations in Algeria and conditions of the study area in order to protect sensitive ecosystems, surface water, as well as urban and rural areas.

Table 4

Grading values and description of selected criteria

| Criteria	Classes	Description	Scores
Ecological criteria			
Surface water (m)	d < 1000	Unsuitable	0
	1000 < d < 2000	Less-suitable	1
	2000 < d < 3000	Suitable	5
	3000 < d	Highly-suitable	10
Residential area (m)	0 < d < 1000	Less-suitable	1
	1000 < d < 2000	Suitable	5
	2000 < d	Highly-suitable	10
Sensitive ecosystems (m)	d < 500	Unsuitable	0
	500 < d < 1500	Less-suitable	1
	1500 < d < 3000	Suitable	5
	3000 < d	Highly-suitable	10
Socio-economic criteria			
Distance from roads (m)	0 < d < 500	Highly-suitable	10
	500 < d < 1000	Suitable	5
	1000 < d	Less-suitable	1
Slope (degree)	$0° < \alpha < 10°$	Highly-suitable	10
	$10° < \alpha < 25°$	Suitable	5
	$25° < \alpha < 45$	Less-suitable	1
	$45° < \alpha$	Unsuitable	0
Settlement (m)	0 < d < 1000	Less-suitable	1
	1000 < d < 2000	Suitable	5
	2000 < d	Highly-suitable	10
Land use			
	Barren land	Highly-suitable	10
	Pastures & agricultural area	Suitable	5
	Orchards	Less-suitable	1
	Built up (urbanized & industrial area)	Unsuitable	0
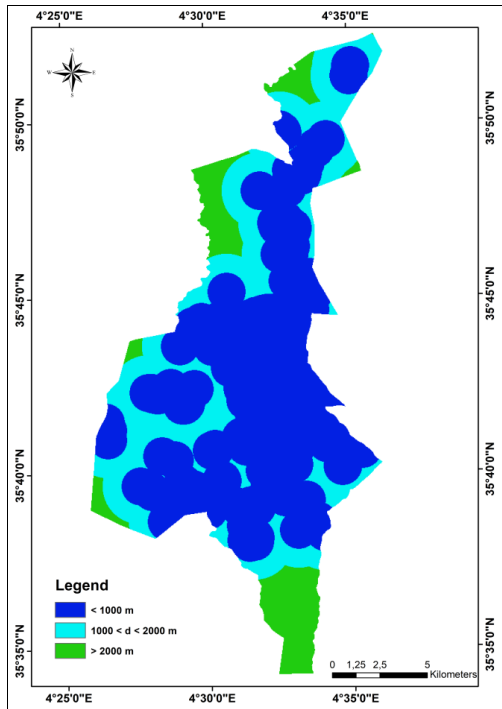
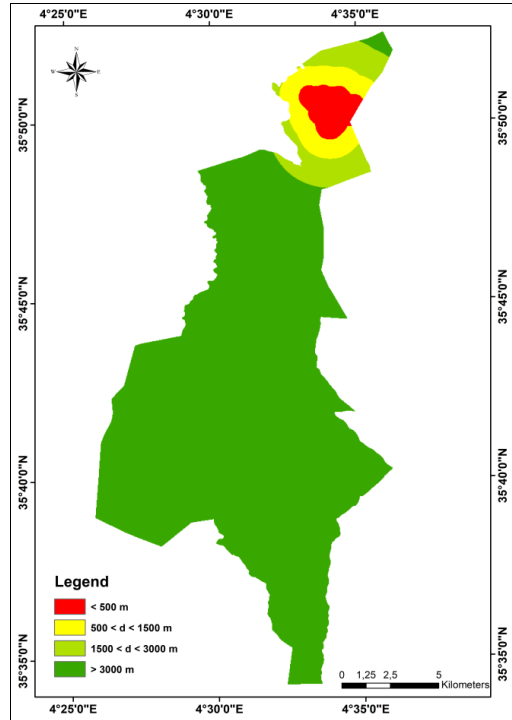Fig. 2 – Map of distance to residential area.

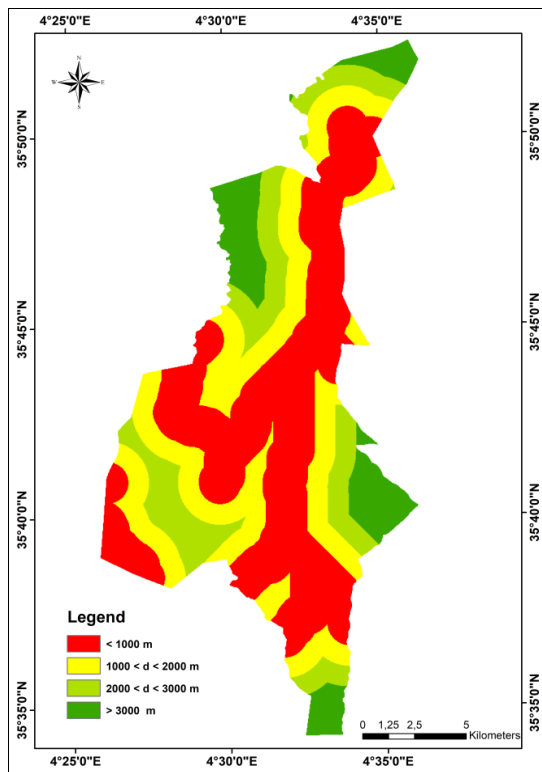Fig. 3 – Map of sensitive ecosystems.

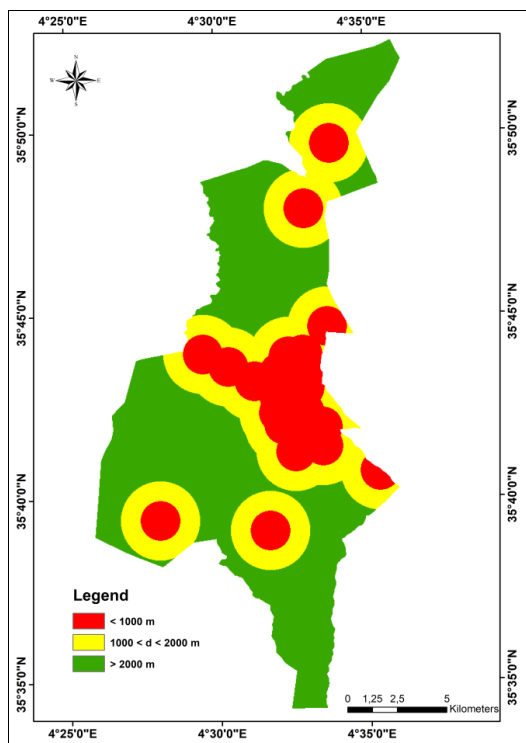Fig. 4 – Map of distance to surface water.

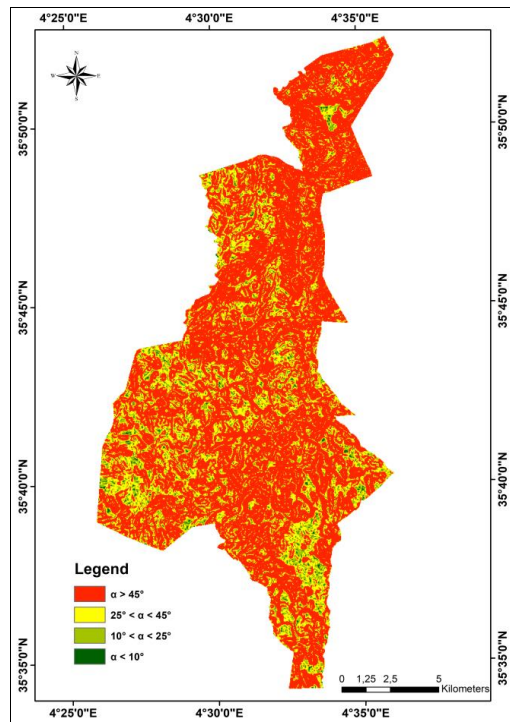Fig. 5 – Map of distance to settlement.
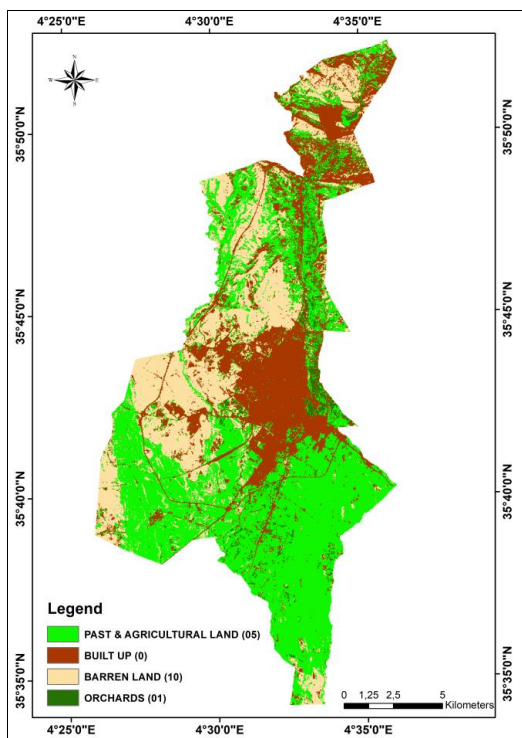

Fig. 6 – Map of slope.

Fig. 7 – Map of land use.
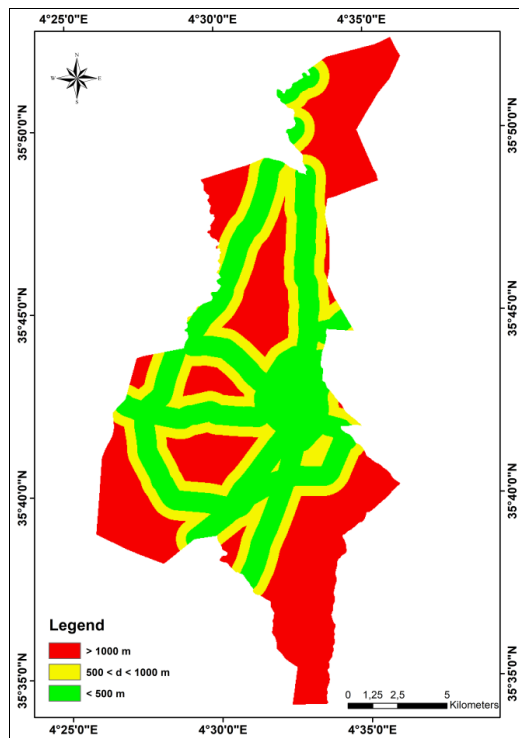
Fig. 8 – Map of distance to roads.

Table 5

Areas of selected priorities according to the index overlay method.

Selected Priorities	Highly Suitable	Suitable	Moderately Suitable	Less Suitable	Unsuitable	Sum of suitability
Area (km²)	1.16	11.03	17.65	33.28	170.08	233.2
Area (%)	0.50	4.73	7.73	14.27	72.93	100
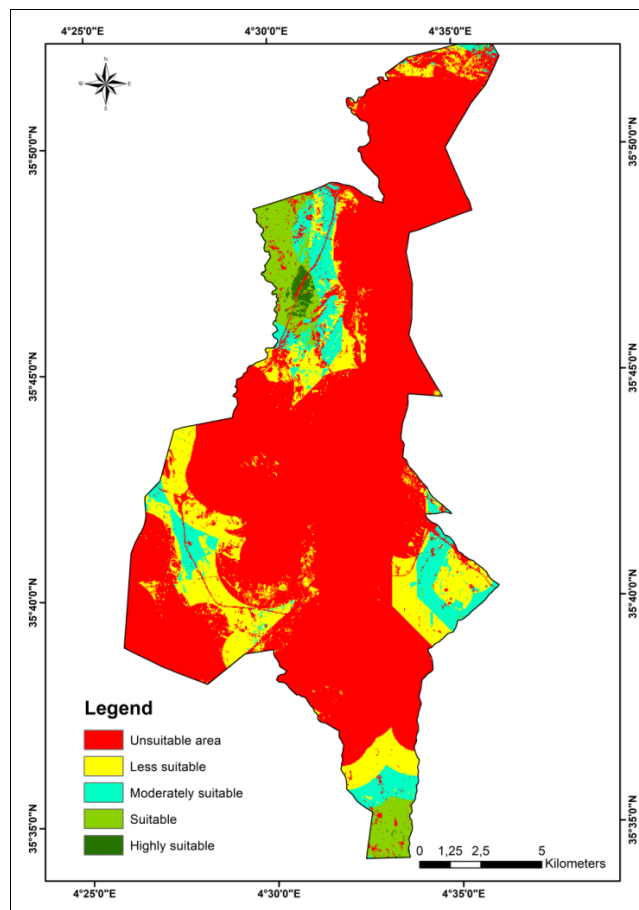
Fig. 9 – Landfill suitability map and area recommended for siting.

4.1. Ecological criteria

4.1.1. Surface Waters

Surface water is an important parameter to consider when setting up landfills. To avoid surface water pollution by landfill leachate[1], one should consider the minimum distance from surface water (Sener *et al.*, 2010). Oued K'sob is the main river that provides water for agricultural land irrigation in the study area. In this research, we have suggested bands at a gradually increasing distance and with a deviation of 1000 m (Fig. 2). For distances under the legal limits (1000 m), we assigned a score of zero, while areas over 3000 m were scored as 10 (Alavi *et al.*, 2013). The score was incrementally

---

[1] It has an adverse impact on groundwater quality, as well as on living beings. It contains high levels of organic, inorganic, heavy metal, and xenobiotic matter, which percolates through the subsoil and contaminates the groundwater.

increased as distance from the buffer zone increased as well (Table 4); the results presented in Fig. 4 show that surface waters must be 1000 m away from the selected landfill. Places that are at distances under 1000 m are unsuitable, places that are between 1000 m–2000 m away are less suitable, places between 2000 m–3000 m away are moderately suitable and places 3000 m away are highly suitable.

4.1.2. Sensitive Ecosystems

A landfill should not be located near any sensitive ecosystem such as lakes, dams, or wetlands (Alavi *et al.*, 2013; Sener *et al.*, 2010). M'sila is located near some sensitive areas, such as Ksob dam (With a capacity of 50 million cubic meters of water intended for the irrigation of 13,000 ha). For this reason, a 500 m buffer was placed around all sensitive ecosystems. Therefore, a score of 0 was assigned when the distance to a sensitive ecosystem was under 500 m. However, when the distance from the boundary was increased, the score rose accordingly, based on the expert opinion judgement. Therefore, if the distance to a sensitive ecosystem was over 3000 m, a score of 10 was allocated (Table 4); thus, the areas will be highly suitable for landfill sites (Fig. 3).

4.1.3. Residential area

Because of odour, dust and noise, the landfill sites' proximity to urban and rural areas can have an impact on the population and the landscape (Uyan, 2014; Tchobanoglous *et al.*, 1993). For that, the landfill site should not be placed near a residential or urban area, so as to avoid adversely affecting land value and future development, and to protect the general public from possible environmental hazards stemming from landfill sites. In this study, scores of 0 and 10 were given respectively to a distance under 1000 m and over 2000 m to a residential area. The results presented in Fig. 2 show areas that are at distances under 1000 m to residences to be unsuitable (Nas *et al.*, 2010), areas at between 1000 m–2000 m away to be less suitable, and areas that over 2000 m away – highly suitable.

4.2. SOCIO-ECONOMIC CRITERIA

4.2.1. Land Uses

Due to its reliance on an understanding both of the natural environment and the kinds of land uses envisaged, land use planning when performing site selection is an important criterion; therefore, based on the general land uses in this area, land uses were divided into the residential, agricultural, industrial, activity-dedicated and unused lands. Disposal of MSW onto built-up lands is strictly forbidden; consequently, built-up lands were deemed unsuitable for landfill sites and received a score of 0.

The unused lands, with a score of 10, were ranked highly suitable because of the easy clearing, good terrain and low economic values. Pastures and agricultural lands were ranked moderately suitable, barren land was ranked highly suitable because of the light vegetation and orchards were ranked unsuitable as they are not suitable for siting landfills (Fig. 7).

4.2.2. Distance to Roads

Distance to roads is an important criterion; hence, closer distances to main roads received higher scores. According to environmental experts, the distance between a landfill and a main road should be under 500 m. To assess this criterion, 500 m buffer zones were established around all roads. Distances of 500–1000 m received scores of 5. The highest score, that of 10, was assigned to a distance under 500 m (Table 4). The results shown in Fig. 8 indicate that distances greater than 1000 m from roads are less suitable, a distance between 500 m and 1000 m may be considered suitable, which corresponds to the study of Allen *et al.* (2002) who affirmed that a distance over 1 km away from main roads should be avoided. The most suitable distance from the road is under 500 m for easy accessibility.

4.2.3. Slope

Land slope is a basic parameter for the construction and operation of a landfill site. Sites with steep slopes are usually not technically suitable for landfill construction. The values of the slope distribution in M'sila range between 0 and over 45°, as demonstrated in Fig. 6.

The very steep areas (>45%), the steep areas (25 – 45%), the inclined planes areas (10 – 25%) and the slightly sloping areas (<10%) received scores of 0, 1, 5, and 10, respectively (Table 4). The most suitable areas were considered to be the inclined planes (10 – 25%) with a score of 5, while the slightly sloping areas (<10%), with a score of 10 (Kontos *et al.*, 2005), may be regarded as most appropriate areas. Those areas exceeding a 45° – slope were deemed not appropriate for a landfill site, which is accordance with the study of Guiqin *et al.* (2009) who affirmed that a slope greater than 40° is not suitable as a landfill site.

4.2.4. Distance from settlements

Locating a landfill near urban centres and villages can cause a negative environmental impact including odour, noise caused by vehicles and mechanical equipment, traffic, and dust. According to environmental experts, landfills at a distance of under 1000 m from population centres are not allowed, whereas those situated more than 2000 m away are highly suitable.

5. CONCLUSIONS

Disposing municipal solid waste to open dumps leads to many environmental and public health concerns in M'sila. In order to consider all criteria for landfill site identification within this extended area, we have applied a combined methodology of GIS and AHP. The landfill site selection criteria taken into consideration include proximity to major roads, built-up areas, land use, sensitive ecosystems, slope and water bodies. GIS was employed to digitize all the spatial features related to suitably siting landfill areas.

In this study, different data from various parameters were obtained and prepared in a GIS environment. Then, we used AHP to establish the relative importance of criteria to each other, and the SAW method to evaluate land suitability. The results showed that among the studied criteria, sensitive ecosystems and surface waters were the most important ones. The sensitive ecosystems were the major criteria in this case study, while the least important criterion was proximity to roads.

The purpose of this study was to pursue an appropriate selection process by taking into account environmental issues, and to suggest an appropriate site for landfills using GIS and multi-criteria decision-making techniques (AHP) so as to facilitate the choice of a suitable location.

As a result, approximately 0.5% of the entire study region was highly suitable for landfilling, while 4.73% was only suitable. These sites are easy to access for the disposal of solid waste. They are located in the northern and southern part of the study area. These are the most suitable classes, which could be suitable from an environmental, transport and socio-economic point of view.

REFERENCES

Abdelli, I.S., Asnoune, M., Arab, Z., Abdelmalek, F., Addou, A. (2017), *Management of household waste in sanitary landfill of Mostaganem district (Western Algeria)*. J Mater Cycles Waste Manag, **19**, pp. 265–281 (2017). https://doi.org/10.1007/s10163-015-0415-6.

Abedi-Varaki, M., Davtalab, M. (2016), *Site selection for installing plasma incinerator reactor using the GIS in Rudsar county, Iran*. Environmental Monitoring and Assessment, **188**(6), p. 353.

Ahmed, M., Karuturi, V.S. (2019), *Solid waste dumping site selection using GIS-based multi-criteria spatial modeling: a case study in Logia town, Afar region, Ethiopia*. Geology, Ecology, and Landscapes. https://doi.org/10.1080/24749508.2019.1703311.

Barakat, A., Hilali, A., El Baghdadi, Touhami, F. (2017), *Landfill site selection with GIS-based multi-criteria evaluation technique. A case study in Béni Mellal-Khouribga Region, Morocco*. Environmental Earth Sciences, **76**(*12*), p. 413, DOI: 10.1007/s12665-017-6757-8.

Alanbari, M.A. *et al*. (2014), *Modeling landfill suitability based on GIS and multicriteria decision analysis: case study in Al-Mahaweelqadaa*. Natural Science, **6**, pp. 828–851.

Alavi, M.R., Mokhtarani, N., Mokhtarani, B. (2013), *Municipal solid waste landfill site selection with geographic information systems and analytical hierarchy process: A case study in Mahshahr County, Iran*. Waste Manag. Res, **31**, pp. 98–105.

AND (National Waste Agency), (2014), *Characterization of household and similar waste in the northern, semi-arid and arid areas of Algeria*, Algiers, 2014.

Awomeso, J.A. *et al*. (2010), *Waste disposal and pollution management in urban areas: a workable remedy for the environment in developing countries*. American Journal of Environmental Sciences, **6**(*1*), pp. 26–32.

Bendjoudi, Z., Taleb, F., Abdelmalek, F., Addou, A. (2009), *Healthcare waste management in Algeria and Mostaganem department.* Waste Management, **29**(*4*), pp. 1383–1387 https://doi.org/10.1016/j.wasman.2008.10.008.

Bhushan, N., Rai, K. (2004), *Strategic decision making: applying the analytic hierarchy process*. Springer, New York, p. 172.

Bilgehan, N. *et al*. (2008), *Selection of MSW landfill site for Konya, Turkey using GIS and multi-criteria evaluation*. Environ Monit Assess, **160**, pp. 491–500.

Carone, E., Sansò, P. (2010), *Individuazione di aree idonee per la realizzazione di discariche RSU mediante tecniche GIS: esempio di applicazione in provincia di Brindisi*. Geologi e Territorio, **4** – 2009/**1** – 2010, pp. 3–10.

Chang, N., Parvathinathanb, G., Breden, J.B. (2008), *Combining GIS with fuzzy multicriteria decisionmaking for landfill siting in a fast-growing urban region*. Journal of Environmental Management, **87**, pp. 139–153. doi:10.1016/j.jenvman.2007.01.011.

Delgado, O.B., Mendoza, M., Granados, E.L., Geneletti, D. (2008), *Analysis of land suitability for the siting of inter-municipal landfills in the Cuitzeo Lake Basin, Mexico*. Waste Management (New York, N.Y.), **28**, pp. 1137–1146. doi:10.1016/j. wasman.2007.07.002.

Demesouka, O.E., Vavatsikos, A.P., Anagnostopoulos, K.P. (2013), *Suitability analysis for siting MSW landfills and its multicriteria spatial decision support system: Method, implementation and case study*. Waste Manag, **33**, pp. 1190–1206.

Drobne, S., Lisec, A. (2009), *Multi-attribute decision analysis in GIS: weighted linear combination and ordered weighted averaging*. Informatica, **33**, pp. 459–474.

Ebistu, T.A., Minale, A.S. (2013), *Solid waste dumping site suitability analysis using geographic information system (gis) and remote sensing for bahir dar town, north western ethiopia*. African Journal Of Environmental Science and Technology, **7**(*11*), pp. 976−989.

El Alfy, Z., Elhadary, R., Elashry, A. (2010), *Integrating GIS and MCDM to Deal with landfill site selection*. Int. J. Eng. Technol, **10**, pp. 32–42.

Erkut, E., Moran, S.R. (1991), *Locating obnoxious facilities in the public sector: An application of the hierarchy process to municipal landfill siting decisions*. Socio-Economic Planning Sciences*, **25**(*2*), pp. 89–102. doi:10.1016/0038-0121(91)90007-E.

Eskandari, M., Homaee, M., Falamaki, A. (2016), *Landfill site selection for municipal solid waste in mountainous areas with landslide susceptibility*. Environ Sci Pollut Res, 23, pp. 12423–12434. https :// doi.org/10.1007/s1135 6-016-6459-x

Gbanie, S.P., Tengbe, P.B., Momoh, J.S., Medo, J., Kabba, V.T.S. (2013), *Modelling landfill location using Geographic Information System (GIS) and Multi-Criteria Decision Analysis (MCDA): case study Bo, Southern Sierra Leone*. Appl Geogr, **36**, pp. 3–12.

Gizachew, K., Suryabhagavan, K.V., Mekuria, A., Hameed, S. (2012), *GIS-based solid waste landfill site selection in Addis Ababa, Ethiopia*. International Journal of Ecology and Environmental Sciences, **38**, pp. 59−72.

Gomez-Delgado, M., Tarantola, S. (2006), *Global sensitivity analysis, GIS and multi-criteria evaluation for a sustainable planning of a hazardous waste disposal site in Spain*. International Journal of Geographical Information Science*, **20**(*4*), pp. 449–466. doi:10.1080/13658810600607709.

Guerrero, L.A., Maas, G., Hogland, W. (2013), *Solid waste management challenges for cities in developing countries*. Waste Manag, **33**, pp. 220–232.

Hossein, Y. *et al*. (2018), *Landfill Site Selection Using a Multi-Criteria Decision-Making Method: A Case Study of the Salafcheghan Special Economic Zone, Iran*. Sustainability, **10**(*4*), p. 1107.

José, A.A., Teresa, L. (2006), *Consistency in the analytic hierarchy process: a new approach*. International Journal of Uncertainty, Fuzziness and Knowledge-Based Systems, **14**(*4*), pp. 445−459.

Kamali, M. *et al*. (2017), *Delphi-AHP and weighted index overlay-GIS approaches for industrial site selection case study: large extractive industrial units in Iran*. Journal of Settlements and Spatial Planning, **8**(*2*), pp. 99–105.

Kara, C., Doratli, N. (2012), *Application of GIS/AHP in siting sanitary landfill: A case study in Northern Cyprus*. Waste Manag. Res, **30**, pp. 966–980.

Asif, K., Chaudhry, M. N., Ashraf, U., Syed, M.A. (2019), *GIS-Based Multi-Criteria Evaluation of Landfill Site Selection in Lahore, Pakistan*. Polish Journal of Environmental Studies. DOI: 10.15244/pjoes/95181.

Khairul, M., Simare-mare, Siahaan, A. P. U. (2016), *Decision Support System in Selecting The Appropriate Laptop Using Simple Additive Weighting*, International Journal of Recent Trends in Engineering & Research, **2**(*12*), pp. 215–222.

Khan, D., Samadder, S.R. (2014), *Municipal solid waste management using geographical information system aided methods: a mini review*. Waste Management & Research, **32**, pp. 1049–1062.

Kodwo, M. *et al*. (2015), *Municipal solid waste characterization and quantification as a measure towards effective waste management in Ghana*. Waste Management, **46**, pp. 15–27. https://doi.org/10.1016/j.wasman.2015.09.009.

Kontos, T.D., Halvadakis, C.P. (2002), *Development of a Geographic Information System (GIS) for land evaluation for landfill siting: the case of Lemnos Island*. In: 7th national conference of Hellenic cartographic society, Mytilene, Lesvos, pp. 98–107.

Kontos, T.D., Komilis, D.P., Halvadakis, C.P. (2005), *Siting MSW landfills with a spatial multiple criteria analysis methodology*. Waste Manag, **25**, pp. 818–832.

Kontos, T.D., Komilis, D.P., Halvadakis, C.P. (2003), *Siting MSW landfills on Lesvos island with a GIS based methodology*. Waste Management & Research, **21**, pp. 262–277.

Malc-zewski, J. (1997), *Propagation of errors in multicriteria location analysis: A case study*. In G. Fandel & T. Gal (Eds.), Multiple criteria decision making, pp. 154–155.

Minghua, Z., Xiumin, F., Rovetta, A., Qichang, H., Vicentini, F., Bingkai, L. (2009), *Municipal solid waste management in Pudong New Area, China*. Waste Manag, **29**, pp. 1227–1233.

Moeinaddini, M., Khorasani, N., Danehkar, A., Darvishsefat, A.A., Zienalyan, M. (2010), *Siting MSW landfill using weighted linear combination and aNalytical Hierarchy Process (AHP) methodology in GIS environment (case study: Karaj)*, Waste Management, **30**, pp. 912–920.

Hafidi, M. (2015), *L'impact et la Gestion des Déchets Solides – Région Marrakech-SAFI-, HELMUT REIFELD ABIR IBOURK,* 2015, Konrad-Adenauer-Stiftung E.V., Bureau du Maroc.

Mojtaba, B. *et al*. (2019), *Landfill site selection using GIS-based multi-criteria evaluation (case study: SaharKhiz Region located in Gilan Province in Iran*. SN Applied Sciences, **1**, p. 1082. https://doi.org/10.1007/s42452-019-1109-9.

Nas, B., Cay, T., Iscan, F., Berktay, A. (2010), *Selection of MSW landfill site for Konya, Turkey using GIS and multi-criteria evaluation*. Environmental Monitoring and Assessment, **160**(*1*), pp. 491–500. DOI: 10.1007/s10661-008-0713-8.

Nemouchi, H. (2005), *Crise multidimensionnelle des villes algériennes: entre discours et réalité, la gestion du patrimoine foncier le cas de la ville de Skikda (nord-est algérien)*. Université de Caen, Basse-Normandie.

Nishanth, T., Prakash, M.N., Vijith, H. (2010), *Suitable site determination for urban solid waste disposal using GIS and Remote sensing techniques in Kottayam Municipality.* India. International Journal Of Geomatics And Geosciences, **1**(*2*), pp. 197–210.

Pinar, Y.G., Akgun, H. (2014), *Landfill site selection utilizing TOPSIS methodology and clay liner geotechnical characterization: a case study for Ankara, Turkey*. Bull Eng Geol Environ, **73**, pp. 369–388. https ://doi.org/10.1007/ s1006 4-013-0562-8.

Pires, A., Chang, N.B., Martinho, G. (2011), *An AHP-based fuzzy interval TOPSIS assessment for sustainable expansion of the solid waste management system in Setúbal Peninsula, Portugal*. Resour. Conserv. Recycl, **56**, pp. 7–21.

Programming and budget monitoring department DPAT. (2017), M'sila by the numbers.

Rahman, M., Sultana, K. R., Hoque, M. A. (2008), *Suitable Sites for Urban Solid Waste Disposal Using GIS Approach in Khulna City, Bangladesh*. Environmental Science Discipline, **45**(*1*), pp.11–22. http://www-sul.stanford.edu/ depts/gis/whatgis.html.

Ramjeawon, T., Beerachee, B. (2008), *Site selection of sanitary landfills on the small island of Mauritius using the analytical hierarchy process multi-criteria method*. Waste Manag. Res, **26**, pp. 439–447.

Saaty, T. L. (1980), *The analytic hierarchy process*. McGraw-Hill International, New York, p. 287.

Safaa, M. (2012), *La gestion des déchets ménagers au Caire: les habitants en question*. Égypte/Monde arabe, Troisième, document 8, mis en ligne le 01 septembre 2012. URL: http://ema.revues.org/3003; DOI: 10.4000/ema.3003.

Sarptas, H., Alpaslan, N., Dolgen, D. (2005), *GIS supported solid wastemanagement in coastal areas*. Water Science and Technology, **51**(*11*), pp. 213–220.

Sener, S., Sener, E., Nas, B., Karagüzel, R. (2010), *Combining AHP with GIS for landfill site selection: a case study in the Lake Beysehir catchment area (Konya, Turkey)*. Waste Manag, **30**, pp. 2037–2046.

Sener, S., Sener, E., Karagüzel, R. (2011), *Solid waste disposal site selection with GIS and AHP methodology: A case study in Senirkent–Uluborlu (Isparta) Basin, Turkey*. Environ. Monit. Assess, **173**, pp. 533–554.

Sener, B., Suzen, L., Doyuran, V. (2006), *Landfill site selection by using geographic information systems*. Environmental Geology, **49**, pp. 376–388. doi:10.1007/ s00254-005-0075-2.

Sharifi, M., Hadidi, M., Vessali, E., Mosstafakhani, P., Taheri, K., Shahoie, S., Khodamoradpour, M. (2009), *Integrating multi-criteria decision analysis for a GIS-based hazardous waste landfill sitting in Kurdistan Province, western Iran*. Waste Manag, **29**, pp. 2740–2758.

Siddiqui, M.Z., Everett; J.W., Vieux, B.E. (1996), *Landfill siting using geographic information systems: A demonstration*. Journal of Environmental Engineering, **122**(*6*), pp. 515–523. doi:10.1061/(ASCE) 0733–9372(1996)122:6(515).

Aliouche, S. *et al*. (2017), *Modalités de sélection des sites d'enfouissement technique en Algérie et leur prise en charge par les instruments d'aménagement du territoire et d'urbanisme*. Déchets Sciences et Techniques – N°75 – Décembre 2017, INSA de Lyon, France.

Soroudi, M., Omrani, G., Moataar, F., Jozi, S.A. (2018), *A comprehensive multi-criteria decision making-based land capability assessment for municipal solid waste landfill siting*. Environ. Sci. Pollut. Res, **25**, pp. 27877–27889. https://doi.org/10.1007/s11356-018-2765-9.

Tchobanoglous, G., Theisen, H., Vigil, S. A. (1993), *Integrated solid waste management, engineering principles and management issues*, 2nd edn. McGraw-Hill, New York.

United Nations. (2017) *World population prospects*: *2017 revision population database*. Retrieved from http://www.un.org/esa/population/unpop.htm.

Uyan, M. (2014), *MSW landfill site selection by combining AHP with GIS for Konya, Turkey*. Environmental Earth Sciences, **71**(**4**), pp. 1629–1639, DOI: 10.1007/s12665-013-2567-9.

Vatalis, K., Manoliadis, O. (2002), *A two-level multicriteria DSS for landfill site selection using GIS: Case study in Western Macedonia, Greece*. Journal of Geographic Information and Decision Analysis, **6**(*1*), pp. 49–56.

Yan, W. *et al* (2017), *In situ measurement of alkali metals in an MSW incinerator using a spontaneous emission spectrum*. Appl. Sci. **7**, p. 263. https://doi.org/10.3390/app7030263.

Yesilnacar, M.I., Cetin, H. (2005), *Site selection for hazardous wastes: A case study from the GAP area, Turkey.* Engineering Geology, **81**, pp. 371–388.

Yoon, K., Hwang, C.L. (1995), *Multiple Attribute Decision Making: an Introduction*. Sage Publication Inc., London, 83 p.

Yukalang, N., Clarke, B., Ross, K. (2017), *Barriers to effective municipal solid waste management in a rapidly urbanizing area in Thailand*. Int. J. Environ. Res. Public Health, **14**(*9*), p. 1013. https://doi.org/10.3390/ijerph14091013.

THE TYPOLOGY OF THE WORLD'S MACRO-REGIONS

JIŘÍ ANDĚL[*], JAN D. BLÁHA[**], IVAN BIČÍK[***]

Abstract. The article deals with changing differences among the world's macro-regions. It examines whether these differences tend to expand or not. Do convergent or divergent trends prevail within the global system? Changes are studied on the basis of the so-called world's macro-regions that have a high degree of social, economic, and cultural homogeneity. In the parts 'The Forming of the World's Macro-Regions' and 'The Typology of the World's Macro-Regions' the authors explain different macro-regions including their typology. The core part of this article critically evaluates trends in the development of the world's macro-regions; changes in the basic indicators in different macro-regions between 1990 and 2016 are explained. Contradictory trends (divergence and convergence) often appear. The findings are further discussed in a broader geopolitical framework.

1. INTRODUCTION

The ongoing global changes strongly influence the current structure of the world, as well as the changing nature of the world's different regions. These changes, however, are diverse. Thus, the crucial question is whether such uneven change dynamics depend on the level of wealth, or rather on lower-than-average development. This study examines the following aspect: are the gaps among the different world regions widening or not? In other words, is it convergence that prevails within the global system, or is it divergence? To address this issue, the authors have chosen the following intermediate steps:

(1) Geographical units were chosen where global processes would be examined;

(2) These units were sorted into classes (the typology was established) using different economic and social data, with respect to geographical position;

(3) Suitable indicators were chosen.

One of the key questions examined in this study is whether the global trends of the post-bipolar world have now a tendency to reverse. The long-time dominance of the "West" (seen as the core of the global system – see Wallerstein, 1979), which was typical throughout the entirety of the 20th century (Taylor, 1989; Lindert & Williamson, 2001; Landes, 1998; Novotný, 2007; Pieterse, 2011; Brauer & Dymitrow, 2017), seems to be slowing down or even disappearing. Rapid economic growth of many semi-peripheral and especially peripheral countries was enhanced by the financial and economic crisis and stagnation of the most developed countries (Hampl, 2014). Many questions related to this goal have already been answered in our previous work (Anděl, Bičík & Bláha, 2020).

Many economists support this trend referring to the dynamic progress of BRICS states (Brazil, Russia, India, China, and South Africa). A number of political scientists and political geographers support this idea, too, and talk about the "end of North Atlantic dominance" and the "end of the unipolar world" (Layne, 2006; Zakaria, 2008; Pieterse, 2011; Bradshaw, 2009).

---

* Associate Professor, Department of Geography Jan Evangelista Purkyně University in Ústí nad Labem, Pasteurova 15, 400 96 Ústí nad Labem, Czech Republic, jiri.andel@ujep.cz.

** Associate Professor, Department of Geography, Jan Evangelista Purkyně University in Ústí nad Labem, Pasteurova 15, 400 96 Ústí nad Labem, Czech Republic, jd@jackdaniel.cz.

*** Associate Professor, Department of Geography, Jan Evangelista Purkyně University in Ústí nad Labem, Pasteurova 15, 400 96 Ústí nad Labem, Czech Republic, ivan.bicik@natur.cuni.cz.

Both divergent and convergent trends are examined using the world's macro-regions that were defined in the other authors' publications (Anděl, Bičík & Zavadská, 2017; Anděl, Bičík & Bláha, 2018a; Anděl, Bičík & Bláha, 2020 etc.). Macro-regions are explained further on in the text. According to Wallerstein (1991), they can be divided into core, semiperipheral, and peripheral regions. Trends are evaluated using the appropriate indicators, such as gross domestic product, literacy, or life expectancy.

2. THE FORMING OF THE WORLD´S MACRO-REGIONS

Divergent and convergent trends of the contemporary globalized world are difficult to assess when only nation states are taken into account. Such an analysis would have only partial results – bigger regions (the world's macro-regions) are more convenient in this case.

The World's macro-regions should be economically, socially, and culturally homogeneous. They are expected to be contiguous and similar in size. When creating these regions, different authors use different approaches: social-economic (Morris, 1972), social-cultural (De Blij & Muller, 1997; Huntington 1996; Fellmann, Getis & Getis, 2008), or technical-economic ones (Cole, 1996).

The approach adopted in this study (Anděl, Bičík & Bláha, 2018b) is based on the following ideas and methodical frameworks. The World is divided into ten relatively homogeneous units (unlike continents that are much more heterogeneous). These macro-regions are evaluated as single units; subsequently, possible internal differentiation are discussed. For the sake of comparison, similar indicators are used for all regions.

From the methodical standpoint, it is a synthesis combining four relatively different concepts: those adopted by De Blij & Muller (1997), Cole (1996), Huntington (1996), and Hampl (2009). Social and cultural aspects ("civilizations") that roughly reflect Huntington's concepts (1996, see Fig. 1) form the most important factor. Secondly, economic interconnection and similarities are taken into consideration as regards the level of economic development. Thirdly, geographical complexity (in the sense of internal integrity) is also seen as an important factor.

Fig. 1 – Civilizations according to Huntington (1996).
Source: Huntington (1996).

Huntington's (1996) work reveals some interesting findings that are closely related to the topic of the present study. We have summarized them in the following eight points.

1. For the first time in history, global politics has a multi-polar and at the same time multi-civilizational (multi-cultural) character; modernization is no longer a synonym for the "westernization" of non-Western societies, and its result is not even universal civilization in some meaningful challenge of the word.

2. The power balance among civilizations (cultural regions of the world) is changing: the influence of the "West" is relatively declining (i); the economic, military and political power of Asian "civilizations" is growing (ii); a demographic revolution is taking place in Islamic countries, which has had destabilizing effects both for those countries in and of themselves, as well as for the rest of the world (iii); in general, "non-Western" countries are rediscovering the values of their own cultures and gaining political and economic power (iv).

3. A world order based on civilizations is born. States that are culturally close cooperate with each other, and macro-regions are created. Efforts to "enforce" a company from one civilization to another are not successful. The states of the macro-region are grouped around the leaders of said states, the leaders of their civilization.

4. Universalist demands are increasingly leading the "West" into conflicts with other civilizations, with Islamic countries, as Russia and China are becoming more serious. It appears there is the threat of local conflicts shifting towards a wider global conflict.

5. The survival of the "West" depends on the United States confirming its Western identity, and on whether the people of the "West" recognize that their civilization is unique, though not universal. Global conflict can be avoided if the leaders of the world's powers accept the multi-civilizational character of the world.

6. The "West" is currently the most powerful civilization and will remain so in the near future. However, its power in relation to other civilizations is declining. By promoting their values and protecting their interests, the "West" presents non-Western societies with an easy choice. Some of them are trying to imitate the West, thus more or less adding to its values, while others societies, especially Confucian and Islamic societies, are instead trying to increase their economic and military force so that they can stand up to the "West" and reach a "balance" in their relationship with it.

7. After the end of the Cold War, at the turn of the 9th decade of the 20th century, it became, therefore, the main axis of global politics, given the interaction between the economic and cultural power of the West and the economic and cultural power of non-Western civilizations.

8. Today, the world is made up of seven or eight major civilizations. The most important states of the world (economically and politically) more often than not come from different civilizations (the USA, the EU, Japan, China, Russia, India, Iran, Turkey). The main models of political and economic development differ from civilization to civilization, and differences between civilizations are key issues of contemporary international life. The "West", which has long enjoyed its dominant position in the world, is losing power, which shifts to non-Western societies. Global politics has already acquired a multi-polar and multi-civilizational (multi-cultural) character in the globalizing world.

Assigning appropriate names to the world's macro-regions poses a real challenge. The different concepts mentioned above often include the geographical position of respective regions on the globe and such names are sometimes rather complicated (South-western Asia and Northern Africa or some of the regions used by Huntington). This study uses the terms coined by Hampl (2009), with two exceptions (the Angloamerican macro-region and the Indonesian macro-region).

The economic standards of various macro-regions, as well as convergent (divergent) trends are evaluated by representative indicators, reflecting economic, social, and demographic aspects. Economic well-being is measured with the aid different indices aggregated into the Human Development Index (HDI; Stanton, 2007). HDI is made up of the Gross Domestic Product (GDP), the Expectancy Index, and the Educational Index. The latter has been modified into Literacy Rate for the purpose of this study.

In out humble opinion (Anděl, Bičík & Bláha, 2018a, 2020), the World is divided into ten contiguous macro-regions. These are as homogeneous as possible in terms of social and economic development and cultural integrity (Fig. 2).

1. The European macro-region (except for Belarus and Ukraine, that are part of the Russian macro-region)
- is based on the concepts of European civilization that include cultural, social, and ethical values,
- has very high living standards (the highest life expectancy of all – 78 years for men, 83 for women, a literacy rate close to 100%),
- has the biggest share of the world's gross domestic product (25.6%),
- is quite homogeneous, both economically and culturally,
- the idea of European identity is important through the existence of the European Union.

Fig. 2 – The world's macro-regions, as defined by Anděl, Bičík & Bláha (2018a, 2020), modified.
Source: Anděl, Bičík & Bláha (2018a, 2020).

2. The Angloamerican macro-region
- covers the United States of America, Canada, and Greenland,
- most of its people speak English,
- enjoys high prosperity, includes the most economically developed parts of the world,
- has the highest share of world's gross domestic product (25.3%),
- has high level of economic a cultural homogenity,
- is rather homogeneous, both economically and culturally.

3. The Russian macro-region (Northern Eurasia)
- is identical to the former Soviet Union (except for Moldova, and the three Baltic countries),
- is the second largest of the world's macro-regions according to area (16.2%),
- the heritage of former Soviet Union acts as the main integrating factor,
- has a large distance between the main economic centers of the macro-region,
- industrial branches generate low added value,
- has a focus on the export of raw materials and weapons,
- natural conditions vary greatly across the region.

4. The Australian-Oceanic macro-region
- is the least populous of all macro-regions (only 0.5% of the world's population),
- has a very low population density (just 4.5 people per sq km),
- enjoys significant cultural and linguistic diversity,
- displays a stark contrast between the population of Australia and New Zealand on the one hand, and some Pacific islands on the other.

5. The Sino-Japanese macro-region, including China, Japan, the Korean Peninsula, Taiwan and Mongolia (Eastern Asia)
- holds a high share of the world's population (22.6%) and economy (22.0% by GDP),
- is the second most populous of the world's macro-regions and the third strongest by GDP,
- has had high dynamics of economic development in last 60/30 years in Japan/China
- its national economic systems are export-oriented,
- deals with complicated relations between communist and democratic countries,
- faces a high number of nature-related risks (extremelly polluted environment, desertification, volcanic activity, earthquakes, tsunamis).

6. The Indonesian macro-region (South-East Asia)
- is a special macro-region that includes countless islands, channels and straits,
- its economic activities tend to be clustered around the coastal area,
- has a long colonial past, as well as a relatively recent creation of independent states,
- has caused the geographic isolation of the islamic country of Indonesia from other Islamic countries,
- is greatly influenced both by the Chinese and the Indian macro-regions,
- copes with a number of social and economic problems,
- has extraordinarily high linguistic diversity.

7. The Indian macro-region
- covers the former area of British India (India, Pakistan, Bangladesh), Afganistan and Nepal,
- is the most populous of macro-regions (23.7% of the world's population),
- deals with overpopulation, high birthrate and relatively low mortality,
- religion plays an important role (Hinduism and Islam)
- having a common history under the British rule is a typical integrating factor,
- due to poor economic conditions, GDP per capita is the lowest among macro-regions,
- has a high proportion of rural population,
- has a low life expectancy (67 years for men, 70 for women)
- has a high literacy rate (43%),
- enjoys a high degree of cultural and economic heterogeneity.

8. The Islamic macro-region
- is made up of a belt of predominantly Islamic countries, from Morocco in West to Iran in the East,
- the Islamic religion is the most important integrating factor,
- internal cultural and ethnic differences often lead to high tensions within the macro-region,
- the economic progress of many of its countries is based on oil and gas extraction,
- encompasses the most conflict-prone areas of the contemporary Word, repeatedly plagued by foreing interference (the United States, Russia, China).

9. The Latin American macro-region
- covers the southern and central part of the Americas up to the US-Mexican border,
- has high level of integration based on the use of Romance languages and on the Christian religion,

- has a high rate of urbanization and a low population density,
- deals with widespread crime (often linked to the drug business),
- has extreme economic disparities between its countries.

10. The African macro-region
- includes the African countries located south of Morocco, Algeria, Tunisia, Libya and Egypt,
- is the largest of the world's macro-regions (18.4% of Earth´s landmass),
- tackles poverty, widespread illiteracy (one third of the population cannot read or write), frequent epidemics, overpopulation, ethnic tensions, and colonial heritage as the typical and integrating factors into the macro-region,
- undemocratic regimes prevail, often under military rule,
- produces just 2% of the world's nominal GDP,
- economic and cultural differences are extraordinarily high, caused mainly by complex ethnic patterns,
- many states of the macro-region are nowadays plagued by ethnic and religious tensions,
- a high incidence of corruption and so-called tribalism are typical aspects of the region.

At the turn of the 3rd decade of the 21st century, we are seeing an increase in the prices of goods on world markets. This includes food, oil, precious metals, strategic metals, industrial products and other goods. Economists and political scientists are asking the question whether we are at the beginning of a new, longer-running economic supercycle that may have an impact on changing the balance of power between the world's macro-regions. The supercycle is defined as a long period of rising prices of goods and services as a consequence of strong economic growth. Perič (2021) points out that in the 20th century the world experienced a supercycle only three times.

The first supercycle was caused by industrialization and the subsequent development of urbanization in the United States associated with the First World War. The result has been, among other things, a significant improvement in the US's economic and geopolitical standing in the world. The second supercycle was associated with the reindustrialization of (Western) Europe and Japan after the Second World War, which again brought an improvement in the economic and geopolitical position of these two regions on the world stage. The third supercycle was brought about by the post-1990 industrialization and urbanization of China. Over the past 20 years we have had the opportunity to observe its unprecedented economic growth and success in gaining an important geopolitical position in the world. All three of these supercycles were driven by demand related to the revolutionary process of industrialization and urbanization. At the same time, there was a lack of capacity in the required volume of several product categories, especially energy, metals and minerals.

Perič (2021) points out that in the next 10–15 years we may very well see two potential triggers for greater economic expansion, which could lead to the beginning of a new supercycle. One is a country capable of influencing world economy and commodity prices just like China did 30 years ago. That country is India, where not only strong industrialization and urbanization can be expected in the near future, but given its potential in finance, informatics, commercial services and, of course, a huge number of educated young people, a significant shift in building a post-industrial society can also take place.

As in China thirty years ago, these changes are very likely to bring significant economic growth to India and possibly an improvement in its geopolitical position in the world. The second possible impetus for the new supercycle is the expected large-scale construction of new energy infrastructure to support climate goals, which several countries have included in their strategic development plans. An extensive fiscal stimulus related to the Covid-19 pandemic could also help trigger the supercycle (Perič, 2021).

3. THE TYPOLOGY OF THE WORLD'S MACRO-REGIONS

The Economic prosperity of a country or region is routinely measured by gross domestic product (GDP) per capita. According to this standard, the European macro-region ranks 1: the European share of the world's population equals 7.3%, while that of the world's GDP is 25.6%. Similar numbers apply for the Angloamerican macro-region (4.9% of the world's population, 25.3% of world's GDP) and the Australian-Oceanic macro-region (0.5% and 2.2%, respectively).

The European and Angloamerican macro-regions combined make up more than half of the world's economy. Four macro-regions (Russian, Sino-Japanese, Islamic, and Latin American) have roughly equal shares in the world's total population number and GDP. Major inequalities, however, can be noted in the African macro-region (13.4% of the world's population, 2.2% of the world's GDP), the Indian macro-region (23.7% and 3.4%), and the Indonesian macro-region (8.5% and 2.9%).

The above-mentioned differences become very clear when GDP per capita (measured by purchasing power parity, PPP) is taken into consideration. GDP per capita (PPP) in the most economically developed regions is more than ten times higher than corresponding figures for the poorest regions. The comparison of GDP per capita (without PPP correction) would show even higher inequalities (25:1) – see Table 1.

Table 1

The world's macro-regions according to population and GDP (2016)

No.	Macro-region	1	2	3	4	5
1	European	541	7.3	19.4	25.6	35.9
2	Angloamerican	363	4.9	19.2	25.3	52.9
3	Russian	286	3.8	2.4	3.2	8.4
4	Australian-Oceanic	39	0.5	1.7	2.2	43.6
5	Sino-Japanese	1,668	22.6	16.7	22.0	10.0
6	Indonesian	629	8.5	2.2	2.9	3.5
7	Indian	1,755	23.7	2.6	3.4	1.5
8	Islamic	502	6.8	4.3	5.7	8.6
9	Latin American	630	8.5	5.6	7.4	8.9
10	African	994	13.4	1.7	2.2	1.7
	Total	7,407	100.0	75.8	100.0	10.0*

1 – Population (millions); 2 – Population (%); 3 – GDP (trillions); 4 – GDP (%); 5 – GDP per capita (thousands of USD).
Source: the World Bank, the CIA World Factbook, the United Nations. Note: * mean value.

The literacy rate surpasses 90% in most macro-regions, with the exception of the Indian (57%), African (64%), and Islamic (75%) ones. The most economically advanced regions also show the highest levels of life expectancy; at the other end of the spectrum, the African macro-region is at the bottom of the list (life expectancy is 57 years for men, 60 for women). The Russian, Indian, Indonesian, and Sino-Japanese macro-regions as a whole also display relatively low figures; Japan itself, however, belongs among the countries with the highest life expectancy.

The World's macro-regions can be sorted into different classes according to social and economic standards. The European and Angloamerican macro-regions are undoubtedly the most developed ones, making up over 50% of the world's economy. The Australian-Oceanic macro-region also has very good values (GDP per capita, economic prosperity); however, in this region there are more pronounced internal differences (to be discussed further on). The Russian and Sino-Japanese macro-regions are comparable in terms of social and economic standards; the same applies for the Islamic and Latin American macro-regions. A critical situation persists in the African macro-region, where GDP per capita is more than ten times lower in comparison to Europe. More than one third of the

population is illiterate in Africa. The Indonesian macro-region, still below the world's average, has rather good prospects for the future (social aspects, literacy rate).

Table 2

Main indicators of the world's macro-regions (2016)

No.	Macro-region	1	2	3	4	5	6	7	8
1	European	3.7	7.3	106	25.6	100	78/83	***	***
2	Angloamerican	16.0	4.9	17	25.3	100	77/82	***	***
3	Russian	16.2	3.8	13	3.2	100	65/75	**	***
4	Australian-Oceanic	6.2	0.5	5	2.2	95	75/79	**	*
5	Sino-Japanese	8.6	22.6	141	22.0	95	66/70	*	***
6	Indonesian	3.3	8.5	140	2.9	91	68/74	**	*
7	Indian	3.7	23.7	344	3.4	57	67/70	**	*
8	Islamic	8.9	6.8	41	5.8	75	71/75	**	***
9	Latin American	15.0	8.5	31	7.4	90	72/79	**	***
10	African	18.4	13.4	40	2.2	64	57/60	*	*
	Total	100.0	100.0	54	100.0	80	68/72	.	.

1 – Area (%) ; 2 – Population (%); 3 – Population density (sqkm); 4 – GDP (%); 5 – Literacy Rate (%);
6 – Life Expentancy (years M/F); 7 – Homogeneity (economic); 8 – Homogeneity (cultural).
Source: the World Bank, the CIA World Factbook, the United Nations. Note: *, ** and *** represent the
level of homogeneity (from the bottom – up).

In addition to economic prosperity, the economic and cultural homogeneity of the world's macro-regions is also examined. The indicators shown in Table 2 allow us to formulate general conclusions and create different types of macro-regions (Fig. 3).

Fig. 3 – The typology of the world's macro-regions.

3.1. Type I – The European, Angloamerican, and Australian-Oceanic macro-regions

These regions, also called *core regions*, display high levels for all parameters (GDP per capita in excess of 35,000 USD, a literacy rate of 95% or more, a life expectancy of 75 years for men, 79 for women). These macro-regions are quite homogeneous regarding economic prosperity (all subregions

are well developed) and cultural patterns (all belong to one single civilization, *the western civilization*, as defined by Huntington, 1996, Fig. 1). The only exception is cultural heterogeneity in the case of the Australian-Oceanic macro-region where pronounced differences exist between Australia and New Zealand on one side, and the Pacific islands on the other. An interesting work dedicated to the macro-regions of the world was submitted by Polonský (2012), who defined the same 10 macro-regions of the world as the authors of the presented study. In his work, the author evaluated the integrated power potential of macro-regions. Polonský (2012) defines the integrated power potential as an indicator consisting of the values of GDP per capita, the share of the population in the total population of the world, and the share of the area of the macro-region in the land area of the Earth. An interesting finding of the author's is the fact that the share in power potential of the Type 1 macro-regions decreased from 1950 to 2008 from 48.8% to 34.0%. The European macro-region dropped from 24.4% to 16.3% (Germany decreased from 4.4% to 2.6%, Great Britain from 4.5% to 2.2% and France from 3.6% to 2.2%), the Angloamerican macro-region from 22.8% to 16.3% (the USA went from 22.8% to 14.5%) and the Australian-Oceanic macro-region went from 1.6% to 1.4%.

Values of Type I macro-regions (2016):
- 25.9% of total area, 12.7% of total population, 53.1% of total GDP
- 8 members of the "G20" platform (France, Germany, Italy, the United Kingdom, the European Union, the USA, Canada and Australia; see chapter 5).

3.2. Type II – The Russian, Sino-Japanese, and Latin American macro-regions

Most parameters show values around the world's average (GDP per capita 15,000 to 20,000 USD, a literacy rate of 95% or more, a life expectancy of 65–70 years for men, 70–79 for women). Cultural homogeneity for these *semiperipheral regions* is rather high (Orthodox, Chinese, Japanese, and Latin-American civilizations), while economic homogeneity is around average. According to Polonský (2012), the integrated power potential of Type 2 macro-regions for the 1950–2008 period increased from 30.3% to 37.5%. However, the change in the integrated power potential of individual macro-regions of this type is remarkable. While in the Russian macro-region we noted a decrease from 9.6% to 4.4% over the period under review, the share of the Sino-Japanese macro-region increased from 12.6% to 24.4% (China increased from 9.0% to 17.2%, and Japan from 3.1% to 4.4%) and the share of the Latin American macro-region remained virtually unchanged (only slightly increasing from 8.1% to 8.7%). As already mentioned several times in this article, this increase in the integrated power potential of Type II macro-regions can be "accounted for" primarily by the rapid growth of China's economy since the 1990s.

Values of Type II macro-regions (2016):
- 39.8% of total area, 34.9% of total population, 32.6% of total GDP
- 7 members of the "G20" platform (Russia, China, Japan, South Korea, Mexico, Argentina, Brasil).

3.3. Type IIa and IIb – Islamic and Indonesian macro-regions

These regions show similar levels of life expectancy (roughly 65 years for men, 75 years for women) and economic performance. Economic homogeneity is rather low. Literacy rate, however, varies significantly – in the Islamic macro-region it is quite low, especially women's literacy rate. The Islamic macro-region is culturally quite homogeneous, while in the Indonesian macro-region the opposite is true. The integrated power potential of Type IIA and IIB macro-regions over a period of 58 years, from 1950 to 2008 increased from 8.0% to 12.1% (Polonský 2012). The Islamic macroregion (increase from 4.2% to 6.2%) and the Indonesian macroregion (increase from 3.8% to 5.9%) contributed equally to this increase in integrated power potential. As shown in points throughout the

paper, the increase in the integrated power potential of this type of macro-region can be mainly "accounted for" by the dynamic development of the population of both macro-regions of this type.

Values of type IIa and IIb macro-regions (2016):

- 12.2% of total area, 15.3% of total population, 8.7% of total GDP
- 3 members of the "G20" platform (Saudi Arabia, Turkey, Indonesia).

3.4. Type III – Indian and African macro-regions

All indicators point to very low values (GDP per capita barely reaches 4,000 USD, the literacy rate is below 65%, life expectancy is also low). Economic and cultural heterogeneity is quite high in both macro-regions. The existing civilization, as defined by Huntington (1996), is extremely diverse ethnically in these *peripheral macro-regions*. A slight increase in the integrated power potential was also observed for Type III. The increase from 13.0% in 1950 to 16.4% in 2008 is mainly due to the population explosion of the Indian macro-region, mainly in India. While the Indian macro-region increased its integrated power potential from 8.2% to 11.1% (by almost 3%, India increased from 6.6% to 8.8%) over the period under review, the integrated power potential of the African macro-region changed only slightly, from 4.8% to 5.3%.

Values of Type III macro-regions (2016):

- 22.1% of total area, 37.1% of total population, 5.6% of total GDP
- 2 members of the "G20" platform (India and South Africa).

4. THE WORLD'S MACRO-REGIONS: CURRENT TRENDS

This part analyses changes in population and GDP in different regions over the 1990–2016 period. Tables 2 and 3 show the positioning of the different world macro-regions within the global system. Different dynamics in different parts of the world can be compared.

In terms of total GDP, Europe was part of the dominant world regions in 1990: with about 10% of the world's population, the European macro-region accounted for almost one third of the world's economy (measured by GDP). A similar ratio (GDP per capita) was applied to the Australian-Oceanic macro-region – the population of this part of the world, however, is twenty times lower.

The Angloamerican macro-region was the most economically advanced in the early 1990s. GDP per capita exceeded that of Europe by 50% (though nominal GDP was slightly lower). The European and Angloamerican macro-regions combined accounted for more than 60% of global GDP. On the contrary, the four weakest macro-regions (African, Indian, Indonesian, and Islamic) made up only 7.3% of the global GDP, with roughly 43% of the world's population. The difference between the strongest and weakest regions (Angloamerican vs. Indian) measured by GDP per capita was quite confounding – 62:1.

GDP per capita (the mean value for the whole world) rose 2.5 times between 1990 and 2016. Such an increase, however, was uneven when considered region by region. Developing countries (regions) show the fastest progress – also due to rather low starting levels. The Indonesian, Indian, Islamic, and African macro-regions now account for 53% of the world's population and 10.8% of the world's GDP. The most advanced regions (Angloamerican and European) produce 50.9% of world's GDP, which means a significant decrease compared to 1990. Moreover, the share of developed regions in terms of the world's population dropped to 12.2%. The differences between the strongest and weakest regions (Angloamerican vs. African and Indian) measured by GDP became much smaller (35:1).

Table 3

The world's macro-regions according to population and GDP (1990)

No.	Macro-region	1	2	3	4	5
1	European	508	9.9	6.8	31.8	13.0
2	Angloamerican	277	5.4	6.1	28.3	21.8
3	Russian	280	5.4	1.5	6.9	5.3
4	Australian-Oceanic	28	0.5	0.4	1.7	12.7
5	Sino-Japanese	1.320	25.5	4.1	19.0	3.1
6	Indonesian	437	8.5	0.3	1.6	0.8
7	Indian	1.100	21.4	0.4	1.9	0.4
8	Islamic	255	4.9	0.5	2.5	2.1
9	Latin American	481	9.3	1.1	5.0	2.2
10	African	483	9.4	0.3	1.3	0.6
	Total	5,167	100.0	21.5	100.0	4.1*

1 – Population (millions); 2 – Population (%); 3 – GDP (trillions); 4 – GDP (%); 5 –
GDP per capita (thousands of USD).
Source: The Calendario Atlante De Agostini, the World Bank, the CIA World Factbook, the United Nations.
Note: * mean value.

A comparison between Tables 2 and 3 shows that convergent trends prevail – in other words, the differences between the world's macro-regions are becoming smaller. More detailed characteristics such as differences among economic sectors (which are quite important) are not taken into consideration here.

Table 4 shows a different approach that enables the measurement of relative changes of GDP per capita in different regions. The Angloamerican region had the highest GDP per capita in 1990 as well as in 2016. These values are compared to the GDP of other macro-regions. Thanks to the fact that in 1990 all developing regions displayed rather low figures, their increase (in relative terms) was 2.8 to 4 times higher than that of developed regions over the past 26 years.

In other words, differences among regions decreased. From this perspective, we may discuss whether it is appropriate for other countries in Eastern Asia to share the same region as China and Japan owing to very different starting positions. Still, the Sino-Japanese macro-region shows significantly higher changes of GDP than the world's average over the 1990–2016 period.

The Indonesian macro-region recorded the highest increase in GDP per capita compared to the Angloamerican macro-region: the index rose from 3.7 (800 USD) to 6.6 (3,500 USD). Conversely, the Russian macro-region lost lost a significant amount (from 24.3 in 1990 to 15.8 in 2016).

Table 4

Changes in GDP per capita in different world macro-regions (1990, 2016)

No.	Macro-region	1	2	3	4	5	6
1	European	13	59.6	35.9	67.9	2.76	8 th
2	Angloamerican	21.8	100.0	52.9	100.0	2.43	9 th
3	Russian	5.3	24.3	8.4	15.8	1.58	10 th
4	Australian-Oceanic	12.7	58.3	43.6	82.4	3.43	5 th
5	Sino-Japanese	3.1	14.2	10.0	18.9	3.23	6 th
6	Indonesian	0.8	3.7	3.5	6.6	4.38	1 th
7	Indian	0.4	1.6	1.5	2.8	4.29	2 th
8	Islamic	2.1	12.4	8.6	16.2	4.10	3 th
9	Latin American	2.2	9.6	8.9	16.8	4.50	4 th
10	African	0.6	2.8	1.7	3.2	2.83	7 th
	Total	4.1	10.8	10.0	18.9	2.44	.

1 – GDP per capita 1990 (thousands USD); 2 – GDP per capita 1990 related to the Angloamerican macro-region (%); 3 – GDP per capita 2016 (thousands USD); 4 – GDP per capita 2016 related to the Angloamerican macro-region (%); 5 – Index 2016/1990 – GDP per capita in 2016 related to GDP per capita in 1990; 6 – Rank (sorted by index).
Source: the World Bank, the CIA World Factbook, the United Nations.

5. THE NEW POSITION RUSSIA, CHINA, INDIA AND BRASIL
IN GLOBAL ECONOMY

By the middle of the first decade of the 21st century, the tendencies of changes in "leadership" in the world economy were already evident. The roles of various informal groupings of developed countries into different "G groups" were also discussed. In connection with the emergence and establishment of new centers of economic and political power, the former emerging economies of China, India, Russia and Brazil and their new position and role in the world economy were most frequently mentioned. Everyone is familiar with the relatively new term "BRIC", respectively BRICS, a grouping of four countries, Brazil, Russia, India and China, to which South Africa was added in 2011. This designation, still BRIC at the time, was first used by Goldman Sachs investment bank in 2001. According to this report, some time between 2035 and 2040, the total GDP of these four countries will surpass the GDP of the six currently most developed economies in the world (the USA, Japan, Germany, Great Britain, France and Italy) (Haggett, 2001).

It is clear that more attention needs to be paid to two trends that shape the growth of the economies of the four major emerging world economies (China, India, Russia and Brazil), which have different conditions and trajectories of economic (and social) development compared to previous world economy leaders. The second trend is the stagnation of several regions, especially in Africa and part of the Islamic macro-region.

The informal G20 group was founded in 1999 with the aim of studying, reviewing, and promoting high-level discussions regarding policy issues pertaining to the promotion of international financial stability. The G20 is the latest in a series of post-World War II initiatives aimed at the international coordination of global economic policy. France, Germany, Italy, the United Kingdom, the European Union and the European Central Bank (the European macro-region), the USA, Canada (Angloamerican), Russia (Russian), China, Japan, South Korea (Sino-Japanese), India (Indian), Indonesia (Indonesian), Saudi Arabia, Turkey (Islamic), Mexico, Argentina, Brasil (Latin American), South Africa (African) and Australia (Australian-Oceanic) are part of the "G20" global world platform. Economic development, territorial and cultural attributes were respected when selecting the members of the "G20" platform.

In assessing the current development of these four economies, a number of questions arise, the most important of which seems to be the following: Can this aggressive growth of the BRIC economies be maintained for the following 20–30 years or is the current development only a situation where large amounts of money are sought abroad for new investment opportunities and are found today, especially in these four economies? A similar topic has been discussed with China for 20 years, but as the data in Tables 5 and 6 show, containing the GDP growth of these four countries and three advanced economies since 1990, it still works in China. Of course, it is very difficult to assess the economies of the BRIC countries as a whole. Each of them has their own particular type of economic development. The consequences of these changes will be reflected not only in the transformation of the world economy, but also in the redistribution of wealth and poverty reduction in the World (Haggett, 2001).

However, these four countries are well aware of their special standing in global politics and are trying to use every opportunity to clarify practices in the emerging global economy. Following the outbreak of the global crisis of 2009, the economies of these countries represented protruding islands in the sinking world economy and the hope of a faster solution to the global economic problems brought about by the crisis. The economies of the four countries are also expected to play a positive role in the coming crisis following the end of the Covid-19 pandemic.

Table 5

GDP and GDP per capita – annualized growth rates for the 1990–2015 period

Country	Marco-region	1	2
Germany	European	3.1	2.9
United Kingdom	European	3.6	3.1
France	European	2.6	2.2
USA	Angloamerican	4.6	3.6
Canada	Angloamerican	3.9	2.9
Russia	Russian	3.6	5.9
Japan	Sino-Japanese	3.2	2.8
China	Sino-Japanese	14.3	3.7
Indonesia	Indonesian	7.6	6.1
Turkey	Islamic	5.9	4.5
Saudi Arabia	Islamic	7.1	4.3
Iran	Islamic	-1.7	-3
India	Indian	13.3	7.7
Pakistan	Indian	6.8	4.6
Mexico	Latin American	5.7	4
Brasil	Latin American	5.7	4.3
Argentina	Latin American	5.9	4.7

1 – GDP annualized growth rate 1990–2015 (%); 2 – GDP *per capita* annualized growth rate 1990–2015 (%).
Source: List of countries by GDP growth 1980–2010. Wikipedia, available March 25th, 2021.

Table 6

GDP per capita between 1990 and 2019 in select countries (%)

Rok	Germany	USA	Russia	Japan	China	India	Brasil
1990	5.26	1.86	-3.00	5.20	3.80	5.53	-4.30
1991	5.11	-0.19	-5.05	3.35	9.20	1.06	1.51
1992	2.23	3.34	-14.53	0.97	14.20	5.48	-0.47
1993	-0.80	2.69	-8.67	0.25	14.00	4.77	4.67
1994	2.66	4.06	-12.57	1.10	13.10	6.65	5.33
1995	1.89	2.54	-4.14	1.96	10.90	7.57	4.42
1996	0.99	3.75	-3.60	2.75	10.00	7.56	2.15
1997	1.80	4.55	1.40	1.57	9.30	4.05	3.37
1998	2.03	4.22	-5.30	-2.05	7.80	6.19	0.04
1999	2.01	4.49	6.40	-0.14	7.60	7.39	0.25
2000	3.21	3.69	10.00	2.86	8.40	4.03	4.31
2001	1.24	0.76	5.09	0.18	8.30	5.22	1.31
2002	0.00	1.61	4.74	0.26	9.10	3.77	2.66
2003	-0.22	2.52	7.35	1.41	10.00	8.37	1.15
2004	1.06	3.65	7.14	2.74	10.10	8.28	5.72
2005	0.78	3.08	6.40	1.93	10.40	9.35	3.16
2006	2.87	2.87	7.40	2.40	11.60	9.67	3.97
2007	2.48	2.00	8.10	2.10	13.00	9.06	5.67
2008	1.30	1.10	7.30	-0.70	9.00	7.09	5.08
2009	-5.71	-2.54	-7.80	-5.42	9.40	7.86	-0.13
2010	4.18	2.56	4.50	4.19	10.64	8.50	7.53
2011	3.93	1.55	4.30	-0.12	9.55	5.24	3.97
2012	0.42	2.25	4.00	1.49	7.86	5.46	1.92
2013	0.44	1.84	1.76	2.01	7.77	6.39	3.01
2014	2.21	2.53	0.74	0.38	7.43	7.41	0.51

Table 6 (continued)

1015	1.49	2.91	-1.97	1.22	7.04	8.00	-3.55
2016	2.23	1.64	0.19	0.52	6.85	8.26	-3.28
2017	2.60	2.37	1.83	2.17	6.95	7.04	1.32
2018	1.27	2.93	2.54	0.32	6.75	6.12	1.32
2019	0.56	2.16	1.34	0.65	5.95	4.18	1.14

Source: GDP growth (annual%) – Germany, USA, Russia, Japan, China, India, Brasil, China. | Data (worldbank.org), available March 25th, 2021.

6. CONCLUSIONS

The above-mentioned changes happened over quite a short stretch of time of just 26 years. That being said, the positions of different macro-regions (and nation states) on the global stage are undergoing significant shifts. The type of changes depends on the indicators used as well as on the nature of regions (developed vs. developing). As an example, life expectancy or literacy rate show clear convergent trends, though the speed with which change occurrs remains uneven.

The Lorenz curve proves that the former dominance of Angloamerican and European macro-regions (measured by GDP) became significantly weaker (50.9% of world's GDP in 2018, down from 60.1% in 1990) (Anděl, Bičík & Bláha, 2020). However, the economic progress of the poorest macro-regions (African and Indian) is not really fast (an increase from 3.2% to 5.6% – share of world's GDP). The Islamic macro-region shows the best improvements (a change from 2.5 to 5.7%).

In total, the graphs show slight convergent trends as regards the distribution of population and GDP in the 1990–2016 period. The world average GDP per capita increased 2.5 times between 1990 and 2016 (from 4,100 USD to 10,000 USD). While in 1990 there were only four macro-regions that showcased above-average figures, in 2016 there were seven such macro-regions. Some 45.6% of the world's population now live in below-average regions (the African, Indian, and Indonesian macro-regions), while in 1990 the figure was 79%.

There are great inequalities between individual types of macro-regions. Type I (European, Angloamerican, and Australian-Oceanic macro-regions) for example, obtains 12.7% of total population only, but generates 53.1% of the total GDP and its 7 countries + the EU and the ECB belong to the "G20" platform. On the other hand, Type III (Indian and African macro-regions), with 37.1% of the total population, generates a meager 5.6% of the total GDP, while its 2 countries are part only of the "G20" platform.

A number of scholars have strived to explain the above-mentioned inequalities including the effects on society. Regional differences are reflected in the changing patterns of international labour markets and in the creation of global production chains (Hampl, 2009, 2014). The study carried out by Cox (2012) examines the qualitative aspects of global economy that are inevitably linked, on the one hand, with science, research, and technologies, and with structures and the financial strength of multinational corporations on the other.

The ongoing global changes, however, should not be examined purely from the economic standpoint. Uneven economic development and distribution of wealth is crucial for the reshaping of the global power structure; it has, however, a number of social, cultural, and environmental consequences (Giddens, 1990; Jackson, 2000; Haggett, 2001; Layne, 2006; Holton, 2006; Zakaria, 2008). Some scholars emphasize the geopolitical aspects of the above-mentioned changes (Pieterse, 2011; Agnew, 2009; Acemoglu & Robinson, 2012).

The changing character of the world's macro-regions may explain some reasons for the dynamic changes suffered by selected areas or nation-states like China or India (Turner, 2016). The borders of the world's macro-regions and their stability (increasing or decreasing) have become a new research direction (Longo, 2017). The authors of this article are preparing a new study that ought to interpret

the findings (core, semi-peripheral, and peripheral macro-regions) and expand the time scope of the research (including a comparison with the era of the bipolar world).

REFERENCES

Acemoglu, D., Robinson, J. A. (2012), *Why Nations Fail: The Origins of Power, Prosperity, and Poverty*. London: Profile Books.

Agnew, J. A. (2009), *Globalization and Sovereignty*. Lanham: Rowman & Littlefield Publishers.

Anděl, J., Bičík, I., Bláha, J. D. (2018a), *Concepts and Delimitation of the World's Macro-regions*. Miscellanea Geographica – Regional Studies on Development, **22**, *1*, s. 16–21.doi: 10.2478/mgrsd-2018-0001.

Anděl, J., Bičík, I., Bláha, J. D. (2018b), *Macro-regional Differentiation of the World: Authors' Concept and its Application*. Miscellanea Geographica – Regional Studies on Development, **22**, *3*, s. 1–6.doi: DOI: 10.2478/mgrsd-2018-0025.

Anděl, J., Bláha, J. D., Bičík, I. (2020), *World's macro-regions: divergent and convergent trends since early 1970s*. Acta Geographica Universitatis Comenianae, **64**, *2*, pp. 141–159.

Bell, D. (1973), *The Coming of Post-Industrial Society: A Venture in Social Forecasting*. New York, Basic Books.

Bradshaw, M. J. (2009), *The Geopolitics of Global Energy Security*. Geography Compass, **3**, *5*, pp. 1920–1937.

Brauer, R., Dymitrow, M. (2017), *Human Geography and the hinterland: The case of Torsten Hägerstrand's 'belated' recognition*, Moravian Geographical Reports, **25**,*2*, s. 74–84.

Cole, J. (1996), *Geography of the World's Major Regions*. New York: Routledge.

Cox, M. (2012), *Power Shifts, Economic Change and the Decline of the West?* International Relations, **26**, *4*, s. 369–388. doi: 10.1177/0047117812461336.

De Blij, H. J., Muller, P. O. (1997), *Geography: Regions and Concepts*. New York: Wiley.

Fellmann, J. D., Getis, A., Getis, J. (2008), *Human Geography: Landscapes of Human Activities*. New York: McGraw-Hill.

Giddens, A. (1990), *The Consequences of Modernity*. Policy Press, Cambridge.

Haggett, P. (2001), *Globalization*. In: Geography a Global Synthesis. G. Canale & C.S.p.A, Harlow, pp. 584–613.

Hampl, M. (2009), *Globální systém: stav, současné tendence a možné perspektivy distribuce mocenského potenciálu (Global System: Situation, Contemporary Tendencies and Possible Perspectives of the Power Potential Distribution)*. Geografie, **114**, *1*, s. 1–20.

Hampl, M. (2014), *Je nástup konvergenčních tendencí v diferenciaci globálního systému potvrzením obecných představ o vývoji územních a sociálních hierarchií? (Does the Onset of Trends Towards Convergence within the Differentiation of the Global System Confirm the General Assumptions about the Development of Territorial and Social Hierarchies?)*. Geografie, **119**, *1*, s. 26–49.

Holton, R. (2006), *Globalizace*. In: Harrington, A. *et al*. eds., Moderní sociální teorie, Portál, Praha, pp. 385–410.

Huntington, S. (1996), *The Clash of Civilization and the Remaking of World Order*. New York: Simon and Schuster.

Jackson, P. (2000), *Rematerializing social and cultural geography*, Social & Cultural Geography, **1**, *1*, s. 9–14.

Landes, D. S. (1998), *The Wealth and Poverty of Nations: Why Some are so Rich and Some so Poor*. New York: W.W. Norton.

Layne, Ch. (2006), *The uUipolar Illusion Revisited. The Coming end of the United States' Unipolar Moment*. International Security, **31**, *2*, s. 7–41. doi: 10.1162/isec.2006.31.2.7.

Lindert, P. H., Williamson, J., G. (2001), *Does Globalization Make the World More Unequal?* NBER Working Paper No. 8228. doi: 10.3386/w8228. http://www.nber.org/papers/w8228.

Longo, M. (2017), *From sovereignty to imperium: borders, frontiers and the specter of neo-imperialism*, Geopolitics, **22**, *4, s.* 757–771.

Morris, J. W. (1972), *World Geography*. New York, McGraw-Hill.

Novotný, J. (2007), *On the Measurement of Regional Inequality: Does Spatial Dimension of Income Inequality Matter?* The Annals of Regional Science, **41**, *3*, s. 563–580. doi: 10.1007/s00168-007-0113-y.

Perič, J. (2021), *Možno stojíme na prahu ďalšieho komoditného supercyklu*. Trend, **11**, s. 6.

Pieterse, J. N. (2011), *Global Rebalancing: Crisis and the East–South Turn*. Development and Change, **42**, *1*, s. 22–48. doi: 10.1111/j.1467-7660.2010.01686.x.

Polonský, F. (2012), *World Regional Structures: Representations, Perceptions and Objectifications*. Dissertation work, Faculty of Science, Charles University, Prague, 163 p.

Stanton, E. A. (2007), *The Human Development Index: A History*. University of Massachusetts Amherst, Political Economy Research Institute.

Taylor, P. J. (1989), *Political Geography: World-Economy, Nation-State and Locality*. Harlow: Longman Scientific & Technical.

Turner, O. (2016), *China, India and the US rebalance to the Asia Pacific: the geopolitics of rising identities*, Geopolitics, **21**, *4*, s. 922–944.

Wallerstein, I. (1979), *The Capitalist World-Economy*. Cambridge: Cambridge University Press.

Wallerstein, I. (1991), *Geopolitics and Geoculture*. Cambridge, MA: Cambridge University Press.

Zakaria, F. (2008), *The Post-American World*. New York, London: Norton.

RELATIONSHIP BETWEEN LULC CHARACTERISTIC AND LST USING REMOTE SENSING AND GIS, CASE STUDY GUELMA (ALGERIA)

IMEN GUECHI[*], HALIMA GHERRAZ[**], DJAMEL ALKAMA[***]

Abstract. Urbanization is a phenomenon that is driven by humans. It has significantly influenced biodiversity, ecosystem processes and regional climate. Like all medium-sized cities in Algeria, Guelma is affected by the rapid and massive urban growth which has increased the land use/land cover (LULC) changes. Thus, it generates climate change. This work explores the relationship between the LULC characteristic and LST, based on remote sensing & GIS. A time-series of Landsat images TM, ETM+ and OLI/TIRS data and various geospatial approaches as well as the urban – rural gradient, multi-buffer ring, statistics and the techniques used in urban landscape metrics were used in order to facilitate the analysis. The findings have revealed that urban/built-up areas of Guelma city have increased by 12%. However, the agricultural and forest areas have witnessed a reduction of 15% and 3%. The average temperature of the urban setting was 38.27 C° in 1986, whereas in 2019 it reached 41.90 C°. When the average temperature values for every class were calculated, it was observed that the lowest values were in forest bodies with 27.26 C° in 1986 and 37.78 C° in 2019. There is a possible rise in LST over time scale owing to the substitution of green cover by urban soil areas. For instance, there was a noticeable increase of 3.65°C in mean LST for urban areas. The increased urban LST values are due to the broad region, the low fragmentation degree of landscape and complex outlines, which in turn lead to reduced forest LST values. In comparison to the LST of the sprawl form, the LST of compact form is low. This investigation provides us with clear understanding of the impact that the urbanization, composition and form of landscape has on LST. These findings have significant theoretical and managerial implications.

1. INTRODUCTION

Urbanization is one of the most important factors triggering a transition in (LULC) (Pal *et al.*, 2017). It is an urban phenomenon that has drawn the attention of researchers in the 21st century (Spence *et al.*, 2009). Urban areas such as cities and towns comprise more than half of the world`s population. This number is expected to rise to about five billion by 2030. UNFPA also predicts that much of this urbanization that would occur in Africa and Asia would bring enormous social, economic and environmental problems (UNFPA, 2017). Change in land use/land cover (LULC) has a major impact on climate through various pathways. Those pathways are found to modulate the surface energy balance which affects the land surface temperature (LST). This leads to changes in the region's micro-climate (Wang *et al.*, 2018; Gogoi *et al.*, 2019; Jain *et al.*, 2017). This local temperature variation has a negative effect on both people and the environment because it hinders air quality, increases energy consumption, affects biological control and human health (Meineke *et al.*, 2014; Plocoste *et al.*, 2014). LST is considered a significant urban climate indicator in which the temperature in urban environments and the increasing areas of built-up surfaces is higher than in areas covered by vegetation and water. Therefore, studying the impact of urbanization on LST is important because it can disrupt a wide variety of natural processes (Carleton *et al.*, 2016; Tan *et al.*, 2020). In addition, the surface climate

---

* Ph.D., Department of Architecture, Laboratory of Evaluation of Quality in Architecture and In-built Environment, University of Arbi Ben M'hidi, Oum El Bouaghie, Algeria, guechi.imen@gmail.com.
** Ph.D., Department of Architecture, Laboratory of Evaluation of Quality in Architecture and In-built Environment, University of Arbi Ben M'hidi, Oum El Bouaghie, Algeria, halima.gherraz@gmail.com.
*** Professor, Department of Architecture, University of Guelma, Algeria, dj.alkama@gmail.com.

can be affected by changes in urban space and by the removal of vegetation due to urbanization (Das *et al.*, 2020).

Compared to conventional observation methods which are used at meteorological stations, remote sense tracking of LST provides a wide range of measurements and good spatial consistency. This technique has therefore grown rapidly in thermal environmental research (Liu *et al.*, 2016; Wang *et al.*, 2018). The use of remote sensing data in conjunction with Geographic Information Systems (GIS) is effective in mapping urban areas, modelling urban growth, monitoring LULC's dynamic changes and estimating LST (Kimuku *et al.*, 2017). By incorporating thermal remote sensing, LST information is available from a series of satellite sensors (such as Landsat, MODIS, and ASTER) which cover an extensive part of the earth's surface. At different temporal scales, thermal imaging generates full spatial coverage in comparison to the air temperatures from the weather stations (Myint *et al.*, 2013). Therefore, the relationship between LST and (LULC) change should be investigated in order to address further regional environmental issues and provide a basis for regional planning (Pal *et al.*, 2017). For the effective use and management of natural resources, it is very important to quantify the causes and consequences of LULC shift. (Li *et al.*, 2018).

Several items of research have been published to study: first the relationship between LST / LULC (an increase in land surface temperatures (LST) is one of the main effects of LULC changes) especially in urban centres (Aboelnour and Engel, 2018; Pal and Ziaul, 2017). Second, the relationship between LST and the Landscape patterns which are based on the use of different LST inverting methods has been studied (Brown *et al.*, 2016). The study has also shown that underlying landscape trends have an important impact on LST (Peng *et al.*, 2016; Estoque *et al.*, 2017). Third, the relation between urban form and climate was explored by spatial distribution and the use of morphological indices (Martinelli *et al.*, 2017). There are various approaches and techniques for analysing urban form indices, including the use of spatial metrics (Yang *et al.*, 2016; Boogaard *et al.*, 2017; Santos *et al.*, 2017). They are also commonly used to assess the effects of landscape trends on surface landscape temperature (LST) (Asgarian *et al.*, 2015; Chen and Yu, 2017). Fourth, the relationships between LST, Normalized Difference built-up Index (NDBI), and Normalized Difference Vegetation Index (NDVI) were established using Linear Regression (Guha *et al.*, 2018; Ferrelli *et al.*, 2018). The present study will provide an in-depth analysis of the relation between the LULC characteristic (Urban density, urban form, Landscape pattern and land cover types) and LST by the integration of a geographical and economic approach in the same case study to determine the main effects of landscape characteristic on LST.

Guelma is affected by rapid and massive urban growth which has strongly disrupted the space. This urban growth generates profound spatial and environmental transformations (Guechi *et al.*, 2017). The local authorities of Guelma have revised the Master Plan for Development and Urban Planning (PDAU) in 2013 so as to provide solution for land availability for the future urbanization of Guelma municipality. They have recourse to the inter-communal group of Guelma as part of the postponement of urban growth from the municipality of Guelma to neighbouring municipalities. It included the chief city of Guelma, and the three neighbouring communes including El Fdjouj, Belkhair and Ben Djarah. The position of Guelma in the centre places these communes in its field of attraction. It suffers from the burden of the communes of the wilaya in general and the neighbouring communes in particular. Due to their proximity to the large urban centre and containing land with high agricultural potential, the towns of Belkheir, El Fedjoudj and Bendjerrah have not experienced the desired growth. This raises the potential to exploit agricultural land and forests for urban purposes. Reducing vegetation and replacing it with impermeable surfaces, such as asphalt and concrete, is directly related to urbanization factors that have environmental and social consequences (Mitchell, 2011).

This research objective is to determine and analyse the relationship between LULC characteristics and land surface temperature (LST) in the context of urbanization from 1986 to 2019 in Guelma, using remote sensing & GIS. In order to investigate the urban expansion in Guelma, the time-series satellite images with supervised technique for classification of Maximum Likelihood (MLC) is

employed. Also, in order to determine and analyse the connection between LST and main LULC characteristics (Urban density, urban form, Landscape pattern and land cover types), a multi-buffer ring method, quantitative Study of LST and Landscape metrics technique of land cover are applied.

2. STUDY AREA

Our case study (Guelma inter-municipal grouping) is situated in the centre of Guelma province, northeast Algeria. It is approximately "60 km" south of the Mediterranean Sea 36°27′43″N – 7°25′33″E and 305 m above sea level (Fig. 1). This region occupies a total area of 282.11 km². It has a semi-arid climate with cool winters. It has an average annual temperature of 21.5 °C and 150.3 mm average of annual rainfall (Aouissi, 2010.). It is possible to distinguish two periods in the year, eight months of cold and wet weather from October to May and four months of hot and dry weather from June to September. It is a group of four municipalities (the chief town of the Wilaya, the municipality of Bendjarah, the municipality of Belkhair and the municipality of el Fdjouj). They are in a context of an agricultural vocation par excellence. The position of Guelma in the centre places these municipalities in its field of attraction.
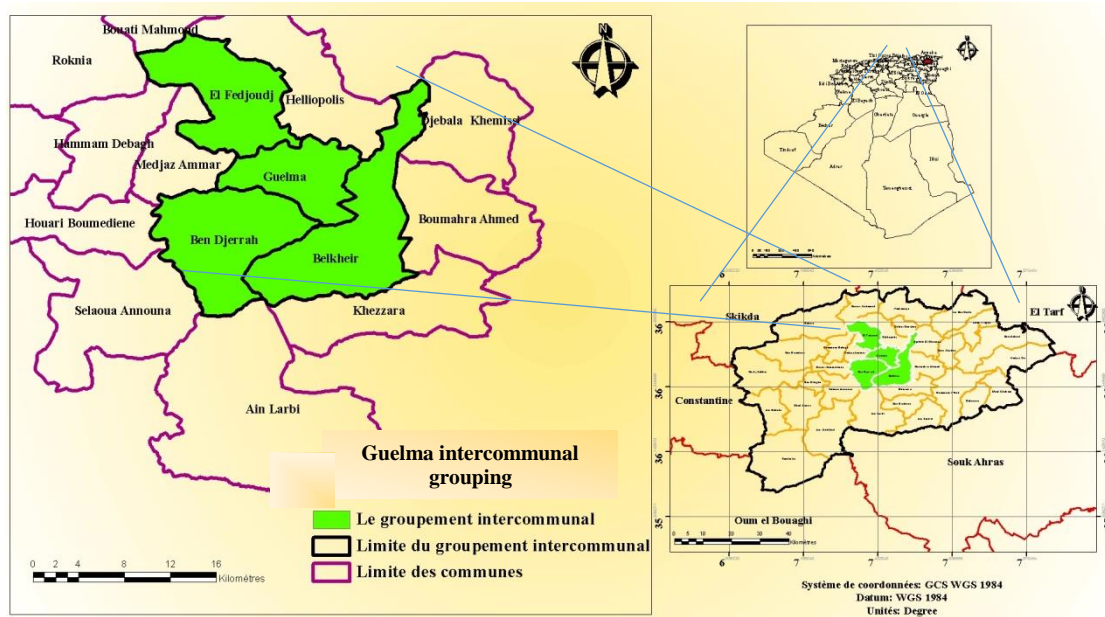

Fig. 1 – Location map of Guelma inter-communal grouping.

3. METHDOLOGY

3.1. Image acquisition and pre-processing

The main data sets in this analysis were time series of Landsat images which were captured by Landsat TM, Landsat ETM+, and Landsat Operational Land Imager (OLI)/Thermal Infrared Sensor (TIRS) sensors. The data are presented in Table 1. The selected satellite data was cloud-free. All datasets have been downloaded as a georeferenced data set from the website of the United States Geological Survey (USGS) (https:/earthexplorer.usgs.gov). Satellite images were acquired at an interval of 4–5 years during the same season (the dry season) in order to prevent phenological

variability. The Image processing software ArcGIS Spatial Analyst (version 10.5), Environment for Visualizing Images (ENVI) version 5.0, Fragstat 4.2 and Excel were used for conducting the statistical analysis.

Table 1

Landsat data specification used in the study

LANDSAT_SCENE_ID	SPACECRAFT_ID	Acquisition Date	UTM_ZONE	Spatial Resolution
LT51930351986180FUI00	**L5_TM**	**29/06/1986**	**32**	**30**
LT51930351990159FUI00	**L5_TM**	**08/06/1990**	**32**	**30**
LT51930351996160FUI00	**L5_TM**	**08/06/1996**	**32**	**30**
LE71930352000179FUI00	**L7_ETM**	**27/06/2000**	**32**	**30**
LE71930352005176EDC00	**L7_ETM**	**25/06/2005**	**32**	**30**
LE71930352010174EDC00	**L7_ETM**	**23/06/2010**	**32**	**30**
LC81930352015180LGN01	**LANDSAT_8**	**29/06/2015**	**32**	**30**
LC81930352019159LGN00	**LANDSAT_8**	**19/06/2019**	**32**	**30**

In this research, after using a radiometric calibration, the fast line-of-sight atmospheric analysis of hypercube (FLAASH) was used for atmospheric correction in ENVI5.1 software. Some parameters are considered for running FLAASH including satellite overpass time, sensor altitude, geographical location, region-related specific atmospheric model, and solar zenith angle of the satellite images acquired by Landsat 5, 7, and 8. The Flowchart Fig. 2 shows the methodology adopted for the following study.
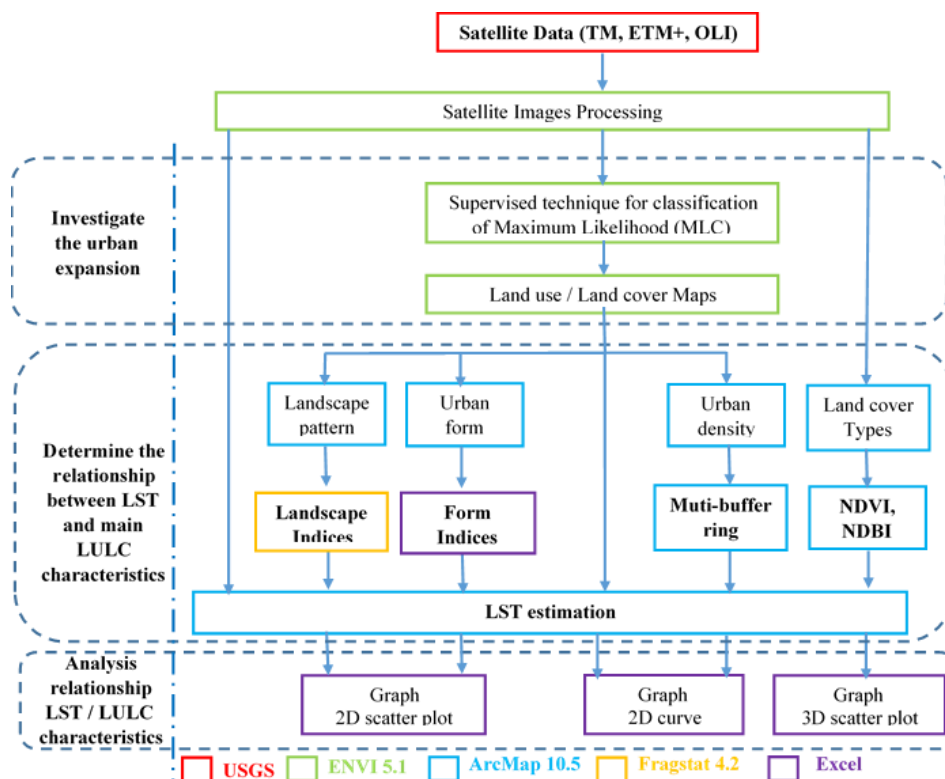

Fig. 2 – Flow chart explaining the methodology.

3.2. Classification of satellite images

Remotely sensed data are commonly used for mapping land use and cover maps. Supervised technique for classification of Maximum Likelihood (MLC) is employed in this study. MLC which is used in a variety of applications is the most generally used supervised classification (Pushpendra *et al.*, 2014). MLC doesn't only perform better than the other parametric classifications but it also considers the variance-covariance within the class distributions (Erdas, 1999). Images from the years 1986, 1990, 1996, 2000, 2005, 2010, 2015 and 2019 were classified with the software ENVI 5.1 so as to obtain land cover distribution. Composite imagery with false colour band combination of bands RGB = 543 for Landsat 8, RGB = 432 for Landsat 5TM and Landsat 7 ETM+ was utilized to obtain better visualization of the urban environments. Four signature classes were selected for the classification including urban, forest, agricultural and bare land. Residential buildings, highways, industries, commercial buildings illustrate the urban area. The bare land represents the soil and unused land. The agricultural land represents both the areas with and without vegetation. Training areas have been developed by selecting one or more polygons for each class. Pixels were taken to be the training pixels for a specific class within the training area. Then, Confusion Matrix Using Ground Truth ROIs in ENVI5.0 was used in this analysis to test the accuracy of maximum likelihood classification. The Kappa coefficient was also obtained for each year.

3.3. LULC characteristics

3.3.1. Urban density

From a socio-economic point of view, cities are perceived as magnets that provide people with different social and economic opportunities. Cities can draw or repel residents, money, as well as business investment (Fonseka *et al.*, 2019.). This feature of the city is well illustrated by the multi-buffer approach which demonstrates the city's distribution outward from its centre (Fonseka *et al.*, 2019; Rahman, 2016). The position of Guelma in the centre, places these municipalities in its attraction sector. Taking into consideration the idea of magnetic cities, the multi-buffer ring method was employed. From 1 km to 16 km, the multi-buffer rings are created in Arc GIS (using the multiple ring buffer option) for every 1km distance from Guelma centre to outside. Then, the classified intersection with land cover for all dates is carried out. Later on, the urban area class is calculated for a distance of 16 km. The density is extracted by the equation that follows:

Urban density = (Urban area per ring) / (Total area of ring)……….(1)

3.3.2. Urban form Indices

In this study, we opted to use the most elementary arithmetic indices (Guérois, 2003). To measure the urban form of the inter-municipal Grouping of Guelma, several form indices were set up based on the different geometric relationships between the following elementary values including the perimeter, the surface area and the axes digitation distances (Table 2).

Table 2

Urban form Indices

Urban forme indices	Objectif	Formuler
I1 (Perimetercontortion index)	describe the degree of irregularity of the contour shape	$I_1 = 4\pi A/P^2$
I2 (The Stretch Index)	measures the stretch, or span of the shape	$I_2 = L2/L1$
I3, I4, I5 (Disc filling indices)	measure disc filling of the shape	$I_3 = \pi(R_{ci})^2/A$, $I_4 = R_{ci}/R_{cc}$, $I_5 = A/\pi(R_{cc})^2$
I6 (The digitation index)	identify more clearly the digested forms	$I_6 = 1/(1+D)$

P: perimeter, *A*: shape area, **L2**: the length of longest axis, **L1**: the length of longest perpendicular axis, **R_{ci}**: radius of the largest circle, **R_{cc}**: radius of the smallest circumscribed circle.

3.3.3. Landscape Pattern Indices

Indices were chosen from patch type and landscape level to quantitatively describe the characteristics of LC's landscape patterns. Landscape level indices are used to define the overall LC status characteristics, whereas, patch type indices concentrate on LCT types morphology and structure. The selected landscape indices including total area (CA), percent landscape (PLAN), largest patch index (LPI), mean patch area (AREA_MN), landscape shape index (LSI), Euclidean nearest neighbour distance (ENN). These are typical and frequently utilized hints in landscape research.

In order to quantitatively investigate the correlation between the landscape pattern indices, the LST and the underlying surface coverage area, ArcGIS ' fishing net feature was used to extract 15 * 17 samples with a 1400 m 1400 m grid unit. The sampled fields were then superimposed with the vector map LC and LST. After that they were converted to a grid file. In order to estimate the indices for the landscape pattern, the grid data were input into Frag stats 4.2.

3.3.4. Land Cover Types

– The **NDVI** index is a measure of the surface vegetation quantity and vigour. For the reason that vegetation is well reflected in the near infrared part of the spectrum, NDVI has become a simple graphic indicator for assessing target vegetation coverage. Several researches focused on understanding the LST-NDVI relationship (Lo *et al.*, 1997). The NDVI images were calculated with the equation (2). $NDVI = NIR – Red/NIR + Red$ …..... (2) where Red and NIR are the spectral reflectance of vegetation, NIR : is the near infrared band, *Red*: is the red band

– **NDBI is** another index used in this study that is sensitive to the built-up area. It is derived by the following equation: $NDBI = (R_{SWIR} – R_{NIR})/(R_{SWIR} + R_{NIR})$ ……… (3)
Where, R_{SWIR} and R_{NIR} are the spectral reflectance.

3.4. LST Estimation

The thermal infrared bands of different Landsat image types (band 6 of Landsat 5 TM, Landsat 7 ETM+ and band 10 of Landsat 8) (Landsat (7), 2011; Landsat (8), 2015) were utilized to estimate LST of the inter-municipal grouping of Guelma. Landsat OLI-TIRS had two thermal bands which are band 10 and band 11. Since band 11 displays striping, only band 10 was used here. A single window algorithm based on NDVI was utilized to extract land surface emissivity (LSE). The steps below are employed to retrieve LST from thermal images and NDVI images.

a – Radiance image calculation

The raw digital number (DN) values of TM and ETM+ have been converted to luminance radiation or top-of-atmospheric (TOA) radiance by means of equation (1) (Chander *et al.*, 2003).

$$L\lambda = (L_{max} – L_{min})/(QCAL_{max} – QCAL_{min}) \times (DN – QCAL_{min}) + L_{min} \text{ …….(4)}$$

where,

DN: is the pixel digital number for band 6, $L_{max} = 17, 04$ (mW/cm2sr·$\Box$m) is spectral at-sensor radiance that is scaled to $QCAL_{max}$, $L_{min}= 0$(mW/cm^{2}sr·$\Box$m) is spectral at-sensor radiance that is scaled to $QCAL_{min}$, $QCAL_{max} = 255$ is Maximum quantized calibrated pixel value corresponding to L_{max}, $QCAL_{min} = 0$ is the minimum quantized calibrated pixel value corresponding to L_{min}.

For Landsat OLI-TIRS the equation (5) is used (USGS, 2014). $L\lambda = M_L \times DN + A_L$ …... (5) where, M_L: is the specific multiplicative rescaling factor band DN: is the pixel digital number for band 10

A_L: is the specific additive rescaling factor band from the metadata.

b – Radiant temperature calculation

The following equation (6) was used to calculate radiant temperature by the use of radiance images which were obtained from thermal bands (Chander *et al.*, 2009). $Tk = K2/In(K1/L\lambda + 1)$……… (6) Where, Tk : is the temperature in Kelvin (K), $K1$: is the prelaunch calibration of constant 1 in unit of W/ (m^2sr·µm), $K2$: is the prelaunch calibration constant 2 in Kelvin.

c – Emissivity calculation:

The emissivity is calculated with the following equation $\varepsilon = 0.004\,p_v + 0.986$ …… (7) Where, p_v: is the vegetation proportion which can be derived from the NDVI image based on the following equation (6). $P_V = {}'\left(\frac{NDVI - NDVI_{min}}{NDVI_{max} - NDVI_{min}}\right)^2$ ……… (8)

d – LST Calculation

Outputs derived from (5) and (7) were then used as inputs to estimate the LST using the equation below. $LST = T_k/(1 + ((\lambda T_k)/p)\,In\,\varepsilon)$………(9) Where, λ : is the central wavelength (in µm) of the Landsat thermal band, $p = 1.438 \times 10^{-2}\,mK$.

3.5. The Relationship between LULC characteristics and LST

This study's main consideration was to define the relation between LST/LULC characteristics. In order to determine and analyse the mean LST values for land cover change and land use, class zonal statistics in ArcGIS were used. The relation between LST /LULC characteristics was statistically analysed in Excel software by means of regression analysis and trend analysis.

4. RESULTS

4.1. Precision evaluation report of LU / LC classification

The urban land cover classification results in the inter-municipal grouping of Guelma from 1986 to 2019 are shown in Fig. 3.

4.2. Spatio-temporal Pattern of LU/LC Dynamics and its Relationship with LST

The spatial LU/LC maps of inter-municipal grouping of Guelma are shown in Fig. 3. It is clear that there has been an urban expansion in the inter-municipal grouping of Guelma in the last 33 years. This growth is concentrated in the Guelma municipality which is very significant compared to the other municipalities. Guelma is regarded as one of the Algerian cities which fulfils very important urban functions. Those functions exert an influence on both the adjacent communes and even on the rest of the communes of the province, as indicated in the (PDAU 2013).
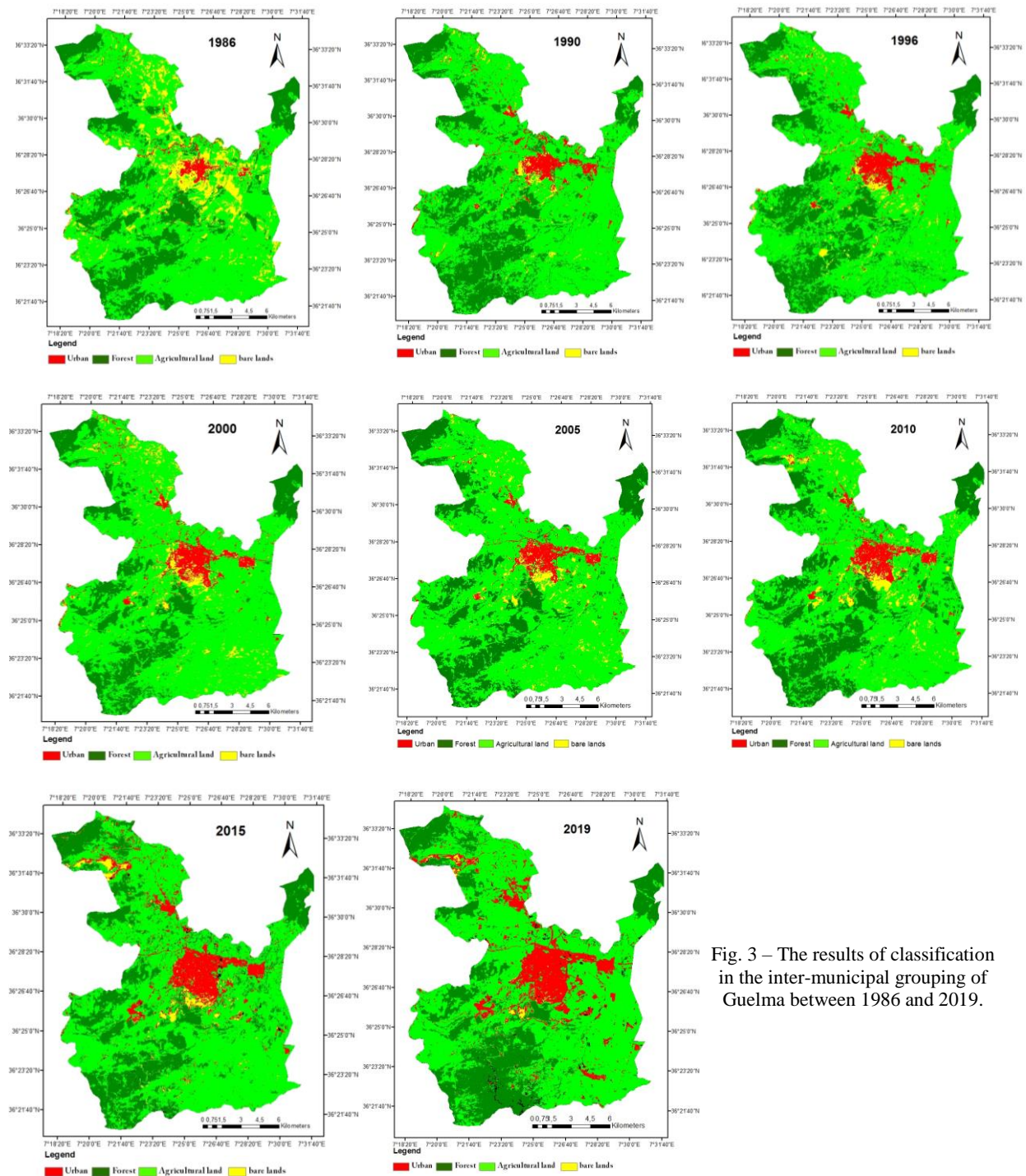
Fig. 3 – The results of classification in the inter-municipal grouping of Guelma between 1986 and 2019.

To further explain urbanization during the study period in Guelma's inter-municipal classification, the areas of different land cover and their changes were calculated, and are presented in Fig. 4.
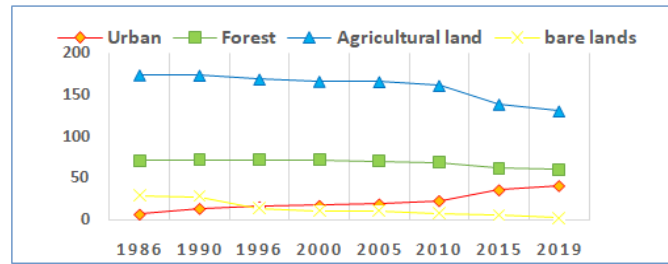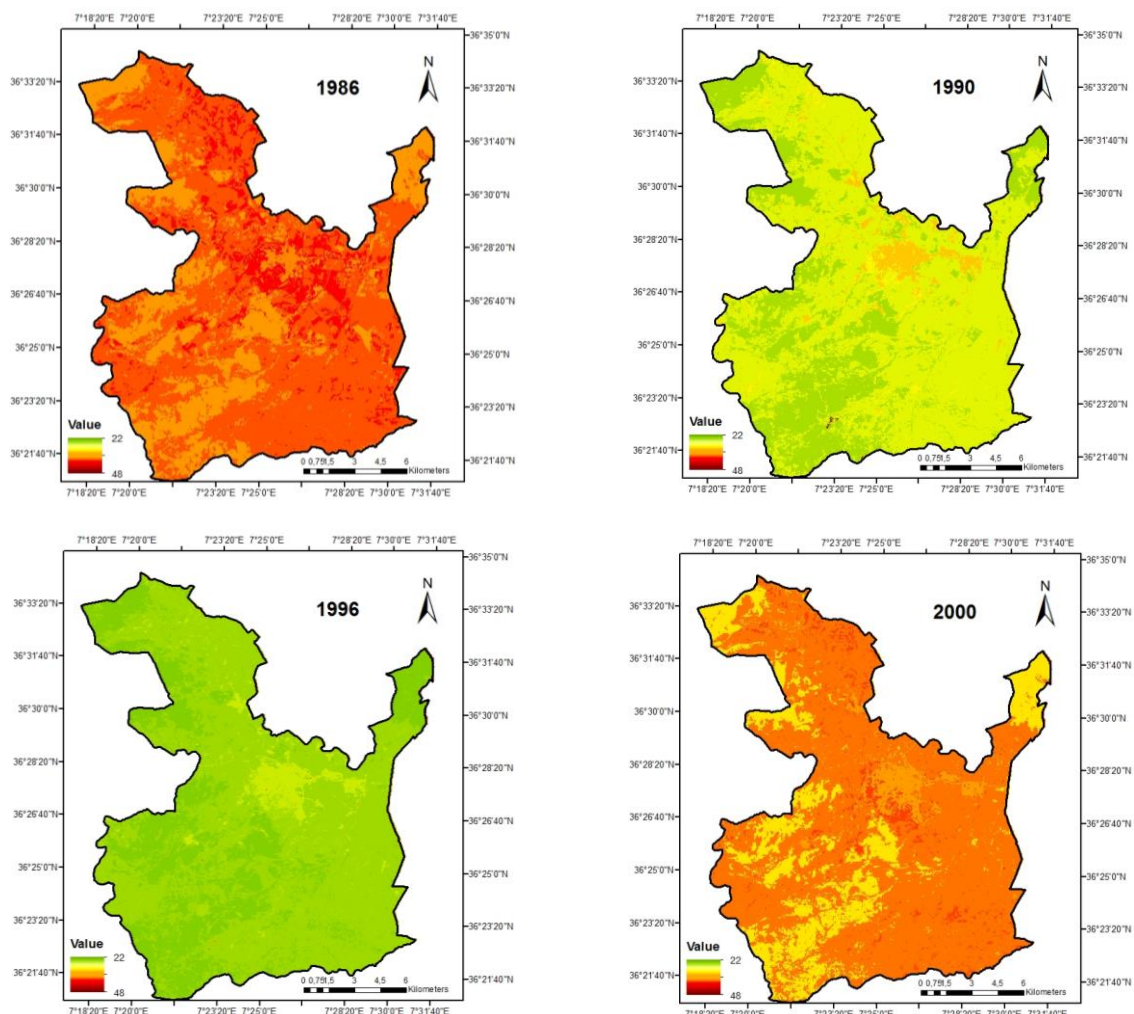
Fig. 4 – Urban land cover change in the inter-municipal grouping of Guelma from 1986 to 2019.

Fig. 4 reveals that there is a rising trend in the urban area from "6, 5 km²" to "40, 88 km²" in 1986 and 2019 respectively. However, the area of bare land, agriculture land and forest has decreased. For the bare land, the area decreases from 29.33 km² in 1986 to 1.98 km² in 2019. For the agricultural land, the surface has decreased from 173.22 ha in 1990 to 130.48 ha in 2019. For the forest, the area has decreased from 71.14 km² in 2005 to 60.34 km² in 2019. Based on these findings, it is concluded that the urban land cover increase is directly proportional to the reduction in green cover especially in the last period. The result of analysis is consistent with Guechi *et al.*, 2017.
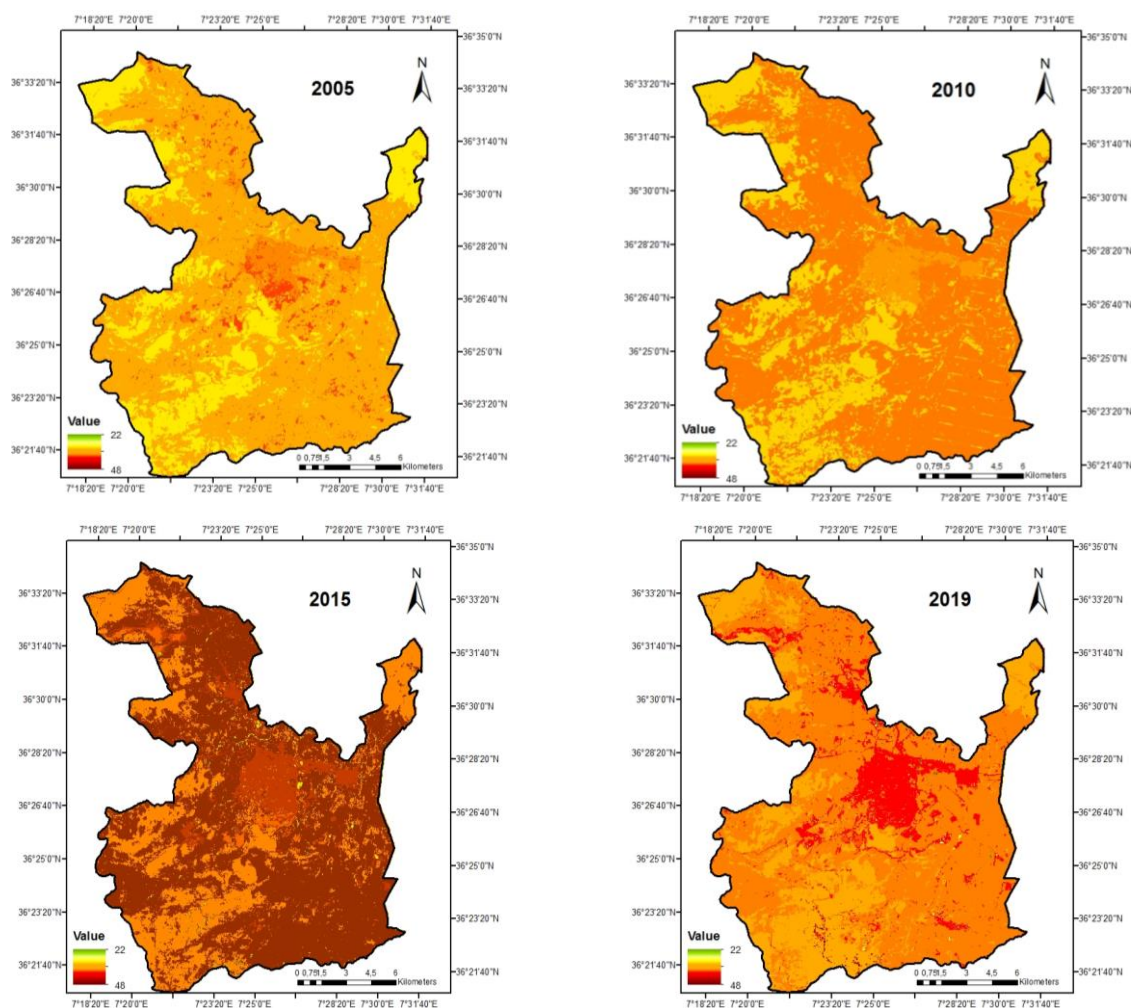
Fig. 5 – Mean land surface temperature in the inter-municipal grouping of Guelma
for corresponding years to land cover classification.

The LSTs estimated from Landsat images are shown in Fig. 5 which reveals a clear gradient between urban areas, bare land, agriculture land and forests from 1986 to 2019. It illustrates the temperature increase in urban setting in the 1990 and 1996. This is principally owing to higher radiant temperatures in urban surface materials. The results of this analysis are consistent with other studies related to the rise in LST due to the changing of LULC (Carleton *et al.*, 2016; Tan *et al.*, 2020; Das *et al.*, 2020). However, for the years: 2000, 2005, 2010 and 2015, agricultural land had the highest temperature owing to the absence of vegetation. The mean temperature values of LST for each class are presented in Table 3.

Table 3

Mean LST (C°) for corresponding urban land cover

	1986	1990	1996	2000	2005	2010	2015	2019
Urban	38.25	31.43	27.24	35.61	37.17	33.33	47.05	41.90
Forest	37.12	26.55	22.51	31.17	33.90	27.46	44.02	37.78
Agricultural land	40.12	29.75	25.33	36.53	37.96	33.46	47.74	40.80
Bare lands	41.31	30.79	25.56	37.53	37.98	32.83	46.21	40.07

In 1986, the average temperature of urban settings was 38.27 C°, whereas, in 2019 it reached 41.90 C°. When the average temperature values for every class are calculated, the lowest temperature values were observed in forest bodies with 27.26 C° in 1986 and 37.78 C° in 2019. It is found to be the same result with Aboelnour and Engel, 2018; Pal and Ziaul, 2017.

4.3. Urban density and its relationship with LST

After classification, multi-buffer rings are created for every 1 km distance from 1 km to 16km from Guelma centre to outside.
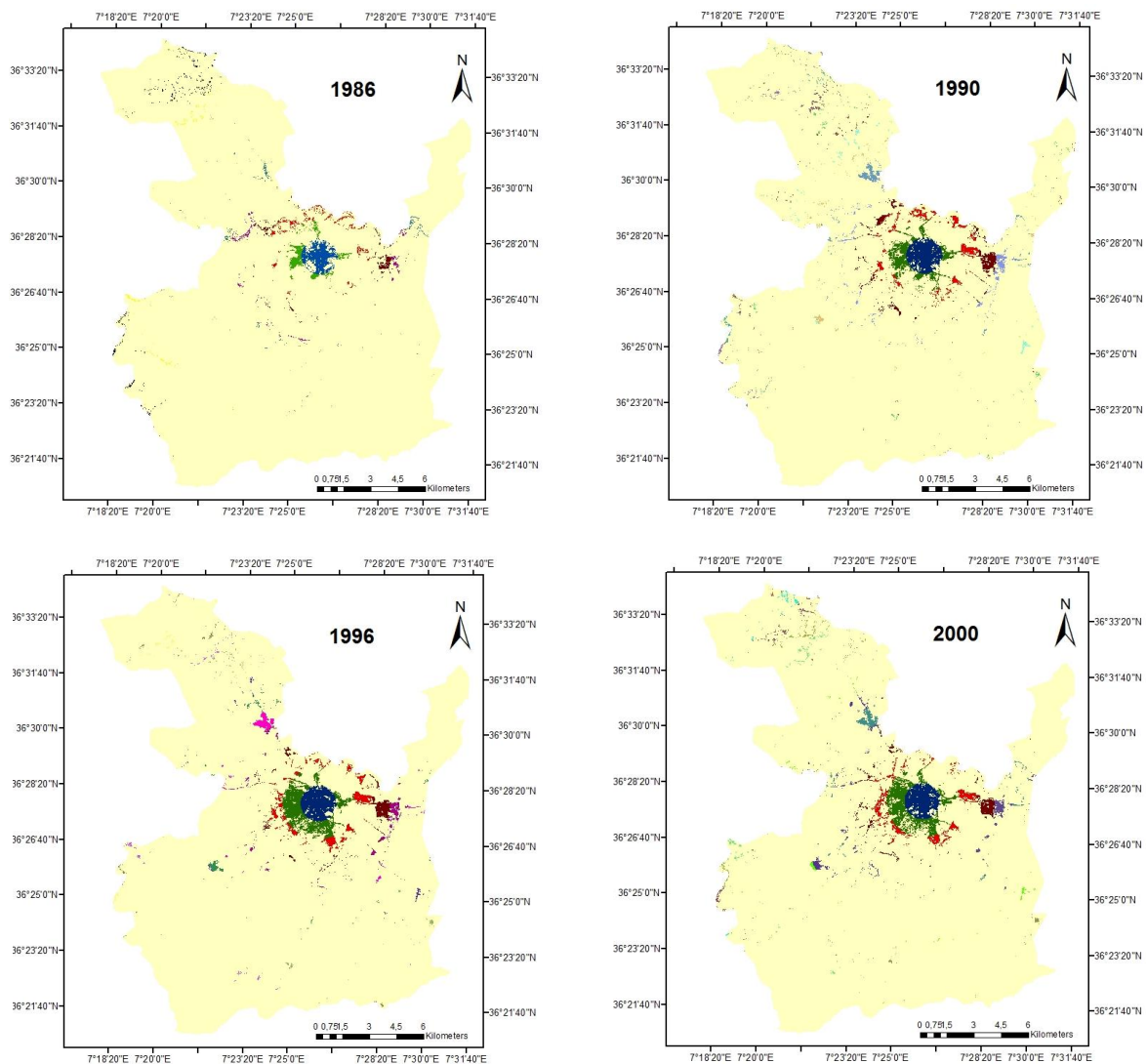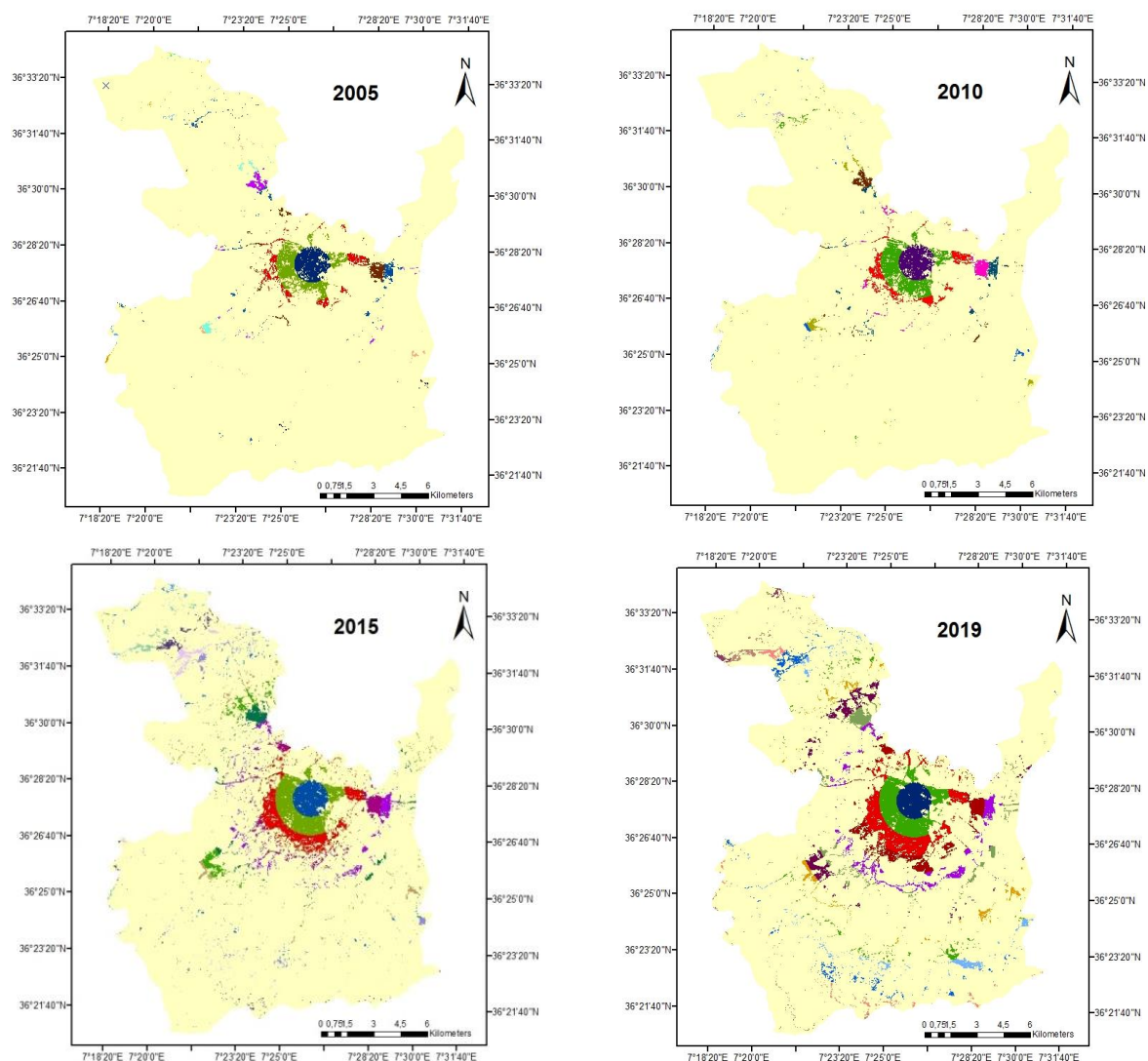
Fig. 6 – Multi-buffer ring analysis of the inter-municipal grouping
of Guelma from 1986 to 2019.

The principle aim of applying the method of multi-buffer ring is to determine the spatial and temporal relationships (Fonseka *et al.*, 2019). Some attractive patterns in the urban land distribution throughout a variety of buffer zones can be observed in Fig. 6. The various zones or rings have embodied various densities. A pattern analysis was applied to obtain the relationship of urban density shift and mean LST in the inter-municipal grouping of Guelma. The findings are presented in Fig. 6.
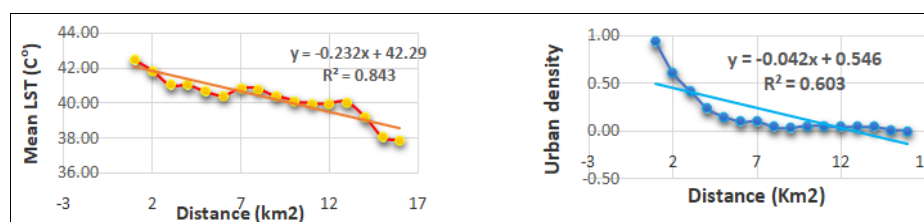

Fig. 7 – Trend analysis of average urban density, average temperature with distance
from the city centre of Guelma.

As predicted, it is clear that in both diagrams the density in the inter-municipal grouping of Guelma in 2019 tends to decline outward from the centre. It is the same for the mean LST. However, it is difficult to validate the precise relationship between urban density and LST by in-situ measurements because emissivity can be affected by some factors, such as the composition of all land cover classes within each pixel which was also proven by past research (Fonseka *et al.*, 2019; Ahmad *et al.*, 2016).

4.4. Urban form and its relationship with LST

The form indices and mean LST are calculated and presented in Table 4. The indices' values equal to one express a compact form, whereas the indices close to zero imply an excessive sprawl (Guérois, 2003).

Table 4

Mean LST (C°) for corresponding urban form indices

	I1	I2	I3	I4	I5	I6	Mean LST	Min LST	Max LST
Guelma	0,3	0,61	0,58	0,44	0,34	0,18	41,76	38,82	49,74
Bel Khair	0,54	0,6	0,57	0,51	0,46	0,47	41,77	39,82	44,97
Ben Djarah	0,41	0,73	0,46	0,43	0,44	0,65	41,49	39,13	45,58
El Fjouj	0,22	0,36	0,35	0,27	0,21	0,42	42	40,4	44,01

According to Table 4, we can say that the city of El Fdjouje had a more spread out and warmer form. The urban form of Guelma and Belkhir is elongated and less compact with a medium temperature in contrast to that of the municipality of Bendjarah, which has a compact non-elongated shape and a lower temperature compared to the other municipalities. Therefore, we can say that the elongated urban form is warmer than the compact form.

4.5. Landscape patterns and its relationship with LST

Based on data of June 19th, 2019, the grid samples of LC and LST are presented in Fig. 8. The quantitative relation between LST and each LC's landscape pattern was studied and represented in Figs. 9, 10 and 11.
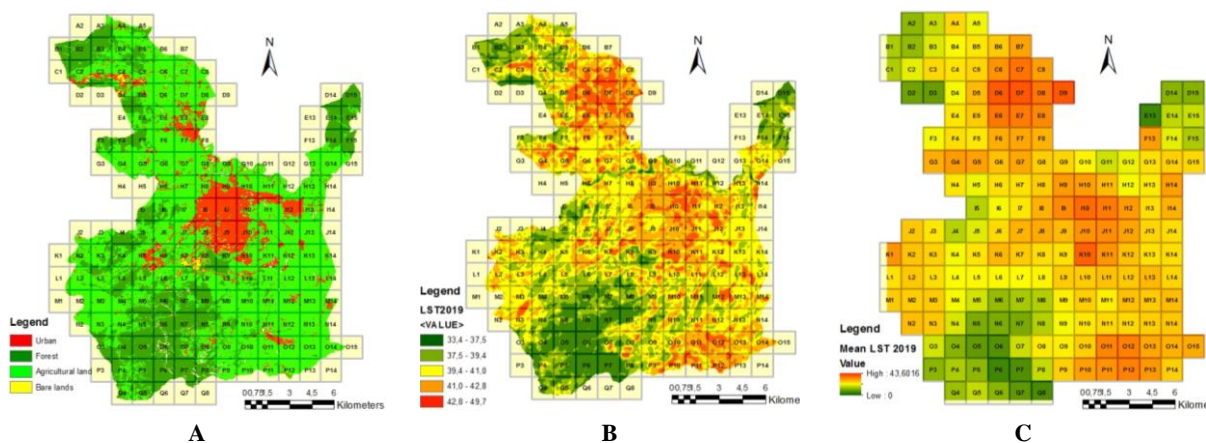

A   **B**   **C**

Fig. 8 – Sample grid in the study area. (A) Slice of LC figure, (B) Slice of LST figure and (C) Slice of mean LST figure.
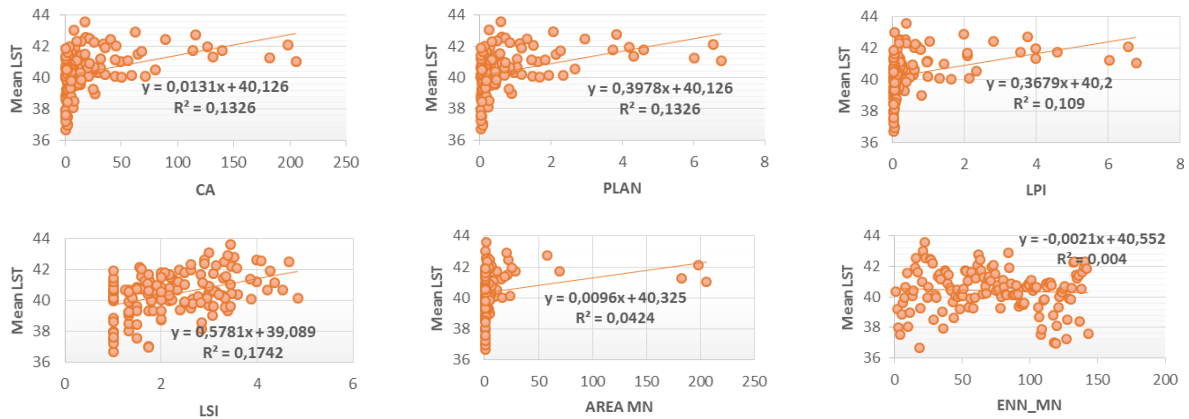
Fig. 9 – The relationship between urban Landscape Pattern Indices and LST.

For the urban space, Fig. 9 reveals that there is a positive relationship between the mean LST and CA R = 0.36, PLAN R= 0.36, LPI R= 0.31, LSI R= 0.41, AREA-MN R= 0.20 and a negative relationship with ENN-MN. Since CA is important, a large PLAND and LPI signifies a huge part of the area's urban and large patch size. Thus, the LST average is high. Having a large ENN MN indicated a fragmented and dispersed urban surface distribution. This indicates that the LST average is low. A large LSI signifies a complex form of the urban surface which leads to massive surface contact with the environment. Therefore, the average LST around it increases the same as the results with Hongyu *et al.*, 2019.

According to Fig. 10, we note that there is a negative relationship between the mean LST and CA R = - 0.67, PLAN R= - 0.67, LPI R= - 0.68, LSI R= - 0.14, AREA-MN R= - 0.64 and a positive one with ENN-MN R= 0.26. High fragmentation signifies a mean dispersed GL distribution and long distances between patches. The complex shape of the forest area landscape, important CA, large PLAND and LPI, and large patch size which mean a huge part of land have low mean LST. The results are the same with Li *et al.*, 2013.
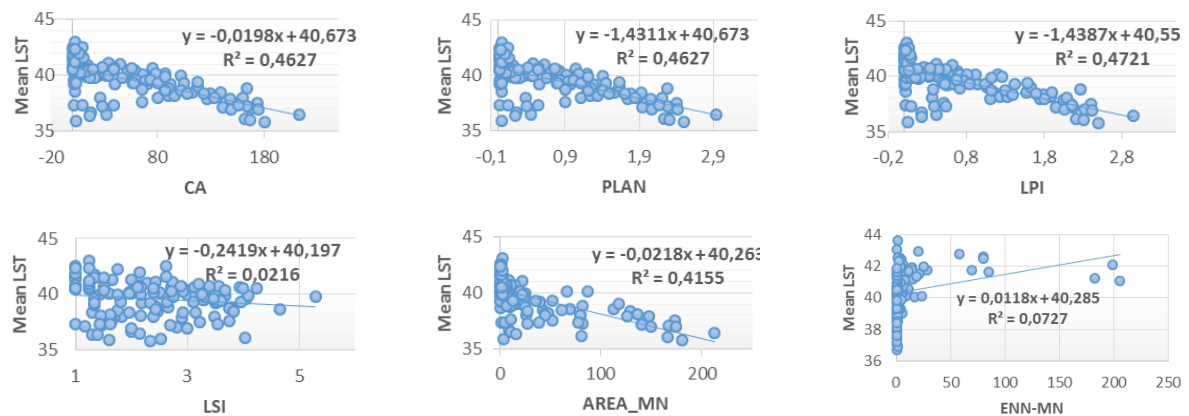

Fig. 10 – The relationship between forest Landscape Pattern Indices and LST.

According to Fig. 11, just as the urban space, the indices of the agricultural land (CA, PLAN, and LPI) display positive correlations with LST, except LSI, which displays a negative correlation. This contrasts what is reported in most previous studies (Li *et al.*, 2013; Hongyu *et al.*, 2019).
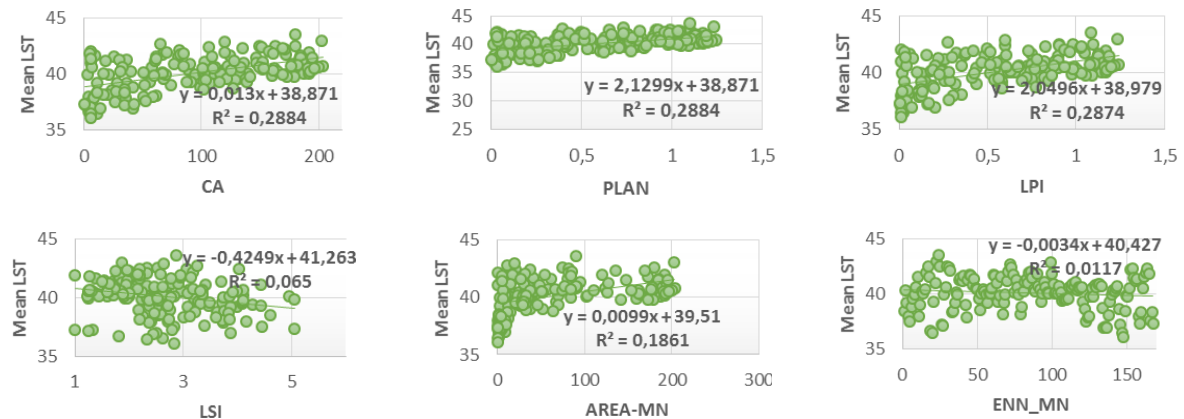
Fig. 11 – The relationship between agriculture Landscape Pattern Indices and LST.

4.6. Spatiotemporal Pattern of NDVI, NDBI Dynamics
and Its Relationship with LST

In order to determine the relationship between NDBI, NDVI and LST, 168 sample points randomly collected from LST, NDBI and NDVI images were used to perform the appropriate regression. The coefficients of the Pearson correlation were calculated and presented in Table 5.

Table 5

LST- NDVI, LST-NDBI relationships from 1986 to 2019.

	1986	1990	1996	2000	2005	2010	2015	2019
NDVI, LST correlation coefficient	-0.68	-0.72	-0.74	-0.83	-0.78	-0.69	-0.68	-0.72
NDBI, LST correlation coefficient	0.47	0.65	0.66	0.60	0.50	0.40	0.52	0.50

The NDVI is negatively correlated with LST. Thus, the areas with the least vegetation are experiencing higher LST. On the other hand, the NDBI and the LST are positively correlated. The results are similar to those found by Naserikia *et al.*, 2019, Mathew, Khandelwal, &Kaul, 2018.

The average and weak correlation between LST and NDBI in 1986, 2000, 2005, 2010, 2015 and 2019 might be correlated with a higher LST. In order to determine the correlation between LST (dependent variable), NDBI and NDVI (independent variables), the multiple linear regressions were utilized. The data utilized in the regression model are represented in a graphic form with a 3D space in Fig. 12.

The LST range in the 3D scatterplot was presented in the form of balls which change in terms of size and colour according to the LST values of each year. The larger-sized balls had high LSTs, low vegetation, and high built-up features. However, the root with smaller balls displays a low LST, low built-up, but highly-vegetated pixels (Naserikia *et al.*, 2019). The red colours, which represent the hotter spots, increased particularly in 1986, 2000, 2005, 2010, 2015 and 2019. On this note, the ones in 2015 showed greater hotter spots than the ones from the other years. It was noticed that in 1990 and 1996, the number of balls which are characterized with reasonably fresh surface temperatures was significantly higher. The value of LST increases with the increasing surface brightness NDBI and reducing vegetation NDVI on the surface (1986, 2000, 2005, 2010 and 2015), and vice versa.
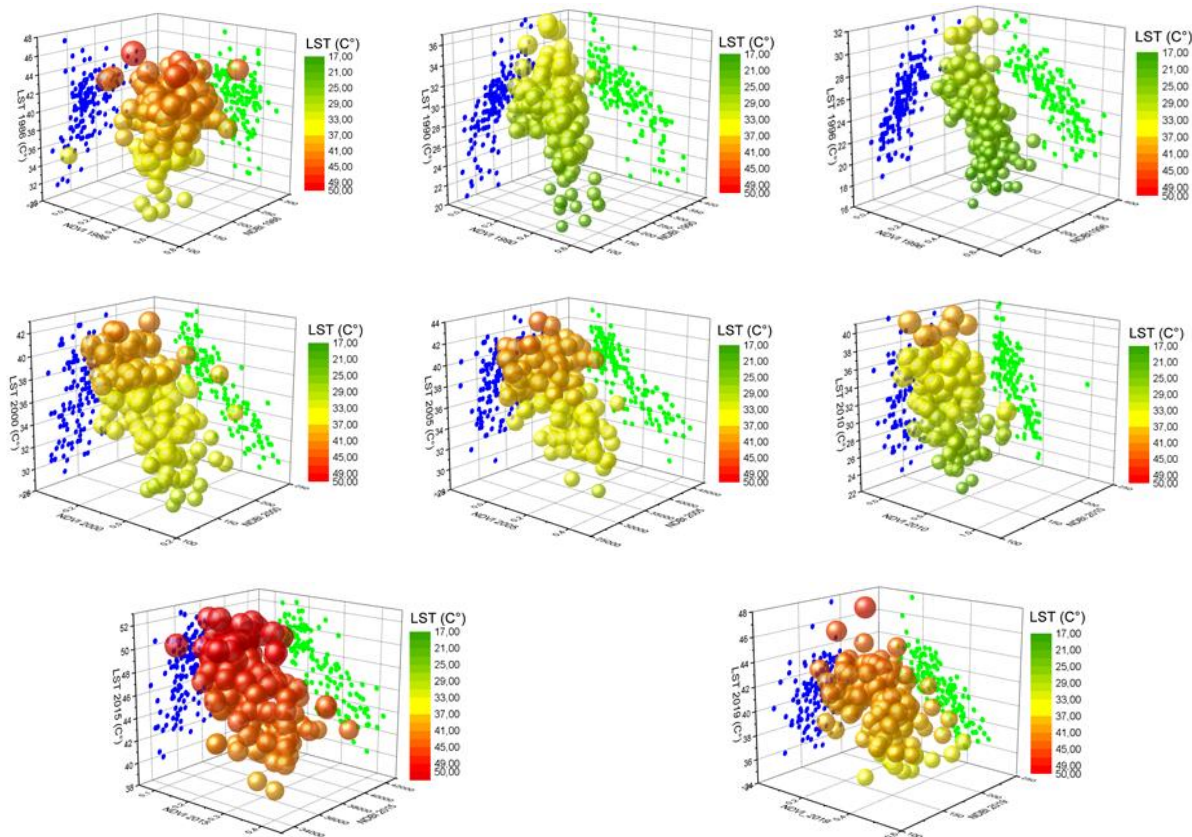
Fig. 12 – 3D scatterplots of the LST- NDVI and LST-NDBI relationships from 1986 to 2019.

5. DISCUSSIONS

5.1. Urban expansion: A mutation of LU / LC and its intensification on LST

Like all medium-sized cities in Algeria, Guelma is affected by rapid and massive urban growth which has strongly disrupted the space (Fig. 3, Fig. 4). Thus, profound spatial and environmental transformations are being generated. The position of Guelma in the centre places these communes in its attraction range (Guechi *et al.*, 2017; PDAU., 2013). Because of its environmental attraction, the city has undergone explosive impermeable growth in the form of residential, commercial, retail, transit networks, and parking lots. This growth was at the expense of transforming LU / LC classes such as urban, agriculture, forests and bare lands. This modification pattern in LU / LC dynamics has significantly altered the scenario of the LST distribution (Wang *et al.*, 2018; Gogoi *et al.*, 2019; Zhao *et al.*, 2013; Li *et al.*, 2018; Pal and Ziaul, 2017; Weng *et al.*, 2004).

Vegetation also displays lower temperatures compared to urban areas along the time scale. This can be best clarified by the fact that through the transpiration cycle, forest or vegetation can reduce the amount of heat contained in the soil or the soil surface. Compared to vegetation areas, higher temperature values are recorded in both urban and bare lands. These results were found to be in line with the actual studies (Fonseka *et al.*, 2019; Gong *et al.*, 2006). Urban areas experience higher temperatures principally owing to the construction materials used. One reason for having high temperature values for bare land is that the majority of bare fields are in areas where there is ongoing development and reduction in vegetation cover (Fonseka *et al*., 2019).

As presented in Fig. 5 and Table 3, agricultural land has the highest temperature in the years of 2000, 2005, 2010 and 2015 owing to the absence of vegetation. The period of last June in Guelma is known as the time of barley and wheat harvest. However, on 19/06/2019, the LST of the urban space displayed the most important value compared to the LST of the agricultural land, the forest and the bare land, although the agricultural land displays land without vegetation. These results confirm that the strong urbanization which marked the past years has exerted an influence on the increase of LST. (Das *et al.*, 2020; Zhao *et al.*, 2013; Li *et al.*, 2018).There is a possible rise in LST over time due to the substitution of green cover by urban soil areas. Generally, there was a noticeable increase in the mean LST of 3.65 C° for urban areas. In this research, the majority of the urban expansion resulted from the conversion of the green cover. The problem in this case study is that the future urbanization of the municipality of Guelma will be directed towards the neighbouring municipalities (the revision of the PDAU 2013) which are surrounded by land with high agricultural potential (Fig. 4). It is well known that the gradual replacement of natural surfaces by constructed surfaces, through urbanization, is the main reason of the LST increase.

5.2. Landscape characteristic effect on LST

In this analysis, the temperature variation and standard deviation show that there are significant differences in a particular form of land-cover as well as the similarities between various types of land-covers. More studies that are recent have shown similar findings (Gogoi *et al.*, 2019; Das *et al.*, 2020).

In this research, the broad region, the low degree of fragmentation of the landscape, and complex outlines have led to reduced forest LST values and increased urban LST values (Fig. 9, Fig. 10). However, like the urban space, the indices of the agricultural land (CA, PLAN, and LPI) display positive correlations with LST, while LSI displays a negative correlation (Fig. 11). These results are explained by the absence of the green cover in most of the agricultural land because of the harvest. Thus, the bare ground reflects an important quantity of the temperature. For LSI, the complex composition of spaces where this displays vegetation is explained by the deprivation of the LST valuations. Our findings are consistent with several other studies reported in literature in other regions. Estoque *et al.* 2017 has found that the difference between the mean LST of built-up land and vegetation cover was 2.7°C in 1987 and 3.4°C in 2015. However, Boyan *et al.*, 2018 have found a gap of 1.3°C.

Therefore, NDVI and NDBI are not sufficient indices for the analysis of LST in towns dominated by barren land which absorbs a significant volume of solar radiation. Mathew *et al.*, 2018 have also demonstrated the ineffectiveness of NDBI in Surface LST Intensity studies, because bare soils and dry vegetation covers show a high spectral reflection in the SWIR band, resulting in positive NDBI values for drier plants and low NDBI values for barren soil compared to built-up areas. It is the same for GUELMA, especially in the summer. A negative relationship was found between vegetation indices and LST (Table 5), which was most likely owing to the impact of surface thermal inertia and evapotranspiration. Moreover, the relationship between the LST variations and NDVI variations is supposed to be direct.

6. CONCLUSIONS

Multidisciplinary theories and methods were used in this research to analyse the effect of LULC characteristics on the LST. The results show that in the inter-communal grouping of Guelma the LULC type has changed significantly. The urban/built-up areas of Guelma city have dramatically expanded, whereas the green cover has declined. These results indicate that the changes in the area's LULC type are related to the rapid and massive urban growth. The LSTs of different LCs are significantly different. Changes to LULC have been followed by changes to the LST. In the 1990s, 1996 having much green cover, the temperature of the urban setting was the most important, while the

years 1986, 2000, 2005, 2010 and 2015, which witnessed the reduction of vegetation, agricultural land, bare land and built-up areas had almost the same temperature. This confirms the role of vegetation in decreasing LST. Moreover, the variation in temperature between the urban setting and forest areas has significantly widened. Therefore, the excessive presence of vegetation was a crucial factor that influences LST. Landscape level indices are used to define the overall LC status characteristics, whereas patch type indices concentrate on the LCT types' morphology and structure. The selected landscape indices include total area (CA), percent landscape (PLAN), largest patch index (LPI), mean patch area (AREA_MN), landscape shape index (LSI), and the Euclidean nearest neighbour distance (ENN). These are typical and frequently used hints in landscape research. For the urban space, we note that there is a positive relationship between the mean LST and CA, PLAN, LPI, LSI, AREAMN, and a negative relationship with ENN-MN, and vice versa for forest area. Broad regions, a low landscape fragmentation degree and complex outlines have reduced forest LST values and increased urban LST values. In comparison to the LST of the sprawl form, the LST of the compact form is low. The results of the LST/NDVI and LST/NDBI relationship have shown a negative correlation and positive relationship, respectively. In the context of LST /NDVI, it can be said that a higher NDVI led to a lower LST and vice versa for the relation between LST/NDBI, where the depletion of green cover had a significant role in the escalation of LST, since vegetation can lower temperatures.

Overall, findings have proved the ability of Landsat multi-temporal images that can precisely measure the trend of transition in LULC and LST in Guelma. Furthermore, the combination of RS and GIS may offer a beneficial tool for surveying, tracking the landscape and the extent of land-cover shifts. Consequently, the knowledge obtained from the outputs of change identification will help to explain the complexities of LULC transition to help policymakers anticipate and schedule future changes in Guelma, achieve long-term stabilization of soil and water supplies and their effects on climate change, and thereby define the evolution of urban building lands.

REFERENCES

Aboelnour M, Engel, BA (2018), *Application of remote sensing techniques and geographic information systems to analyse land surface temperature in response to land use/land cover change in Greater Cairo Region*, Egypt. Journal of Geographic Information System **10**(*01*): 57.

Ahmad, F., & Goparaju, L. (2016), *Analysis of urban sprawl dynamics using geospatial technology in Ranchi City, Jharkhand, India*. Journal of Environmental Geography, **9**(*1–2*), pp. 7–13.

Aouissi, A. (2010.), *Microbiologie et physico-chimie de l'eau des puits et des sources de la région de Guelma (Nord-est de l'Algérie)*. Thèse de Magistère, Université 8 Mai 1945. Guelma, Algerie.

Asgarian, A., Amiri, B. J., & Sakieh, Y. (2015), *Assessing the effect of green cover spatial patterns on urban land surface temperature using landscape metrics approach*. Urban Ecosystems, **18**(*1*), pp. 209–222.

Benenson, W., Harris, J., Stöcker, H., & Lutz, H. (2002*), Handbook of Physics*. New York, NY, USA: Springer.

Boogaard, F., Vojinovic, Z., Chen, Y. C., Kluck, J., & Lin, T. P. (2017), *High resolution decision maps for urban planning: A combined analysis of urban flooding and thermal stress potential in Asia and Europe*. In MATEC Web of Conferences (Vol. **103**, pp. 04012). EDP Sciences.

Boori, M. S., Netzband, M., Choudhary, K., & Voženílek, V. (2015), *Monitoring and modeling of urban sprawl through remote sensing and GIS in Kuala Lumpur, Malaysia*. Ecological Processes, **4**(*1*), 15.

Brown, D. R. N., Jorgenson, M. T., Kielland, K., Verbyla, D. L., Prakash, A., & Koch, J. C. (2016), *Landscape effects of wildfire on permafrost distribution in interior Alaska derived from remote sensing*. Remote Sensing, **8**(*8*).

Carleton, T., & Hsiang, S. (2016), *Social and economic impacts of climate*. Science.

Chander, G., & Markham, B. (2003), *Revised Landsat-5 TM radiometric calibration procedures and post-calibration dynamic ranges*. IEEE Transactions on Geoscience and Remote Sensing, **41** (*11*), pp. 2674–2677.

Chander, G., Markham, B., & Helder, D. (2009), *Summary of current radiometric calibration coefficients for Landsat MSS, TM, ETM+, and EO-1 ALI sensors*. Remote Sensing of Environment, **113**(*5*), pp. 893–903.

Chen, Y., & Yu, S. (2017), *Impacts of urban landscape patterns on urban thermal variations in Guangzhou, China*. International journal of applied earth observation and geoinformation, **54**, pp. 65–71.

Das, N., Mondal, P., Sutradhar, S., & Ghosh, R. (2020), *Assessment of variation of land use/land cover and its impact on land surface temperature of Asansol subdivision*. The Egyptian Journal of Remote Sensing and Space Science.

Estoque, R. C., &Murayama, Y. (2017), *Monitoring surface urban heat island formation in a tropical mountain city using Landsat data (1987–2015)*. ISPRS Journal of Photogrammetry and Remote Sensing, **133**, pp. 18–29.

Estoque, R., Murayama, Y., & Myint, S. (2017), *Effects of landscape composition and pattern on land surface temperature:An urban heat island study in themegacities of Southeast Asia. Sci.* Total Environ, 577.

Ferrelli, F., Huamantinco Cisneros, M.A., Delgado, A.L., & Piccolo, M.C. (2018), *Spatial and temporal analysis of the LST-NDVI relationship for the study of land cover changes and their contribution to urban planning in Monte* Hermoso, Argentina.

Fonseka, H., Zhang, H., Sun, Y., Su, H., & Lin., H. L. (2019.), *Urbanization and Its Impacts on Land Surface Temperature in Colombo Metropolitan Area, Sri Lanka, from 1988 to 2016.* Remote sensing.

Gogoi, P.P., Vinoj, V., Swain, D., Roberts, G., Dash, J., & Tripathy, S. (2019), *Land use and land cover change effect on surface temperature over Eastern India.* Scientific reports, **9**(*1*), pp. 1–10.

Gong, A., Chen, Y., Li, J., Gong, H., & Li, X. (s.d.). (2006), *Spatial distribution patterns of the urban heat island based on remote sensing images: A case study in Beijing, China.* In Proceedings of the 2006 IEEE International Geoscience Remote Sensing Symposiu.

Green, K., Kempka, D., & Lackey, L. (1994), *Using remote sensing to detect and monitor land-cover and land-use change.* Photogrammetric Engineering & Remote Sensing, **60**, pp. 331–337.

Guechi I., Alkama Dj . (2017), *Apport de la télédétection pour la cartographie diachronique de l'étalement urbain et l'analyse morphologique de l'agglomération de Guelma.* Courrier du Savoir – N°**24**, pp.73–80.

Guha, S., Govil, H., Dey, A., & Gill, N. (2018), *Analytical study of land surface temperature with NDVI and NDBI using Landsat 8 OLI and TIRS data in Florence and Naples city,* Italy. European Journal of Remote Sensing, **51**(*1*), 667–678.

Hongyu, D., Jinquan, A., Yongli, C., & Liu, H. J. (2019), *Combined Effects of the Surface Urban Heat Islandwith Landscape Composition and Configuration Based on Remote Sensing*: A Case Study of Shanghai, China. Sustainability.

Imhoff, M., Zhang, P., Wolfe, R., & Bounoua, L. (2010), *Remote sensing of the urban heat island effect across biomes in the continental USA.* Remote Sens. Environ, **114** (*3*), pp. 504–513.

Inc, E. (1999), *Erdas Field Guide.* Erdas Inc. Atlanta, Georgia.

Jain, M., Dimri, A. P., & Niyogi, D. (2017), *Land-Air Interactions over Urban-Rural Transects Using Satellite Observations: Analysis over Delhi, India from 1991–2016.* Remote Sensing, **9**(*12*), 1283.

Jensen, J. (1995), *Introductory Digital Image Processing a Remote Sensing Perspective* (éd. Second Edition). New Jersey, Englewood Cliffs: Prentice-Hall.

Junxiang, L., Conghe, S., Lu, C., Feige, Z., Xianlei, M., & Jianguo, W. (2011), *Impacts of landscape structure on surface urban heat islands: a case study of Shanghai, China. Remote Sens.* Environ, **115**, pp. 3249–3263.

Kam, T. (1995), *Integrating GIS and remote sensing techniques for urban land-cover and land-use analysis.* Geocarto International, **10**, pp. 39–49.

Killian, J. (2014), *Magnet-Cities.* Available online: https://home.Kpmg.Com/uk/en/home/insights/2014/07/magnetcities. Html.

Kimuku, C.W. and Ngigi, M. (2017), *Study of Urban Heat Island Trends to Aid in Urban Planning in Nakuru County-Kenya.* Journal of Geographic Information System, **9**, pp. 309–325.

Kong, F., Yin, H., James, P., Hutyra, L., & He, H. (2014), *Effects of spatial pattern ofgreenspace on urban cooling in a large metropolitan area of eastern China.* Landsc. Urban Plan, **128**, pp. 35–47.

Kumar, K., Bhaskar, P., & Padmakumari, K. (2012). *Estimation of land surface temperature to study urban heat island effect using LANDSAT ETM+ image.* Int. J. Eng. Sci. Technol, **4** (*2*), pp. 771–778.

Landsat, N. (. (s.d.), *Science Data Users Handbook.* 2011–03–11. Consulté le October 23, 2019, sur http://landsathandbook.gsfc.nasa.gov/inst_cal/prog_sect8_2.html.

Landsat, N. (s.d.), *Science Data Users Handbook.* 2015-june. http://landsat.usgs.gov/l8handbook.php. Accessed 30 September 2019.

Li, B.,Wang,W., Bai, L.,Wang,W.,& Chen, N. (2018), *Effects of spatio-temporal landscape patterns on land surface temperature: a case study of Xi'an city, China.* Environmental Monitoring and Assessment, **190**(*7*), 419.

Li, X., Zhou, W., & Ouyang, Z. (2013), *Relationship between land surface temperature and spatial pattern of greenspace: What are the e_ects of spatial resolution? Landsc.* Urban Plan, **114**, pp. 1–8.

Liu, S., Su, H., Zhang, R., Tian, J., & Wang, W. (2016), *Estimating the surface air temperature by model. Advances in Meteorology.*

Lo, C., Quattrochi, D., & Luvall, J. (1997). *Application of high-resolution thermal infrared remote sensing and GIS to assess the urban heat island effect.* Int. J. Remote Sens, **18**, pp. 287–304.

Loveland, T., Sohl, S., Stehman, A., Gallant, K., & Sayler, N. D. (2002), *A strategy for estimating the rates of recent United States land-cover changes, Photogrammetric Engineering & Remote Sensing.* **68**(*10*), pp. 1091–1099.

Maimaitiyiming, M., Ghulam, A., Tiyip, T., Pla, F., Latorre-Carmona, P., Halik, Ü., Caetano, M. (2014), *E_ects of green space spatial pattern on land surface temperature: Implications for sustainable urban planning and climate change adaptation.* ISPRS J. Photogramm. Remote Sens, **89**, pp. 59–66.

Martinelli, L., & Matzarakis, A. (2017), *Influence of height/width proportions on the thermal comfort of courtyard typology for Italian climate zones.* Sustainable Cities and Society, **29**, pp. 97–106.

Mathew, A., Khandelwal, S., & Kaul, N. (2018), *Spatio-temporal variations of surface temperatures of Ahmedabad city and its relationship with vegetation and urbanization parameters as indicators of surface temperatures.* Remote Sens. Appl. Soc. Environ.

Meineke, E., Dunn, R., & Frank, S. (2014), *Early pest development and loss of biological control are associated with urban warming.* Biol. Lett.

Mitchell, B. C. (2011). *Urbanization and Land Surface Temperature in Pinellas County, Florida, Graduate Theses and Dissertations.* Récupéré sur http://scholarcommons.usf.edu/etd/3250.

Myint, S., Wentz, E., Brazel, A., & Quattrochi, D. (2013), *The impact of distinct anthropogenic and vegetation features on urban warming.* Landscape Ecol, **28** (*5*), pp. 959–978.

Naserikia, M., Asadi Shamsabadi, E., Rafieian, M., & Leal Filho, W. (2019), *The urban heat island in an urban context: A case study of Mashhad, Iran.* International Journal of Environmental Research and Public Health, **16**(*3*), 313.

Pal, S., & Ziaul, S. (2017), *Detection of land use and land cover change and land surface temperature in English Bazar urban centre.* Egyptian Journal of Remote Sensing and Space Science, **20**(*1*), pp. 125–145.

Pal, S., & Ziaul, S.K. (2017), *Detection of land use and land cover change and land surface temperature in English Bazar urban centre. The Egyptian Journal of Remote Sensing and Space Science*, **20**(*1*), pp. 125–145.

Peng, J., Xie, P., Liu, Y., & Ma, J. (2016), *Urban thermal environment dynamics and associated landscape pattern factors: A case study in the Beijing metropolitan region.* Remote Sens. Environ, **173**, pp. 145–155.

Plocoste, T., Jacoby-Koaly, S., Molinié, J., & Petit, R. (2014), *Evidence of the effect of an urban heat island on air quality near a landfill.* Urban Clim, **10**, pp. 745–757.

Pushpendra, S., Singh., Vivekanand.T, & Anil.K. (2014), *Analysis of Supervised Maximum Likelihood Classification for Remote Sensing Image,* IEEE International Conference on Recent Advances and Innovations in Engineering (ICRAIE – 2014). Jaipur, India.

Quattrochi, D., & Luvall, J. (1999), *Thermal infrared remote sensing for analysis of landscape ecological processes: methods and applications*. Landscape Ecol, **14** (*6*), pp. 577–598.

Radhi, H., Fikry, F., & Sharples, S. (2013), *Impacts of urbanisation on the thermal behaviour of new built up environments: a scoping study of the urban heat island in Bahrain*. Landscape Urban Planning , **113**, pp. 47–61.

Rahman, M. (2016), *Detection of land use/land cover changes and urban sprawl in Al-Khobar, Saudi Arabia: An analysis of multi-temporal remote sensing data.* Int. J. Geo Inf.

Ridd, M., & Liu, J. (1998), *A comparison of four algorithms for change detection in an urban environment. Remote Sensing of Environment*, **63**, pp. 95–100.

Rizwan, A., Dennis, L., & Chunho, L. (2008), *A review on the generation, determination and mitigation of Urban Heat Island.* J. Environ. Sci., **20** (*1*), pp. 120–128.

Santos, R. G., Prata-Shimomura, A. R., Correia, E., Franco, M. D. A. R., & Lopes, A. S. (2017), *Morfologia Urbana e Corredores de Ventilação como subsídio à Resiliência Urbana*. Revista LABVERDE, **8**(*2*), pp. 12–37.

Singh, A. (1989), *Digital change detection techniques using remotely-sensed data.* International Journal of Remote Sensing, **10**, pp. 989–1003.

Sohl, T. (1999), *Change analysis in the United Arab Emirates: An investigation of techniques* . Photogrammetric Engineering & Remote Sensing, **65**(*4*), pp. 475–484.

Spence, M., Annez, P., & Buckley, R. (2009), *Urbanization and Growth. Washington*, DC, USA: Word Bank.

Sun, H., Forsythe, W., & Waters, N. (2007), *Modeling urban land use change and urban sprawl*: Calgary, Alberta, Canada. Netw. Spat. Econ, **7**.

Tan, J., Yu, D., Li, Q., Tan, X., & Zhou, W. (2020), *Spatial relationship between land-use/land-cover change and land surface temperature in the Dongting Lake area, China*. Scientific Reports, **10**(*1*), pp. 1–9.

UNFPA. (Retrieved February 12, 2017, from http://www.unfpa.org/urbanization .). Urbanization.

USGS. (2014), *Using the USGS Landsat 8 product*. Retrieved December 11, 2014 from https://landsat.usgs.gov/using-usgs-landsat-8-product.

Voogt, J., & Oke, T. (2003), *Remote sensing of urban climates.* Remote Sensing of Environment, **3**(*86*), pp. 70–84.

Wang, R., Derdouri, A., & Murayama, Y. (2018), *Spatiotemporal simulation of future land use/cover change scenarios in the Tokyo metropolitan area*. Sustainability, **10**(*6*), 2056.

Wang, Y. C., Hu, B. K., Myint, S. W., Feng, C. C., Chow, W. T., & Passy, P. F. (2018), *Patterns of land change and their potential impacts on land surface temperature change in Yangon*, Myanmar. Science of the Total Environment, **643**, pp. 738–750.

Weng, Q. (2009), *Thermal infrared remote sensing for urban climate and environmental studies: methods, applications, and trends. ISPRS J.* Photogrammetry Remote Sens, **64** (*4*), pp. 335–344.

Yang, F., & Chen, L. (2016), *Developing a thermal atlas for climate-responsive urban design based on empirical modeling and urban morphological analysis.* Energy and Buildings, **111**, pp. 120–130.

Yang, X., & Lo, C. (2002), *Using a time series of satellite imagery to detect land use and land cover changes in Atlanta, Georgia metropolitan area.* International Journal of Remote Sensing, **9**, pp. 1775–1798.

Yuan, F., & Bauer, M. (2007), *Comparison of impervious surface area and normalized difference vegetation index as indicators of surface urban heat island effects in Landsat imagery*. Remote Sens. Environ, **106** (*3*), pp. 375–386.

Yuan, F., Sawaya, K. E., Loeffelholz, B. C., & Bauer, M. E. (2005), *Land cover mapping and change analysis in the Twin Cities Metropolitan Area with Landsat remote sensing*. Remote Sensing of Environment, **98**(*2.3*), pp. 317–328.

Zhou, W., Huang, G., & Cadenasso, M. (2011), *Does spatial configuration matter? Understanding the e_ects of land cover pattern on land surface temperature in urban landscapes*. Landsc. Urban Plan, **102**, pp. 54–63.

Zhou, W., Qian, Y., Li, X., Li, W., & Han, L. (2014), *Relationships between land cover and the surface urban heat island: seasonal variability and effects of spatial and thematic resolution of land cover data on predicting land surface temperatures*. Landscape Ecol, **29** (*1*), pp. 153–167.